

MEMBRANE-LOCALIZED TRANSCRIPTION REGULATORS: UNDERSTANDING
POST-TRANSLATIONAL REGULATION AND SINGLE-MOLECULE DYNAMICS OF
TCPB IN *VIBRIO CHOLERAE*

By

Lucas Maurice Demey

A DISSERTATION

Submitted to
Michigan State University
in partial fulfillment of the requirements
for the degree of

Microbiology and Molecular Genetics – Doctor of Philosophy

2022

ABSTRACT

MEMBRANE-LOCALIZED TRANSCRIPTION REGULATORS: UNDERSTANDING POST-TRANSLATIONAL REGULATION AND SINGLE-MOLECULE DYNAMICS OF TCP P IN *VIBRIO CHOLERAE*

By

Lucas Maurice Demey

Vibrio cholerae is a Gram-negative gastrointestinal pathogen that has evolved an elegant regulatory system to precisely time production of essential virulence factors. A key step in this regulatory system is the transcription of a soluble AraC-like transcription factor, ToxT. ToxR and TcpP, two membrane-localized transcription regulators (MLTRs), positively regulate *toxT*. Much work has contributed to our understanding of TcpP and ToxR regulation, yet major gaps remain in our knowledge of these MLTRs.

MLTRs are unique one-component signal transduction systems because they respond to extracellular stimuli by influencing gene transcription from their location in the cytoplasmic membrane. In Chapter 2, I explore the prevalence and diversity of MLTRs within prokaryotes to enhance our understanding of TcpP and ToxR. I show that MLTRs are far more common among prokaryotes than previously anticipated and that MLTRs are an understudied class of transcription regulators. In Chapter 3, I describe the use of super-resolution single-molecule tracking to investigate how TcpP, a model MLTR, identifies the *toxT* promoter. I provide evidence that TcpP binds to the *toxT* promoter independent of ToxR, and TcpP transitions to a specific diffusion state. The data support the first biophysical model for how TcpP-like MLTRs locate their target promoters.

TcpP is subject to a form of post-translational regulation known as regulated intramembrane proteolysis (RIP). RIP of TcpP results in its complete inactivation,

resulting in loss of virulence factor production. TcpH inhibits RIP of TcpP under certain pH and temperature conditions. In Chapter 4, I describe the mechanism TcpH employs to inhibit TcpP RIP while *V. cholerae* is present in the mouse gastrointestinal tract. I demonstrate that the dietary fatty acid α -linolenic acid enhances inhibition. I also show that α -linolenic acid promotes TcpH-mediated inhibition of TcpP RIP by increasing association of both proteins with detergent-resistant membrane (DRM) domains. My work provides the first evidence that DRMs influence virulence factor transcription in *V. cholerae* and that a dietary fatty acid promotes *V. cholerae* pathogenesis.

“Two things that remain eternally true and complement each other, in my view are: don’t snuff out your inspiration and power of imagination, don’t become a slave to the model; and the other, take a model and study it, for otherwise your inspiration won’t take on material form.”

— Vincent van Gogh

ACKNOWLEDGEMENTS

First, I would like to thank Vic for deciding to take a chance on me and for introducing me to TcpP and TcpH. From the start to the end of my PhD journey Vic has helped me to become a better communicator, better writer, a critical thinker, and a leader. While these skills have helped me to become a better scientist, these skills have all translated into almost every aspect of my life and have forever changed me for the better. I would also like to thank my committee members, Neal Hammer, Heedeok Hong, Lee Kroos, Chris Waters, who both challenged me and encouraged me throughout my graduate career.

Of course, I also need to thank the entire DiRita lab who have been my rock. They were there through all my ups and downs, encouraging me when needed, and imploring me to focus on one topic at a time when I found a new paper I loved. First, I would like to thank Rhia who is the heart of the lab and keeps everything together in the midst of all the chaos that comes with research. I would also like to thank Ted and Beth who took the brunt of my science ranting. Ted and Beth (aka, Bethanol) are both selfless people who always take time to help and to offer advice. Lastly, but not least, I would like to thank Ritam who has always been an endless source of encouragement and a steadfast friend. To the DiRita lab, I entered the MMG department with the goal of earning a PhD, but I will be leaving with you as lifelong friends.

Outside of MSU I also was privileged to have support from my mother, father, sister, and brother-in-law who encouraged me throughout graduate school. Last, but not

least, I need to thank John Nelson. Whether he knows it or not, John was really my first scientific mentor. Every day John was pushing me to question the status quo and to think outside of the box. Working for John was the best thing I could have ever done to prepare for my PhD journey. I am eternally grateful for what I learned while working for John.

TABLE OF CONTENTS

LIST OF TABLES	x
LIST OF FIGURES	xi
KEY TO ABBREVIATIONS	xiv
Chapter 1 – Introduction	1
1.1 – <i>Vibrio cholerae</i>	2
1.2 – <i>V. cholerae</i> Pathogenesis	3
1.3 – Regulation of the Virulence Cascade	4
1.4 – Concluding Remarks	9
Chapter 2 – Membrane-Localized Transcription Regulators within Prokaryotes	12
2.1 – Abstract	13
2.2 – Introduction	13
2.3 – Materials and Methods	18
2.3.1 – MLTR screen using the MIST database	18
2.3.2 – MLTR domain and gene neighborhood analysis	18
2.4 – Results	19
2.4.1 – The <i>Vibrio</i> genus	19
2.4.2 – The <i>Salmonella</i> and <i>Escherichia</i> Genera	24
2.4.3 – The <i>Yersinia</i> Genus	30
2.4.4 – The <i>Enterococcus</i> and <i>Lactobacillus</i> genera	34
2.4.5 – The <i>Staphylococcus</i> genus	40
2.5 – Discussion	43
Chapter 3 – Independent Promoter Recognition by TcpP Precedes Cooperative Promoter Activation by TcpP and ToxR	45
3.1 – Preface	46
3.2 – Abstract	46
3.3 – Introduction	47
3.4 – Materials and Methods	50
3.4.1 – Bacterial strains and growth conditions	50
3.4.2 – Plasmid construction	50
3.4.3 – Bacterial strain construction	51
3.4.4 – Growth Curves	51
3.4.5 – Real-time quantitative PCR (RT-qPCR)	52
3.4.6 – Protein electrophoresis and immunodetection	52
3.4.7 – Single-Molecule Microscopy	53
3.4.8 – Data Analysis	54
3.5 – Results	54

3.5.1 – Single-molecule tracking of TcpP-PAmCherry is useful to study promoter identification, but cannot probe regulated-intramembrane proteolysis	54
3.5.2 – Baseline Dynamics of TcpP-PAmCherry	56
3.5.3 – Mutation of the <i>toxTpro</i> Decreases the Slow Diffusion State Occupancy	60
3.5.4 –ToxR Promotes TcpP-PAmCherry Association with the Slow and Fast Diffusion States	63
3.5.5 – Mutation of the TcpP Helix-Turn-Helix Domain Reduces the Percentage of Slowly Diffusing TcpP-PAmCherry	68
3.6 – Discussion	69
 Chapter 4 – Co-Association of TcpP and TcpH within Detergent-Resistant Membranes Stimulates TcpH-Dependent Inhibition of Regulated Intramembrane Proteolysis of TcpP in <i>Vibrio cholerae</i>	75
4.1 – Abstract	76
4.2 – Introduction	77
4.3 – Methods and Materials	79
4.3.1 – Bacterial strains, plasmids, and growth conditions	79
4.3.2 – Plasmid construction	81
4.3.3 – Mutant construction	81
4.3.4 – Growth curves	82
4.3.5 – Western blots	82
4.3.6 – Enzyme Linked-Immunosorbent Assay (ELISA)	83
4.3.7 – Infant Mouse Colonization	83
4.3.8 – Real-time quantitative PCR (RT-qPCR)	84
4.3.9 – β -Galactosidase activity assay	84
4.3.10 – Subcellular Fractionation	85
4.3.11 – Triton X-100 Subcellular Fractionation	86
4.3.12 – Co-affinity precipitation	87
4.4 – Results	88
4.4.1 – TcpH Maintains <i>in vitro</i> Activity Upon Alteration of its Transmembrane and Periplasmic Domains	88
4.4.2 – TcpH TM domain is Critical for Colonization of Infant Mice	91
4.4.3 – The TcpH Transmembrane Domain Protects TcpP from RIP	93
4.4.4 – <i>toxT</i> Transcription is Enhanced with Crude Bile and is Dependent on the TcpH Transmembrane Domain	94
4.4.5 – α -Linolenic Acid Enhances <i>toxT</i> Transcription by Promoting TcpH-Dependent Enhanced RIP Inhibition	96
4.4.6 – Co-Association of TcpP and TcpH with Detergent-Resistant Membranes is Required for Enhanced RIP Inhibition	101
4.4.7 – TcpP and TcpH Interaction is critical for inhibition of RIP	105
4.4.8 – Miltefosine Functions Synergistically with α -Linolenic acid	109
4.5 – Discussion	110
 Chapter 5– Concluding Remarks	118
5.1 – Conclusions and Significance	119
5.2 – Future Directions	121

APPENDICES	127
APPENDIX A: Supplemental Material for Chapter 2	128
APPENDIX B: Distribution of Membrane-Localized Transcription Regulators within the Prokaryotic Domain	142
APPENDIX C: Supplemental Material for Chapter 3	154
APPENDIX D: Supplemental Material for Chapter 4	170
APPENDIX E: Identifying Regions within TcpH Critical for its Function	198
APPENDIX F: Defining the Mechanism of Action of Toxtazin A and Toxtazin B	211
APPENDIX G: Heterogeneous Single-Cell toxT Transcription	217
REFERENCES	222

LIST OF TABLES

Table A.1: Characterized MLTRs and their known cellular response and associated proteins	129
Table A.2: Membrane localized transcription regulators (MLTRs) within the <i>Vibrio</i> genus	131
Table A.3: Membrane localized transcription regulators (MLTRs) within the <i>Escherichia</i> and <i>Salmonella</i> genera	133
Table A.4: Membrane localized transcription regulators (MLTRs) within the <i>Yersinia</i> genus	134
Table A.5: Membrane localized transcription regulators (MLTRs) within the <i>Enterococcus</i> genus	135
Table A.6: Membrane localized transcription regulators (MLTRs) within the <i>Lactobacillus</i> genus	138
Table A.7: Membrane localized transcription regulators (MLTRs) within the <i>Staphylococcus</i> genus	140
Table B.1: Distribution of MLTRs within Bacterial Phyla.....	150
Table C.1: Chapter 3 strain list.....	165
Table C.2: Chapter 3 primer list	168
Table D.1: Chapter 4 strain list.....	188
Table D.2: Chapter 4 primer list	193

LIST OF FIGURES

Figure 1.1: The Virulence cascade in <i>V. cholerae</i>	5
Figure 2.1: Prokaryotic Signal transduction systems.....	15
Figure 2.2: Characterized membrane localized transcription regulators (MLTRs) within Prokaryotes.....	17
Figure 2.3: Representative MLTRs identified within the <i>Vibrio</i> genus	20
Figure 2.4: Representative MLTRs identified within the <i>Escherichia</i> and <i>Salmonella</i> genera.....	26
Figure 2.5: Representative MLTRs identified within the <i>Yersinia</i> genus	31
Figure 2.6: Representative MLTRs identified within the <i>Enterococcus</i> and <i>Lactobacillus</i> genera.....	35
Figure 2.7: Representative <i>Staphylococcus</i> MLTRs identified	42
Figure 3.1: Single-molecule diffusion dynamics of TcpP-PAM.....	58
Figure 3.2: TcpP-PAMCherry diffusion dynamics within live <i>V. cholerae</i> cells containing mutated regions of the <i>toxT</i> promoter (<i>toxTpro</i>).....	61
Figure 3.3: TcpP-PAMCherry diffusion dynamics within live <i>V. cholerae</i> cells lacking ToxRS and regions of the <i>toxT</i> promoter	65
Figure 3.4: Mutation of the DNA binding domain within TcpP reduces the number of TcpP molecules within the slow diffusion state.....	67
Figure 4.1: TcpH transmembrane and periplasmic constructs protect TcpP, support <i>toxT</i> transcription, and virulence factor production.....	90
Figure 4.2: TcpH transmembrane constructs have a colonization defect in infant mice	93
Figure 4.3: α -Linolenic acid stimulates <i>toxT</i> transcription, elevated TcpP levels, and does not increase <i>tcpP</i> transcription	98
Figure 4.4: TcpP and TcpH abundance increases in detergent resistant membranes in the presence of α -linolenic acid.....	103
Figure 4.5: TcpP and TcpH interaction is critical for TcpH-dependent inhibition of RIP	108

Figure 4.6: α -Linolenic acid stimulates co-association of TcpP and TcpH within detergent resistant membranes thereby enhancing TcpH inhibition of RIP	113
Figure C.1: Possible membrane localized transcription regulators (MLTRs) within Gram-negative and Gram-positive bacteria.....	155
Figure C.2: Biochemical characterization of <i>tcpP</i> -PAm strains	156
Figure C.3: TcpH protects TcpP-PAm from proteolysis.....	157
Figure C.4: <i>toxT</i> transcription profile in <i>tcpP</i> -PAm strains.....	158
Figure C.5: PAmCherry does not promote dimerization of TcpP.....	159
Figure C.6: <i>tcpP</i> -PAm strains have growth dynamics similar to WT	160
Figure C.7: Complementation and overexpression of ToxR in <i>tcpP</i> -PAm strains	161
Figure C.8: TcpP-PAmCherry transition plots	162
Figure C.9: ToxR overexpression reduces virulence factor production	164
Figure D.1: TcpH transmembrane and periplasmic constructs growth dynamics are similar to WT.....	175
Figure D.2: TcpH transmembrane and periplasmic constructs support <i>toxT</i> transcription and CtxB production.....	176
Figure D.3: TcpH transmembrane and periplasmic constructs display WT growth in adult mice feces	177
Figure D.4: TcpH transmembrane constructs inhibit RIP of TcpP	178
Figure D.5: Crude bile stimulates <i>toxT</i> transcription in a TcpH dependent manner	179
Figure D.6: α -Linolenic acid stimulates <i>toxT</i> transcription in a TcpH dependent manner	180
Figure D.7: α -Linolenic acid stimulates <i>toxT</i> transcription in a dose dependent manner	181
Figure D.8: <i>toxT</i> transcription is stimulated by crude bile and α -linolenic acid, but <i>tcpP</i> transcription does not change	182
Figure D.9: TcpP levels are elevated in the presence of crude bile and α -linolenic acid	183
Figure D.10: α -Linolenic acid promotes association of TcpP and TcpH with detergent resistant membranes (DRM)	184

Figure D.11: α -Linolenic acid does not promote non-specific protein association with detergent resistant membranes.....	185
Figure D.12: Hsv-His(6x) tagged TcpP constructs remain functional	186
Figure D.13: Miltefosine and α -linolenic acid function synergistically to stimulate <i>toxT</i> transcription.....	187
Figure E.1: TcpH transmembrane and periplasmic constructs remain functional <i>in vitro</i>	201
Figure E.2: Residues within region 136-103 in the periplasmic domain of TcpH are critical for protecting TcpP under non-virulence inducing conditions.....	203
Figure E.3: Overexpression of TcpH transmembrane and periplasmic constructs allows for visualization via western blot.....	204
Figure E.4: TcpH transmembrane and periplasmic constructs Infant mouse colonization and growth in adult mice feces.....	207
Figure E.5: TcpH transmembrane constructs inhibit RIP of TcpP and C_{txB} TcpH remains localized to the cytoplasmic membrane.....	209
Figure F.1: Characterization of toxtazin A and B mechanism of action	215
Figure G.1: Single-cell <i>toxT</i> transcription is heterogenous in <i>V. cholerae</i>	219
Figure G.2: TcpP is sensitive to an unknown protease upon mutation of <i>tsp</i> and <i>yaeL</i>	220

KEY TO ABBREVIATIONS

3,3',5,5'-tetramethylbenzidine	TSB
Accessory Cholera Enterotoxin	Ace
Avian pathogenic <i>E. coli</i>	APEC
CAAX Proteases and Bacteriocin-Processing metalloproteases	CPBP
Cellulose polysaccharide locus	<i>bcs</i>
CFU	Colony forming units
Cholera toxin	CtxAB
Cyclic adenosine monophosphate	cAMP
Cyclic di-peptide cyclic phenylalanine-proline	cyc-phe-pro
Detergent resistant membranes	DRM
Detergent soluble membranes	DSM
Diaminopimelic acid	DAP
Diarrheagenic <i>E. coli</i>	DEC
Dithiobis-succinimidyl propionate	DPS
DNA	Deoxyribonucleic acid
DMSO	Dimethyl sulfoxide
Enteroaggregative <i>E. coli</i>	EAEC
Enterohemorrhagic <i>E. coli</i>	EHEC/STEC
Enteroinvasive <i>E. coli</i>	EIEC
Enteropathogenic <i>E. coli</i>	EPEC
Enterotoxigenic <i>E. coli</i>	ETEC

Enzyme Linked-Immunosorbent Assay	ELISA
ETT2	<i>E. coli</i> type III secretion system 2
Global Regulator of Virulence protein A	GrvA
Guanine nucleotide-binding regulatory protein	Gsa
Histone-like nucleoid structuring protein	H-NS
Isopropyl β -d-1-thiogalactopyranoside	IPTG
Lactic acid bacteria	LAB
Locus of enterocyte effacement	LEE
Lysogeny Broth	LB
Membrane localized transcription regulators	MLTRs
Microbial Signal Transduction Database	MIST
Monosialoganglioside	GM1
Multifunctional Auto processing Repeats-in-toxin	RTX
Multi-transmembrane domain MLTR	MT-MLTR
Nitric oxide	NO
Nitrogen assimilation control	Nac
Non-virulence inducing	non-Vir Ind
Non-virulence-inducing conditions	LB pH 8.5, 37°C, shaking at 210rpm
Optical density	O.D. _{600nm}
Periplasmic domain	Peri
Photoactivatable mCherry	PAmCherry
Poly-unsaturated fatty acids	PUFA
Regulated Intramembrane Proteolysis	RIP

<i>Salmonella</i> pathogenicity island 1	SPI-1
<i>Salmonella</i> pathogenicity island 2	SPI-2
<i>Salmonella</i> pathogenicity island 3	SPI-3
<i>Salmonella</i> typhimurium fimbriae operon	<i>stf</i>
Single-Molecule Analysis by Unsupervised Gibbs sampling	SMAUG
Super-resolution single-molecule tracking	SMT
Tail-specific protease	Tsp
Thiosulfate-citrate-bile salts-sucrose agar	TCBS
Toxin co-regulated pilus	Tcp
<i>toxT</i> promoter	<i>toxTpro</i>
Transmembrane	TM
Triton insoluble	TI
Triton soluble	TS
Type three secretion system	T3SS
Untranslated region	UTR
Uropathogenic <i>E. coli</i>	UPEC
Uropygial gland	Preen gland
Virulence-inducing	Vir Ind
Virulence-inducing conditions	LB pH 6.5, 110 rpm, 30°C
<i>Vibrio</i> Pathogenicity Island 1	VPI-1
<i>Vibrio</i> seventh pandemic island I	VPS-1
<i>Vibrio</i> seventh pandemic island 2	VSP-2
WT	Wild type

Y. enterocolitica chromosomally encoded T3SS

Ysa

Y. enterocolitica plasmid that encoded a T3SS

Ysc

Chapter 1 – Introduction

1.1 – *Vibrio cholerae*

V. cholerae is a Gram-negative free-living marine bacterium that is the agent of the diarrheal disease cholera. Cholera is a life-threatening disease that has been a recurring problem around the world since 1817 when the first of seven recorded cholera pandemics began and continues to pose a significant global burden killing ~95,000 people annually (1–3). Treatment of *V. cholerae* infection currently involves oral rehydration therapy, and antibiotic therapy (4–6). To reduce the burden of *V. cholerae* several vaccines have been developed (7–10). However, despite treatment options and vaccine development these conventional methods to combat *V. cholerae* have been ineffective at reducing the incidence of cholera cases (11–14). To add insult to injury, changes in global climate and temperature are anticipated to allow *V. cholerae* to proliferate in new geographical areas leading to more cholera cases (15). Thus, there is a need for novel treatment methods to combat *V. cholerae* infections. Identification and development of these novel treatment methods will require a deeper understanding of the pathogenesis of *V. cholerae*. Thus, the aim of this work has been to deepen our understanding of virulence gene regulation in *V. cholerae*.

The first six Cholera pandemics were dominated by the Classical biotype of *V. cholerae* and was supplanted by the El Tor biotype during the seventh pandemic. Classical and El Tor biotypes differ in the severity of disease and their proliferation in aquatic environments with El Tor biotypes causing milder disease and better survival in aquatic environments (16). El tor and Classical biotypes also differ by their sensitivity to polymyxin B, acetylmethylcarbinol synthesis, phage sensitivity, hemolysis of sheep enterocytes, chicken erythrocytes agglutination, and their *ctxB* and *tcpA* alleles (17, 18).

In addition, El Tor biotypes acquired the *Vibrio* seventh pandemic island 1 and 2 (VPS-1 and VSP-2) (19). Despite these differences, many genes involved in regulation of virulence factor production are highly conserved between Classical and El Tor biotypes, with intergenic mutations driving differences in virulence factor transcription (20).

1.2 – *V. cholerae* Pathogenesis

V. cholerae infections occur via the fecal-oral route, typically from consumption of undercooked contaminated food or water (21, 22). Once ingested, *V. cholerae* cells must survive the acidic stomach environment to reach the small intestine. Once inside the lumen of the small intestine, *V. cholerae* cells proceed to colonize the middle and distal portions of the small intestine, where they must penetrate the thick mucus layer to reach the epithelial crypt, the primary site of infection (23–25). To proliferate, *V. cholerae* employs a number of virulence factors to establish colonization, suppress the host immune response, and to manipulate host cells to proliferate. To colonize the small intestine, *V. cholerae* cells must compete with the host microbiota via direct killing mediated by the type-6 secretion system, stimulate permeability of the mucus layer (via Hemagglutinin Protease, Neuraminidase, and the Zonula Occludens Toxin), and colonize epithelial cells promoted by the Toxin co-regulated pilus (Tcp) via an unknown mechanism (26–32). In addition to colonization, *V. cholerae* cells must also resist the host-immune response. Host cells are known to produce nitric oxide (NO) in response to bacterial infections, and *V. cholerae* cells sense NO via NorR and detoxify NO via HmpA (33). In addition, *V. cholerae* also reduces the innate epithelial immune defense and mucosal inflammation by secreting membrane vesicles which carry small RNAs (e.g., miR-146a) that inhibit host immunomodulatory micro-RNAs (34). *V. cholerae* further

modulates the host immune response by suppressing chemokine and cytokine mediated recruitment of innate immune cells normally induced in response to cytoskeleton damage via the Multifunctional Autoprocessing Repeats-in-toxin (RTX) (35).

Once at the site of infection, *V. cholerae* cells stimulate fluid accumulation via secretion of cholera toxin (CtxAB) and Accessory Cholera Enterotoxin (Ace). CtxAB is secreted from *V. cholerae* cells and binds to host monosialoganglioside (GM1) (36). Upon binding to host GM1 CtxAB enters host epithelial cells via endocytosis and activates a subunit of the guanine nucleotide-binding regulatory protein (G α) (36). This leads to stimulation of adenylate cyclase activity yielding high levels of cyclic adenosine monophosphate (cAMP) (36). This in turn leads to the inactivation of NHE3 H⁺/Na⁺ transporters and stimulates secretion of Cl⁻ via the cystic fibrosis transmembrane conductance regulator (36). The net effect is an increase in NaCl, as well as Cl⁻, HCO³⁻, Na⁺, K⁺, and H₂O, secretion and a reduction of NaCl absorption resulting in watery diarrhea (36). Ace stimulates Ca²⁺ dependent Cl⁻/HCO³⁻ cotransporters in host cells independent of cAMP (37, 38). Ace mediated fluid accumulation appears to have a role early during infection before CtxAB fluid accumulation dominates.

1.3 – Regulation of the Virulence Cascade

Transcription of *tcpA-F* and *ctxAB* is regulated by ToxT, an AraC like transcription factor (39–42) (Figure 1.1). In the small intestinal lumen, unsaturated fatty acids directly bind to the N-terminal domain of ToxT preventing dimerization and subsequent transcription of *tcpA-F* and *ctxAB* by ToxT (43–46). Inhibition of ToxT activity by unsaturated fatty acids also reduces degradation of ToxT in the cytoplasm (47, 48).

Unsaturated fatty acids serve as a cue to regulate ToxT activity to prevent premature virulence factor transcription and protect the pool of ToxT within the cytoplasm (48). As *V. cholerae* inches closer to the epithelial brush border the concentration of bicarbonate increases, reaching maximal concentration at the surface of epithelial cells due to active secretion of bicarbonate from host cells (49). Bicarbonate stimulates ToxT activity by promoting dimerization of ToxT monomers and also inhibits unsaturated fatty acid antagonism of ToxT activity (50). The available literature indicates that virulence factor transcription occurs maximally at the surface of epithelial cells.

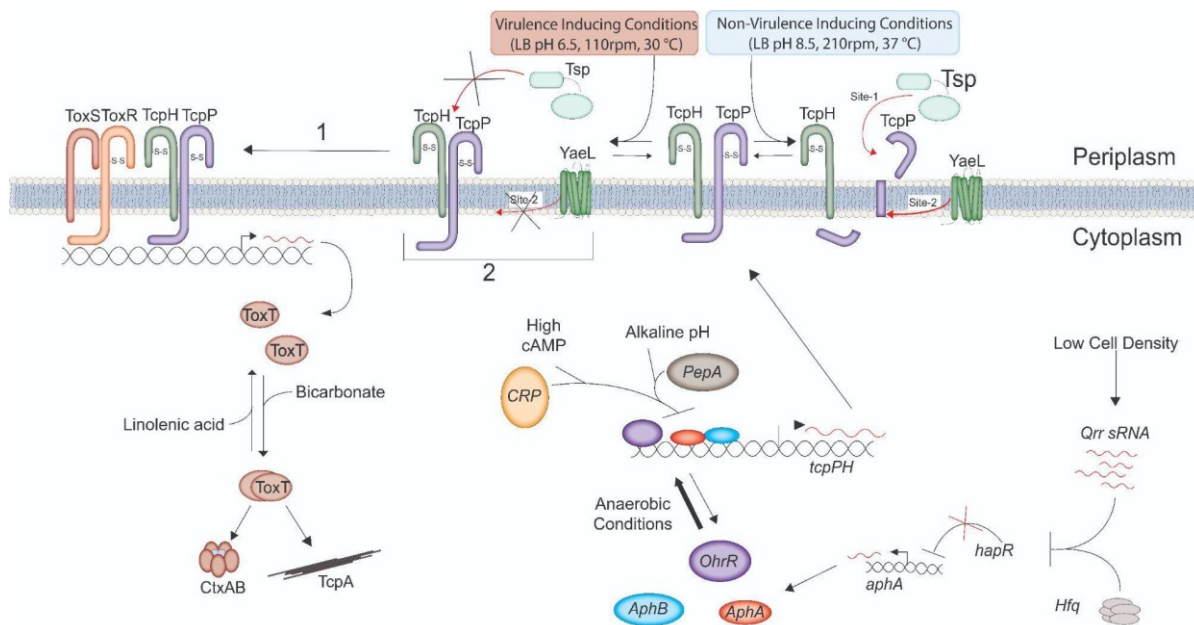


Figure 1.1: The Virulence cascade in *V. cholerae*. Dimerization ToxT stimulates its activity and ability to stimulate *ctxAB* and *tcp* transcription (50, 51). Unsaturated fatty acids, such as α -linolenic acid, inhibit dimerization of ToxT and thereby its activity (43–46). Bicarbonate promotes dimerization of ToxT molecules (50). Transcription of *toxT* is stimulated by ToxR and TcpP and indirectly by their associated proteins, ToxS and TcpH respectively (39–41, 52–57). Currently, it remains unclear how TcpP and ToxR co-localize to the *toxT* promoter while localized to the cytoplasmic (indicated by 1). In addition to identifying the *toxT* promoter, it is currently not understood how TcpH protects TcpP from Regulated Intramembrane Proteolysis (RIP) *in vivo* or *in vitro* (indicated by 2). Once localized to the cytoplasmic membrane, TcpP is prone to RIP, which is stimulated or inhibited by culture conditions (56, 58, 59). Stimulation of RIP of

Figure 1.1 (cont'd)

TcpP occurs under non-virulence inducing conditions (i.e., LB pH 8.5, 210rpm, 37 °C) in a two-step process. RIP of TcpP is initiated by Tsp, cleaving the periplasmic domain of TcpP, and secondly by YaeL removing the cytoplasmic domain from the membrane (58, 59). *tcpP* and *tcpH* are also subject to significant transcriptional regulation. *tcpPH* transcription is negatively regulated by both PepA (under alkaline pH) and catabolite repressor protein (CRP, when levels of cyclic AMP are high) (60–62). *tcpPH* transcription is stimulated by AphA, AphB and OhrR, and their activity is further enhanced by low oxygen concentrations (O₂) further increasing *tcpPH* transcripts (63–65). At high cell density *aphA* transcription is inhibited by HapR (66). At low cell density translation of HapR mRNAs is inhibited by the Quorum regulatory RNAs (Qrr), which are upregulated at low cell density, in association with Hfq (67, 68).

In addition to post-translational regulation of ToxT, transcription of *toxT* is highly regulated and is positively stimulated by TcpP and ToxR, two membrane localized transcription regulators (39–41, 52–55). TcpP and ToxR are bitopic membrane proteins that each contain a cytoplasmic OmpR family DNA-binding domain, a single transmembrane domain, and a periplasmic domain (69). Both ToxR and TcpP bind to the promoter region of the *toxT*, -180 to -60 and -55 to -37 respectively (55, 70, 71). TcpP is absolutely essential for *toxT* transcription while loss of *toxR* can be overcome by overexpression of *tcpP* (39, 55). ToxR is more promiscuous relative to TcpP in its specificity for binding DNA sequences (71–73). It is thought that one of the major biological roles of ToxR is to antagonize the histone-like nucleoid structuring protein (H-NS) to derepress transcription of H-NS target genes (72). It is thought that one mechanism by which ToxR cooperates with TcpP to stimulate *toxT* transcription is by antagonizing H-NS binding to the *toxT* promoter. However, there are still questions regarding how ToxR and TcpP cooperate to stimulate *toxT* transcription. There are several models for cooperative activation of the *toxT* promoter by TcpP and ToxR (71). Several models ascribe ToxR's major role as recruiting TcpP molecules to the *toxT* promoter, and this role is supported by evidence that heterodimerization of TcpP and

ToxR, stimulated by anaerobic conditions, stimulates *toxT* transcription (71, 74). However, data also support an alternative promoter alteration model in which ToxR promotes *toxT* activation by altering the promoter topology promoting TcpP binding without direct recruitment of TcpP by ToxR (71). In this model heterodimerization of TcpP and ToxR would not have an obvious role. Homodimerization of TcpP (stimulated by taurocholate) molecules has been shown to be critical for *toxT* transcription and suggests that TcpP-ToxR heterodimers disassociate prior to interaction with the *toxT* promoter (75–78). As there is data supporting multiple models of cooperativity between TcpP and ToxR it remains unclear how these MLTRs function together to stimulate *toxT* transcription.

Independent of cooperativity, TcpP and ToxR are also sensitive to a form of post-translational regulation known as Regulated Intramembrane Proteolysis (RIP) (56, 58, 59, 79, 80). For both TcpP and ToxR RIP is a two-step process where their periplasmic domains undergo proteolysis first via a site-1 protease/s (TcpP: Tsp, ToxR: DegS and DegP) and their transmembrane domains secondly by a site-2 protease (YaeL, also referred to as RseP) which inactivates both TcpP and ToxR (56, 58, 59, 79, 80). Conditions that promote RIP of TcpP and ToxR inhibit *toxT* transcription. RIP of TcpP and ToxR is inhibited by their associated proteins, ToxS and TcpH respectively, under specific conditions (56, 58, 59, 81, 82). ToxR has been reported to undergo RIP under nutrient limiting conditions, alkaline pH, and in the absence of ToxS (80, 83). Conditions that stimulate RIP of ToxR occur during stationary phase, and RIP of ToxR is critical for *V. cholerae* cells to enter a viable but non-culturable state, which is thought to be important for survival of *V. cholerae* in the environment (80). ToxS has been shown to inhibit RIP of ToxR by directly associating with ToxR molecules in response to bile salts (such as

deoxycholate) (81, 83–85). RIP of TcpP is stimulated by alkaline pH (pH 8.5) and high temperature (37°C), and RIP of TcpP is inhibited by low temperature and mild acidity (30°C and pH 6.5) (56, 58, 59). Similar to ToxS, TcpH is a membrane localized protein which protects TcpP from RIP under specific *in vitro* conditions (56, 58, 59). Currently, it is not clear how TcpH inhibits RIP of TcpP nor is it clear what signals *in vivo* promote TcpH antagonism of RIP.

In addition to post-translational regulation, TcpP transcription is also heavily regulated. Transcription of *tcpPH* is stimulated by AphA and AphB in response to low pH and anoxic conditions (63, 64). Furthermore, AphA transcription is also modulated by cell density of *V. cholerae* (66). Under low cell density LuxO is phosphorylated in response to low concentrations of autoinducers (cholerae autoinducer-1 [CAI-1] and autoinducer-2 [AI-2]) and stimulates transcription of several small regulatory RNAs, *qrr1-4* (67, 68). These regulatory RNAs inhibit translation of HapR thereby relieving repression of *aphA* (66–68). *tcpPH* transcription is also stimulated by OrhR under anoxic conditions (65). Together, AphAB and OrhR function to stimulate transcription of *tcpPH* at low cell density, mildly acidic pH, and anaerobic conditions (Figure 1.1).

Transcription of *tcpPH* is also responsive to nutrient conditions. Under nutrient limiting conditions levels of cAMP are high leading to activation of cAMP receptor protein (CRP). Upon activation of CRP via binding to cAMP, cAMP-CRP inhibits transcription of both the *toxT* and *tcpPH* (60, 61). Conversely, under nutrient rich environments, such as the human gastrointestinal tract, cAMP-CRP levels are low releasing repression of *toxT* and *tcpPH* (60, 61). *tcpPH* transcription is further fine-tuned by PepA, which represses transcription of *tcpPH* under alkaline pH (62).

Taken together, the current body of literature suggests that during the early phase of infection cues in the lumen of the gastrointestinal environment (e.g., acidic pH, low oxygen availability, bile salts, and abundant nutrient availability) elevate *tcpPH* transcription, promote TcpP and ToxR homo/hetero-dimerization, and thereby promote *toxT* transcription. While in the lumen of the small intestine, ToxT is inhibited by high concentrations of unsaturated fatty acids. Once *V. cholerae* reaches the surface of epithelial cells, where bicarbonate concentrations are high, bicarbonate competes with unsaturated fatty acids to stimulate activation of ToxT and thereby downstream virulence factor transcription (i.e., *ctxAB* and *tcpA-F*).

1.4 – Concluding Remarks

V. cholerae is a life-threatening pathogen that continues to pose a major global health burden. *V. cholerae* continues to be a major burden around the globe despite the availability of conventional treatment options. There is a critical need to develop a deeper understanding of *V. cholerae* pathogenesis. There remain major gaps in our knowledge regarding regulation of *toxT* transcription and the function of MLTRs in general.

TcpP and ToxR are unique transcription factors as they are localized to the membrane (i.e., MLTRs). Currently, there are also major questions regarding how membrane localized transcription regulators (MLTRs) in general function from the membrane because only a few DNA binding transcription factors are capable of influencing gene transcription from the membrane. For example, Enterohemorrhagic *Escherichia coli* is a foodborne human gastrointestinal pathogen that stimulates virulence gene transcription in response to mechanical stimuli via GrlA, a membrane bound

transcription factor (86). While localized to the membrane GrlA is not fully active and requires cytoplasmic localization after mechanical stimuli (86). Secondly, within *Salmonella typhimurium* PutA is a bifunctional transcription factor that represses transcription of *putP* (a proline permease) and catalyzes the oxidation of proline (87). In the absence of proline, PutA is localized to the cytoplasm where it can repress *putP* transcription, and in the presence of proline PutA becomes sequestered to the cytoplasmic membrane to oxidize proline and is unable to repress *putP* (87). MLTRs are poorly studied and as such their distribution among bacteria is not understood. To better understand how MLTRs function from the membrane, we conducted a computational screen to identify MLTRs within other bacteria to gain an appreciation for the diversity, conservation, and overall prevalence of MLTRs within bacteria. A summary of our findings is presented in Chapter 2.

Currently, we do not have a complete understanding of how ToxR and TcpP function cooperatively to stimulate *toxT* transcription. There are several models for how TcpP and ToxR function to stimulate *toxT* transcription such as the hand-holding model which states that ToxR displaces H-NS by binding downstream of the *toxT* promoter and recruits TcpP molecules via direct interaction between their cytoplasmic domains (71). Similar to the hand holding model, the catch and release model proposes that ToxR displaces H-NS from the *toxT* promoter and brings TcpP to the *toxT* promoter via direct interaction (71). However, this model suggests that ToxR-TcpP interaction disengages when ToxR binds to the *toxT* promoter allowing TcpP to bind to the proximal region of the *toxT* promoter (71). Thirdly, the membrane recruitment model posits that ToxR recruits TcpP, without direct interaction, to a region within the membrane proximal to the *toxT*

promoter to more efficiently interact with the promoter (71). Lastly, the promoter alteration model hypothesizes that ToxR does not recruit TcpP to the *toxT* promoter directly but rather that ToxR promotes TcpP interaction with the *toxT* promoter by altering the DNA architecture of the *toxT* promoter (71). To decipher the mechanism of cooperativity between TcpP and ToxR, and to gain a deeper understanding for how MLTRs function from the membrane, we measured the dynamics of single TcpP molecules within live *V. cholerae* cells to gain insights into how TcpP finds the *toxT* promoter. This work is presented in Chapter 3.

In addition to not understanding how TcpP and ToxR function from the membrane, we lack a complete understanding of how RIP of TcpP is regulated. As TcpP is essential for *toxT* transcription, we reasoned that RIP of TcpP must be inhibited *in vivo*, so we set out to gain a deeper understanding of this regulation. In Chapter 4 we demonstrate that RIP of TcpP is modulated by a dietary fatty acid, α -linolenic acid. More specifically, we demonstrate that TcpH and TcpP associate with detergent-resistant membranes in the presence of α -linolenic acid, and this event corresponds with antagonism of TcpP RIP and elevated *toxT* transcription.

Chapter 2 – Membrane-Localized Transcription Regulators within Prokaryotes

2.1 – Abstract

To adapt and proliferate bacteria must sense and respond to the ever-changing extracellular environment. One-component transcription regulators are the major tool bacteria employ to adapt their gene transcription to match their changing environment. Membrane-localized transcription regulators (MLTRs) are a family of one-component transcription regulators that respond to extracellular information and influence gene transcription from the cytoplasmic membrane. How MLTRs function to influence transcription of their target genes while localized to the cytoplasmic membrane remains an enigma. To better understand why and how MLTRs localize and function in the cytoplasmic membrane we attempted to understand the prevalence of MLTRs within the *Escherichia*, *Salmonella*, *Yersinia*, *Vibrio*, *Staphylococcus*, *Enterococcus*, and *Lactobacillus* genera. Here we show that MLTRs are highly diverse, horizontally transmissible, and highly prevalent among Gram-positive and Gram-negative bacteria. Our work demonstrates that MLTRs are more common than previously thought, and yet MLTRs remain poorly understood.

2.2 – Introduction

Signal transduction is the process whereby microorganisms regulate their cellular programs according to their extracellular environment. Microorganisms are known to transduce information from outside the cell to the cytoplasm via two-component, one-component, and anti-sigma factor signal transduction systems (88–91). Two-component signal transduction cascades are typically composed of a membrane localized receptor that transfers a phosphate, when stimulated, to a soluble response regulator resulting in

a cellular response, and anti-sigma factors are composed of a membrane localized protein that sequesters an alternative sigma factor, which is an essential component of RNA polymerase and directs it to specific promoters to stimulate transcription, is released from the cytoplasmic membrane, via proteolysis of the anti-sigma factor, under suitable conditions (Figure 2.1) (88–92). One-component signal transduction systems are composed of a single protein that directly detects a stimuli and is then able to directly influence a cellular response (Figure 2.1) (88, 89, 92). Prior studies have revealed that the vast majority of signal transduction systems in bacteria are one-component signal transduction systems (89, 93). The vast majority of one-component signal transduction systems harbor DNA-binding domains or diguanylate/diadenylyl cyclase, or phosphodiesterase, domains which synthesize or breakdown nucleotide second messengers (89, 93–95).

A majority of one-component regulators are predicted to be localized within the cytoplasm, presumably to have unimpeded access to their DNA target(s) (89). Nonetheless, there are one-component regulators that are localized to the cytoplasmic membrane, otherwise known as membrane localized transcription regulators (MLTRs) (Table A.1). Localization to cytoplasmic membrane has been shown to be critical for some MLTRs to influence transcription of their target genes (54, 96). MLTRs are counterintuitive as it would presumably inhibit, or greatly reduce, the ability of a one-component regulator to bind to its target promoter. This is thought to be the main driver that led to the evolution of two-component signal transduction systems. There is evidence of evolution of MLTRs from two-component systems. Within *Pseudomonas aeruginosa*, PilS, the membrane localized histidine kinase, and PilR, the response regulator, together regulate activity of

RpoN (97). *Neisseria gonorrhoeae* was found to encode Rsp, with the membrane localized receptor of *pilS* at its N-terminus and the *pilR* DNA binding domain at its C-terminus, and Rsp represses *pilA* transcription (98). There is clearly an evolutionary pressure for MLTRs within microorganisms, but what constitutes this evolutionary pressure is still unclear.

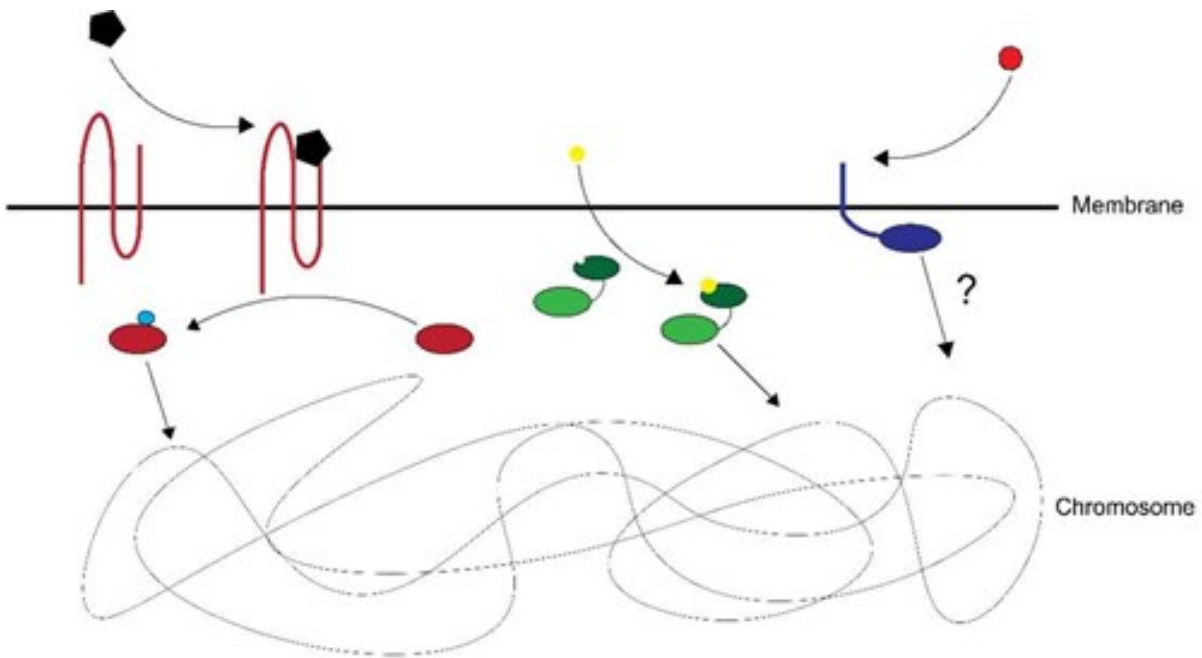


Figure 2.1: **Prokaryotic signal transduction systems.** Signal transduction is known to occur via two-component systems (on the **left**) and one-component systems (**middle** and **right**). Two-component signal transduction systems are commonly composed of a membrane localized histidine kinase that detects an extracellular signal (indicated by the black pentagon) and transfers a phosphate group (indicated by the blue circle) to a soluble response regulator which can influence gene transcription. One-component systems contain both a sensory domain and an output domain, most commonly a DNA binding domain, that influences gene transcription. Canonical one-component systems are localized in the cytoplasm where they are able to respond to a stimuli (indicated by the yellow circle) and directly diffuse to their target promoters to influence gene transcription. Membrane localized transcription regulators (MLTRs) are non-canonical one-component regulators that manage to respond to an extracellular stimuli to influence gene transcription of their target genes while maintaining their localization in the cytoplasmic membrane.

Functional MLTRs are found within prokaryotes and archaea. Due to differences in cellular physiology MLTRs require liberation from the cytoplasmic membrane within eukaryotes, due to the separation of the cytoplasmic membrane and their genomes by the nucleus. Within archaea, MLTRs have only been found to regulate motility and pilin gene transcription in response to dangerous temperatures and nutrient limiting conditions (99, 100). MLTRs are better studied within prokaryotes and have been found to regulate bile salt resistance, toxin production, antibiotic resistance, acid resistance, natural competence, pilin/fimbriae transcription, type-3 secretion systems, biofilm formation, metabolism, and have been implicated in modulation of the human immune system (Figure 2.2 and Table A.1) (52, 71, 101–114). Currently, it remains unclear why MLTRs are localized to the cytoplasmic membrane and how they function from the cytoplasmic membrane. In part, this is due to a lack of information regarding their prevalence. To gain a deeper understanding of MLTRs we utilized the MIST database to gain a better understanding of how prevalent MLTRs are within specific prokaryotic genera. Here we describe our findings and review what is currently known about identified MLTRs. In collaboration with the Jouline lab, we also performed an unbiased screen to identify MLTRs across the prokaryotic domain by screening 10,933 bacterial genomes, present in the MIST database. This ongoing work is presented in Appendix B.

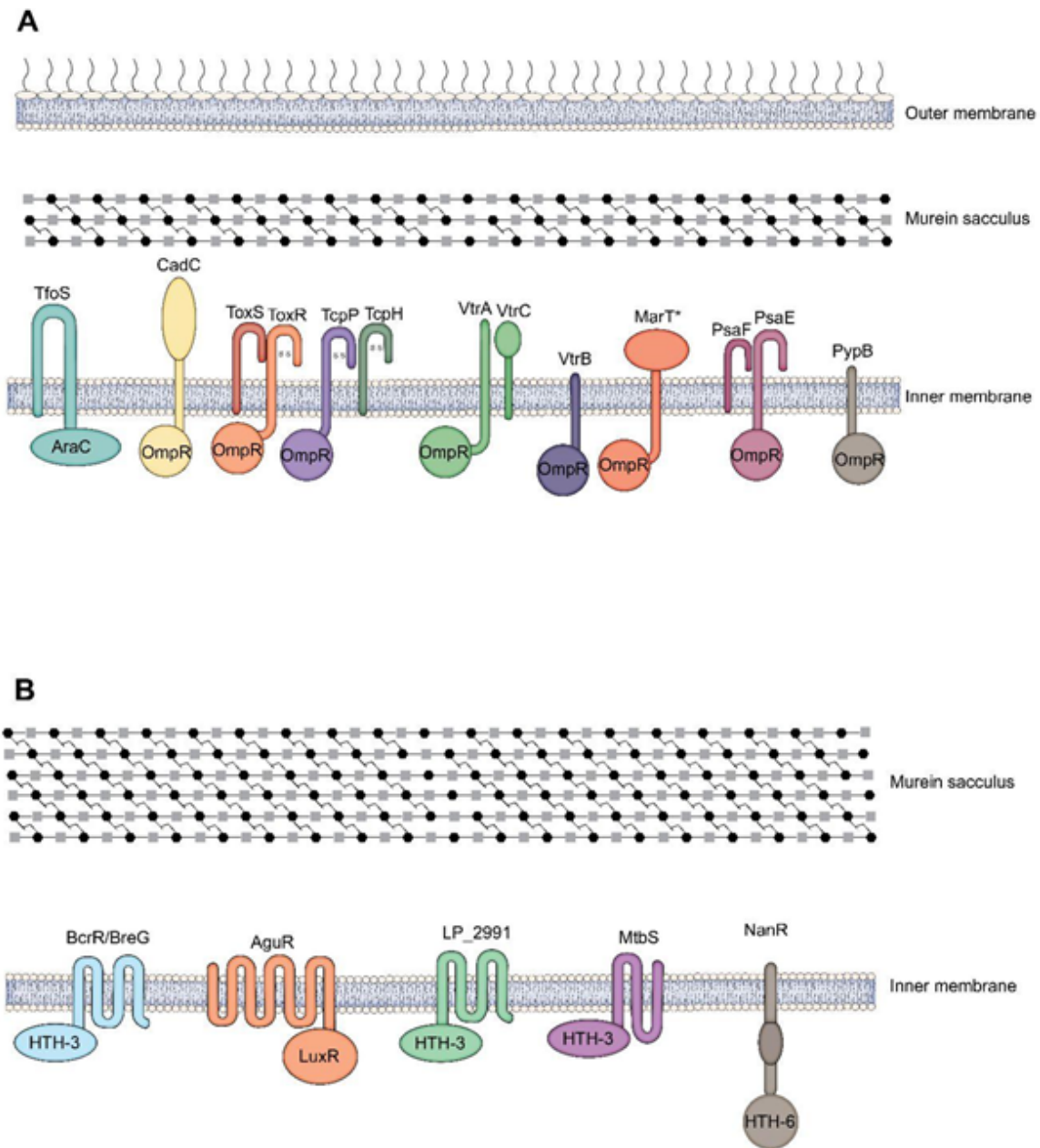


Figure 2.2: **Characterized membrane localized transcription regulators (MLTRs) within Prokaryotes.** MLTRs within Gram-negative(A) and Gram-positive (B) bacteria. DNA binding domains are localized to the cytoplasm for all MLTRs, and the DNA binding domain family for each MLTR is also indicated.

2.3 – Materials and Methods

2.3.1 – MLTR screen using the MIST database

Species from the genus *Vibrio*, *Salmonella*, *Escherichia*, *Yersinia*, *Enterococcus*, *Lactobacillus*, and *Staphylococcus* were included in our analysis. The MIST database does not contain every species within each of the aforementioned genera. As such our analysis is not a comprehensive analysis of each of the mentioned genera. Candidate membrane localized transcription regulators (MLTRs) sequences were acquired from the MIST database (115). Candidate MLTRs were selected based on the presence of a DNA binding domain and at least one transmembrane domain. Of note, the MIST database did not define ToxR, a known MLTR, as having a transmembrane domain. As such, ToxR sequences for *V. cholerae* 01 El Tor, *V. cholerae* 0395, and *V. parahaemolyticus* were acquired manually from NCBI and included in downstream analysis. Finally, MLTRs presented here likely are an underestimate of the true number of MLTRs within these bacteria. Once the candidate MLTRs were acquired the topology of the candidate MLTRs were predicted using the TMHMM server (116). Candidate MLTRs with their DNA binding domain predicted to be localized outside of the cytoplasm were dropped from our analysis. Candidate MLTRs with predicted cytoplasmic DNA binding domains were included in further analysis. See Supplemental File 2.1 for the sequences of MLTRs identified here.

2.3.2 – MLTR domain and gene neighborhood analysis

Predicted MLTRs were separated by genera and follow up phylogenetic analysis of predicted MLTRs were done using the TREND server (117). Predicted MLTRs were

aligned using the FFT-NS-2 algorithm, and phylogenetic trees were generated using the maximum likelihood method with 100 bootstrap replicates. We also interrogated the gene neighborhood using the TREND server with the same settings. Candidate TcpH and ToxS-like genes were identified by their proximity to a MLTR (i.e., overlapping reading frames or immediately upstream or downstream) and the presence of an N-terminal transmembrane domain. MLTRs that clustered with known MLTRs were considered to be related and have similar functions. BLAST was also used to confirm the degree of similarity between MLTRs (118, 119).

2.4 – Results

2.4.1 – The *Vibrio* genus

ToxR was the first identified MLTR and is an ancestral gene conserved within the *Vibrio* and *Photobacterium* genus (53, 120, 121). Members of the *Vibrio* genus are Gram-negative, rod-shaped, mesophilic, and inhabit marine and freshwater environments (122, 123). ToxR is well known for its role in regulating transcription of virulence factors and bile salt resistance in *V. cholerae* via regulation of *toxT*, *cxtAB*, *leuO*, and *ompUT* (39–41, 55, 70, 71, 104, 105, 124–129). ToxR has also been implicated in regulating virulence gene transcription in other pathogenic *Vibrio spp.* directly, via regulation of *ctxAB*, *tdh*, *vvhA*, or indirectly by promoting biofilm formation and bile resistance (126, 130, 131). However, the ToxR regulon has been shown to regulate a diverse set of phenotypes and has a clear role in non-pathogenic *Vibrio spp.* such as regulating hydrostatic pressure response (72, 120). TcpP was later identified within the *Vibrio* Pathogenicity Island 1 (VPI-1) to promote, in coordination with ToxR, *toxT* transcription, and has not been shown to

directly regulate additional genes (39, 52, 54, 55, 132). Among the 14 members of the *Vibrio* genus that were screened for MLTRs, using the MIST database, a total of 70 MLTRs were identified (Figure 2.3 and Table A.2). Of those MLTRs identified, ~23% were found to be ToxR and TcpP homologs. Given that ToxR has been suggested to be an ancestral MLTR within the *Vibrio* genus we anticipated many MLTRs bearing homology to ToxR. However, *V. campbellii*, *V. fluvialis*, and *V. proteolyticus* were found to encode two copies of ToxR (Table A.2). *V. fluvialis* is an emerging pathogen capable of causing gastrointestinal and extragastrintestinal diseases, including acute cholecystitis (133). It remains unclear if multiple copies of ToxR within *V. fluvialis*, *V. campbellii*, or *V. proteolyticus* promote bile salt resistance, but given our current knowledge of ToxR it remains possible.

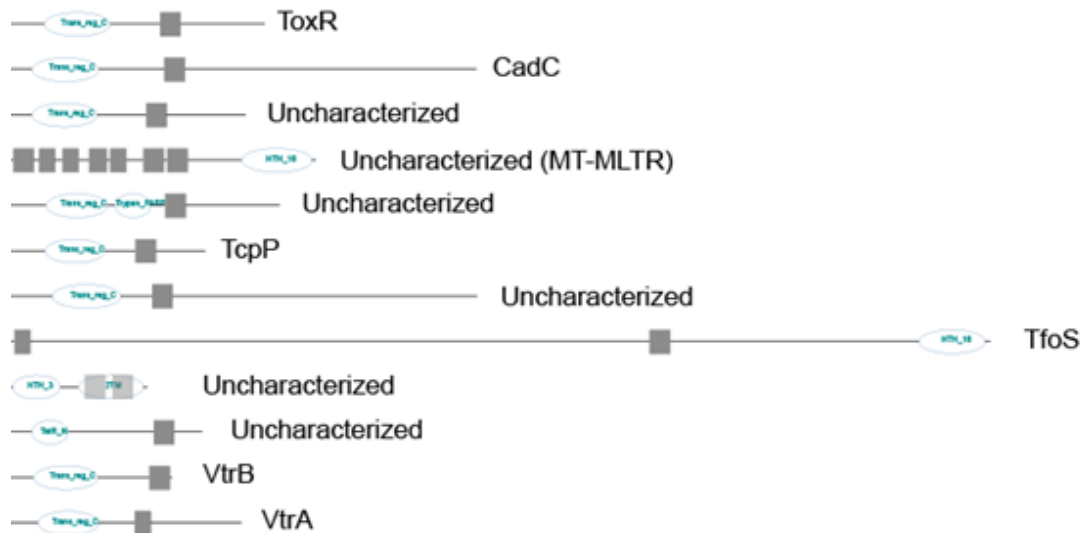


Figure 2.3: **Representative MLTRs identified within the *Vibrio* genus.** Ovals represent protein domains identified and gray squares represent transmembrane domains, see Supplemental Figure 2.1 for view of protein domains. The black line represents the total coding sequence of the MLTR. See Supplemental Figure 2.1 for complete phylogenetic information.

Similarly, *Vibrio fischeri* was found to encode two TcpP homologs (VFA0473 and VFA0860) (Table A.2). Prior work identified VFA0473 (HtbR) as a TcpP homolog and revealed that it plays a role in the symbiotic relationship between *V. fischeri* and *Euprymna scolopes*, the Hawaiian bobtail squid (134). *V. fischeri* is a bioluminescent bacterium that colonizes the light organs of *E. scolopes* to metabolize nutrients provided in exchange for luminescing at night to provide *E. scolopes* camouflage (135–137). *V. fischeri* cells are guided to the *E. scolopes* light organ by following a gradient of N-acetylated sugars where they colonize the light organ and utilize carbon provided by *E. scolopes* to proliferate (138). The symbiotic relationship between *E. scolopes* and *V. fischeri* undergoes daily cycles, growth of *V. fischeri* during the day, *V. fischeri* cells luminesce at night, and *V. fischeri* cells are shed at dawn (139–142). Upon exiting the light organ, *V. fischeri* cells upregulate numerous genes including HbtR (VFA0473) and HbtC, homologs of TcpP and TcpH, respectively (143). It was found that HbtR represses *litR*, via an unknown mechanism, resulting in an increase in motility, chemotaxis, and a reduction in synthesis of extracellular polysaccharides, thus helping *V. fischeri* cells return to a planktonic lifestyle (134). Given the low sequence homology between HbtRC and TcpPH (~26%) it is likely that both TcpPH and HbtRC were acquired by *V. cholerae* and *V. fischeri* independently (134). Within *V. cholerae*, *tcpPH* are encoded within a horizontally acquired pathogenicity island (VPI-1 that encodes the Toxin co-regulated pilus (TCP) operon (144, 145). *V. fischeri* also encodes the TCP gene cluster found within the VPI-1, but eight of the TCP genes are scattered within *V. fischeri*'s genome (146). Secondly, the TCP genes within *V. fischeri* have similar GC content to the rest of its genome and lack any flanking insertion elements that are consistent with horizontal gene

transfer (146). This suggests that the TCP genes, including *hbtRC* were not recently acquired by *V. fischeri* via horizontal gene transfer and leave the possibility that the TCP gene cluster originated within *V. fischeri* (146).

The second TcpP homolog within *V. fischeri* (VFA0860) remains uncharacterized, but a Tn seq screen designed to identify genes essential for pellicle formation in response to L-arabinose revealed that disruption of this VF_A0860 inhibits pellicle formation in *V. fischeri* (147). Pellicle formation in *V. fischeri* in the presence of L-arabinose was dependent on the cellulose polysaccharide locus (*bcs*) as well as motility (147). Deletion of VFA0860 did not inhibit motility of *V. fischeri* but did inhibit pellicle formation in the presence of L-arabinose indicating that VFA0860 may regulate genes within the *bcs* locus (147).

In addition to ToxR and TcpP, we also identified several ToxR-like MLTRs (VtrA/VtrB and VttrA/VttrB) that been identified and implicated in regulation of a type three secretion system (T3SS) within *V. parahaemolyticus* (VtrA and VtrB) and non-01/0139 *V. cholerae* (VttrA and VttrB) respectively (101, 102, 148, 149). *V. parahaemolyticus* contains two sets of gene clusters that encode type three secretion systems (T3SSI and T3SSII) and non-01/0139 *V. cholerae* also encode a T3SS (150–153). Within *V. parahaemolyticus* and non-01/0139 *V. cholerae* VtrA/VttrA promote transcription of *vtrB/vttrB* in response to bile salts, and in turn VtrB/VttrB stimulate transcription of genes within their respective T3SS (102, 154). Within *V. parahaemolyticus*, *vtrA* is co-transcribed with *vtrC*, a TcpH/ToxS like protein, and in the presence of bile salts, the periplasmic domains of VtrA and VtrC form a beta-barrel complex, bridged by a bile salt, to form a heterodimeric complex that stimulates oligomerization of VtrA and thereby

increases *vtrB* transcription (154, 155). Given the similarity between VtrA/VttrA, VttrA is also thought to function similarly with their associated Tcph/ToxS homolog.

From our MLTR search we also found a striking number (20% of MLTRs) of CadC-like MLTRs within pathogenic and non-pathogenic *Vibrio spp.* (Table A.2). *V. cholerae*, like many gastrointestinal pathogens, must survive the acidic conditions within the stomach to reach the nutrient rich gastrointestinal tract. CadC is a MLTR that regulates acid resistance in many Gram-negative organisms (*Escherichia coli*, *Salmonella enterica*, *Vibrio vulnificus*, *Vibrio cholerae*, and *Klebsiella pneumoniae*) (107, 156–163). Activity of CadC is inhibited by LysP (a lysine permease) while concentrations of lysine are low, and CadC remains inactive until extracellular pH is low (~pH 5.8) which stimulates LysP proteolysis, without altering subcellular localization, thereby activating CadC (159, 164, 165). Upon activation, CadC stimulates transcription of *cadAB*, and this results in the conversion of intracellular lysine to cadaverine which is subsequently transported out of the cell by CadB, increasing extracellular pH (107, 166).

TfoS is the only MLTR that was present in all *Vibrio spp.* analyzed here (Table A.2). TfoS is a MLTR that regulates natural competence within *Vibrio spp.* (110, 167). Natural competence is a process by which a bacterium imports exogenous DNA and incorporates the DNA into its genome via homologous recombination (168, 169). Chitin has been shown to be critical for the induction of natural competence in several *Vibrio spp.* (168–170). Chitin is one of the most abundant biopolymers in the ocean and is the major component of copepod exoskeletons, which serve as the environmental reservoir for many *Vibrio spp.* (171–175). In *V. cholerae*, TfoS directly binds chitin via its periplasmic domain, inducing dimerization of TfoS, which promotes transcription of *tfoR*

(110, 167). Once expressed, TfoR interferes with translational suppression of *tfoX* mRNA to thereby promote its translation (110). Once translated TfoX is then able to stimulate the transcription of genes required for DNA uptake (110).

Of the MLTRs identified ~28% displayed no sequence similarity to known *Vibrio* MLTRs despite the majority possessing similar structural features to ToxR/TcpP/CadC/VtrA/VtrA (i.e., cytoplasmic DNA binding domain, single transmembrane domain, and a periplasmic domain) (Table A.2). In addition, we identified a novel multi-transmembrane domain MLTR (MT-MLTR) that encodes an AraC-like helix-turn-helix domain (Table A.2). AraC-like transcription regulators have been implicated in regulating pathways for metabolism of a variety of sugars and function primarily as transcription activators (176). Currently, there are no homologs with known functions. However, based on the presence of this MT-MLTR within pathogenic and non-pathogenic *Vibrio spp.* it is likely not involved in virulence gene regulation. These data indicate that the role of the MT-MLTR is likely to regulate genes important for specific environmental conditions.

2.4.2 – The *Salmonella* and *Escherichia* Genera

Salmonella spp. are rod-shaped, Gram-negative, mesophiles, and facultative intracellular bacterium that can cause severe gastrointestinal disease (177, 178). Specific *Salmonella spp.* (such as *S. enterica serovar Typhi* and *S. enterica serovar Typhimurium*) are capable of causing typhoid fever or non-typhoidal *Salmonella* infections which collectively cause 106-123 million infections and 655,000-755,000 deaths per year (179, 180). *Escherichia spp.* are facultative anaerobic, Gram-negative, bacilli, and are natural

inhabitants of the intestines of humans and many warm-blooded animals (179, 180). Among *Escherichia spp.*, *E. coli* is the most highly associated with human disease and is capable of causing a range of gastrointestinal diseases (179). *E. coli* strains capable of causing diarrheal disease are called diarrheagenic *E. coli* (DEC) (179, 180). The DEC pathotypes are classified as enteropathogenic *E. coli* (EPEC), enterohemorrhagic (Shiga toxin-producing) *E. coli* (EHEC/STEC), enteroaggregative *E. coli* (EAEC), enterotoxigenic *E. coli* (ETEC), and enteroinvasive *E. coli* (EIEC) (179). To respond to acidic conditions of the gastrointestinal tract and to promote colonization, *S. enterica* and *E. coli* both encode characterized CadC and MarT-like MLTRs (107, 165, 181–186). To determine if additional MLTRs are present within members of the *Enterobacteriaceae* family, we screened for MLTRs within the available genomes within the genus of *Salmonella* and *Escherichia* within the MIST database. Across 8 species, we identified a total of 35 MLTRs with only 13 MLTRs homologous to CadC or MarT. The remaining MLTRs were either uncharacterized (~46%) or were VtrB homologs (17%) (Figure 2.4 and Table A.3). Below is a summary of the current knowledge of MarT-like MLTRs within *Salmonella* and *Escherichia spp.* followed by a summary of our findings of the additional MLTRs within members of the *Enterobacteriaceae*.

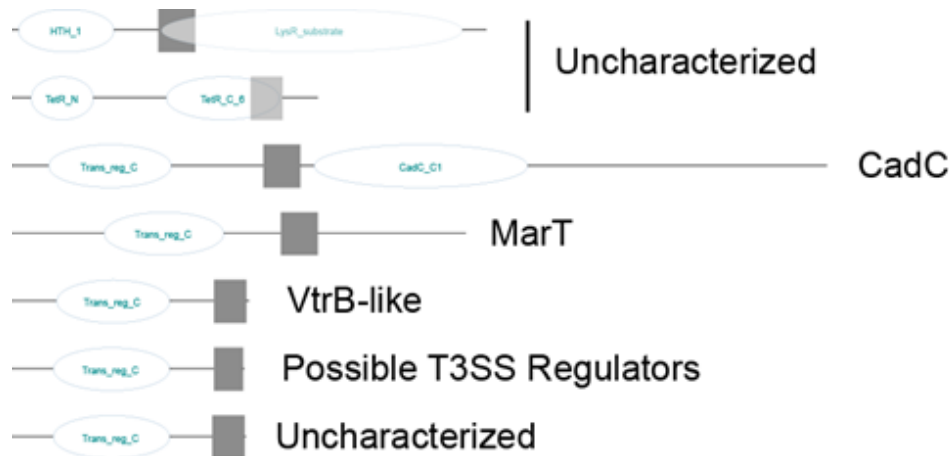


Figure 2.4: **Representative MLTRs identified within the *Escherichia* and *Salmonella* genera.** Ovals represent protein domains identified and grey squares represent transmembrane domains. The black line represents the total coding sequence of the MLTR. See Supplemental Figure 2.2 for complete phylogenetic tree with phylogenetic information and clear view of protein domain names.

Salmonella enterica serovar *Typhimurium* encodes three pathogenicity islands (Salmonella pathogenicity island 1-3 (SPI-1, SPI-2, SPI-3)) that contribute to its pathogenesis (187–190). SPI-1 and SPI-2 encode type III secretion systems (T3SS) that promote host cell invasion, promote systemic infection, support replication within macrophages, and induce programmed cell death of macrophages (189, 191–193). SPI-3 does not encode a T3SS, but it has also been shown to contribute to *Salmonella* pathogenesis by promoting fibronectin binding, which is critical for the formation of host extracellular matrix (i.e., clot formation) (182, 190). A gene encoded within SPI-3, *misL*, is thought to assist gastrointestinal colonization by increasing binding to fibronectin which is at high concentrations at sites where intestinal damage/erosion has occurred (182, 194). Binding to fibronectin could thereby promote colonization of *Salmonella spp.* at sites of active infection/inflammation (182, 194). Secondly, during inflammation epithelial cells

are known to increase fibronectin secretion, and this is also correlated with enhanced *Salmonella* invasion (194). It was previously shown that MisL, encoded within SPI-3, is an outer membrane protein that directly binds to fibronectin (182, 194). Furthermore, it was found that MarT, a MLTR, positively regulates MisL by H-NS antagonism (181). In addition, MarT was also found to function as a general regulator of biofilm formation via an unknown mechanism (183).

Within *E. coli*, GrvA (the Global Regulator of Virulence protein A) and Yqel are MLTRs with homology to MarT and are also important for gastrointestinal colonization of *E. coli* pathotypes (184, 186). EHEC also utilizes a T3SS, encoded with in the locus of enterocyte effacement (LEE), to manipulate host cells to promote proliferation, and also a second, often incomplete, T3SS encoded with in an additional pathogenicity island designated ETT2 (for *E. coli* type III secretion system 2) (195–200). While typically non-functional, ETT2 still contributes to the pathogenesis of several *E. coli* pathotypes (avian pathogenic *E. coli* (APEC), uropathogenic *E. coli* (UPEC), and EHEC). Within APEC and UPEC ETT2 was shown to be critical for motility, serum resistance, and cell adhesion (186, 199, 201, 202).

GrvA indirectly promotes transcription of LEE in response to bicarbonate (184, 203). Transcription of the LEE operon is stimulated by Ler, and during low pH the glutamate-dependent acid resistance system represses *ler* transcription via GadE (184, 204–206). *ler* remains repressed until GrvA represses *gadE* transcription, in response to high concentrations of bicarbonate, and thereby promotes *ler* transcription (184, 203). Given that bicarbonate levels are highest at the surface of epithelial cells, GrvA likely

represses *gadE*, thereby stimulating *ler* transcription, at the surface of epithelial cells, which is also the primary site of EHEC infection (203).

Yqel is encoded within the ETT2 pathogenicity island and is widely distributed among pathogenic and non-pathogenic *E. coli* (186, 195–199). YeqI appears to differentially regulate many genes (>580) involved in many biological pathways (such as motility, adhesion, and environmental signal transduction) in Avian pathogenic *E. coli* (APEC) (186). As such, YeqI was shown to be critical for systemic infection of APEC in chickens (186). This is likely due to a combination of reduced adhesion to DF-1 chicken fibroblast cells, reduced flagella synthesis, and reduced resistance to serum (186). Currently, it is unclear if YeqI is regulated by environmental signals like other MLTRs (such as ToxR and TcpP). However, downstream of Yqel is a single pass transmembrane protein, *yqeJ* (EC3705), whose reading frame overlaps with Yqel. Both TcpP and ToxR have associated single pass transmembrane proteins (TcpH and ToxS respectively) that function to increase stability and reduce degradation of their associated membrane-localized transcription activators (MLTRs) (83, 96, 207). The function of *yqeJ* remains unknown but given its association with a MLTR and domain topology it likely functions to protect or stabilize Yqel and reduce its proteolysis. Furthermore, it was recently shown that Nac (nitrogen assimilation control) transcription regulator stimulates transcription of *yqeJ* (185). Nac is known to play an important role in acid resistance in *E. coli* species (208). Taken together, it is possible that transcription of *yqeJ* during acidic conditions promotes Yqel function, possibly via inhibition of proteolysis.

There were several VtrB-like MLTRs within *Salmonella spp.* (Table A.3). VtrB and VtrB are MLTRs that are known to positively regulate transcription of T3SS within *Vibrio*

spp. (101, 102, 148, 149). *Salmonella enterica serovar Typhimurium* utilizes two T3SS within SPI-1 and SPI-2 (189, 191–193). However, these VtrB-like homologs have not been shown to regulate T3SS within *Salmonella*. They are encoded either upstream or downstream of chaperone-usher type 1 fimbriae genes which members of the chaperone-usher fimbriae family which are adhesive organelles that are highly diverse among *Escherichia* and *Salmonella spp.* (Table A.3) (209). Thus, it is possible that these uncharacterized MLTRs regulate fimbriae gene transcription contributing to pathogenesis or adhesion of *Salmonella* cells to surfaces. None of the VtrB or uncharacterized MLTRs were found to be encoded upstream or downstream of any potential *tcpH/toxS*-like genes (Table A.3). This suggests that these MLTRs may not be regulated by proteolysis, or do not require an accessory protein to inhibit proteolysis like TcpP and ToxR.

A majority of MLTRs identified within *Salmonella* and *Escherichia spp.* are uncharacterized. RS07670, RS12930, and RS11315 are homologs to STM1575 which was found to influence motility within *Salmonella enterica serotype typhimurium* (210, 211). These MLTRs are TetR type regulators which have an N-terminal DNA binding domain along with a C-terminal domain that typically binds to a ligand (212, 213). The TetR family of transcription regulators are known to regulate efflux pumps that promote antibiotic resistance they also bind to a diverse set of ligands (such as heme, biotin, amino acids, fatty acids, uracil, citric acid, nicotinic acid, etc.) (212, 213). Currently, it is unclear if RS07670, RS12930, and RS11315 do regulate motility or if they bind to any ligand. However, as RS07670, RS12930, and RS11315 are TetR regulators, the localization of their C-termini to the cytoplasmic membrane suggests that they interact with a hydrophobic ligand.

Secondly, a separate clade of MLTRs, RS00160, STM0031, RS01180, RS20780, and RS19320, was found to have homology to STM14_0039 which has been implicated as possible T3SS regulator upon computational analysis (214). STM0031 was found to be important for bovine enteric infection in *Salmonella* (215). This further suggests that these potential MLTRs contribute to *Salmonella* virulence and suggests that it is via regulation of T3SS.

2.4.3 – The *Yersinia* Genus

Yersinia spp. are Gram-negative, bacilli shaped, facultative, and non-spore forming bacteria (216). *Yersinia spp.* are known to be the etiological agent of the bubonic plague (i.e., *Yersinia pestis*) and can also cause self-limiting gastrointestinal disease (i.e., *Yersinia enterocolitica*) (216). In addition, *Yersinia ruckeri* is a zoonotic pathogen that primarily infects fish and is the cause of enteric red mouth disease in salmon species (217–219). Within the *Yersinia* genus there have only been two MLTRs identified PsaE and PypB which have been shown to regulate fimbriae and a type IVb pilin respectively (220–225). Our analysis revealed a total of 14 MLTRs within *Y. pestis*, *Y. enterocolitica*, and *Y. ruckeri* with ~36% of the identified MLTRs bearing similarity to PsaE or PypB (Figure 2.5 and Table A.4).

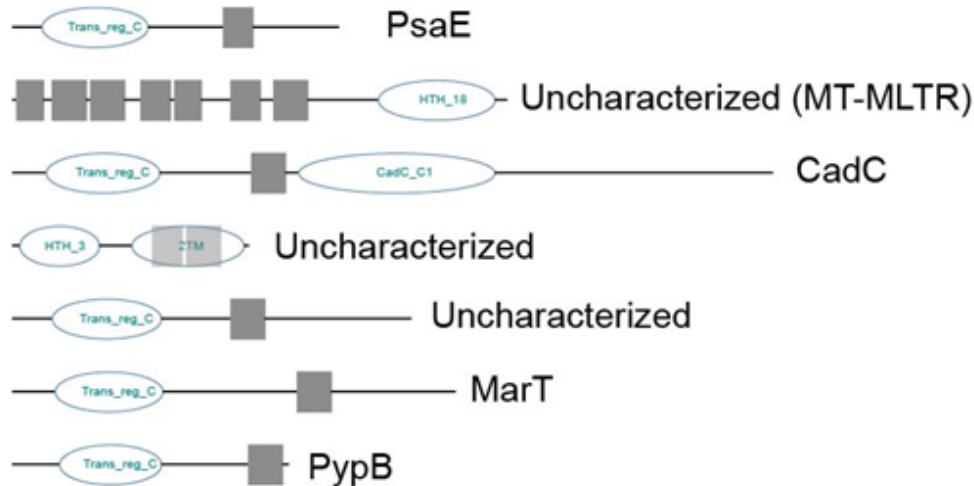


Figure 2.5: **Representative MLTRs identified within the *Yersinia* genus.** Ovals represent protein domains identified and grey squares represent transmembrane domains. The black line represents the total coding sequence of the MLTR. See Supplemental Figure 2.3 for complete phylogenetic tree with phylogenetic information and for a clear view of protein domain names.

Within *Y. pestis*, the *psa* locus encodes genes that are critical for the pathogenesis of *Y. pestis* (226). PsaA, the major subunit of the fimbriae, is positively regulated by high temperature as well as acidic pH, and has been shown to promote host cell adherence and inhibit phagocytosis (222, 225, 227–229). *psaA* is regulated directly by PsaE and indirectly by PsaF (222, 230). PsaE is a MLTR, similar to ToxR and TcpP, and functions to stimulate *psaA* transcription from the cytoplasmic membrane (222, 224). PsaF is important for stability of PsaE and may also enhance the ability of PsaE to stimulate PsaA transcription (221, 230). Levels of both PsaE and PsaF are regulated by temperature and pH. *psaE* mRNA encodes an RNA thermometer within its 5' untranslated region (UTR) which at high temperature (such as 37°C) stabilizes (230). Translation of *psaF* mRNA also requires high temperature but is independent of the *psaE* 5' UTR (221). The exact mechanism of temperature regulation of *psaF* translation remains unclear (221). Similar

to ToxR and TcpP, pH post-translationally regulates levels of PsaE and PsaF (230). Recently, PsaF was shown to sense pH via histidine residues within its periplasmic domain which in turn modulate its ability to protect PsaE from degradation (221). The precise mechanism by which pH influences PsaF function is not known, but it is thought that pH influences the overall structure of PsaF via its periplasmic histidine residues (230).

Similar to other enteric pathogens *Y. enterocolitica* must adhere to host cells to cause disease. *Y. enterocolitica* relies on Myf, a fimbriae similar to CS3 within enterotoxigenic *E. coli* (231, 232). MyfA, the major Myf subunit, is a homolog of PsaA, and is also positively regulated by high temperature and low pH (231). Similar to *psaA*, *myfA* also appears to be regulated by a MLTR and its associated protein, MyfEF (233). MyfE and MyfF appear to be homologs of PsaE and PsaF respectively. As anticipated, we identified both PsaE (YPO_1301) and MyfE (YE1450) within *Y. pestis* and *Y. enterocolitica* (Table A.4).

Y. ruckeri is not known to encode pili similar to PsaA or MyfA. However, genome analysis of *Y. ruckeri* revealed that it encodes a fimbriae gene cluster (the *stf* operon) that is associated with differences in host range and virulence within *S. typhimurium* (234, 235). Upstream of the *stf* operon within *Y. ruckeri* is a MLTR (RS16705) that is a homolog of MarT (Table A.4). Currently, it is unclear if RS16705 regulates the *stf* operon in *Y. ruckeri* but given its proximity to the *stf* operon it remains a possibility.

In addition, several CadC-like MLTRs were identified within *Y. pestis*, *Y. enterocolitica* and *Y. ruckeri* (Table A.4). Of note, RS06955, YPO0804, and YPO0804 are not located upstream or downstream of *cadAB*, which are known to be associated with

cadC. To the best of our knowledge, CadC-like MLTRs have not been characterized within *Yersinia spp.*, but based on homology we anticipate that CadC coordinates acid resistance within *Yersinia spp.*

Early studies on virulence within *Y. pestis* and *Y. enterocolitica* led to the discovery of a large virulence plasmid that encoded a T3SS (the Ysc system) that was critical to virulence of *Y. pestis* and *Y. enterocolitica* (236). Highly virulent strains of *Y. enterocolitica* biovar 1B were found to encode a second chromosomally encoded T3SS (Ysa) that contributed to its virulence that is similar to the T3SS found within the SPI-1 within *Salmonella spp.* (236–238). Genomic analysis of *Y. ruckeri* revealed that it also encodes the *ysa* system, and within the *ysa* system a MLTR (RS13670), bearing homology to PypB, is encoded (239). RS13670 shares sequence similarity to PypB which is a MLTR that has not been reported to regulate genes within the *ysa* locus (220). PypB (YE3623) is a MLTR that stimulates transcription of the *tad* (tight adherence) operon within *Y. enterocolitica* that encodes a Flp type IVb pillin which have been shown to promote microcolony formation, potent biofilms, and to possess promiscuous binding specificity for surfaces (220). *Y. ruckeri* encodes a second homolog of PypB (RS07490) that is encoded upstream of the *tad* operon in *Y. ruckeri*. In addition to homologs of known MLTRs, we also identified several uncharacterized MLTRs with striking similarity to VtrB/PypB but lack sufficient sequence similarity to any characterized transcription factors (Table A.4). Perhaps the most interesting of the uncharacterized MLTRs is YE0935 (an AraC MT-MLTR) which is also found within the *Vibrio* genus. The role of this MT-MLTR remains obscure.

2.4.4 – The *Enterococcus* and *Lactobacillus* genera

Lactic acid bacteria (LAB) are strictly fermentative, aerotolerant, acid tolerant, organotrophs that produce lactic acid as a major metabolic byproduct of glucose (240, 241). LAB utilize a large array of carbohydrates to gain energy which results in the production of lactic acid, in addition to other byproducts (240, 241). Members of the *Enterococcus* and *Lactobacillus* genera are LAB. *Enterococci* are mesophilic non-spore forming Gram-positive ovoid shaped bacterium that grow in pairs or associate in chains (240). *Enterococci* cells are also resistant to desiccation and facultative anaerobes (240). *Lactobacilli* are Gram-positive fermentative anaerobic non-spore forming bacteria that have complex nutritional requirements (240). Members of the *Lactobacilli* and *Enterococci* genera are known to colonize the human gastrointestinal tract and are capable of causing severe disease (240). Only a handful of MLTRs have been identified and characterized within *Enterococci* and *Lactobacilli* spp. (such as BcrR, BreG, and AguR (106, 242, 243). Using the MIST database, we identified 171 potential MLTRs within *Enterococci* and *Lactobacilli* spp. (105 MLTRs and 66 MLTRs respectively) (Figure 2.6, Table A.5, and Table A.6). Surprisingly, BcrR, BreG, and AguR made up only ~16% of identified MLTRs within *Enterococci* spp. and *Lactobacilli* spp. (Table A.5 and Table A.6). Homologs of previously identified MLTRs were found within *Enterococci* and *Lactobacilli* (i.e., MtbS, MmsR, LP_2991 and HcrR) encompassing ~14.6% of identified MLTRs (Table A.5 and Table A.6). The majority of MLTRs identified within *Enterococci* and *Lactobacilli* are uncharacterized (~68%) (Table A.5 and Table A.6). Below is a summary of the current literature surrounding characterized MLTRs within *Enterococci* and *Lactobacilli* along with a summary of our findings regarding the uncharacterized MLTRs.

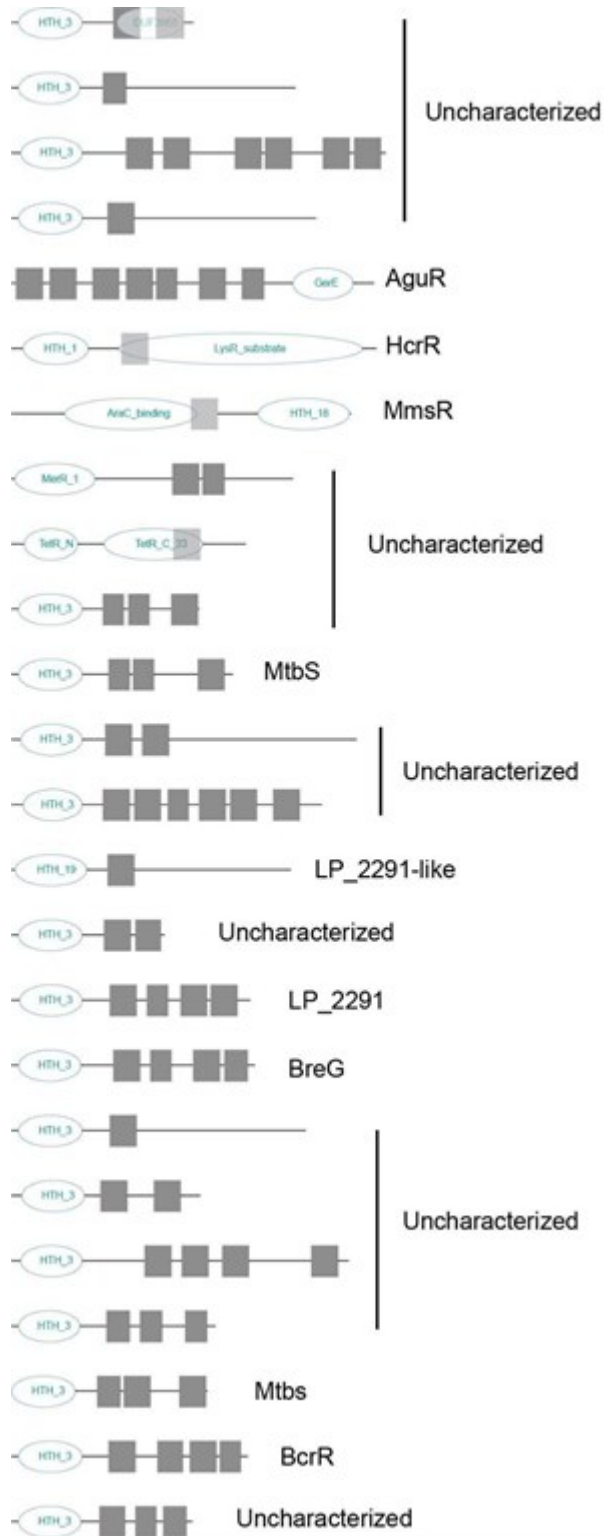


Figure 2.6: **Representative MLTRs identified within the *Enterococcus* and *Lactobacillus* genera.** Ovals represent protein domains identified and grey squares represent transmembrane domains. The black line represents the total coding

Figure 2.6 (cont'd)

sequence of the MLTR. See Supplemental Figure 2.4 for complete phylogenetic tree and for a clear view of protein domain names.

Enterococcus faecalis is a human pathogen commonly associated with nosocomial infections and is commonly found to be resistant to multiple antibiotics, such as vancomycin (244). Bacitracin is a common topical antimicrobial, and it is also used to treat vancomycin resistant *E. faecalis* (245). Bacitracin resistance in *E. faecalis* and *Clostridium perfringens* is regulated by BcrR a MLTR (106, 246). BcrR stimulates transcription of the *bcrABD* operon upon binding to bacitracin and requires membrane localization to function (106, 247, 248). *bcrA* and *bcrB* encode the ATP-binding domain and the membrane spanning domain of the bacitracin ABC transporter (249). It has been shown that the *bcrABD*, *bcrR*, and other genes involved in antibiotic resistance are transmitted between *Enterococcus spp.* via pheromone responsive conjugative plasmids(250–252). Our analysis indicates that BcrR is also present in *Lactobacillus spp.* (Table A.5 and Table A.6).

Similar to BcrR, BreG is a multi-transmembrane domain MLTR that also regulates synthesis of an antibacterial compound and is also encoded within a plasmid (242, 253). LAB are known to use bacteriocins (antibacterial polypeptides) to compete for carbohydrates by inhibiting growth of competing bacteria (242, 254, 255). *Lactobacillus brevis* is a plant-associated LAB that produces two bacteriocins (174A- β and 174A- γ) (242). Synthesis of 174A- β and 174A- γ in *L. brevis* is catalyzed by *breBC* which are encoded within a large plasmid (242, 253). *breBC* are upregulated by BreG, an MLTR with four C-terminal transmembrane domains (242, 253). However, it remains unclear what stimulates BreG activity and BreG transcription in *L. brevis*.

A common feature among LAB is their ability to tolerate acidic conditions, which is necessary given the nature of their metabolism (240). One method of acid resistance employed by *Enterococci* and *Lactobacilli* is the agmatine deiminase system. Within this system, agmatine is imported into the cell via AguD, an agmatine-putrescine antiporter, and agmatine is then broken down into putrescine and carbamoyl phosphate by AguAB, and finally AguC removes a phosphate from carbamoyl phosphate generating ATP, CO₂, and NH₃ (256, 257). AguR stimulates transcription of *aguBDAC* in response to agmatine within *Enterococcus faecalis* (243). Within *Lactococcus lactis* and *Streptococcus mutans* AguR stimulates *aguBDAC* transcription in response to both agmatine and low pH (257–259). The current literature suggests that within *S. mutans*, AguR and AguD function similar to CadC and LysP, where AguR and AguD interact in the absence of agmatine inhibiting transcription of the *aguBDAC* gene cluster (257). Micro-array data indicate that the AguR regulon is much larger than previously anticipated. Deletion of *aguR* resulted in downregulation of 49 genes and upregulation of 41 genes indicating that AguR may have additional regulatory functions (260).

Lactobacilli are known constituents of the human gastrointestinal tract and have been shown to have immunomodulatory roles. *L. plantarum* is a well-studied immunomodulatory *Lactobacilli* that has been used as a probiotic to treat irritable bowel disease, inflammatory bowel disease, and with some success treating allergies (261–265). *L. plantarum* has been shown to promote expansion of regulatory dendritic cells, promote transcription of anti-inflammatory cytokine IL-10, and promote the expansion of regulatory T-cells (266–270). Characterization of genes important for *L. plantarum* immunomodulatory effects revealed that the LamBDCA quorum sensing system,

plantaricin (i.e., bacteriocin) synthesis and its transport, a transcription regulator Ip_2291, and the N-acetyl-glucosamine/galactosamine phosphotransferase system are critical for *L. plantarum*'s immunomodulatory effects (114, 267). A prior study identified Ip_2291 (an MLTR) as a gene involved in modulating pro-inflammatory cytokine production in dendritic cells (114). It was found that Ip_2291 represses *gctA3*, a putative teichoic acid and lipoteichoic acid glycosylation enzyme (114). Modification of lipoteichoic acid (LTA), such as with D-alanyl, has been shown to have effects on cytokine production, and lack of modification of LTA with D-alanyl increases IL-10 secretion (271). These data indicate that Ip_2291 reduces inflammation by repressing *gctA3* thereby reducing the pro-inflammatory nature of its LTA. Currently it is unclear what influences Ip_2291 to repress or derepress *gctA3* transcription.

Our analysis revealed that some *Enterococcus* and *Lactobacillus spp.* encode MtbS homologs (Table A.5 and Table A.6). MtbS is an MLTR recently identified in *Staphylococcus aureus* that has a cryptic role as it promotes soft tissue infection but inhibits skin infection (272). Given that MtbS is not conserved among *Enterococcus* and *Lactobacillus spp.*, this suggests that MtbS was acquired individually by these bacteria, likely by horizontal gene transfer. Of note, *Enterococcus phoeniculicola* was found to encode four MtbS homologs (Table A.5). *E. phoeniculicola* was isolated from the uropygial gland (preen gland) of the Red-billed Wood hoopoe, *Phoeniculus purpureus*, which secretes oils that protect it from bacterial pathogens and predators (273–276). The preen gland is primarily used for maintenance of feathers, waterproofing, and secreting predator deterring odors (274, 277, 278). Antibiotic treatment altered the secretions from the preen gland indicating that bacteria within the preen gland modified the secreted oils

which inhibited bacterial growth (273). *E. pheniculicola* is implicated in modifying the preen gland secretions (273). In addition to the four MtbS-like MLTRs, *E. pheniculicola* has an additional eight MLTRs within its genome (Table A.5). The role of these MLTRs remains unclear. However, given that the preen gland is known to secrete hydrophobic chemicals (i.e., mono and diester waxes, squalene, and alcohols) it is possible that MLTRs are uniquely positioned to sense and respond to the presence of these hydrophobic compounds (277, 278).

Two unique *Lactobacilli* MLTRs, RS06015 and RS09530, were found to be homologs of HcrR and MmsR respectively (Table A.6). HcrR is known to positively regulate *hcrAB* which catalyze the metabolism of hydroxycinnamic acids which are abundant in plants and are utilized by *L. planetarium* (111, 279). MmsR is a regulator of isobutyryl-CoA metabolism in *Pseudomonas aeruginosa* and *Pseudomonas putida* (112). Metabolism of isobutyryl-CoA occurs via methylmalonate semialdehyde dehydrogenase (MmsA) RS09530 and 3-hydroxyisobutyrate dehydrogenase (MmsB) producing propionyl-CoA and CO₂ (112). *mmsA* and *mmsB* are encoded downstream of MmsR, an AraC-type family of regulator, which stimulates transcription of *mmsAB* but the conditions that promote MmsR function are unknown (112).

Both *Enterococci* and *Lactobacilli spp.* were found to encode MLTRs that are associated with plasmids (Table A.5 and Table A.6). LMIV_p072 and HA1_16002 are predicted MLTRs that have been shown to be encoded within plasmids pLMIV and pF262C respectively (280–282). pLMIV is a *Listeria*-associated plasmid and pF262C is associated with *Clostridium perfringens* (280–282). pLMIV has also been incorporated into the genome of pathogenic *Listeria* within hypervariable hotspot 9 (282). However,

neither pLMIV nor pF262C have been shown to have a clear role in virulence for *Listeria spp.* or *Clostridium perfringens*. Thus, it is possible that these plasmid-associated MLTRs may have a role in promoting environmental persistence or proliferation.

2.4.5 – The *Staphylococcus* genus

Staphylococcus spp. are Gram-positive, non-motile, non-spore forming, catalase-positive, cocci, and are facultative anaerobic (283). *Staphylococcus spp.* are natural commensal members of human skin, skin glands, and mucous membranes of humans, other mammals, and birds (283). *Staphylococcus aureus* is a highly studied member of the *Staphylococcus* genus as it is an opportunistic pathogen commonly associated with skin infection, sepsis, endocarditis, osteomyelitis, and necrotizing fasciitis in humans (113). *S. aureus* employs a large number of virulence factors and regulatory proteins to cause disease (see review for more information: (284)). Recently, an MLTR, MbtS, was shown in *S. aureus* to contribute to its pathogenesis via an unknown mechanism (285). In addition, MbtS was also found to be sensitive to degradation by a membrane bound metalloprotease (FtsH) (285). FtsH degrades cytoplasmic membrane proteins that are denatured or loosely folded and is critical for survival of *S. aureus* cells undergoing cellular stress (286, 287). FtsH has been shown to be critical for virulence of *S. aureus* (288). However, FtsH does not directly regulate transcription of virulence factors. Complementation of $\Delta ftsH$ with *mbtS* does not restore virulence of *S. aureus* in a sepsis model or systemic infection (285). Thus, MbtS likely requires FtsH to be liberated from the cytoplasmic membrane to complete its regulatory duties. MbtS also likely functions as a transcription activator and repressor. Loss of *mbtS* lead to a decrease in transcription of 9 genes (such as phosphate transport genes, glycine dehydrogenase,

aminomethyltransferase, and several tRNAs) and an increase in transcription of 8 genes (such as Staphopain A, serine proteases SplA-F, and glycyl-tRNA synthase genes) (285). MbtS potentially regulates many more genes (<200), but to a much lower degree (i.e., 1.4-fold difference) (285). MbtS was found to autoregulate, and this is dependent on FtsH (285). Currently, it is unknown if MbtS recognizes any host or environmental factors to influence its transcription regulation activity. MbtS does not have any known associated protein, like ToxS, TcpH, or PsaF, to inhibit its proteolysis. MbtS is a unique MLTR as it contains three transmembrane domains and virtually no extracellular domain. Given that FtsH is needed for complete MtbS activity, it is possible that MtbS is activated via proteolysis by FtsH and that the biophysical properties of the cytoplasmic membrane affect MtbS sensitivity to FtsH. A second MLTR, NanR, has also been described within *S. aureus* and was found to regulate sialic acid (N-acetylneuraminic acid) metabolism by repressing *nanERKAT* until it binds sialic acid (113).

Upon screening for MLTRs within the Staphylococcus genus we found that only ~23% of all MLTRs identified were homologs of MtbS or NanR (Figure 2.7 and Table A.7). Many of the uncharacterized MLTRs have no associated TcpH/ToxS like genes (Table A.7). RS01135, RS03175, and RS07860 were found to be associated with CAAX Proteases and Bacteriocin-Processing (CPBP) metalloproteases (Table A.7). CPBP metalloproteases are spread throughout all domains of life and thought to be involved in bacteriocin maturation (289). CPBP metalloproteases cleave C-terminal tripeptide 'AAX' from target proteins (290). It is thought that CPBP metalloproteases promote secretion of bacteriocins or possibly degrade bacteriocins (289). Several CPBP metalloproteases were found within bacteriocin operons and have been shown to confer immunity to

bacteriocins in *L. planetarium* and *L. lactobacillus* (291–293). Currently, there is no data to suggest that RS01135, RS03175, and RS07860 are involved in regulating bacteriocin biosynthesis.

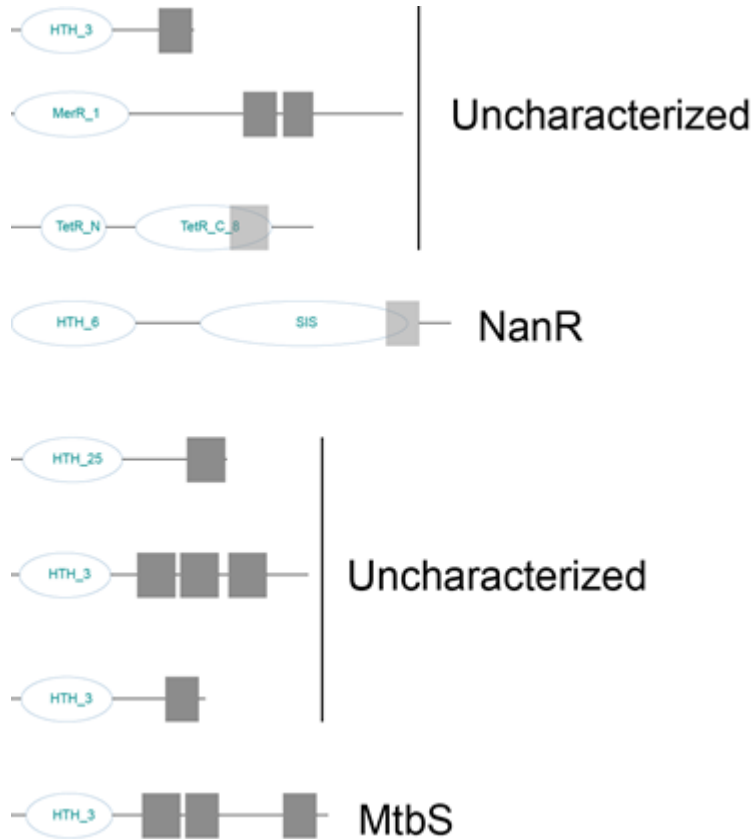


Figure 2.7: **Representative *Staphylococcus* MLTRs identified.** Ovals represent protein domains identified and grey squares represent transmembrane domains. The black line represents the total coding sequence of the MLTR. See Supplemental Figure 2.5 for complete phylogenetic tree with phylogenetic information and for a clear view of protein domain names.

2.5 – Discussion

Here we investigated the prevalence of MLTRs and reviewed the current knowledge of MLTRs within Prokaryotes. We focused our analysis on species closely related to bacteria with previously characterized MLTRs. We found that MLTRs are widespread among Gram-negative and Gram-positive bacteria and that their domain structure is highly diverse. Our analysis revealed that MLTRs within Gram-negatives are more likely to be associated with TcpH- and ToxS-like proteins than MLTRs within Gram-positive bacteria. Surprisingly, Gram-positives appear to be enriched for MLTRs with multiple transmembrane domains. It is currently unclear as to why MLTRs within Gram-positive bacteria are more likely to have multiple transmembrane domains. From our work, and prior work, it is clear that MLTRs can be acquired from horizontal gene transfer, with many MLTRs within Gram-positives associating with plasmids. MLTRs do not appear to have a common regulon. A survey of the literature indicates that MLTRs can influence metabolism, motility, biofilm formation, antibiotic resistance, acid resistance, natural competence, and the human inflammatory response (52, 71, 101–114). Nonetheless, from the work presented here MLTRs within Gram-positive and Gram-negative bacteria are clearly associated with regulating pilin, fimbriae, or T3SS. It remains unclear if this association is due to the fact that pathogenic bacteria are studied more intensely than environmental bacteria, or if this is a trend that is common among all bacteria. Further work is required to understand this.

A major remaining question regarding MLTRs is: why are they localized to the cytoplasmic membrane? Several possibilities exist such as, MLTRs respond to a hydrophobic ligand, their ligand cannot penetrate the cytoplasmic membrane, a

membrane-localized cofactor is required for activity, and MLTRs respond to the cytoplasmic membrane itself (i.e., membrane fluidity, lipid domains, or specific phospholipids influence activity). From our targeted analysis it is clear that the vast majority of MLTRs are uncharacterized and underscores the lack of knowledge we have regarding MLTRs. This work demonstrates the diversity of domain architecture among MLTRs and also reveals distinct differences among MLTR structure within Gram-negative and Gram-positive bacteria.

Chapter 3 – Independent Promoter Recognition by TcpP Precedes Cooperative
Promoter Activation by TcpP and ToxR

3.1 – Preface

Contents of this chapter were published in the journal mBio in 2021 (Citation: Calkins AL, Demey LM, Karlake JD, Donarski ED, Biteen JS, DiRita VJ. Independent Promoter Recognition by TcpP Precedes Cooperative Promoter Activation by TcpP and ToxR. mBio. 2021 Oct 26;12(5):e0221321. doi: 10.1128/mBio.02213-21. Epub 2021 Sep 7. PMID: 34488449.). Per American Society for Microbiology guidelines “An ASM author also retains the right to reuse the full article in his/her dissertation or thesis.”.

3.2 – Abstract

Cholera is a diarrheal disease caused by the Gram-negative bacterium *Vibrio cholerae*. To reach the surface of intestinal epithelial cells, proliferate, and cause disease, *V. cholerae* tightly regulates the production of virulence factors such as cholera toxin (*ctxAB*) and the toxin co-regulated pilus (*tcpA-F*). ToxT is directly responsible for regulating these major virulence factors while TcpP and ToxR indirectly regulate virulence factor production by stimulating *toxT* transcription. TcpP and ToxR are membrane-localized transcription regulators (MLTRs) required to activate *toxT* transcription. To gain a deeper understanding of how MLTRs identify promoter DNA while in the membrane, we tracked the dynamics of single TcpP-PAMCherry molecules in live cells using photoactivated localization microscopy and identified heterogeneous diffusion patterns. Our results provide evidence that: 1) TcpP exists in three biophysical states (fast diffusion, intermediate diffusion, and slow diffusion); 2) TcpP transitions between these different diffusion states; 3) TcpP molecules in the slow diffusion state are interacting with the *toxT* promoter; and 4) ToxR is not essential for TcpP to localize the *toxT* promoter. These data

refine the current model of cooperativity between TcpP and ToxR in stimulating *toxT* transcription and demonstrate that TcpP locates the *toxT* promoter independent of ToxR.

3.3 – Introduction

The Gram-negative bacterium *Vibrio cholerae* infects millions of people each year, causing the diarrheal disease cholera resulting in ~100,000 deaths annually (294, 295), despite treatments available to combat infection, including vaccines, antibiotic therapy, and oral rehydration therapy (7–9, 296–300). With changing climate and growing cases of antibiotic resistant *V. cholerae*, the number of annual cholera infections is projected to continue to increase (15). Thus, gaining deeper insight into the pathogenesis of *V. cholerae* will facilitate development of alternative methods of treatment, thereby reducing the global burden of cholera.

Upon ingestion, typically from contaminated water or food, *V. cholerae* colonizes the crypts of the villi in the distal portion of the small intestine and stimulates production of virulence factors essential for disease progression, such as the toxin co-regulated pilus and cholera toxin (TCP and CtxAB, respectively) (22–25, 31, 301). Transcription of *tcp* and *ctxAB* is directly activated by ToxT (39–42). Transcription of *toxT* is highly regulated and positively stimulated by ToxR and TcpP, two MLTRs, which directly bind to the *toxT* promoter (*toxTpro*), with binding sites at –104 to –68 and –55 to –37, respectively (39, 52–55, 70, 71, 82). TcpP and ToxR are bitopic membrane proteins, each containing a cytoplasmic DNA-binding domain (within the PhoB and OmpR families respectively), a single transmembrane domain, and a periplasmic domain (69). ToxR appears to have an accessory role in *toxT* regulation. Evidence supporting the model that ToxR assists TcpP to *toxT* transcription includes: 1) TcpP binds downstream of ToxR, closer than ToxR to

the putative RNA polymerase binding site on *toxTpro*; and 2) overexpression of TcpP results in ToxR-independent *toxT* transcription activation (39, 55, 70, 71). Furthermore, we have previously measured the single-molecule dynamics of TcpP and noted that deletion of *toxR* decreases but does not eliminate the prevalence of TcpP-DNA binding events (302). However, it remains unclear how TcpP and ToxR identify the *toxTpro* from the cytoplasmic membrane.

Signal transduction pathways in prokaryotes consist of one-component and two-component regulatory systems that manage cellular processes in response to extracellular information such as pH, temperature, chemical gradients, and nutrients (88, 89, 303). One-component regulatory systems combine their input and output functions in a single protein. MLTRs are a unique family of one-component regulators as they function from the cytoplasmic membrane, whereas the majority (~97%) of one-component regulators are localized in the cytoplasm (89). These one-component MLTRs like TcpP and ToxR comprise a sensor domain and an output domain that are separated by a transmembrane domain. MLTRs have been experimentally characterized in other, Gram-positive and Gram-negative, pathogenic bacteria and have been shown to regulate genes important for pathogenesis (such as capsule production, acid tolerance, antibiotic resistance, virulence gene regulation, and natural competence) (107, 110, 181, 190, 249, 285, 304–307). Using the Microbial Signal Transduction Database (MIST), we collected candidate MLTRs from 20 bacterial species and found that the prevalence and diversity of MLTRs is much higher than previously anticipated (Figure C.1). This data indicates that MLTRs are more common among bacteria than previously appreciated. Yet, it remains unclear how MLTRs identify specific promoter(s) while localized to the

cytoplasmic membrane. Some challenges emerge in understanding how MLTRs affect their function of activating transcription in response to external stimuli. For example, diffusion of these regulators is constrained to the cytoplasmic membrane. Additionally, the chromosome structure, which is not static, is known to influence association of a MLTR to its target sequence (308–317). How MLTRs locate their target sequences while bound to the membrane represents a major gap in our knowledge. Here, we investigated the subcellular single-molecule dynamics of TcpP-PAmCherry to understand how TcpP localizes to the *toxTpro* and to develop a general model for how MLTRs identify their DNA targets.

Our approach was to apply super-resolution single-molecule tracking (SMT) in living cells. Previous work demonstrated that TcpP molecules exhibit heterogeneous diffusion patterns (302, 318). Here, we expand upon this earlier work to study the effect of specific mutations, that alter TcpP binding to DNA or the potential association of TcpP with ToxR, on TcpP subcellular mobility. By tracking the movement of TcpP-PAmCherry molecules within single living *V. cholerae* cells, we determined the distributions of the heterogeneous motions of TcpP and detected changes in these diffusion coefficients in response to targeted genetic alterations. From this data, we identify three biophysical states (fast diffusion, intermediate diffusion, and slow diffusion), we propose a biological role corresponding to each state, and we suggest an alternative model of *toxT* activation where TcpP independently identifies the *toxTpro* prior to assistance from ToxR.

3.4 – Materials and Methods

3.4.1 – Bacterial strains and growth conditions

Escherichia coli and *V. cholerae* strains used here can be found in Table B.1. Unless otherwise stated, *E. coli* and *V. cholerae* cells were grown on Lysogeny Broth (LB) plates, or in LB broth at 210 rpm, at 37°C. LB was prepared according to previous descriptions (319). To stimulate virulence, *V. cholerae* cells were diluted from overnight cultures in LB broth and subcultured into virulence-inducing conditions: (LB pH 6.5, 110 rpm, 30 °C; filter sterilized). Here, the LB pH was adjusted by adding HCl (1 N) to pH 6.5 (+/- 0.05) and then the media was filter-sterilized to maintain pH. Where appropriate, antibiotics and cell wall intermediates were added at the following concentrations: streptomycin (100 µg ml⁻¹), ampicillin (100 µg ml⁻¹), and diaminopimelic acid (DAP) (300 µM).

3.4.2 – Plasmid construction

Plasmid vectors were purified using the Qiagen mini prep kit. Plasmid inserts were amplified from *V. cholerae* genomic DNA using Phusion high-fidelity polymerase (Thermo Scientific). Splicing by overlap extension was used to combine the entire plasmid insert sequences together (Table B.2). Plasmid vector was digested by restriction digestion using KpnI-HiFi and XbaI (New England BioLabs) at 37°C for 2 hrs. After digestion the plasmid vector and insert were added to Gibson assembly master mix (1.5 µl insert, 0.5 µl vector, 2 µl master mix) (New England BioLabs) and incubated at 50°C for 1 hr. Assembled plasmid was electroporated into *E. coli* λpir cells and recovered on LB plates with ampicillin and DAP.

3.4.3 – Bacterial strain construction

Strain construction follows the protocol outlined in reference (320). Briefly, *E. coli* λ pir harboring the pKAS plasmid and the donor *V. cholerae* strain were incubated in LB (broth or agar) supplemented with DAP overnight at 37°C. The remaining cells were then spread on LB plates containing ampicillin or TCBS plates containing ampicillin. Counter selection for loss of the pKAS construct by *V. cholerae* cells was done by incubating cells in LB broth for 2 hrs and then for 2 hrs with 2500 $\mu\text{g ml}^{-1}$ streptomycin (both at 37 °C, 210 rpm). 20 μl of this culture was spread onto LB plates containing 2500 $\mu\text{g ml}^{-1}$ of streptomycin and incubated overnight at 37 °C. Streptomycin-resistant colonies were screened for the chromosomal mutation of interest via colony polymerase chain reaction (PCR) using Taq DNA Polymerases (Thermo Fisher). Genomic DNA was purified from possible mutants and sequenced (Genewiz) to validate the exchange. Because *tcpP* and *tcpH* are encoded by on overlapping open reading frames, *tcpH* was cloned downstream of PAmCherry to maintain its transcription, and a stop codon was introduced within the first three codons of the native *tcpH* coding sequence to prevent out-of-frame translation of PAmCherry.

3.4.4 – Growth Curves

V. cholerae strains were initially grown on LB plates containing streptomycin (100 $\mu\text{g ml}^{-1}$) overnight at 37°C, then an individual colony was picked and grown overnight in LB broth at 37°C. *V. cholerae* cells were diluted to an optical density (OD₆₀₀) of 0.01 from the overnight LB broth into a 96 well plate (Cell Pro) with 200 μl of virulence-inducing

media per well. The plate was then incubated at 30°C with shaking every 30 min before each measurement in a SPECTROstar Omega plate reader (BMG LABTECH).

3.4.5 – Real-time quantitative PCR (RT-qPCR)

RNA was extracted from *V. cholerae* cells grown under virulence-inducing conditions. RNA was preserved by resuspending pellet cells in 1 ml Trizol (Sigma aldrich) and then purified using an RNeasy kit (Qiagen). RNA was further purified with Turbo DNase treatment. RNA quantity and quality were measured via UV-Vis spectrophotometry (NanoDrop ND-1000) and by detection of large and small ribosomal subunits via 2% agarose gel. RNA was then converted to cDNA using Superscript III reverse transcriptase (Thermo Scientific). RT-qPCR was performed using 5 ng of cDNA in SYBR green master mix (Applied Biosystems). RecA was used as a housekeeping gene of reference to calculate the threshold values ($\Delta\Delta C_T$) (321, 322). See Table B.2 for primers.

3.4.6 – Protein electrophoresis and immunodetection

After lysis, total protein concentration samples were measured via Bradford assay. Samples were subsequently diluted to 0.5 µg total protein/µl. All SDS page gels contained 12.5 % acrylamide and were run at 90 – 120 volts for 1.5 hrs. Proteins were transferred to nitrocellulose membranes using a semi-dry electroblotter (Fisher Scientific) overnight at 35 mA or for 2 hrs at 200mA. Membranes were blocked with 5 % non-fat milk, 2 % bovine serum albumin in Tris-buffered saline, 0.5 % Tween-20 (TBST) for 1 hr. Membranes were then incubated with primary antibody (α -TcpA 1:100,000; α -TcpP

1:1,000; α -TcpH 1:500; α -ToxR 1:50,000; α -mCherry 1:1,000) diluted in TBST and non-fat Milk (2.5 % w/vol) for an additional hour at room temp with shaking. Membranes were then washed 3 times with TBST. Secondary antibody (Goat anti-Rabbit IgG-HRP 1:2,000) (Sigma) was diluted in TBST and non-fat milk (2.5 % w/vol). Secondary antibody was incubated with the membranes for an additional hour at room temperature with shaking. Membranes were washed again with TBST 3 times and then incubated with SuperSignal HRP Chemiluminescence substrate (Thermo Fisher). Membranes were imaged with an Amersham Imager 600.

3.4.7 – Single-Molecule Microscopy

V. cholerae strains were grown on LB plates containing streptomycin (100 $\mu\text{g ml}^{-1}$) overnight at 37 °C, then an individual colony was picked and grown overnight in LB broth at 37 °C. *V. cholerae* cells were diluted from LB broth into virulence-inducing conditions and grown until they reached mid log-phase. They were then washed and concentrated in M9 minimal media with 0.4 % glycerol. A 1.5 μl droplet of concentrated cells was placed onto an agarose pad (2 % agarose in M9, spread and flattened on a microscope slide) and covered with a coverslip. Cells were imaged at room temperature using an Olympus IX71 inverted epifluorescence microscope with a 100x 1.40 NA oil-immersion objective, a 405-nm laser (Coherent Cube 405-100; 50 W/cm²) for photoactivation and a co-aligned 561-nm laser (Coherent-Sapphire 561-50; 210 W/cm²) for fluorescence excitation. Fluorescence emission was filtered with appropriate filters and captured on a 512 by 512 pixel Photometrics Evolve EMCCD camera. To prevent higher-order excitation during photoactivation, a pair of Uniblitz shutters controlled the laser beams such that samples

were exposed to only one laser at a time. During imaging, the cells were given a 40-ms dose of 405-nm light every 90 s. Images were collected continuously every 40 ms and acquisitions lasted 5 – 7 min each.

3.4.8 – Data Analysis

Recorded single-molecule positions were detected and localized based on point spread function fitting using home-built code, SMALL-LABS (323). This program reduces biases due to background subtraction, increasing the precision of each molecule localization. Subsequent localizations of the same molecule were then connected into trajectories using the Hungarian algorithm (323–325). All trajectories from each movie for a given condition were combined and analyzed together using the Single-Molecule Analysis by Unsupervised Gibbs sampling (SMAUG) algorithm (318). This algorithm considers the collection of steps in all trajectories and uses a Bayesian statistical framework to estimate the parameters of interest: number of mobility states, diffusion coefficient, weight fraction, transition probabilities between states, and noise.

3.5 – Results

3.5.1 – Single-molecule tracking of TcpP-PAmCherry is useful to study promoter identification, but cannot probe regulated-intramembrane proteolysis

To investigate the dynamics of individual TcpP molecules, we generated a *V. cholerae* strain in which the wild type *tcpP* allele is replaced with one expressing TcpP fused at its C-terminus to a photoactivatable fluorescent protein, PAmCherry (*tcpP-PAmCherry*). Levels and activity of TcpP are controlled by a two-step proteolytic process

known as regulated intramembrane proteolysis (RIP) (56, 58, 59). Under RIP-permissive conditions (defined as LB pH 8.5, 37°C, shaking at 210rpm) the C-terminus of TcpP becomes sensitive to proteolysis by Tsp, a site-1 protease, and YaeL, a site-2 protease; this sensitivity results in the inability of the cell to activate *toxT* transcription. Under RIP non-permissive conditions (defined as LB pH 6.5, 30°C, shaking at 110rpm), TcpP is protected from RIP by TcpH (56, 58, 59).

We investigated whether we could assess RIP dynamics using single-molecule tracking. Like wild-type TcpP, TcpP-PAmCherry was sensitive to RIP in the absence of TcpH, indicated by lower levels of TcpP-PAmCherry in *tcpP-PAmCherryΔtcpH* relative to *tcpP-PAmCherry* (Figure C.2A). Secondly, in both *tcpP-PAmCherry* and *tcpP-PAmCherryΔtcpH* a smaller species of TcpP-PAmCherry was observed, referred to as TcpP-PAm* (Figure C.2A). A similar result has been observed for native TcpP in $\Delta yaeL$ cells and indicates RIP (59). Complementation of *tcpP-PAmCherryΔtcpH* with plasmid-encoded *tcpH* resulted in a band with the mass of native TcpP (~29KDa), (Figure C.3). These data indicate that TcpP-PAmCherry resists RIP in a TcpH-dependent fashion similar to native TcpP. As expected, native TcpP was not detected in the absence of TcpH. These data indicate that: 1) TcpP-PAmCherry is sensitive to RIP; 2) TcpH can protect TcpP-PAmCherry from RIP; and 3) addition of PAmCherry to the C-terminus of TcpP reduces RIP of TcpP-PAmCherry relative to TcpP. These conclusions are supported by similar levels of TcpA, CtxB, and *toxT* transcription in *tcpP-PAmCherry* and *tcpP-PAmCherryΔtcpH* (318); (Figures C.2A and Figure C.4). Notwithstanding the detectable levels of TcpP-PAmCherry on immunoblots of total proteins from *tcpP-PAmCherryΔtcpH*, we observed almost no TcpP-PAmCherry molecules in our single-

molecule tracking experiments. As a result, we are unable to collect sufficient data to perform any analysis of *tcpP-PAmCherryΔtcpH* cells. Though we cannot determine how RIP influences TcpP-PAmCherry single-molecule dynamics, fusion of PAmCherry to the C-terminus of TcpP does not affect its ability to stimulate *toxT* transcription (Figure C.4). In addition, activity of TcpP is influenced by homodimerization, mediated by a periplasmic cysteine residue (C207) (77, 78). We sought to determine if addition of PAmCherry to the C-terminus of TcpP promotes its ability to dimerize. To test this, we measured *toxT* transcription in both *tcpP-PAmCherry* and *tcpPC207S-PAmCherry* cells (Figure C.5). We found that PAmCherry does not compensate for loss of C207, suggesting that it does not stimulate dimerization of TcpP-PAmCherry. This data indicates that PAmCherry does not simulate dimerization of TcpP-PAmCherry. Lastly, addition of PAmCherry to the C-terminus of TcpP does not affect the growth rate of *V. cholerae* (Figure C.6). Therefore, TcpP-PAmCherry is an effective tool to understand how TcpP locates the *toxT* promoter from its position in the membrane.

3.5.2 – Baseline Dynamics of TcpP-PAmCherry

Single-Molecule Analysis by Unsupervised Gibbs sampling (SMAUG) characterizes the motion of molecules based on the collection of measured displacements (steps) in their single-molecule trajectories. SMAUG estimates the biophysical descriptors of a system by embedding a Gibbs sampler in a Markov Chain Monte Carlo framework. This non-parametric Bayesian analysis approach determines the most likely number of mobility states and the average diffusion coefficient of single molecules in each state, the population of each state, and the probability of transitioning between different mobility states over the course of a single trajectory (318). In our

previous study, we determined that TcpP-PAmCherry molecules in *V. cholerae* cells transition between multiple biophysical states: fast diffusion, intermediate diffusion, and slow diffusion (318).

Here, we collected a new robust set of TcpP-PAmCherry tracking data in living *V. cholerae* cells (54,454 steps collected from 7601 trajectories) to further refine our analysis and to assign biochemical mechanisms to these biophysical observations (a sample of these tracks is shown in Figure 3.1B). Consistent with our previous results, we ascertained that TcpP-PAmCherry exists in three distinct states (slow diffusion, intermediate diffusion, and fast diffusion; blue, orange, and purple, respectively, in Figure 3.1C). Furthermore, we determined that TcpP-PAmCherry molecules do not freely transition between all the diffusion states: we observe that TcpP-PAmCherry molecules can transition between the fast state (purple) and the intermediate state (orange) and between the intermediate state (orange) and the slow state (blue) freely, but there is no significant probability of transitions directly from the fast diffusion state (purple) to the slow diffusion state (blue) on successive steps (Figure 3.1D). Thus, the intermediate diffusion state represents a critical biochemical intermediate between the slow and fast diffusion states.

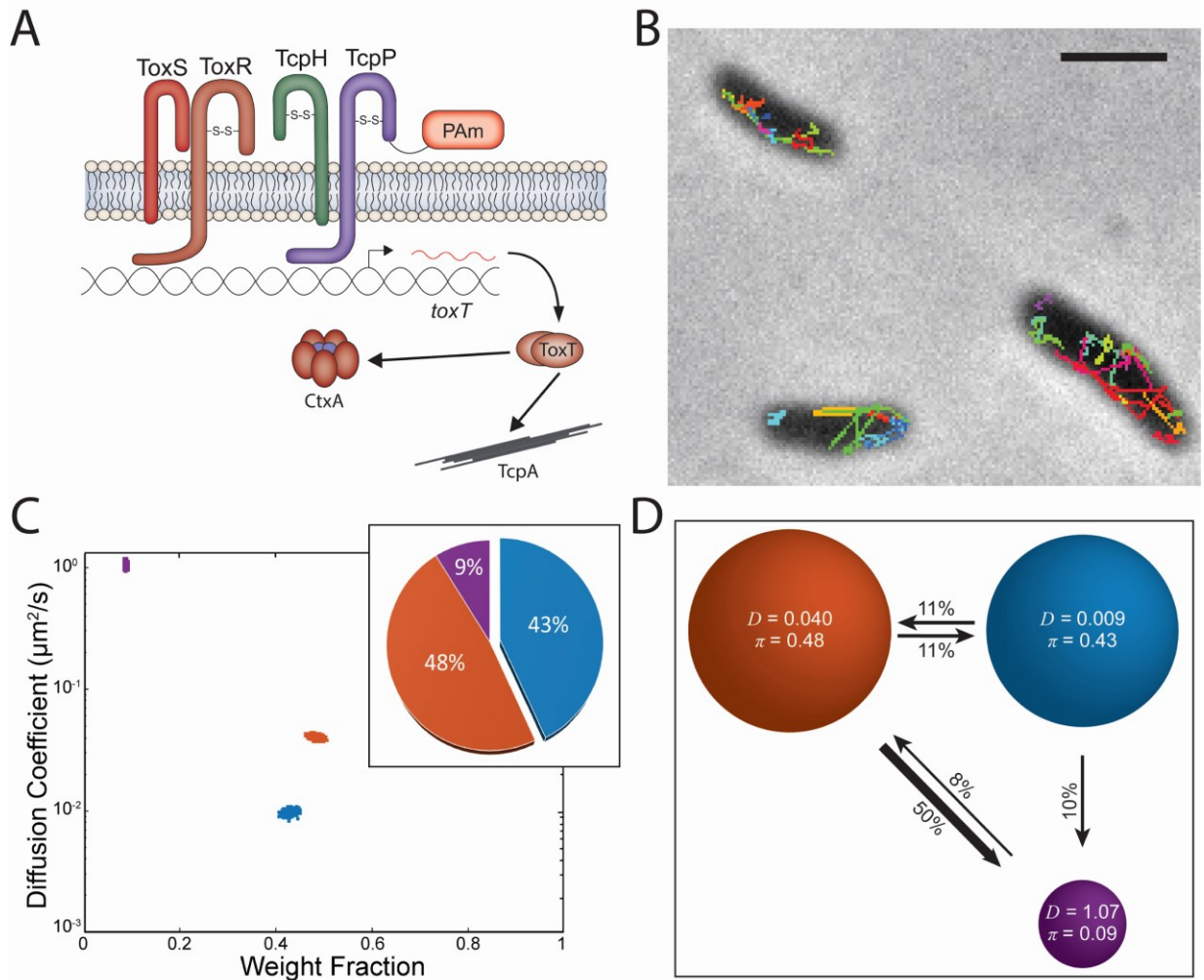


Figure 3.1: Single-molecule diffusion dynamics of TcpP-PAM. A) Model of *tcpP*-PAMCherry. B) Representative single-molecule trajectory maps overlaid on reverse-contrast bright-field image of *V. cholerae* TcpP-PAMCherry. Only trajectories lasting 0.20 s (5 frames) are shown. Trajectories shown in a variety of colors to show diversity of motion observed. Scale bar: 1 μm . C) Average single-molecule diffusion coefficients and weight fraction estimates for TcpP-PAMCherry in live *V. cholerae* cells grown under virulence-inducing conditions. Single-step analysis identifies three distinct diffusion states (fast – purple, intermediate – orange, and slow – blue, respectively). Each point represents the average single-molecule diffusion coefficient vs. weight fraction of TcpP-PAMCherry molecules in each distinct mobility state at each saved iteration of the Bayesian algorithm after convergence. The dataset contains 54,454 steps from 7,601 trajectories. Inset: percentage (weight fraction) of TcpP-PAMCherry in each diffusion state. Colors as in panel. D) Based on the identification of three distinct diffusion states for TcpP-PAMCherry (three circles with colors as in c and with average single-molecule diffusion coefficient, D , indicated in $\mu\text{m}^2/\text{s}$), the average probabilities of transitioning between mobility states at each step are indicated as arrows between those two circles, and the circle areas are proportional to the weight fractions. Low significance transition

Figure 3.1 (cont'd)

probabilities less than 4% are not displayed; for instance, the probability of TcpP-PAmCherry molecules transitioning from the fast diffusion state to the slow diffusion state is 1%. Numbers above the arrows indicate the probability of transition.

The high transition probability of TcpP-PAmCherry molecules from the intermediate diffusion state to the fast diffusion state (50%) is unexpected, as the fast diffusion state represents the smallest population of TcpP-PAmCherry molecules (9%), with a low probability (8%) of TcpP-PAmCherry molecules transitioning from the fast diffusion state back to the intermediate diffusion state (Figure 3.1D). While we cannot directly determine how RIP influences the dynamics of TcpP-PAmCherry, the stark difference in the transition probabilities and the populations of TcpP-PAmCherry in the fast and intermediate diffusion states suggests that fast diffusing TcpP-PAmCherry molecules are potentially sensitive to some form of degradation.

Given this baseline for the dynamics of TcpP-PAmCherry, we hypothesize that: 1) the three diffusion states (slow, intermediate, and fast) are features of TcpP-PAmCherry molecules with three biologically distinct roles; 2) the slow diffusion state is occupied by TcpP-PAmCherry molecules interacting with DNA, such as the *toxTpro*; and 3) the intermediate diffusion state is influenced by ToxR. We further explore these three hypotheses with *V. cholerae* mutants below.

3.5.3 – Mutation of the *toxT* promoter Decreases the Slow Diffusion State Occupancy

We hypothesized that the slow TcpP-PAmCherry diffusion state encompasses molecules specifically interacting with DNA at its binding site in the *toxT* promoter. The molecular weight of chromosomal DNA (chromosome 1: 2.96 Mbp) is much higher than that of any protein. Thus, binding of TcpP-PAmCherry to this promoter on the chromosome should result in an extremely low apparent diffusion rate. To test our hypothesis, we removed key binding sites for TcpP (-55 to -37) and both ToxR and TcpP (-112 to +1) in the *toxT* promoter, generating *tcpP-PAmCherry toxT* promoter Δ (-55-+1) and *tcpP-PAmCherry toxT* promoter Δ (-112-+1) (Figure 3.2), both of which resulted in a drastic reduction in TcpA production, similar to that of a Δ *tcpP* mutant (Figure C.2A). *toxT* transcription was reduced in *tcpP-PAmCherry toxT* promoter Δ (-112-+1), but not in *tcpP-PAmCherry toxT* promoter Δ (-55-+1) (Figure C.4). It is possible that the *toxT* promoter Δ (-55-+1) mutation causes TcpP-PAmCherry and ToxR to stimulate transcription of a non-functional *toxT* mRNA. Regardless, loss of either region of the *toxT* promoter results in loss of production of the TcpA virulence factor.

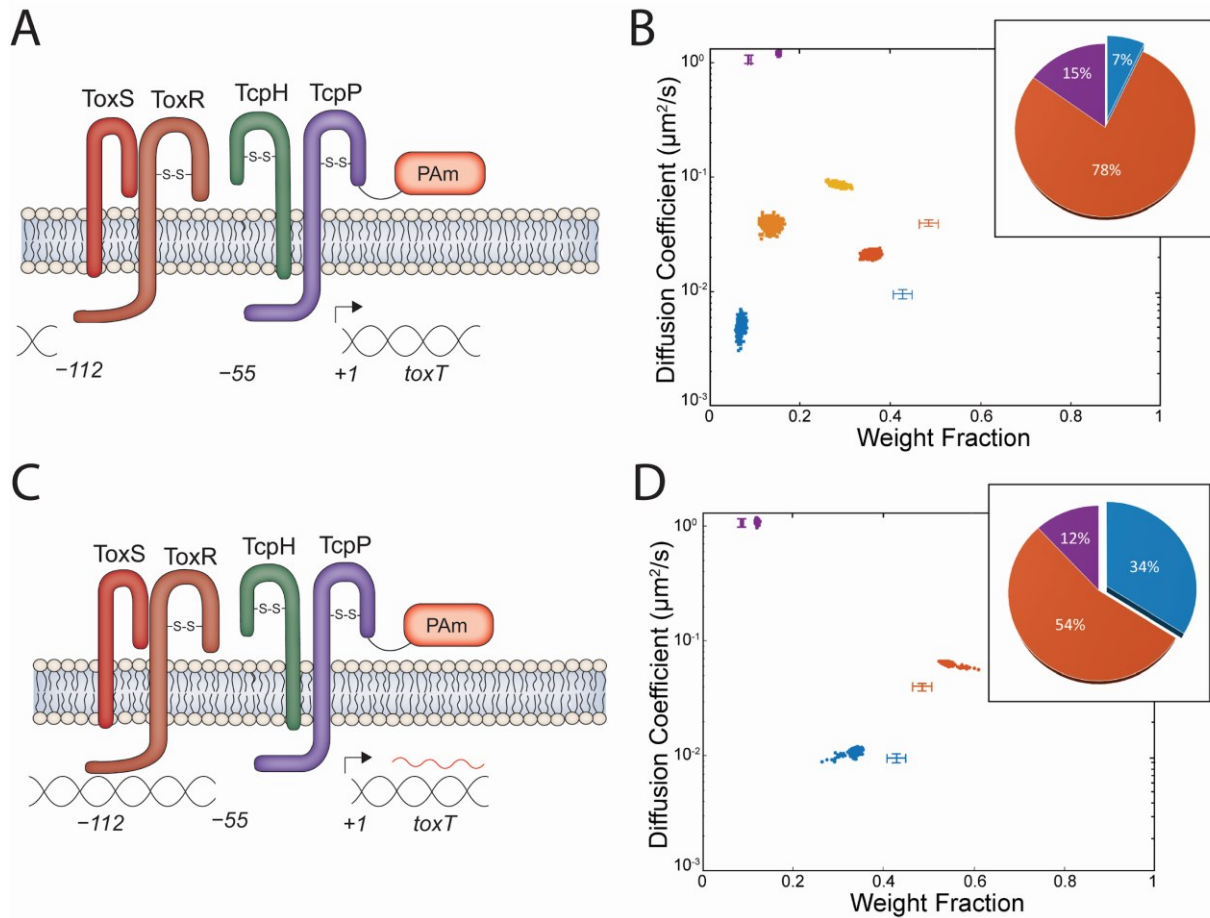


Figure 3.2: **TcpP-PAmCherry** diffusion dynamics within live *V. cholerae* cells containing mutated regions of the *toxT* promoter (*toxTpro*). A) and C) Model of *toxTpro* mutations in *tcpP-PAmCherry toxTpro* $\Delta(-112-+1)$ and *tcpP-PAmCherry toxTpro* $\Delta(-55-+1)$, respectively. B) and D) Average single-molecule diffusion coefficients and weight fraction estimates for TcpP-PAmCherry in live *V. cholerae tcpP-PAmCherry toxTpro* $\Delta(-112-+1)$ (B) and *V. cholerae tcpP-PAmCherry toxTpro* $\Delta(-55-+1)$ (D) grown under virulence-inducing conditions. Single-step analysis identifies five and three distinct diffusion states (fast – purple, intermediate – orange, light orange, and yellow, and slow – blue, respectively). Each point represents the average single-molecule diffusion coefficient vs. weight fraction of TcpP-PAmCherry molecules in each distinct mobility state at each saved iteration of the Bayesian algorithm after convergence. The dataset contains 104,341 steps from 21,274 trajectories for b and 75,841 steps from 11,624 trajectories for d. The data for TcpP-PAmCherry diffusion in wild type *V. cholerae* cells (Figure 3.1C) are provided for reference (cross hairs). Insets: Percentage (weight fraction) of TcpP-PAmCherry in each diffusion state. Colors as in panel.

Relative to the wild type (Figure 3.1), deleting both the ToxR and TcpP binding sites (*toxTpro* $\Delta(-112-+1)$) reduces the percentage of slow diffusing TcpP-PAmCherry to very low levels (7%; Figure 3.2B). Thus, TcpP-PAmCherry in the slow diffusion state requires *toxTpro*; therefore, we propose molecules in this state are bound to *toxTpro*. On the other hand, loss of the TcpP binding site alone (*toxTpro* $\Delta(-55-+1)$) reduces the percentage of slow TcpP-PAmCherry molecules only subtly (from 43% to 34%; Figure 3.2D). This result is consistent with earlier observations demonstrating that association with ToxR can restore the function of TcpP variants otherwise unable to bind the *toxTpro* (39, 55).

Furthermore, our single-step analysis of TcpP-PAmCherry in the *toxTpro* $\Delta(-112-+1)$ cells indicates five distinct TcpP-PAmCherry diffusion states, an increase from three states in the wild type (Figure 3.2B). In particular, the percentage of TcpP-PAmCherry molecules within the intermediate state overall increased (48% to 78%), but our analysis showed that these moderate moving molecules in fact cluster into three distinct sub-states (yellow, light orange, and orange, in Figure 3.2B). These intermediate TcpP-PAmCherry diffusion sub-states appear when TcpP-PAmCherry is unable to associate with the *toxTpro*. Though large-scale changes in the chromosome structure following the promoter deletion may play a role, these intermediate TcpP-PAmCherry diffusion sub-states may represent true biochemical interactions that are too short-lived to precisely distinguish and identify due to our current time resolution of 40 ms/acquisition. Further investigation is required to understand the specific biological roles of these sub-states, but indeed as discussed below, we detect these intermediate sub-states in all the other mutants studied here (Figure 3.3 and Figure 3.4).

3.5.4 –ToxR Promotes TcpP-PAmCherry Association with the Slow and Fast Diffusion States

ToxR is a critical regulator of *toxT* transcription through its role supporting TcpP interaction with the *toxTpro* (39, 55, 70). Prior studies have shown that TcpP and ToxR interact in response to low oxygen concentrations, and ToxR antagonizes H-NS from the *toxTpro* (55, 72, 132). Several models for TcpP-mediated *toxT* transcription implicate ToxR in recruitment of TcpP molecules to the *toxTpro* (39, 54, 55, 70, 71, 302). Another model invokes “promoter alteration” to suggest that ToxR promotes TcpP-*toxTpro* interaction by displacing the histone-like protein (H-NS) and altering DNA topology rather than recruiting TcpP molecules to the *toxTpro* (71).

To examine the role of ToxR in the motion and localization of TcpP-PAmCherry, we deleted *toxR*, and its accessory protein *toxS*, in both the *tcpP-PAmCherry* and the *tcpP-PAmCherry toxTpro* $\Delta(-55-+1)$ backgrounds, resulting in *tcpP-PAmCherry* Δ *toxRS* and *tcpP-PAmCherry* Δ *toxRS toxTpro* $\Delta(-55-+1)$ genotypes. We found that *tcpP-PAmCherry* Δ *toxRS* and *tcpP-PAmCherry* Δ *toxRS toxTpro* $\Delta(-55-+1)$ cells could activate *toxT* transcription, but only *tcpP-PAmCherry* Δ *toxRS* supported virulence factor production (Figures C.2AB and Figure C.4). Complementation of *tcpP-PAmCherry* Δ *toxRS* with *toxR* did not change overall levels of TcpA (Figure C.7). Complementation of *tcpP-PAmCherry* Δ *toxRS toxTpro* $\Delta(-55-+1)$ with ToxR did not restore TcpA to WT levels (Figure C.7). These data show that TcpP-PAmCherry can stimulate *toxT* transcription and bind to the *toxTpro* independent of ToxR. WT TcpP can stimulate *toxT* transcription independent of ToxR, but only upon TcpP overexpression (39, 55). Due to reduced sensitivity of TcpP-PAmCherry to RIP, we measure higher levels of TcpP-

PAmCherry relative to TcpP (Figure C.2A). This observation suggests that cooperativity between ToxR and TcpP is only necessary when levels of TcpP are low (i.e., when TcpP is sensitive to RIP).

The percentage of slowly diffusing TcpP-PAmCherry molecules depends on *toxRS*, as deleting *toxRS* reduces this population in *tcpP-PAmCherry ΔtoxRS* from 43% to 20% (Figure 3.3B). This *toxRS* dependence is maintained even in the absence of the TcpP binding site within the *toxT* promoter; the slow population in *tcpP-PAmCherry ΔtoxRS toxTproΔ(-55-+1)* is reduced to 8% from 34% in *tcpP-PAmCherry toxTproΔ(-55-+1)* (Figure 3.3D). Indeed, the TcpP-PAmCherry dynamics are very similar for *tcpP-PAmCherry toxTproΔ(-112-+1)* (Figure 3.2B) and *tcpP-PAmCherry ΔtoxRS toxTproΔ(-55-+1)* (Figure 3.3D). The major difference between TcpP-PAmCherry diffusion dynamics is the loss of the light orange intermediate diffusion sub-state in *tcpP-PAmCherry ΔtoxRS toxTproΔ(-55-+1)* (Figure 3.3D). These data indicate that, in addition to the slow diffusion state, the presence of ToxR is critical for TcpP-PAmCherry molecules to exist in one of the intermediate sub-state diffusion states (i.e., the light orange diffusion state).

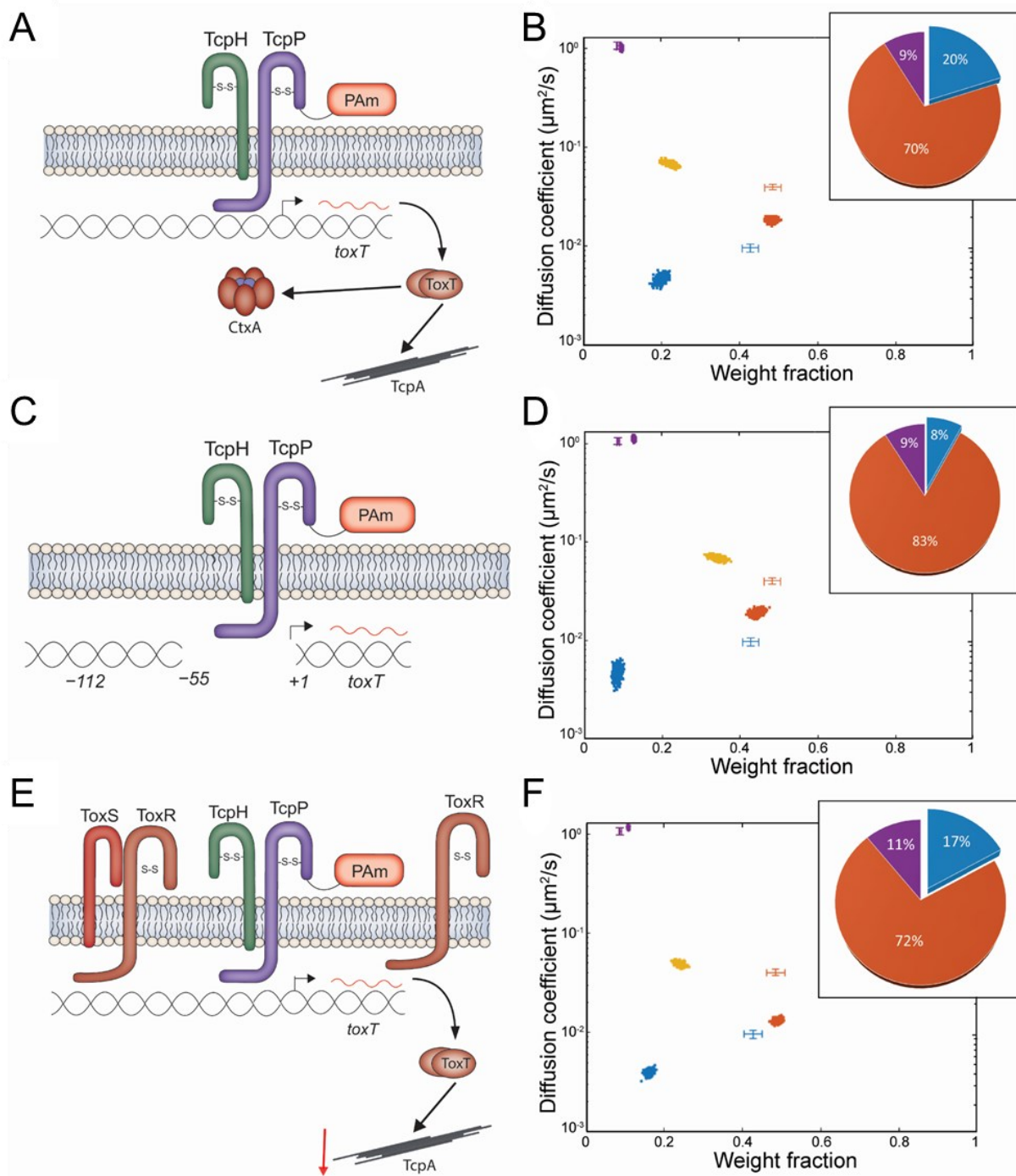


Figure 3.3: **TcpP-PAmCherry** diffusion dynamics within live *V. cholerae* cells lacking **ToxRS** and regions of the **toxT** promoter. A), C), and E) Model of *tcpP-PAmCherry* Δ *toxRS*, *tcpP-PAmCherry* Δ *toxRS* *toxTpro* Δ (-55+1), and *tcpP-PAmCherry* pMMB66eh-*toxR*, respectively. B), D) and F) Average single-molecule diffusion coefficients and weight fraction estimates for **TcpP-PAmCherry** in live *V. cholerae* *tcpP-PAmCherry* Δ *toxRS* (B), *V. cholerae* *tcpP-PAmCherry* Δ *toxRS*

Figure 3.3 (cont'd)

toxTpro $\Delta(-55-+1)$ (D), and *tcpP-PAmCherry* pMMB66eh-*toxR* (F) grown under virulence-inducing conditions. *tcpP-PAmCherry* pMMB66eh-*toxR* was grown in the presence of 1mM IPTG. Single-step analysis identifies four distinct diffusion states (fast – purple, intermediate – yellow and orange, and slow – blue, respectively). Each point represents the average single-molecule diffusion coefficient vs. weight fraction of TcpP-PAmCherry molecules in each distinct mobility state at each saved iteration of the Bayesian algorithm after convergence. The dataset contains 80,005 steps from 11,069 trajectories for b, 58,577 steps from 11,314 trajectories for d, and 134,071 steps from 19,509 trajectories for f. The data for TcpP-PAmCherry diffusion in wild type *V. cholerae* cells (Figure 3.1C) are provided for reference (cross hairs).

As shown in Figure 3.1D, we found that TcpP-PAmCherry molecules do not freely transition between all the diffusion states: the intermediate diffusion state is an important diffusion state for TcpP-PAmCherry molecules to transition between the fast and the slow diffusion states. Since the ToxR-TcpP interaction is proposed to enable TcpP to associate with the transcription complex at *toxTpro* (39, 55), we reasoned that ToxR is responsible for the preferred intermediate-to-slow state transition of TcpP-PAmCherry. However, in Δ *toxRS* (Figure 3.3B) like in the wild-type (Figure 3.1C), only TcpP-PAmCherry molecules in the slowest of the intermediate diffusion sub-states were likely to transition to the slow diffusion state (orange and blue diffusion states, respectively, Figure C.8B). These transition probabilities suggest that ToxR is not responsible for the restricted transition of TcpP-PAmCherry between the slow and fast diffusion states. Furthermore, the absence of ToxR reduced the probability of TcpP-PAmCherry entering the fast diffusion state and increased the probability of TcpP-PAmCherry leaving the fast diffusion state (Figure 3.1D and Figure C.8B). Taken together, these data indicated that ToxR sequesters a portion of the total TcpP-PAmCherry population away from the *toxTpro*. We reasoned that increased levels of ToxR might sequester TcpP molecules to an inactive state

(represented by the intermediate diffusion state). To test this hypothesis, we overexpressed ToxR in a *tcpP-PAmCherry* background and quantified virulence factor transcription (i.e., *TcpA*) (Figure C.9). We found that elevated ToxR levels reduced virulence factor levels in both WT and *tcpP-PAmCherry* cells. Furthermore, overexpression of ToxR also decreased the percentage of *TcpP-PAmCherry* in the slow diffusion state (17% vs 43%) and resulted the formation of a sub-intermediate diffusion state, similar to *tcpP-PAmCherry* Δ *toxRS* (Figure C.4B). These data suggest that elevated levels of ToxR can repress *toxT* transcription by reducing the percentage of *TcpP* molecules entering the slow diffusion state.

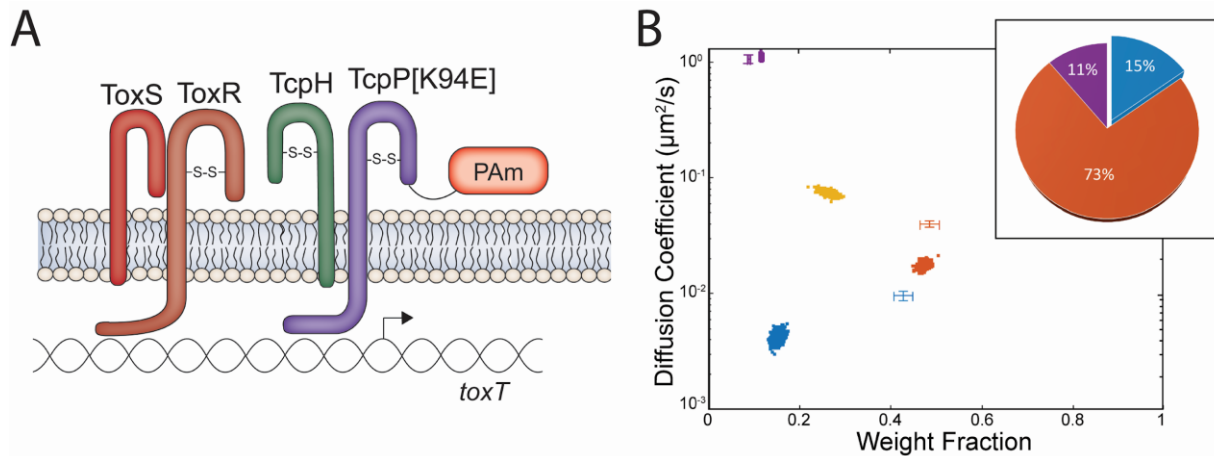


Figure 3.4: Mutation of the DNA binding domain within *TcpP* reduces the number of *TcpP* molecules within the slow diffusion state. A) Model of *tcpP*-[K94E]-*PAmCherry*. B) Diffusion dynamics of a DNA binding deficient *TcpP*-*PAmCherry* variant within live *V. cholerae* cells. Average single-molecule diffusion coefficients and weight fraction estimates for *TcpP*-[K94E]-*PAmCherry* in live *V. cholerae* *tcpP*-[K94E]-*PAmCherry* grown under virulence-inducing conditions. Single-step analysis identifies four distinct diffusion states (fast – purple, intermediate – yellow and orange, and slow – blue, respectively). Each point represents the average single-molecule diffusion coefficient vs. weight fraction of *TcpP*-[K94E]-*PAmCherry* molecules in each distinct mobility state at each saved iteration of the Bayesian algorithm after convergence. The dataset contains 52,565 steps from 8,056 trajectories. The data for *TcpP*-*PAmCherry*

Figure 3.4 (cont'd)

diffusion in wild type *V. cholerae* cells (Figure 3.1C) are provided for reference (cross hairs). Inset: Percentage (weight fraction) of TcpP-[K94E]-PAmCherry in each diffusion state. Colors as in panel.

3.5.5 – Mutation of the TcpP Helix-Turn-Helix Domain Reduces the Percentage of Slowly Diffusing TcpP-PAmCherry

Based on results shown in Figure 3.1C, we proposed that TcpP-PAmCherry molecules in the slow diffusion state are bound to *toxTpro*, and we found that removing the *toxTpro* binding sites (Figure 3.2) or eliminating *toxR* (Figure 3.3) significantly reduces this bound state population. Previous studies demonstrated that TcpP does not require DNA binding capability to activate *toxT* transcription if ToxR is present (39, 55). To examine this finding further by SMT, we used a *tcpP-PAMCherry* allele with a mutation (K94E) that inhibits TcpP from binding to the *toxTpro* (55). This mutation results in greatly reduced *toxT* transcription and TcpA levels (Figures C.2A and Figure C.4). The levels of TcpP[K94E]-PAmCherry is elevated compared with TcpP-PAmCherry (Figure C.2A), consistent with earlier evidence that the K94E substitution increases TcpP stability (55). In addition to TcpP[K94E]-PAmCherry being unable to stimulate *toxT* transcription, a lower percentage of TcpP[K94E]-PAmCherry molecules are detected in the slowest-diffusing state than for TcpP-PAmCherry (15% vs. 43%; Figure 3.4B). Furthermore, TcpP[K94E]-PAmCherry molecules have an additional intermediate diffusion sub-state, similar to both *tcpP-PAMCherry* Δ *toxRS* and *tcpP-PAMCherry* Δ *toxRS* *toxTpro* Δ (-55-+1) (Figure 3.4B).

3.6 – Discussion

How MLTRs find their target sequences from the membrane represents a major gap in knowledge. Here, we started to address this by investigating single-molecule dynamics of TcpP-PAmCherry. Taken together with previous work, the data presented here demonstrate that TcpP-PAmCherry molecules diffuse in at least three distinct biophysical states (fast, intermediate, and slow diffusion), but do not freely transition between all diffusion states (318). We hypothesized that each of these biochemical states have distinct biological roles. Specifically, we hypothesized that the slow diffusion state represented TcpP-PAmCherry molecules interacting with the *toxTpro*. To test this hypothesis, we made targeted deletions to the *toxTpro* and of *toxRS*, and we mutated the TcpP DNA binding domain (K94E). Our biophysical measurements of these mutations support the hypothesis that the slow diffusion state is occupied by TcpP-PAmCherry molecules interacting specifically with DNA at *toxTpro*. Additionally, we observed that TcpP-PAmCherry molecules only transition to the slow diffusion state from the intermediate diffusion state, and that ToxR is not responsible for this transition specificity. These data support a modified promoter alteration model (71) in which ToxR binds to the distal region of the *toxTpro* to promote TcpP binding to the proximal region of the *toxTpro* or, in the absence of its binding site, ToxR directly interacts with TcpP to stimulate *toxT* transcription. Our data do not suggest that ToxR directs or recruits TcpP to the *toxTpro*.

While ToxR is critical for TcpP to stimulate *toxT* transcription (39, 52, 55), our data demonstrate that TcpP-PAmCherry can support *toxT* transcription and virulence factor production without ToxR, which may be a consequence of the greater stability of TcpP-PAmCherry compared to native TcpP (Figure C.2A and Figure C.4). Moreover, our single-

molecule imaging finds a higher percentage of the TcpP-PAmCherry molecules in the slow diffusion state in *tcpP-PAmCherry ΔtoxRS* cells compared to *tcpP-PAmCherry ΔtoxRS toxTproΔ(-55→+1)* (Figure 3.3). In addition, prior DNase I footprinting experiments have demonstrated that in cells lacking *toxR* TcpP protects a larger region of the *toxTpro* (-100 to -32), i.e., TcpP protects most of the ToxR binding and TcpP binding sites in *ΔtoxRS* (39). Taken together, these results indicate that: 1) ToxR is not essential for TcpP to locate the *toxTpro*; and 2) TcpP is able to interact with the *toxTpro* independent of ToxR. In addition, our data show that *ΔtoxRS* reduces the percentage of DNA-bound TcpP-PAmCherry but does not decrease the probability of TcpP-PAmCherry molecules transitioning from the intermediate state to the bound state (Figure 3.3 and Figure C.8B). Despite a reduction in the percentage of DNA-bound TcpP-PAmCherry, TcpP-PAmCherry stimulates WT *toxT* transcription independent of ToxR (Figure C.4). These data support the promoter alteration model (71) in which, rather than ToxR recruiting TcpP to the *toxTpro*, ToxR assists TcpP to stimulate *toxT* transcription once TcpP independently associates with the *toxTpro*. Counterintuitively, in the absence of ToxRS TcpP-PAmCherry molecules have a lower probability of exiting the slow diffusion state (Figure C.8B). Given that RIP of TcpP-PAmCherry impedes our ability to image TcpP-PAmCherry, these data suggest that TcpP-PAmCherry molecules might be sensitive to RIP while interacting with the *toxTpro*, and that ToxRS may inhibit RIP of TcpP while interacting with the *toxTpro*. If this is the case, given that we are unable to image TcpP-PAmCherry molecules that are sensitive to RIP, it might explain why we observe a lower percentage of TcpP-PAmCherry molecules in the slow diffusion state and yet we observe WT *toxT* transcription in the absence of ToxRS. However, future

experiments are required to determine if ToxRS inhibits RIP of TcpP while interacting with the *toxTpro*.

Under certain conditions ToxR can negatively influence *toxT* transcription. In response to stationary-phase accumulation of the cyclic di-peptide cyclic phenylalanine-proline (cyc-phe-pro), ToxR stimulates production of LeuO, resulting in down-regulation of the *tcpP* regulator *aphA* (326, 327). Our data suggests that ToxR can also reduce *toxT* transcription by influencing TcpP-PAmCherry single molecule dynamics (Figure C.8B). Deletion of *toxRS* reduces the overall probability of TcpP-PAmCherry molecules transitioning between the intermediate and fast diffusion states (Figure C.8B). Moreover, elevated levels of ToxR reduce both the percentage of TcpP-PAmCherry in the slow diffusion state and virulence factor production (Figure 3.3F and Figure C.9), suggesting that ToxR can antagonize *toxT* transcription by promoting transition of TcpP molecules to the fast or sub-intermediate diffusion states. A similar phenotype has been reported previously (39). Lastly, prior electrophoretic mobility shift assays also indicate that ToxR can sequester TcpP from the *toxTpro*. In Δ *toxRS* cells TcpP is able to bind to the *toxTpro* -73–+45 (*toxTpro* lacking the ToxR binding region), but not in the presence of ToxR molecules (39). It remains unclear how ToxR sequesters TcpP-PAmCherry molecules from the slow diffusion state. However, we hypothesize that ToxR promotes TcpP molecules to transition away from the slow diffusion state to prevent aberrant *toxT* transcription. Follow-up experiments are required to test this hypothesis.

Currently, the biological roles of the intermediate diffusion states (or intermediate diffusion sub-states) are unclear, but the intermediate states are certainly important, as TcpP molecules transition to the *toxTpro*-bound state from them. There is nearly a 10-

fold difference in diffusion coefficients between the slow and intermediate diffusion states (0.044 $\mu\text{m}^2/\text{sec}$ vs. 0.006 $\mu\text{m}^2/\text{sec}$ respectively; Figure 3.1C). This difference cannot be explained by dimerization or interaction of ToxR and TcpP-PAmCherry alone: the mobility of membrane-localized proteins scales linearly with the number of transmembrane helices, such that increasing the number of transmembrane helices via dimerization from one to two would only reduce the diffusion coefficient by a factor of two (328). One possibility is that TcpP-PAmCherry molecules undergo fast diffusion in less protein dense areas of the cytoplasmic membrane relative to TcpP-PAmCherry molecules undergoing intermediate diffusion. Prior single molecule analysis of 209 membrane localized proteins in *Bacillus subtilis* revealed that only 6% of all membrane proteins imaged were homogeneously distributed throughout the cytoplasmic membrane (328, 329). Heterogeneous distribution of membrane localized proteins in *B. subtilis* suggests that similar distribution of membrane localized proteins in *V. cholerae* can occur. It remains unclear as to why the vast majority of these membrane localized proteins in *B. subtilis* have heterogeneous diffusion dynamics. One possibility is that these membrane localized proteins have different preferences for lipid ordered and lipid disordered membrane domains. Prior studies have demonstrated that transmembrane domain properties (e.g., surface area, length, and post-translational modifications) are major factors in determining lipid ordered or lipid disordered membrane domain preference (330). We are currently exploring if lipid ordered and lipid disordered membrane domains influence diffusion dynamics of TcpP molecules within the fast and intermediate diffusion states.

Alternatively, it is possible that the diffusion coefficients of TcpP-PAmCherry molecules in the intermediate state are undergoing non-specific interactions with DNA

whereas the slowest TcpP-PAmCherry molecules are specifically bound at *toxTpro*. Our data show that there are some slow moving TcpP-PAmCherry molecules when major regions of the *toxTpro* are deleted or when key residues within the DNA binding domain of TcpP are mutated (i.e., *tcpP[K94E]-PAmCherry*; Figure 3.2 and 3.4). When considering our alternative model of non-specific DNA binding by TcpP, our data suggest two possibilities: 1) TcpP-PAmCherry molecules in the slow diffusion state represent TcpP molecules that make both specific and non-specific interactions with DNA; or 2) TcpP-PAmCherry molecules in the slow diffusion state interact specifically with non-*toxTpro* DNA (i.e., TcpP regulates additional genes). Several genes appear to have altered gene transcription upon deletion of *tcpPH* (331). However, these experiments have yet to be replicated. Thus, future experiments would be required to test these hypotheses.

These results provide deep insights that further expand the model of cooperativity between ToxR and TcpP-PAmCherry. Our data demonstrate that ToxR assists TcpP to associate with the *toxTpro* even in the absence of the TcpP binding site, further supporting the established model of cooperativity between TcpP and ToxR. The data also show that TcpP can locate the *toxTpro*, interact with the *toxTpro*, and stimulate *toxT* transcription independent of ToxR. This supports the promoter alteration model in which TcpP molecules independently associate with the *toxTpro* while ToxR enhances this association by altering *toxTpro* topology to stimulate *toxT* transcription. In addition to independently associating with the *toxTpro*, these data show that ToxR promotes transition of TcpP molecules to the fast and sub-intermediate diffusion states, shifting the equilibrium of TcpP molecules away from the *toxTpro*. The mechanism by which ToxR promotes transition of TcpP molecules away from the slow diffusion state is currently

unclear but will be the subject of future investigation. Given that *toxT* transcription is highly regulated, we speculate that sequestration of TcpP molecules from the *toxT* promoter is yet another mechanism to fine tune *toxT* transcription. It is probable that other MLTRs, found in both Gram-negative and Gram-positive bacteria, have similar biophysical properties (Figure C.1). Continued exploration of MLTR biophysical properties could be leveraged to develop alternative strategies to inhibit MLTRs to treat bacterial infections without exacerbating the global antibiotic resistance crisis.

Chapter 4 – Co-Association of TcpP and TcpH within Detergent-Resistant Membranes
Stimulates TcpH-Dependent Inhibition of Regulated Intramembrane Proteolysis of TcpP
in *Vibrio cholerae*

4.1 – Abstract

Vibrio cholerae is a Gram-negative gastrointestinal pathogen responsible for the diarrheal disease cholera. *V. cholerae* produces virulence factors such as cholera enterotoxin (CT) and the toxin co-regulated pilus (TCP) to cause disease. Transcription of these is activated directly by a transcription regulator, ToxT, and indirectly by two single-pass membrane-localized transcription regulators (MLTR), ToxR and TcpP, that promote the transcription of *toxT*. TcpP abundance and activity are controlled via TcpH, a single-pass transmembrane protein, and a two-step proteolytic process known as Regulated Intramembrane Proteolysis (RIP). The mechanism of TcpH mediated protection of TcpP represents a major gap in our understanding of *V. cholerae* pathogenesis. Absence of *tcpH* leads to unimpeded degradation of TcpP *in vitro* and a colonization defect in a neonate mouse model of *V. cholerae* colonization. Here, we show that TcpH protects TcpP from RIP via direct interaction. We also demonstrate that a dietary fatty acid, α -linolenic acid, promotes TcpH-dependent inhibition of RIP via co-association of TcpP and TcpH molecules within detergent-resistant membranes (DRMs) (also known as lipid rafts). Taken together our data support a model where *V. cholerae* cells utilize exogenous α -linolenic acid to remodel their phospholipid bilayer *in vivo* leading to co-association of TcpP and TcpH within DRMs where RIP of TcpP is strongly inhibited by TcpH thereby promoting *V. cholerae* pathogenesis.

4.2 – Introduction

V. cholerae tightly regulates transcription of its virulence factors, such as cholera toxin (CtxAB) and the toxin co-regulated pilus (TcpA-F) to reach the optimal site of infection, the crypt of intestinal villi (332–337). Transcription of these essential virulence factors is regulated by ToxT, an AraC-like transcription factor (338–341). Similarly, transcription of *toxT* is highly regulated and positively stimulated by TcpP and ToxR, two membrane-localized transcription regulators (MLTR) (342–345).

TcpP and ToxR are bitopic membrane proteins that each contain a cytoplasmic DNA-binding domain, a single transmembrane domain, and a periplasmic domain (346). Both ToxR and TcpP directly bind to the promoter region of *toxT*, at -180 to -60 and -55 to -37, respectively (340, 347, 348). While ToxR directly binds to the *toxT* promoter, ToxR alone is unable to directly stimulate *toxT* transcription (340). However, TcpP is required for *toxT* transcription, presumably because TcpP facilitates transcription through direct interaction with RNA polymerase due to its binding sequence being near the -35 site (340, 347). Unlike ToxR, transcription of *tcpP* is tightly regulated by multiple transcription factors, further demonstrating the critical importance of TcpP (60–63, 65, 67, 349, 350).

TcpP is also post-translationally regulated by two proteases, Tail-specific protease (Tsp) and YaeL, through a process known as Regulated Intramembrane Proteolysis (RIP) (96, 351, 352). RIP is a form of gene regulation conserved across all domains of life that allows organisms to rapidly respond to extracellular cues, commonly by liberating a transcription factor or a sigma factor, from membrane sequestration (353). Two well-characterized systems controlled by RIP mechanisms are the extracytoplasmic stress

response in *E. coli* and regulation of sporulation in *Bacillus subtilis*. These systems require RIP of RseA and SpoIVFB to release their respective sigma factors (σ^E and pro- σ^K) from the membrane to influence gene transcription(354–360). Similarly, both systems have their respective TcpH analog, RseB and BofA, which function to prevent RIP of RseA and SpoIVFB via different mechanisms (355, 361–366). Regulation of TcpP by this mechanism diverges from these canonical systems because transcription activity of TcpP is not activated by RIP but is rather inactivated by RIP, which removes TcpP from the cytoplasmic membrane thereby leading to a decrease in *toxT* transcription (96, 351, 352).

Our current understanding of RIP of TcpP remains limited. Under RIP-permissive conditions *in vitro* (e.g. LB pH 8.5, 37°C, 210rpm), TcpP is sensitive to proteolysis by tail-specific protease (Tsp; site-1 protease), and subsequently by YaeL protease (site-2 protease) (96, 351, 352). RIP of TcpP is inhibited by its associated protein, TcpH, under specific *in vitro* conditions (e.g. LB pH 6.5, 30°C, 110rpm) (96, 351, 352). Without TcpH present, TcpP is constitutively sensitive to RIP (96, 351, 352). However, the mechanism by which TcpH inhibits RIP and how TcpH-dependent RIP inhibition is modulated by extracellular stimuli remains unknown.

In this report we provide evidence that TcpH protects TcpP from RIP via direct interaction. Furthermore, we explore the role of the membrane in regulating TcpP-TcpH association and present data that the two molecules interact within both detergent-resistant and detergent-soluble membranes (DRM and DSM, respectively). DRM and DSM (i.e., lipid-ordered and lipid-disordered membrane domains) are known to form in both eukaryotic and prokaryotic organisms (367–372). In prokaryotes, lipid-ordered membrane domains are small phospholipid domains (~10-200 nm) that exist within both

inner and outer membranes (373). They are composed of saturated phospholipids and hopanoids (or cholesterol in eukaryotic cells) that tightly interact, resulting in a structured membrane region with low fluidity. Conversely, lipid-disordered membrane domains are enriched in unsaturated phospholipids resulting in high fluidity (367–369, 371–380). Due to these differences lipid-ordered and lipid-disordered membrane domains can be separated based on solubility in non-ionic detergents, and we refer to them as detergent-resistant membranes (DRM) and detergent-soluble membranes (DSM), respectively. Our data suggest that *in vivo* TcpP and TcpH preferentially associate with DRMs. This leads to enhanced inhibition of RIP by TcpH, thereby resulting in elevated TcpP levels, and *toxT* transcription. We also show that utilization of exogenous α -linolenic acid, a long chain poly-unsaturated fatty acid present *in vivo*, stimulates TcpP and TcpH association within DRMs. Data generated here support a model where, once *V. cholerae* cells enter the gastrointestinal tract, cellular uptake of α -linolenic acid results in modification of the phospholipid profile and leads to an increase the abundance of TcpP and TcpH molecules within DRMs thereby stimulating inhibition of RIP.

4.3 – Methods and Materials

4.3.1 – Bacterial strains, plasmids, and growth conditions

All *V. cholerae* strains used in this study were of the classical biotype (0395) (See Table D.1 for a complete list of bacterial strains). Unless otherwise stated *Escherichia coli* and *V. cholerae* were grown at 37°C in Luria-Bertani (LB) with vigorous shaking (210 rpm). LB was prepared as previously described (381). To stimulate virulence factor production, *V. cholerae* strains were subcultured, to an O.D. of 0.01, from an overnight

LB culture and grown under virulence inducing conditions (Vir Ind; 30°C, LB pH 6.5, and 110 rpm) or non-virulence inducing conditions (non-Vir Ind; 37°C, LB pH 8.5, and 210 rpm). Media used for both Vir Ind and non-Vir Ind were sterilized using 1L 0.22 µm vacuum filtration units (Sigma) following pH adjustment.

Ex-vivo mouse fecal experiments with sterile and non-sterile mouse fecal media were conducted aerobically at 37°C in 48 well plates (Sigma) with shaking (210 rpms). Sterile mice fecal samples were collected from C57 Black female mice on 4 separate days and stored at -80°C. After collection mice fecal samples were homogenized, via mortar and pestle, and then suspended in M9 minimal media. The final concentration of mice fecal media was 9% w/v. The mice fecal media was then spun down (2450xg for 10 min) to remove insoluble material. The supernatant was collected, and filter sterilized using a 0.45 µm syringe filter (Sigma). Non-sterile mice fecal samples were collected from C57 Black female mice on three separate days. Mice fecal matter was directly resuspended in M9 media to a final concentration of 9% w/v. Mice fecal media was then incubated at room temperature for 1 hour while shaking on a table top shaker. Mice fecal media was spun down (2450xg for 10 min). The supernatant was collected and used directly for the growth curve. *V. cholerae* cell density was determined by counting CFU's on LB agar plates supplemented with streptomycin. Microbiota in mice fecal matter were not found to be resistant to streptomycin.

Unless otherwise stated, antibiotics were used at the following concentrations: ampicillin (100 µg/ml), chloramphenicol (30 µg/ml), and streptomycin (100 µg/ml). Overexpression of constructs by pBAD18 was induced by culturing strains in LB containing 0.1% arabinose.

4.3.2 – Plasmid construction

Briefly, DNA fragments 500 bp upstream and downstream of the target gene were amplified using Phusion high-fidelity polymerase (Thermo Scientific) (see Table D.2 for list of primers used). Insert fragments containing desired mutations were connected by splicing via overlap extension PCR. Plasmid vectors (pKAS32 and pBAD18) were isolated from bacterial strains using the Qiagen Miniprep kit. Plasmid vectors were then digested with KpnI-HiFi and XbaI (New England BioLabs) at 37°C for 2 hours. Insert and vector fragments were then added to Gibson assembly master mix (New England BioLabs) and incubated at 50°C for 30 minutes. Plasmids were then introduced to *E. coli* ET12567 $\Delta dapA$ (λ pir +) by electroporation. pKAS32 plasmids were then transferred to *V. cholerae* strains via mating on LB agar plates at 30°C overnight. pBAD18 plasmids were introduced into *V. cholerae* strains via electroporation.

4.3.3 – Mutant construction

Mutants were constructed as previously described (320). *V. cholerae* harboring pKAS32 derivatives were grown in 2 ml LB for 2 hours at 37°C. Streptomycin was then added to cultures to a final concentration of 2500 μ g/ml and incubated for an additional 2 hours. After a total of 4 hours of incubation, 20 μ l of culture was spread on LB agar plates containing streptomycin (2500 μ g/ml) and incubated at 37°C overnight. Colonies that were resistant to streptomycin were screened via colony PCR to confirm presence of the desired mutation. Genomic DNA was then isolated from potential mutants and the region of interest was then amplified via PCR and validated by sequencing (GeneWiz).

4.3.4 – Growth curves

V. cholerae strains were subcultured from an overnight culture to a final optical density (600 nm) of 0.01 in 200 µl of virulence inducing media per well of a 96 well plate. The plate was then incubated at 30°C in a SPECTROstar Omega plate reader (BMG LABTECH), with shaking and optical density measurements every 30 minutes.

4.3.5 – Western blots

After whole cell lysis, the total protein concentration of each sample was measured via Bradford assay (Sigma Aldrich). Samples were subsequently diluted to a final concentration of 0.5 µg total protein/µl. All SDS page gels contained 12.5% acrylamide and were run at 90-120 volts for 1.5 hours. Proteins were transferred to nitrocellulose membranes using a semi dry electroblotter (Fisher Scientific) overnight at 35 mA or for 2 hours at 200mA. Membranes were blocked with 15 ml of blocking buffer (5% non-fat milk, 2% bovine serum albumin, 0.5% Tween-20, in Tris-buffered saline) for 1 hour at room temperature. Primary antibodies were diluted in 5% non-fat milk and Tris-buffered saline (α -TcpH 1:500, α -TcpP 1:1,000, α -RNA polymerase β' 1:1,000 and α -TcpA 1:100,000) and incubated with the membranes for 1 hour at room temperature. Membranes were washed three times for 5-15 minutes with Tris-buffered saline. Secondary antibodies (Sigma Aldrich) were diluted in 5% non-fat milk in Tris-buffered saline (Goat anti-Rabbit IgG-HRP 1:2,000 and Mouse anti-Rabbit IgG-HRP 1:2,000) and incubated as before. Membranes were washed three times for 5-15 minutes with Tris-buffered saline and then incubated with SuperSignal HRP Chemiluminescence substrate (Thermo Fisher). Membranes were imaged with an Amersham Imager 600.

4.3.6 – Enzyme Linked-Immunosorbent Assay (ELISA)

ELISAs were performed as previously described (382). *V. cholerae* cells were subcultured from overnight cultures to an optical density of 0.01 in 10 ml of LB pH 6.5. Cultures were incubated at 30 °C for a total of 24 hours. Cells were collected by centrifugation at 2450X g for 15 minutes. 1 ml of culture supernatant was collected and the remaining supernatant was discarded. All steps of EILSA were performed at room temperature. 10 µl of culture supernatant was added to 140 µl PBS-T (phosphate buffered saline, 0.05% Tween-20, 0.1% BSA) in row A of plates coated with GM1 (monosialotetrahexosylganglioside). Samples were diluted (1:3) down each column and incubated at room temperature for 1 hour. Plates were then washed with PBS-T three times. Primary (α -CtxB 1:8000, Sigma Aldrich) and secondary antibody (Goat anti-Rabbit IgG-HRP 1:5,000, Sigma Aldrich) were diluted in PBS-T. 100 µl of diluted antibody was added to each well and incubated for 1 hour at room temperature. Plates were again washed with PBS-T as before. 100 µl of TBS (3,3',5,5'-tetramethylbenzidine, Sigma) was added to each well and incubated for 5-10 minutes. The reaction stopped by addition of 100 µl of 2M sulfuric acid and the optical density (450 nm) was measured for each well using SPECTROstar Omega plate reader (BMG LABTECH).

4.3.7 – Infant Mouse Colonization

Infant mouse colonization experiments were performed as previously described (383). Briefly, three- to six- day old CD-1 mice (Charles River, Wilmington, MA) were orogastrically inoculated with $\sim 1 \times 10^6$ bacterial cells after 2 hours of separation from their

mothers. Infant mice were kept at 30°C in sterile bedding and euthanized about 21 hours after infection. Mouse intestines (small and large) were weighed in 3 ml PBS and homogenized. Homogenates were then serially diluted in PBS, spread on LB plates containing streptomycin, and incubated at 37°C overnight.

4.3.8 – Real-time quantitative PCR (RT-qPCR)

RT-qPCR experiments were performed as previously described (384). RNA was preserved by resuspending *V. cholerae* cells in 1 ml of Trizol (Sigma Aldrich) and then extracted from cells using an RNEasy kit (Qiagen) according to manufacturer's instructions. RNA was then treated with Turbo DNase for 30 minutes at 37°C. After DNase treatment, RNA quality was determined by detection of large and small ribosomal subunits via 2% agarose gel. RNA quantity was then measured using a Nanodrop spectrophotometer (Thermo Scientific). cDNA was generated from DNase treated RNA using Superscript III reverse transcriptase (Thermo Scientific) as previously described (384). 5 ng of cDNA was used with SYBR green master mix (Applied Biosystems) to perform the RT-qPCR. *recA* was used as a housekeeping gene of reference to calculate the threshold values ($\Delta\Delta C_T$) (385). See Table D.2 for primers.

4.3.9 – β -Galactosidase activity assay

V. cholerae cells were subcultured from overnight cultures to an optical density of 0.01 in 50 ml of LB pH 6.5. *V. cholerae* strains were grown for 4 hours under Vir Ind conditions. Following incubation cultures were centrifuged (2450 X g 15 minutes),

resuspended in 1 ml LB, and then 200 µl of the culture resuspension was transferred to fresh media (Vir Ind, Vir Ind supplemented with crude bile/ cholate and deoxycholate (purified bile)/ α-linolenic acid, or non-Vir Ind). Cultures were grown for an additional 4 hours under their indicated condition. At the indicated time point (4 hours or 8 hours) 1.5 ml of culture was removed, centrifuged (4000 X g 15 minutes), and resuspended in 1 ml of Z-buffer (Na₂HPO₄ 60mM, NaH₂PO₄ 40mM, KCl 10mM, MgSO₄ 1mM, β-mercaptoethanol 50mM, pH7.0). β-galactosidase activity and Miller units were determined as previously described (386).

4.3.10 – Subcellular Fractionation

Cells were fractionated following the Tris-sucrose-EDTA method (200mM Tris-HCl pH 8.5, 500mM sucrose, 1mM EDTA, pH 8.0) (387). *V. cholerae* cells were subcultured from overnight cultures to an optical density of 0.01 in 50 ml of LB pH 6.5. After 2 hours of incubation, plasmids were induced by the addition of arabinose (final concentration of 0.1%) at 30°C with mild shaking (110 rpm), and then cultured for an additional 5 hours. All steps of the fractionation procedure were performed on ice as follows (387). Spheroplast fractions (i.e., cytoplasm and the cytoplasmic membrane) were resuspended in 500 µl 0.45% NaCl. To lyse the spheroplasts 50 µl of 10% SDS were added, and samples were then boiled for 5-10 minutes. Periplasmic fractions were concentrated using trichloroacetic acid (TCA) (387, 388). Pelleted whole cells were resuspended in 50-200 µl of resuspension buffer (50mM Tris-HCl, 50mM EDTA, pH 8.0). Cells were then lysed by the addition of lysis buffer (10mM Tris-HCl, 1% SDS) and boiled for 5-10 minutes. All fractions were stored at -20 °C until use.

Soluble and insoluble fractionation of *V. cholerae* cells was performed as described by Miller *et. al.*, with modifications (342). Initial steps of the Tris-sucrose-EDTA extraction were followed regarding growth and collection of *V. cholerae* cells. Following collection, cells were resuspended in 10 ml of lysis buffer (10 mM Tris HCl pH 8.0, 750mM sucrose, EDTA-free protease inhibitor, 2mM EDTA, 50 µg/ml lysozyme, 10 U/ml DNase 1) and incubated on ice for 20 minutes. Cells underwent two rounds of lysis via French press (7,000-10,000 psi). Cellular debris was removed by centrifugation (1200 X g for 10 minutes) and supernatant was retained. Insoluble (i.e., the inner and outer membrane) and soluble fractions were separated by ultracentrifugation (100,000 x g for 2 hours at 4 °C). The pellet, containing the membrane fraction, was collected and resuspended in 500 µl 5mM EDTA and 25% sucrose. The insoluble membrane fraction underwent a second round of ultracentrifugation and was then collected. All samples were stored at -80°C until further use.

4.3.11 – Triton X-100 Subcellular Fractionation

V. cholerae cells were subcultured from overnight cultures to an optical density of 0.01 in 50 ml of LB pH 6.5 and grown under Vir Ind for 6-8 hours. Cells were then pelleted by centrifugation (2450 X g 15 minutes), and resuspended in 500 µl of phosphate buffered saline (pH 7.4). Cells were then pelleted by centrifugation (2450 X g 15 minutes).

For spheroplast fractionation, cells were resuspended in 100 µl of 200mM Tris HCl. After resuspension, components were added sequentially to each sample: 200 µl of 200mM Tris HCl and 1M sucrose, 20 µl of 10mM EDTA, 20 µl of lysozyme (10mg/ml), 10 µl of protease inhibitor cocktail (Sigma), and 600 µl of H₂O. Samples were then incubated

at room temperature for 30 minutes. After room temperature incubation 700 μ l of 2% Triton X-100, 50mM Tris HCl, and 10mM MgCl₂ was added.

For gentle cell lysis, pelleted cells were resuspended in 5 ml of Triton X-100 buffer (1% Triton X-100, 10mM imidazole, 500mM HEPES, 10% glycerol, 2M MgCl₂). Samples then underwent three rounds of freeze-thaw lysis in 180 proof ethanol at -80°C.

Triton X-100 soluble and insoluble membrane fractions were then separated by ultracentrifugation (100,000 X g 1 hour). The supernatant (i.e., the Triton X-100 soluble fraction; TS) and the pellet (i.e., the Triton X-100 insoluble fraction; TI) were collected. The TI fraction was resuspended in 500 μ l of 2% SDS and 10mM imidazole. The TS fraction was concentrated using Amicon protein concentrators with a 10KDa cutoff (Sigma).

4.3.12 – Co-affinity precipitation

For co-affinity precipitation experiments *V. cholerae* cells were grown as described in the Triton X-100 Subcellular Fractionation section. After cells were suspended in PBS, proteins were cross linked by adding 1mM Dithiobis(succinimidyl propionate) (DPS) to cell suspensions and samples were incubated on ice for 30 minutes. DPS was quenched by adding Tris HCl pH 8.5 to final concentration of 1M and incubating cells on ice for an additional 15 minutes. Cells were then pelleted by centrifugation (2450 X g 15 minutes) and TI and TS fractions were collected via the gentle cell lysis method discussed in the Triton X-100 Subcellular Fractionation section. TI fractions were resuspended in 5ml of 2% sodium dodecyl-sulfate and 10mM imidazole. After collection of TI and TS fractions 100 μ l of His-affinity gel (i.e., Ni-NTA Magnetic Agarose Beads) (ZYMO Research) and

10 μ l of protease inhibitor cocktail (Sigma) was added to the TI and TS fractions and samples were incubated on a rocking platform overnight at 4°C. TI samples were then incubated at 40°C for 20 minutes to completely solubilize the sample. Samples were then centrifuged (2450 X g 15 minutes) and Ni-NTA agarose beads were washed three times with either Triton X-100 buffer or 2% sodium dodecyl-sulfate and 10mM imidazole. between wash steps TI Ni-NTA agarose beads were incubated at 40°C for 5 minutes. Equal volume of laemmli buffer was added to each sample (BIO-RAD) and then boiled for 5 minutes. Boiled samples were then used directly for western blot analysis.

4.4 – Results

4.4.1 – TcpH Maintains *in vitro* Activity Upon Alteration of its Transmembrane and Periplasmic Domains

To identify regions within TcpH that are critical for its role in protecting TcpP from RIP we constructed chimeric transmembrane domain fusions (TM) and periplasmic TcpH deletion constructs (Peri). We generated several *tcpH* constructs (as described in Experimental Procedures), but due to stability issues only two TM and one Peri constructs [ToxS TcpH, EpsM TcpH, and TcpH Δ 119-103, respectively] are discussed; the allele encoding each was recombined into the *V. cholerae* genome so as not disrupt the *tcpP* coding sequence are under normal *tcpPH* transcriptional control (Figure 4.1A). Growth dynamics of the resulting strains were unaffected in comparison with wild-type *V. cholerae* in virulence inducing (Vir Ind) conditions (Figure D.1A). We evaluated the constructs also by measuring TcpP levels, *toxT* transcription, and TcpA and CtxB production *in vitro* (Figure 4.1B and Figure D.2). All the TcpH constructs protected TcpP similar to WT TcpH

or better than $\Delta tcpH$ (Figure 4.1B). This suggests that the TcpH constructs are capable of inhibiting RIP of TcpP and thereby the TcpH TM and Peri constructs support TcpP function to stimulate *toxT* transcription.

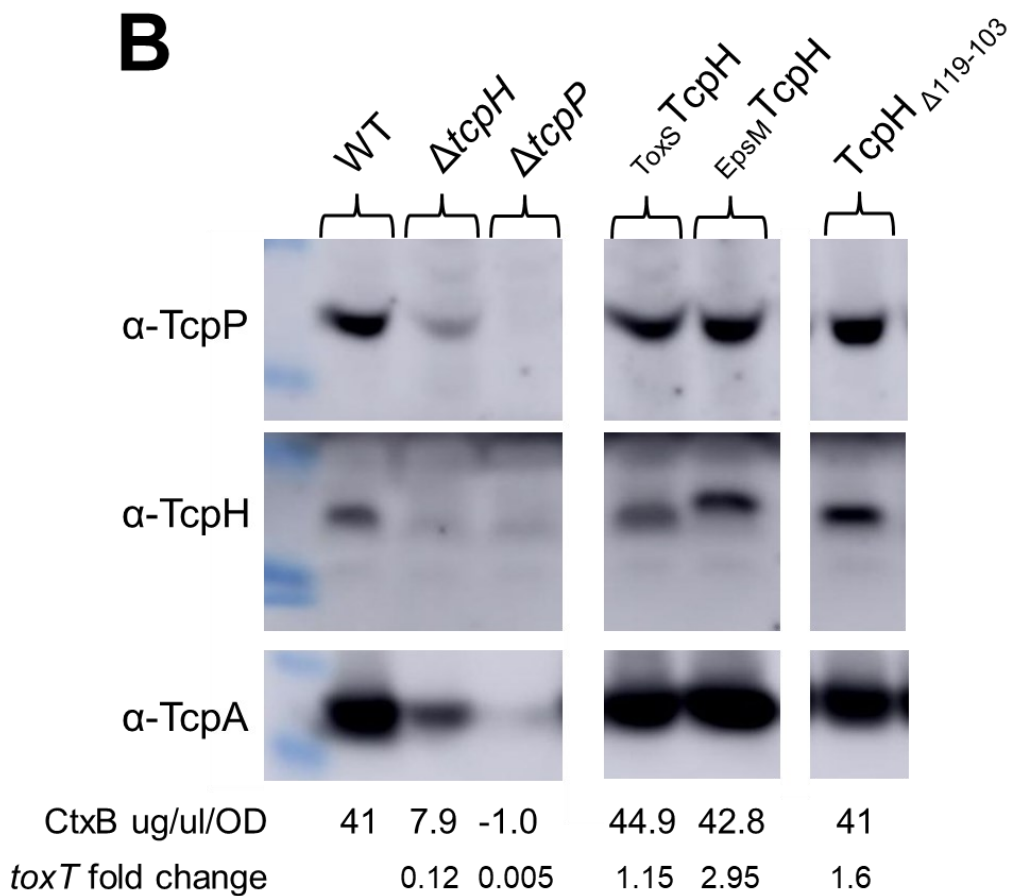
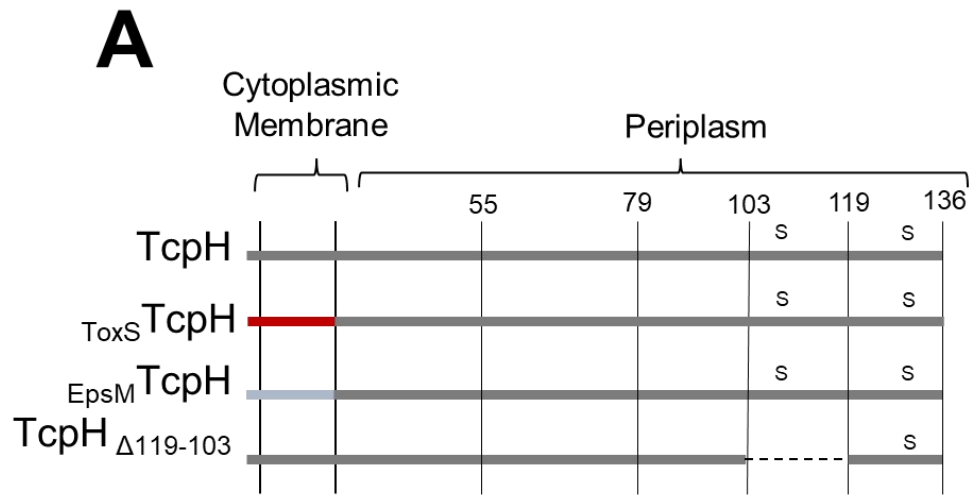


Figure 4.1: **TcpH transmembrane and periplasmic constructs protect TcpP, support *toxT* transcription, and virulence factor production.** A) Diagram of TcpH

Figure 4.1 (cont'd)

transmembrane constructs (E_{psM} TcpH and T_{oxS} TcpH) and periplasmic construct (TcpH $_{\Delta 119-103}$). TcpH has a single transmembrane domain (also a Sec signal sequence), at its N-terminus, and two periplasmic cysteine residues (C114 and C132), represented by “s”. The transmembrane domain of TcpH was replaced with the transmembrane domain of ToxS (T_{oxS} TcpH) and EpsM (E_{psM} TcpH) as both ToxS and EpsM are known to be localized to the cytoplasmic membrane with similar domain topology at TcpH (207, 389). As the majority of TcpH is localized in the periplasm, we also reasoned that the periplasmic domain was critical for TcpH function. In-frame deletion of periplasmic residues are indicated by a dashed line, based on TcpH secondary structure. B and C) *in vitro* characterization of TcpH transmembrane and periplasmic chromosomal constructs grown under virulence inducing conditions. B) Western blots of whole-cell lysates probed with α -TcpP (top), α -TcpH (middle), and α -TcpA (bottom). In addition, CtxB levels and *toxT* transcription were also determined for the TcpH transmembrane and periplasmic constructs. Average CtxB levels and *toxT* fold change (relative to WT) for each strain are indicated below the western blot. See Figure D.2 for full view of the data. See Figure E.1 for full view of western blots in panel B.

4.4.2 – TcpH TM domain is Critical for Colonization of Infant Mice

In vitro experiments indicate that the TM and Peri domain of TcpH can withstand considerable modifications and still maintain function. Thus, we tested the fitness of the TcpH TM and Peri constructs *in vivo*. We infected infant mice with the TcpH TM and Peri constructs (Figure 4.2A). Despite TcpH-dependent virulence gene transcription profiles of strains expressing T_{oxS} TcpH, and E_{psM} TcpH being analogous to cells expressing wild-type TcpH *in vitro*, these strains colonized infant mice to significantly lower levels than wild type, more closely resembling a $\Delta tcpH$ strain (Figure 4.2A). TcpH $_{\Delta 119-103}$ supported the same level of TcpH-dependent virulence gene transcription *in vitro* as both T_{oxS} TcpH and E_{psM} TcpH, but colonized infant mice to a similar degree as wild type (Figure 4.2A). The inocula of T_{oxS} TcpH and E_{psM} TcpH used to infect infant mice produced similar levels of TcpA compared to wild type (Figure 4.2B). We concluded that the colonization defects of the TM TcpH constructs were likely due to an inability of strains lacking the natural

TcpH transmembrane domain to express colonization factors – particularly TcpA – *in vivo*.

To determine whether the presence of other microbes in the gastrointestinal tract might influence the ability of strains expressing TcpH with altered TM domains to support virulence gene transcription, we cultured wild type and the TcpH constructs (TM and Peri) aerobically in both filter sterilized and non-sterile (i.e., non-filtered) mouse fecal media for 21hrs at 37°C (Figure D.3). All strains exhibited similar growth rates and final cell densities in both filter sterilized and non-sterile mice fecal media (Figure D.3). In addition, we quantified TcpA levels in cell lysates after 21 hours of growth in sterile mouse fecal media. While the growth rates were very similar between wild type and strains expressing altered TcpH proteins, the strains expressing T_{oxS} TcpH and E_{psM} TcpH produced TcpA levels below that of wild type (Figure 4.2C). The strain expressing the TcpH protein with a periplasmic deletion was unaffected for TcpA transcription (Figure 4.2C). Taken together, these data suggest that the TcpH transmembrane domain is critical for TcpH to respond to cues present in the gastrointestinal tract and protect TcpP from RIP, thereby supporting downstream virulence factor production. Due to their WT levels of colonization and ability to support WT levels of TcpA synthesis in mouse fecal media we chose to exclude the TcpH Peri construct from further experiments.

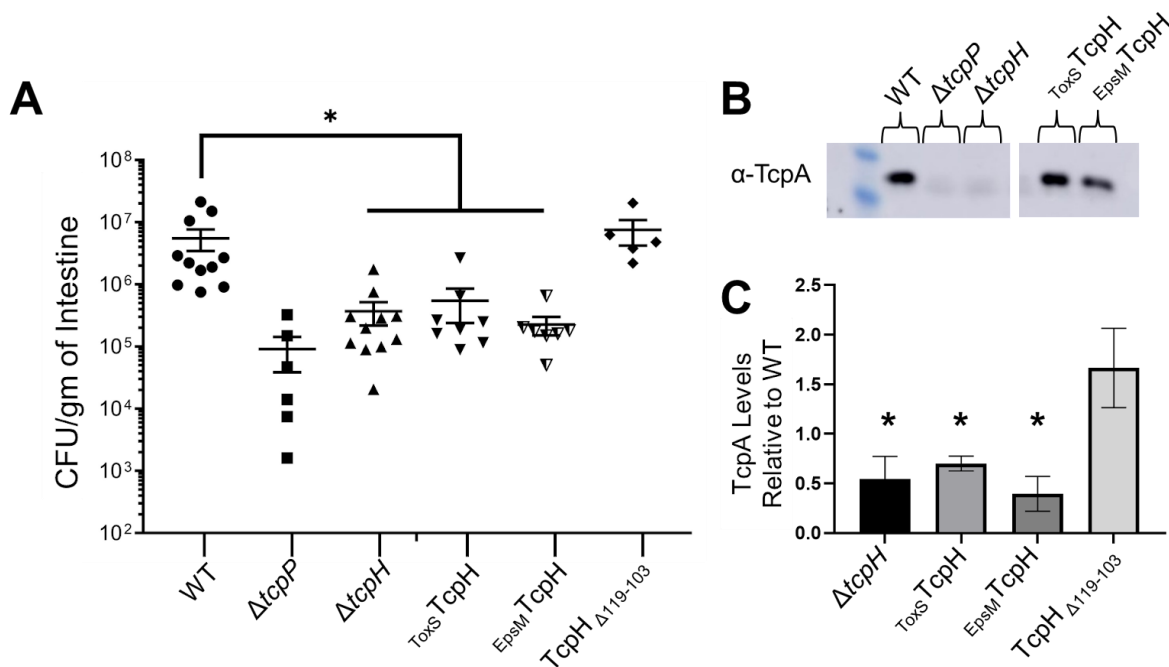


Figure 4.2: TcpH transmembrane constructs have a colonization defect in infant mice. A) Colony forming units per gram of 3-6 day old infant mouse intestine. Infant mice were orally infected with $\sim 1 \times 10^6$ cells and intestines were harvested 21 hours post infection. Mouse intestines were homogenized, serially diluted, and plated on LB plates containing streptomycin. Asterisk indicates a p-value of less than 0.05. A Mann-Whitney U test was used to determine statistical significance between WT and each TcpH transmembrane construct. The horizontal line indicates the average CFU/gm of intestine and is an average of 5-11 biological replicates. Error bars indicate the standard error of the mean. B) Western blots of initial inoculums used to infect infant mice in panel A. C) Relative TcpA levels after 21 h of aerobic growth in sterile mice fecal media (9% w/v). TcpA levels were determined via densitometry, calculated using ImageJ. Averages represent three biological replicates. Error bars represent standard deviation of the mean. A one-tailed Student's t-test was used to determine statistical significance. * Indicates a p-value less than 0.05 and that there is a statistical difference between WT and the indicated sample.

4.4.3 – The TcpH Transmembrane Domain Protects TcpP from RIP

Our data suggests that inhibition of RIP is critical for WT colonization and that TcpP is subject to RIP *in vivo* when TcpH lacks its normal transmembrane domain. While the TM TcpH constructs do support higher levels of TcpP than a $\Delta tcpH$ mutant, it was still unclear if the TM TcpH constructs specifically inhibited RIP of TcpP. In the absence of

TcpH, TcpP is sensitive to degradation and undergoes RIP. Loss of both *tcpH* and *yaeL* leads to the formation of TcpP*, an intermediate degradation product formed by cleavage of TcpP by Tsp alone. TcpP* lacks most of its periplasmic domain and therefore has a lower molecular weight (19 KDa) compared to WT TcpP (~29 KDa), thus allowing us to determine the RIP status of TcpP via western blot. Inhibition of RIP of TcpP, by a functional TcpH, can be observed by the presence of a full sized TcpP band and no TcpP* band. Alternatively, when RIP is left unchecked, the smaller TcpP* band accumulates. When TcpH, _{ToxS}TcpH, or _{EpsM}TcpH constructs were ectopically expressed in a $\Delta tcpH/\Delta yaeL$ mutant background only full length TcpP was observed (Figure D.4). These data show that RIP of TcpP is inhibited by all TM constructs. Given the *in vivo* data, these data further suggest that the TM TcpH constructs are unable to inhibit RIP of TcpP *in vivo*.

4.4.4 – *toxT* Transcription is Enhanced with Crude Bile and is Dependent on the TcpH Transmembrane Domain

Data presented here and other published data indicate that TcpH-dependent RIP inhibition is affected by different *in vitro* and *in vivo* environmental signals and that the trans-membrane domain of TcpH is critical for that function (96, 351, 352). *Vibrio* species use exogenous fatty acids present in bile via the VolA and FadL/FadD pathways (390–394), resulting in modification of phospholipid composition in *Vibrio* species, and influencing growth rate, biofilm formation, and motility (394, 395). Given that TcpH and TcpP require membrane localization, we hypothesized that phospholipid changes, stimulated by fatty acids present in the gastrointestinal tract, would stimulate inhibition of RIP via TcpH.

To test this we supplemented media with Bovine Crude Bile (0.4%), which contains various fatty acids that have been shown to be incorporated into the bacterial membrane (394), and measured *toxT* transcription using a plasmid-based transcription reporter (pBH6119-*toxT*::*GFP*). In wild type cells, *toxT* transcription was elevated in the presence of crude bile, while TcpH TM constructs did not support increased *toxT* transcription (Figure D.5A). This suggested that native TcpH is responding to changes in phospholipid composition to inhibit RIP of TcpP, and that TcpH with the altered transmembrane domain is unable to respond and/or sense the same change. As a negative control, we also measured *toxT* transcription under non-inducing conditions, known to stimulate RIP of TcpP (96, 351, 352), in these conditions *toxT* transcription was indeed reduced (Figure D.5A). In addition, we measured *toxT* transcription in $\Delta tcpP$ and $\Delta tcpH$ cells with and without crude bile present, and we observed no increase in *toxT* transcription (Figure D.5A). This indicates that our *toxT* transcription reporter is accurate, and that the conditions used here do not promote TcpP function in the absence of TcpH. Secondly, we measured *toxT* transcript levels in WT cells grown in the presence of crude bile via RT-qPCR (Figure D.5B). Similar to our transcription reporter, we observed an increase in *toxT* transcription. While *toxT* transcription is elevated in the presence of α -linolenic acid in WT cells, the fold increase in *toxT* transcription is not the same for both methods used (Figure D.5AB). We believe the difference in the fold increase in *toxT* transcription when quantifying *toxT* mRNA, via RT-qPCR, or GFP fluorescence, from the *toxT*::GFP reporter, is due to the maturation time of GFP molecules (~30 minutes). Additionally, it is unknown if α -linolenic can reduce fluorescence of GFP directly or reduce translation of GFP mRNAs via direct interaction. These are also potential mechanisms could lead to overall

reduced increase in *toxT* transcription observed via the *toxT*::GFP reporter. Regardless, both methods used to quantify *toxT* transcription, RT-qPCR and the *toxT*::GFP reporter, demonstrate that there is a statistically significant increase in *toxT* transcription in WT cells in the presence of α -linolenic. Lastly, we found that native TcpH and TcpH with an altered TM have similar growth rates in crude bile supplemented Vir Ind media (Figure D.1B). These data support a hypothesis that TcpH responds to host stimuli, specifically fatty acids or constituents of crude bile, and antagonizes RIP of TcpP which in turn leads to increased *toxT* transcription. Given that elevated *toxT* transcription requires TcpH to have its native transmembrane domain, we hypothesize that TcpH senses changes in phospholipid composition or membrane fluidity, via its transmembrane domain, to inhibit RIP of TcpP.

4.4.5 – α -Linolenic Acid Enhances *toxT* Transcription by Promoting TcpH-Dependent Enhanced RIP Inhibition

Crude Bile is a mixture of saturated and unsaturated fatty acids, as well as bile salts (e.g., cholate and deoxycholate). We sought to determine whether bile salts or fatty acids in crude bile were responsible for elevated *toxT* transcription in WT. To test this, we supplemented virulence inducing media with cholate/deoxycholate (Purified Bile) (100 μ M of each), palmitic acid (500 μ M), stearic acid (500 μ M), linoleic (500 μ M), α -linolenic acid (500 μ M), arachidonic acid (500 μ M), and docosahexaenoic acid (500 μ M). Using the *toxT*::GFP transcription reporter plasmid, we observed elevated *toxT* transcription in wild type cells with only crude bile or α -linolenic acid present (Figure 4.3A). Addition of crude bile or α -linolenic acid did not result in increased *toxT* transcription in $\Delta tcpH$ or $\Delta tcpP$ cells (Figure 4.3A), demonstrating that TcpH is still needed to inhibit RIP and TcpP is

necessary to promote *toxT* transcription. Lastly, none of the purified components of crude bile resulted in statistically significant increased levels of *toxT* transcription in cells expressing E_{psM} TcpH or T_{oxS} TcpH (Figure 4.3A and Figure D.6, respectively). In addition, we also found that α -linolenic acid stimulates *toxT* transcription in a dose-dependent manner (Figure D.7). To confirm our results, we measured *toxT* mRNA levels using RT-PCR in WT cells grown under the same conditions. Consistent with the reporter plasmid data, we found that *toxT* mRNA was elevated in the presence of α -linolenic acid (~2.5 fold) (Figure D.8A). There was no difference in growth rate between WT and the TcpH TM constructs when cultured with α -linolenic acid (Figure D.1D). Considering that cells expressing T_{oxS} TcpH and E_{psM} TcpH do not colonize mice as well as those expressing native TcpH, these data suggest that TcpH responds to changes in phospholipid composition or membrane fluidity stimulated by α -linolenic acid, and that modifying the TM domain of TcpH renders the protein unable to respond to these changes to enhance inhibition of RIP.

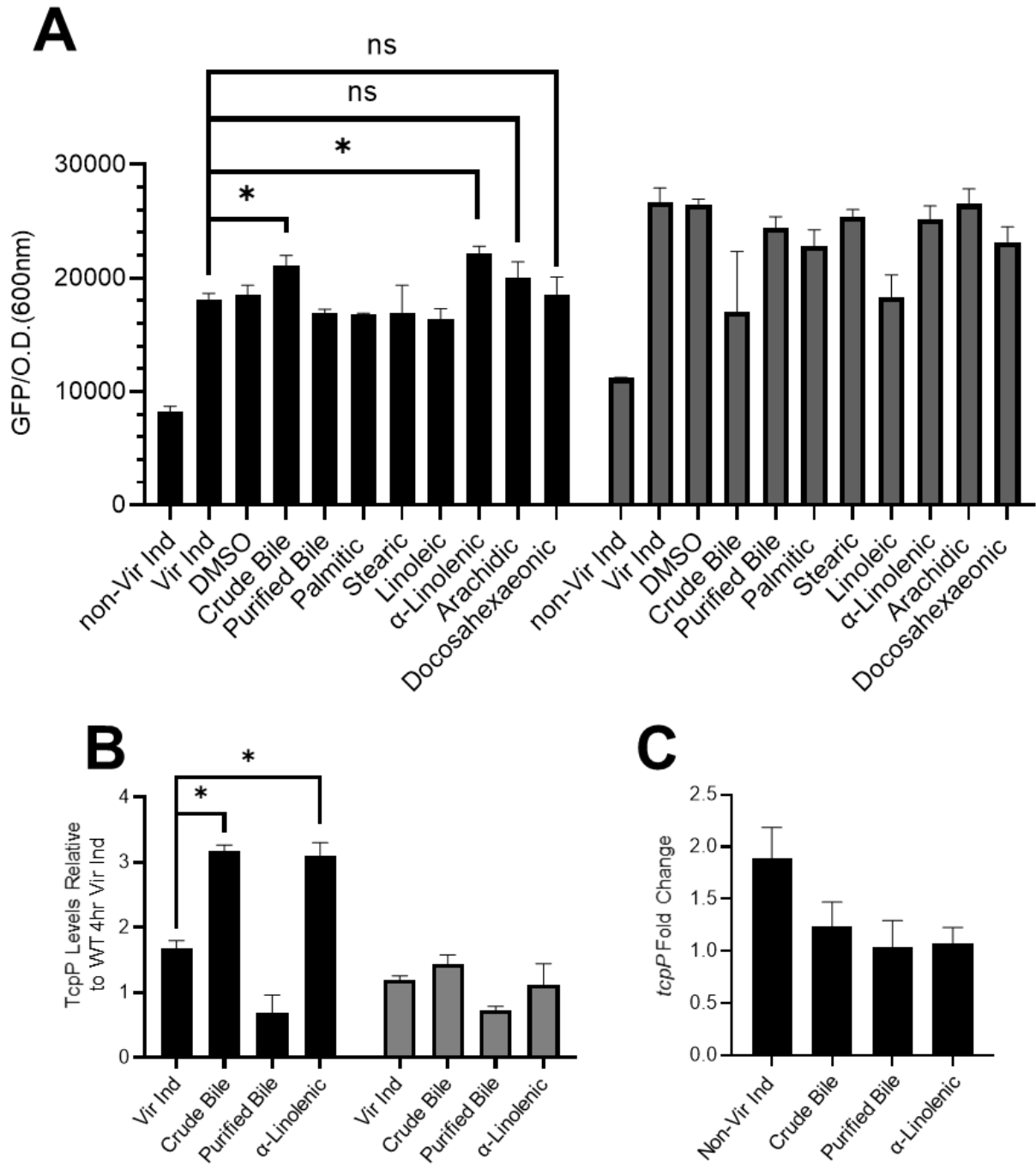


Figure 4.3: α -Linolenic acid stimulates *toxT* transcription, elevated TcpP levels, and does not increase *tcpP* transcription. A) *toxT* transcription in WT (black bars) and $E_{psM}TcpH$ (gray bars) was determined using a plasmid based *toxT::GFP* transcription reporter. See supplemental methods for information on how *V. cholerae*

Figure 4.3 (cont'd)

cells were cultured. *toxT* transcription was determined by measuring GFP fluorescence (excitation 488nm and emission 515nm) and optical density (600nm). The data here are an average of three or more biological replicates and error bars represent the standard error of the mean. Two-tailed Student's t-test was used to determine statistical significance. * Indicates a p-value of less than 0.05. B) TcpP levels in WT (black bars) and E_{psM} TcpH (gray bars) relative to WT cells cultured under virulence inducing conditions (see supplemental methods for details on growth conditions). Densitometry, calculated by ImageJ, was used to determine relative abundance of TcpP. Averages represent three biological replicates. Error bars represent standard error of the mean. Two-tailed Student's t-test was used to determine statistical significance. * Indicates a p-value of less than 0.05. C) *tcpP* transcription in WT *V. cholerae* cells using RT-qPCR, determined via $\Delta\Delta C_T$ method. Cells were incubated in Vir Ind for 4hrs and then transferred to indicated conditions for an additional 4hrs. RNA was collected at the 8hr time point. *tcpP* transcription is relative to WT Vir Ind. Averages represent three biological replicates and error bars represent standard error of the mean.

We reasoned that enhanced *toxT* transcription in the presence of crude bile or α -linolenic acid was due to inhibition of RIP, leading in turn to elevated levels of TcpP. Thus, we quantified TcpP levels under virulence inducing conditions supplemented with crude bile or α -linolenic acid (Figure 4.3B, see Figure D.9 for a view of western blots used to quantify TcpP levels). TcpP levels in wild type cells were significantly elevated in the presence of crude bile or α -linolenic acid (Figure 4.3B). In contrast, TcpP levels in cells expressing E_{psM} TcpH grown with or without α -linolenic acid were similar (Figure 4.3B). Furthermore, loss of TcpH led to degradation of TcpP under all conditions indicating that Tsp and YaeL activity is not inhibited by the addition of crude bile or α -linolenic acid (Figure D.9). We conclude that i) elevated *toxT* transcription in the presence of crude bile or α -linolenic acid is due to enhanced inhibition of RIP via TcpH and ii) that altering the phospholipid composition of the cells with exogenous crude bile or α -linolenic acid enhances the TcpH function in RIP inhibition through a mechanism that requires the native transmembrane domain.

As TcpP levels are elevated upon supplementation of crude bile or α -linolenic acid, we considered it possible that elevated *tcpP* transcription could also contribute to elevated TcpP levels. In support of this, linoleic acid has been shown to rapidly diffuse into the cytoplasm of *V. cholerae* (46, 396). To determine if *tcpP* transcription is influenced by crude bile or α -linolenic acid we measured *tcpP* transcription in wild type *V. cholerae* cells using both RT-PCR and a transcription reporter, *tcpP::lacZ*. Neither crude bile nor linoleic acid supplementation led to increased *tcpP* transcription (Figure 4.3C and Figure D.8B). These data indicate that crude bile and α -linolenic acid influence TcpP levels post-transcriptionally supporting the hypothesis that these conditions lead to RIP inhibition by TcpH.

We analyzed the fatty acid profile of phospholipids from *V. cholerae* cells cultured with and without α -linolenic acid to determine if α -linolenic acid is incorporated into the cytoplasmic membrane under our conditions (Figure D.8C). In the presence of α -linolenic acid more than 80% of acyl chains within *V. cholerae* were 18:3. This is consistent with prior published data (394, 395) and demonstrates that under our conditions *V. cholerae* cells are remodeling the fatty acid content of their phospholipids. Given that the vast majority of fatty acids detected are 18:3, this data suggests that *V. cholerae* cells are directly utilizing exogenous α -linolenic acid for phospholipid synthesis (Figure D.8D).

4.4.6 – Co-Association of TcpP and TcpH with Detergent-Resistant Membranes is Required for Enhanced RIP Inhibition

Collectively these data demonstrate that under conditions that modify phospholipid composition, TcpP levels are enhanced, and *toxT* transcription is increased. Elevated levels of TcpP are due to enhanced inhibition of RIP by TcpH rather than increased *tcpP* transcription, and this inhibitory function requires the native TcpH TM domain. In addition to α -linolenic acid, arachidonic and docosahexaenoic acid modify phospholipid composition in *V. cholerae* (394). Despite causing similar changes to the phospholipid profile, these polyunsaturated fatty acids do not have a significant effect on *toxT* transcription (Figure 4.3A and Figure D.6). These data indicate the phospholipid profile is not predictive of TcpH dependent inhibition of RIP. Exogenous fatty acids can be utilized directly as acyl chains in *de novo* phospholipid synthesis (397, 398). Thus, while gross phospholipid composition can remain similar upon supplementation of α -linolenic, arachidonic, and docosahexaenoic acid, (i.e., relative abundance of cardiolipin, phosphatidylglycerol, and phosphatidylethanolamine) the overall biophysical properties of the cytoplasmic membrane (i.e., membrane fluidity) can differ due to differences in acyl chain composition. We reasoned that the differences in observed TcpH-dependent enhanced RIP inhibition could be due to differences in the biophysical properties of the cytoplasmic membrane (i.e., membrane fluidity).

Poly-unsaturated fatty acids (PUFA), such as omega-3 fatty acids, have been shown to influence lipid-ordered membrane domains within the cytoplasmic membrane of T-cells (399, 400). Lipid-ordered membrane domains, also called lipid rafts, are regions of the membrane that are enriched in saturated fatty acids, cholesterol (or hopanoids for

some bacterial species), and proteins with specific TM domain qualities (typically long TM domain(s) and low surface area) (372, 379, 401). As a result, lipid ordered membrane domains tend to be thicker and less fluid than other areas of the membrane (372). n3-PUFA (i.e., omega-3 fatty acids) increase the size and stability of lipid-ordered membrane domains (372, 399, 400). We hypothesized that TcpP and TcpH molecules are able to associate within lipid-ordered membrane domains and that α -linolenic acid supplementation increases association of TcpP and TcpH molecules with the lipid-ordered membrane domain.

Lipid ordered membrane domains, also known as detergent resistant membranes (DRMs), were discovered due to their insolubility in Triton X-100 (376, 402). Triton X-100 has been used in both eukaryotic and prokaryotic organisms to isolate lipid ordered and disordered membrane domains (367–372). Thus, to test our hypotheses we utilized Triton X-100 to separate lipid ordered and lipid disordered membrane domains from cellular lysates.

Under Vir Ind conditions, TcpP and TcpH associate with Triton X-100 insoluble (TI; considered to be enriched with lipid ordered membrane domains) and Triton X-100 soluble membrane fractions (TS; considered to be enriched with lipid disordered membrane domains) (Figure 4.4AB). Supplementation with α -linolenic acid resulted in an increase of both TcpP and TcpH in the TI fraction (Figure 4.4AB and Figure D.10). These data support the hypothesis that α -linolenic acid promotes enhanced RIP inhibition by increasing association of TcpP and TcpH with Triton X-100 insoluble membrane domains. Similar to TcpH, E_{psM} TcpH also associated with both the TI and TS membrane fractions (Figure 4.4CD). In contrast to native TcpH, there was no observable increase in E_{psM} TcpH

levels in the TI fraction upon supplementation of α -linolenic acid (Figure 4.4CD). These data suggest that E_{psM} TcpH is unable to support enhanced RIP inhibition due to an inability to increase association with lipid ordered membrane domains.

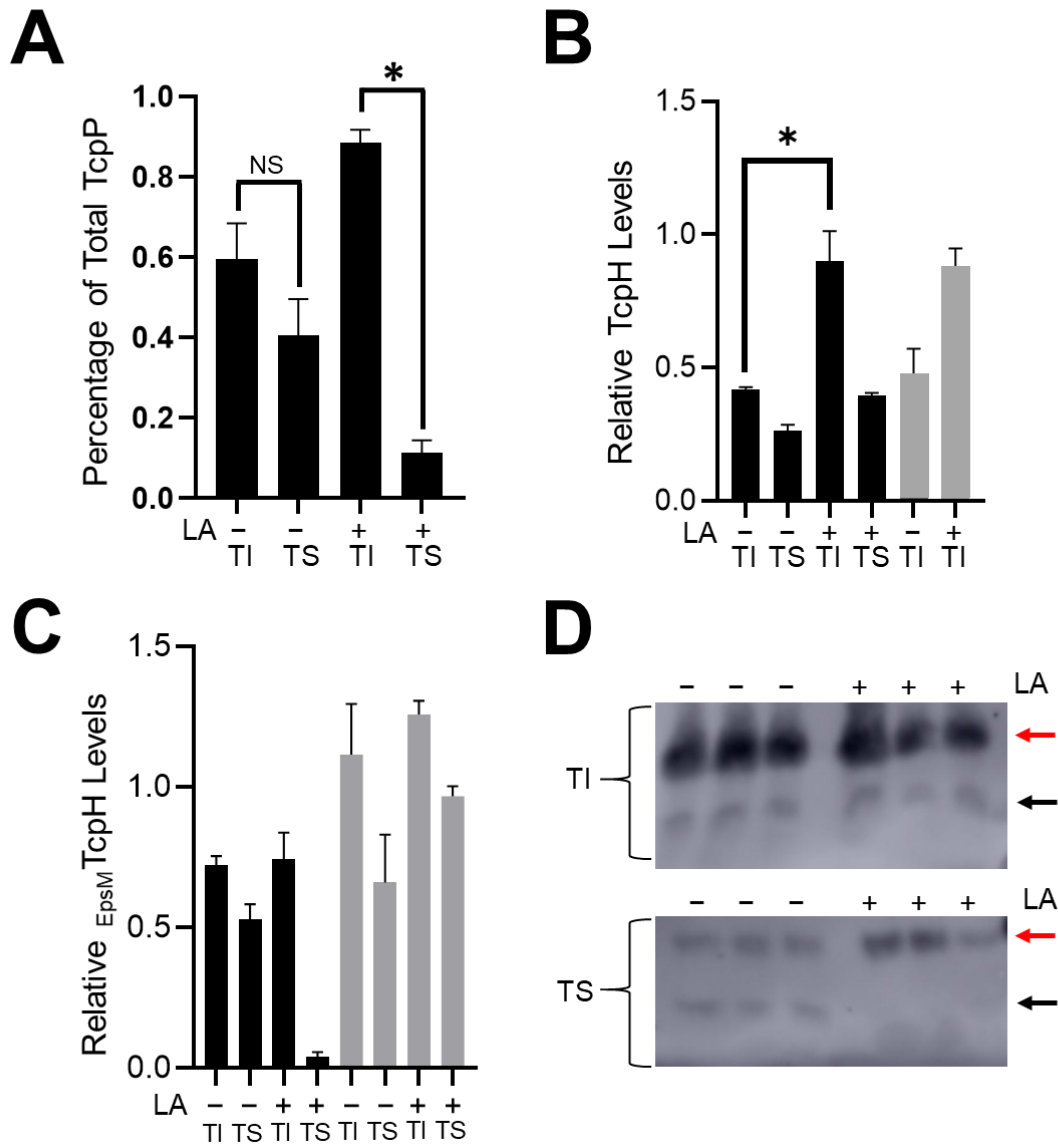


Figure 4.4: **TcP and TcPH abundance increases in detergent resistant membranes in the presence of α -linolenic acid.** A) Percentage of total TcP molecules within the Triton soluble (i.e., TS; lipid disordered) and Triton insoluble (i.e., TI; lipid ordered) fractions in WT cells. Percentage of TcP within the TI and TS fractions was calculated by normalizing to the total amount TcP in both the TI and TS fractions. Non-normalized TcP levels were measured via densitometry using ImageJ. B)

Figure 4.4 (cont'd)

Relative levels of TcpH within the TI and TS membrane fractions measured via densitometry using ImageJ. C) Relative levels of $E_{psM}TcpH$ in TS and TI fractions measured via densitometry using ImageJ. B and C) Black bars indicate TI and TS membrane fractions collected by spheroplast lysis, and gray bars indicate TI and TS samples collected using a gentle freeze thaw lysis. Cells that were cultured in α -linolenic acid (LA, 500 μ M) are indicated by +. TcpH and $E_{psM}TcpH$ levels were normalized to a non-specific band (19KDa) that is equally distributed within TI and TS fractions (see panel D and Figure D.11A). D) Representative western blots of $E_{psM}TcpH$ TI and TS membrane fractions. Black arrows mark the TcpH bands, and red arrows mark the non-specific band that serves as a loading control. The data here are an average of three or more biological replicates, and error bars represent the standard error of the mean. A two-tailed student's T-test was used to determine statistical significance. * indicates a p-value less than 0.05, and NS indicates a lack of statistical significance (i.e., p-value greater than 0.05).

Prior studies revealed that studying lipid ordered membrane domains with this biochemical method can yield dramatically different results with changes in detergent concentration and temperature (403). To determine if our results were robust, we performed the same experiments with an alternative biochemical method to extract lipid ordered membrane domains. By altering the lysis method and the temperature at which cell lysis occurs we found the same TI and TS association trend for TcpH and $E_{psM}TcpH$ with and without α -linolenic acid present (Figure 4.4BC). We found a shift in the percentage of TcpP molecules present in the TI and TS fraction (~40% of TcpP molecules were present in the TI fraction and the remaining ~60% was present in the TS) under Vir Ind conditions (Figure D.10B). However, upon supplementation of α -linolenic acid to Vir Ind conditions, we found TcpP molecules maintained their preference for the TI fraction despite the change in our extraction method (Figure D.10B). All told, these data suggest that enhanced RIP inhibition occurs due to increased association of both TcpP and TcpH with the TI fraction, and that the TM domain of TcpH drives this association with the TI fraction upon α -linolenic acid supplementation.

Excluding $E_{psM}TcpH$, it remained unclear if α -linolenic acid supplementation induced a general association of membrane proteins to the TI fraction. To test this, we quantified levels of a loading control, a 19KDa non-specific band, in TI and TS fractions with and without α -linolenic acid (Figure D.11A). We found that there was no change in TI or TS abundance of the loading control with α -linolenic acid supplementation (Figure D.11). These data indicate that α -linolenic acid supplementation does not induce a general association of proteins with the TI fraction. In addition, we took an unbiased approach and characterized the proteome of the TI and TS fractions collected from WT cells (Supplemental File 4.1). Similarly, we found that α -linolenic acid supplementation does not induce a general association with the TI fraction for all proteins detected. Furthermore, we also found that with α -linolenic acid supplementation the TI fraction had a higher association of 16:0 fatty acids and lower association of 18:3 fatty acids than the TS fraction (Figure D.11B). This is consistent with prior studies that indicate that lipid ordered membrane domains are enriched with saturated fatty acids (377).

4.4.7 – TcpP and TcpH Interaction is critical for inhibition of RIP

Our data indicate that increased association of TcpP and TcpH molecules in the TI fraction results in enhanced RIP inhibition. The mechanism underlying this RIP inhibition remains unclear. Prior studies have indicated that lipid-ordered membrane domains (which are also Triton insoluble) function as protein concentrators and thereby promote interaction between membrane localized proteins (50). We hypothesized that enhanced co-association within the TI fraction increased RIP inhibition due to direct interaction between TcpP and TcpH. To test direct TcpP-TcpH interaction, we used a co-affinity precipitation approach. We genetically fused a His(6x)-Hsv or Hsv-His(6x) tag to

the C-terminus and N-terminus, respectively, of TcpP, resulting in *tcpP-His-Hsv* and *Hsv-His-tcpP*. We could then extract TcpP from membrane fractions using NTA-Ni beads and identify TcpH and TcpP in elution fractions with α -TcpH and α -Hsv antibody. Proteins tagged at the amino-terminus are described with the tag noted first (e.g., Hsv-His-TcpP), while those tagged at the carboxy-terminus are described with the tag noted second (e.g., TcpP-His-Hsv).

First, we tested if both the N- and C- terminally-tagged proteins (Hsv-His-TcpP and TcpP-His-Hsv, respectively) function like native TcpP by measuring CtxB production after induction of the fusion proteins with arabinose under Vir Ind conditions. CtxB production was similar to that from cells expressing native TcpP, irrespective of which terminus the tag was placed (Figure D12).

Co-precipitation experiments indicated that the C-terminally-tagged TcpP could associate with TcpH, while the N-terminally-tagged TcpP could not (Figure 4.5AB). Physical interaction between the C-terminally tagged TcpP and TcpH also correlated to protection from RIP, as determined by assessing the stability of the tagged proteins in cells expressing the first-site RIP protease Tsp but lacking the second protease YaeL. In such cells, the product of Tsp action on TcpP accumulates in the cell because the second-site protease YaeL is not present to eliminate it (26, 27). We observed greater accumulation of TcpP degradation intermediates (between 24KDa and 19KDa) in cells expressing N-terminally-tagged-TcpP compared to those expressing C-terminally-tagged TcpP (Figure 4.5C). The 24 kDa TcpP degradation intermediate from N-terminally-tagged TcpP is also observed in cells expressing native TcpP in the absence of TcpH (Figure 4.5CD). Considering that the N-terminally-tagged TcpP is sensitive to RIP even with TcpH

present suggests a defect in its association with TcpH and its recognition by the RIP proteases. Despite this defect, N-terminally-tagged TcpP is capable of supporting WT CtxB production (Figure D12). We believe that this is the result of overexpression of N-terminally-tagged TcpP. Native expression of TcpP leads to accumulation of only TcpP* in a $\Delta tcpH \Delta yaeL$ background (Figure D.4), but overexpression of TcpP in a $\Delta tcpP \Delta tcpH \Delta yaeL$ background yields both full length and TcpP* (Figure 4.5D). These data indicate that artificial elevation of TcpP levels, via overexpression, can outpace RIP of TcpP.

These data also indicate that TcpP-His-Hsv, compared to Hsv-His-TcpP, is less sensitive to RIP in the presence of TcpH. Prior studies have demonstrated that modification of the C-terminus of TcpP can lead to TcpH-independent resistance to RIP (78). To determine if the addition of His-Hsv to the C-terminus of TcpP promotes resistance to RIP independent of TcpH we expressed *tcpP-His-Hsv* and *tcpP* in a $\Delta tcpP \Delta tcpH \Delta yaeL$ background. We found that TcpP* accumulated in both *tcpP* or *tcpP-His-Hsv* expressing cells (~17KDa) (Figure 4.5D). These data show that addition of His(6x)-Hsv to the C-terminus of TcpP does not abrogate the need for TcpH to protect TcpP-His-Hsv from RIP (Figure 4.5D). In summary, our data indicates that TcpP and TcpH interact and that TcpP-TcpH interaction is important for inhibition of RIP of TcpP.

It remains unclear why Hsv-His-TcpP is unable to interact with TcpH. Our prior single-molecule tracking studies indicate that TcpP may be sensitive to RIP while interacting with the *toxT* promoter (74). The Hsv tag is enriched with negatively charged amino acids (Hsv amino acid sequence: QPELAPEDPED). Given that DNA has an intrinsic negative charge, the addition of Hsv-His(6x) to the N-terminus of TcpP may promote a conformation that is similar to the conformation that TcpP molecules adopt

when actively interacting with DNA. It remains unclear if this is the case and requires additional experiments to test this hypothesis.

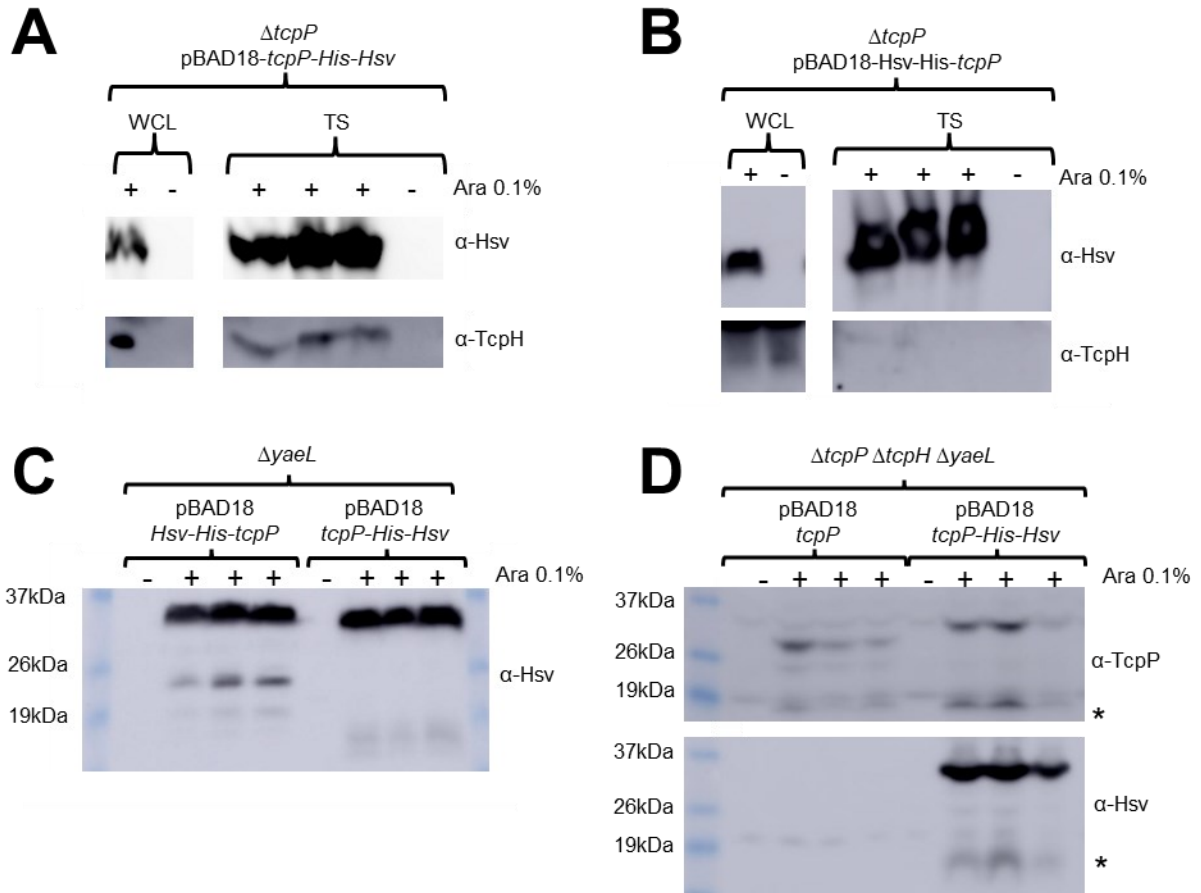


Figure 4.5: TcpP and TcpH interaction is critical for TcpH-dependent inhibition of RIP. A and B) Co-affinity precipitation of ectopically expressed *tcpP*-His-Hsv (A), *Hsv*-His-*tcpP* (B). The data here represent three biological replicates. Triton soluble (TS). C) Ectopic transcription of *Hsv*-His-*tcpP* and *tcpP*-His-Hsv in $\Delta yaeL$ cells under virulence inducing conditions. *Hsv*-His-TcpP is more sensitive to RIP than *TcpP*-His-Hsv, as seen by accumulation of *TcpP* degradation intermediates between 26 and 19 kDa. D) Ectopic transcription of *tcpP* and *tcpP*-His-Hsv in $\Delta tcpP \Delta tcpH \Delta yaeL$ cells under virulence inducing conditions. Samples were probed with α -*TcpP* (top) and α -*Hsv* (bottom) antibodies. *TcpP*-His-Hsv remains sensitive to RIP as accumulation of *TcpP** is observed in *tcpP*-His-Hsv expressing cells, similar to *TcpP*. *: indicates accumulation of *TcpP**. A-D) *tcpP* constructs were all ectopically expressed from pBAD18 using arabinose (Ara 0.1% w/v). + indicates arabinose was added to the culture. Samples presented here represent three biological replicates.

4.4.8 – Miltefosine Functions Synergistically with α -Linolenic acid

Staphylococcus aureus relies on lipid ordered membrane domains to recruit and promote oligomerization of flotillin, which in turn promotes antibiotic resistance (45). Miltefosine, a drug used to treat Leishmaniasis and certain types of cancers, inhibited flotillin association with lipid ordered membrane domains in *S. aureus* (45, 75). Our data indicate that α -linolenic acid enhances *toxT* transcription by promoting association of TcpP and TcpH molecules within lipid ordered membrane domains. We hypothesized that miltefosine treatment would inhibit TcpH dependent enhanced RIP inhibition in the presence of α -linolenic acid. Instead, we observed that miltefosine alone functioned similar to α -linolenic acid (Figure D.13A). Treatment with both miltefosine and α -linolenic acid resulted in a ~7-fold increase in TcpP levels relative to Vir Ind conditions (Figure D.13B). Our data also demonstrate that miltefosine also promoted association of TcpP molecules with the TI fraction like α -linolenic acid (Figure D.13C). Miltefosine did not promote *toxT* transcription in $\Delta tcpH$ and $E_{psM}TcpH$ cells (Figure D.13A). Taken together, these data indicate that miltefosine functions synergistically with α -linolenic acid to increase levels of TcpP in *V. cholerae* and is not effective at inhibiting lipid ordered domain formation in *V. cholerae*. Miltefosine is known to associate with lipid ordered domains and requires lipid ordered domains to enter cells (76, 77). Secondly, miltefosine has also been shown to increase membrane fluidity (78). Other n3-PUFA, similar to α -linolenic acid, are also capable of increasing membrane fluidity, and they have been shown to drive aggregation and stabilization of lipid ordered membrane domains (47, 69, 70). Given that miltefosine and α -linolenic acid function synergistically to promote TcpH-dependent

antagonism of RIP, these data suggest that α -linolenic acid promotes lipid ordered domain aggregation, and thereby increases lipid ordered domain size in *V. cholerae* cells.

4.5 – Discussion

Canonical RIP systems act by releasing an anti-sigma factor from the cytoplasmic membrane to influence gene transcription. Many membrane localized transcription regulators (MLTRs), in addition to TcpP and ToxR, are sensitive to RIP (e.g., CadC) (165, 272). However, RIP of MLTRs, such as TcpP, results in their inactivation, typically leading to decreased gene transcription. The fundamental mechanisms of RIP for TcpP are understood, in terms of the primary proteases that work in the two-step pathway (351, 352), but many of the regulatory mechanisms influencing these have been less well understood. It is clear that TcpH is essential to inhibit RIP of TcpP, and that its ability to protect TcpP from RIP changes in response to temperature and pH (96, 351, 352). ToxR is a well-studied MLTR, similar to TcpP and is sensitive to RIP (57, 404). ToxR is protected from RIP by ToxS, a single pass transmembrane protein analogous to TcpH (80, 343). Prior work indicates that: i) ToxR undergoes RIP during late stationary phase (i.e., alkaline pH and nutrient limiting conditions); ii) ToxS antagonizes RIP of ToxR via direct interaction; and iii) deoxycholate increases interaction between ToxR and ToxS (79, 83, 85, 405). Similar to what is understood about ToxR, our data indicate that RIP of TcpP is inhibited by direct interaction with TcpH. Our data indicate that α -linolenic acid, a host dietary fatty acid, plays a role in inhibiting RIP by increasing the local concentration of TcpP and TcpH within detergent resistant membranes (DRM) (i.e., lipid ordered membrane domains). Whether this fatty acid plays any role in ToxR RIP inhibition remains to be discovered.

α -Linolenic acid is an essential omega-3 fatty acid used to synthesize arachidonic and docosahexaenoic acid humans and mice (406, 407). α -Linolenic acid is acquired via dietary supplementation and is present in milk, meats, dairy products, soybean oil, and plant seeds (e.g., pomegranate, tung seeds, rapeseed, flax seed, and marigold seeds) (408–414). It is considered a beneficial dietary fatty acid as it is a precursor to omega-3, omega-6, and conjugated α -linolenic acids, and has health benefits ranging from anti-carcinogenic, anti-atherogenic, anti-inflammatory, improved memory, and anti-diabetic activity (415–423). *V. cholerae* uses exogenous long-chain fatty acids, such as α -linolenic acid, to remodel its phospholipid composition (394, 395). Long-chain fatty acids are transported across the outer membrane by FadL into the periplasmic space where FadD covalently modifies the fatty acids by adding an acyl-CoA group, resulting in formation of long-chain fatty acyl-CoA (LCFA-CoA) (390–393). LCFA-CoAs then bind to FadR, the principal regulator of fatty acid biosynthesis in *V. cholerae*, resulting in a conformational change inhibiting FadR from binding to DNA (424–426). This leads to decreased biosynthesis of unsaturated fatty acids (i.e., decrease in *fabAB* transcription) and increased transcription, due to a lack of repression by FadR, of genes required for transport, activation, and beta-oxidation of long-chain fatty acids (i.e., *fadL*, *fadD*, *fadBA*, *fadE*, and *fadH*) (424–426).

Utilization of exogenous fatty acids remodels phospholipid composition in *Vibrio* spp. (394, 395, 427) and has an impact on pathogenicity, motility, and antibiotic resistance via unknown mechanisms (395). Our work demonstrates that: i) *toxT* transcription is enhanced in the presence of α -linolenic acid; ii) TcpP levels are significantly elevated in the presence of α -linolenic acid; iii) the *tcpP* transcript level is not

increased with exogenous α -linolenic acid; iiiv) TcpP and TcpH avidly associate within detergent resistant membranes (DRM; hypothesized to be lipid-ordered domains) in the presence of α -linolenic acid; v) TcpP and TcpH interaction is important for inhibition of RIP; and vi) enhanced *toxT* transcription in the presence of α -linolenic acid is dependent on co-association of TcpP and TcpH in the DRM membrane fraction. Our data support a model where, once present in the gastrointestinal tract, *V. cholerae* cells take up and incorporate α -linolenic acid into phospholipids, thereby altering the composition of the cytoplasmic membrane. This influences TcpH and TcpP molecules to increase their association with lipid ordered membrane domains via an unknown mechanism. N-3 polyunsaturated lipids (i.e., omega-3 fatty acids) are known to increase lipid ordered domain size in eukaryotes by promoting aggregation of existing lipid ordered membrane microdomains (399, 400). As lipid ordered membrane domains are known to be relatively small in size (10-200 nm) (373), this may lead to an increase in the local concentration of TcpP and TcpH molecules thereby allowing TcpH to enhance RIP inhibition of TcpP via direct interaction with TcpP (Figure 4.6).

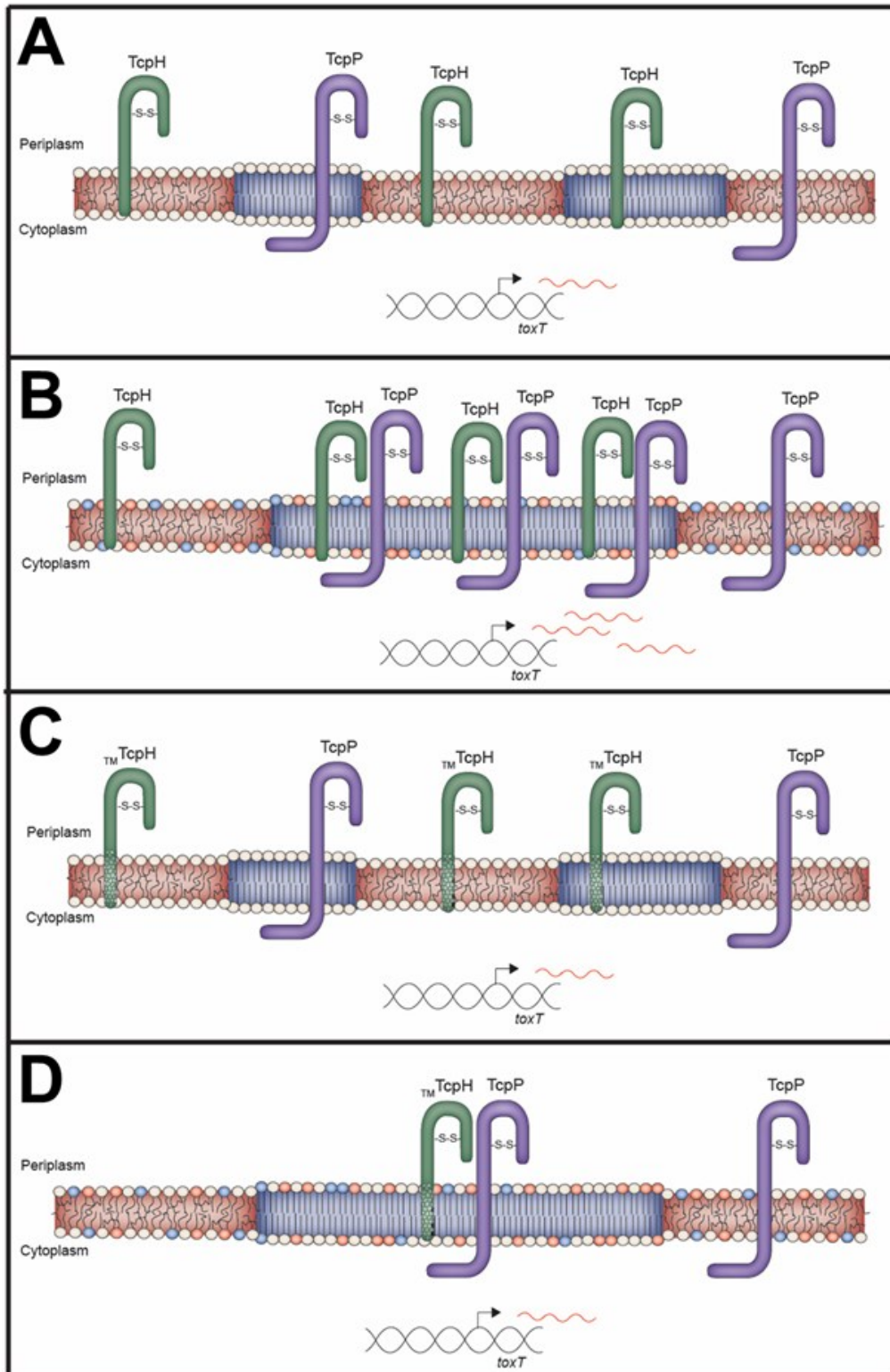


Figure 4.6: α -Linolenic acid stimulates co-association of TcpP and TcpH within detergent resistant membranes thereby enhancing TcpH inhibition of RIP. Under virulence inducing (Vir Ind) conditions (LB pH6.5, 30°C, 110rpm) TcpH inhibits RIP of TcpP and *toxT* transcription is stimulated. Under these conditions, TcpP and TcpH

Figure 4.6 (cont'd)

molecules are associated with lipid-ordered (blue) and lipid-disordered (red) membrane domains. A) in WT cells TcpP and TcpH molecules associate with both lipid ordered and lipid disordered membrane domains, and C) a similar trend is observed for TcpH transmembrane constructs (T_M TcpH). B and D) When α -linolenic acid is present *V. cholerae* cells have been shown to uptake it (via FadL/FadD) and this leads to changes in the overall phospholipid profile of *V. cholerae*, indicated by the blue and orange phospholipids (391, 392, 428, 429). Polyunsaturated fatty acids, such as α -linolenic acid, have also been shown to increase lipid ordered domain size by stimulating aggregation of small lipid ordered domains (430, 431). B) Under these conditions, a majority of TcpP and TcpH molecules transition to lipid ordered membrane domains leading to enhanced inhibition of RIP by TcpH. The net result of α -linolenic acid supplementation is an increase in *toxT* transcription, indicated by an increase in red *toxT* mRNA. D) Modification of TcpH transmembrane domain prevents TcpH molecules from transitioning to lipid ordered domains in the presence of α -linolenic acid, likely due to increased surface area and shorter length of the transmembrane domain. This inhibits TcpH from enhanced inhibition of RIP and does not result in an increase in *toxT* transcription.

Previous studies have investigated the role of exogenous fatty acids on the pathogenesis of *V. cholerae*. These concluded that FadD is required for wild-type *toxT* transcription through a mechanism involving its effect on TcpP levels (432, 433). These prior publications support our model as accumulation of α -linolenic acid in the periplasmic space or within the cytoplasmic membrane, due to loss of *fadD*, results in a reduction in TcpP levels, rather than an increase (432, 433). This work indicates that free α -linolenic acid (i.e., not incorporated in phospholipids) within the periplasmic space, cytoplasm, or within the cytoplasmic membrane, does not promote TcpH mediated inhibition of RIP. When considering this with the data presented here, this indicates that α -linolenic acid needs to be incorporated into the cytoplasmic membrane as a phospholipid to have any effect on TcpH function.

Lipid ordered and lipid disordered membrane domains were discovered due to the insolubility of the lipid ordered membrane domain (initially referred to as detergent

resistant membranes) in Triton X-100 and other non-ionic detergents (376, 402). This biochemical method has been used to separate lipid ordered (DRM) and lipid disordered (DSM) membrane domains in many Eukarya and Bacteria, including Gram-negative and Gram-positive bacteria (367–372). Data generated from the biochemical-based separation of lipid ordered and lipid disordered membrane domains has been verified by alternative methods (e.g., fluorescent microscopy, single-molecule tracking, and synthetic membrane vesicles) (434). Due to a lack of literature on lipid ordered and lipid disordered membrane domains in *V. cholerae*, we performed additional experiments to determine if our biochemical extraction method faithfully enriched for lipid ordered membrane domains and lipid disordered membrane domains within the DRM and DSM (i.e., TI and TS) respectively. In the presence of α -linolenic acid, we found that the TI fraction had a higher association of 16:0 fatty acids and a lower association of 18:3 fatty acids compared to the TS fraction (Figure D.11B). These characteristics are consistent with lipid ordered membrane domain and suggest that the TI and TS fractions presented here are enriched in lipid ordered and lipid disordered membrane domains respectively.

Transmembrane domain length and surface area are major factors in determining the preference of a protein for lipid ordered (enriched with proteins having longer TM domain and low surface area) or lipid disordered (enriched with proteins having shorter TM domain and high surface area) membrane domains (435). We demonstrated that native TcpH and TcpP increase localization within the lipid ordered membrane domain in the presence of α -linolenic acid while E_{psM} TcpH does not (Figure 4.4). E_{psM} TcpH has a shorter TM domain than TcpH (20 amino acids vs 22 amino acids) and a higher overall surface area (108 \AA^2 vs 92 \AA^2), see reference for TM domain surface area calculations

(436). Thus, we hypothesize that the TM domain properties of E_{psM} TcpH molecules inhibit its transition from the TS fraction to the TI fraction in the presence of α -linolenic acid. Alternatively, it is also possible that TcpH, and not E_{psM} TcpH, undergoes post-translational modification (e.g., palmitoylation) within its TM domain. We view this as unlikely as TcpH is not predicted to have a palmitoylation site within its TM domain. In addition, it also appears that the surface area of the transmembrane domain of TcpP influences its function. Prior analysis of TcpP transmembrane domain revealed that mutation of L152 and W162/S163 with alanine (which reduces the overall surface area of the transmembrane domain) increased *toxT* transcription (437). It remains unclear why these mutations increase TcpP function, but given the data presented here, it is possible that TcpPL152A and TcpP W162A/S163A may have a greater propensity than TcpP to associate within DRMs (i.e., lipid ordered membrane domain).

Based on our data and the literature, we hypothesize that phospholipid remodeling of *V. cholerae* occurs in the lumen during the initial stages of infection. Our data suggests that this remodeling promotes TcpH mediated inhibition of RIP and promotes *toxT* transcription. However, unsaturated fatty acids are also known to inhibit degradation and activity of ToxT (i.e., inhibit *tcpA-F* and *ctxAB* transcription) (46, 396). This likely prevents premature transcription of TCP which is known to stimulate microcolony formation and thereby could inhibit penetration of the mucus layer (438). Bicarbonate, which is present at high concentrations at the surface of epithelial cells, competes with unsaturated fatty acids to activate ToxT once *V. cholerae* reaches the surface of epithelial cells, its primary site of infection (48, 50, 439). There is also evidence that bicarbonate represses *toxT* transcription (439). This indicates that transcription of *toxT*, stimulated by enhanced RIP

antagonism, during early infection (i.e., the lumen) is critical for *V. cholerae* to cause disease. This adds a new level of regulation to the ToxR regulon and yet another dietary host factor that modulates *toxT* transcription in *V. cholerae*. α -linolenic acid represents the first *in vivo* signal that modulates RIP of TcpP, and, to the best of our knowledge, the first evidence that lipid ordered and lipid disordered membrane domains exist in *V. cholerae*. The data presented here further expands our knowledge of the complex virulence regulatory cascade in *V. cholerae*.

Chapter 5– Concluding Remarks

5.1 – Conclusions and Significance

Signal transduction is essential for organisms to respond and adapt to their environments. Mechanisms of signal transduction in prokaryotic organisms are composed of one-component, two-component, and anti-sigma factor signal transduction systems (88–91). Membrane localized transcription regulators (MLTRs) are unique one-component regulators that manage to influence gene transcription from the cytoplasmic membrane. Within *V. cholerae*, two MLTRs, TcpP and ToxR, positively regulate *toxT* transcription thereby promoting virulence (39–41, 52–55). Due to their sub-cellular localization both TcpP and ToxR are sensitive to Regulated Intramembrane Proteolysis (RIP) (56, 58, 59, 80, 440). Prior to the work presented in Chapter 2 and Appendix B the prevalence and diversity of MLTRs within the prokaryotic domain was not known. We demonstrate that MLTRs are more prevalent and diverse among prokaryotes than previously understood. Our analysis revealed that MLTRs in Gram-negative bacteria are more likely to have a TcpH/ToxS-like associated protein, and MLTRs within Gram-positive organisms are more likely to have more than one transmembrane domain. Our data indicate that specific genera are enriched with MLTRs. This work emphasizes that MLTRs represent a class of one-component regulators that are understudied and represents a large gap in our knowledge of signal transduction in the prokaryotic domain.

One of the fundamental questions regarding MLTRs is how they manage to influence gene transcription from the cytoplasmic membrane. Using TcpP as a model MLTR, we addressed this gap in knowledge in Chapter 3 by using super-resolution single-molecule tracking (SMT) to measure the biophysical properties of individual TcpP molecules. We found that TcpP molecules exist in three biophysical states (fast,

intermediate, and slow), and we also found that TcpP molecules are unable to transition directly between the slow and fast diffusion states. Secondly, we found that the native level of ToxR does not drive the ordered transition of TcpP molecules between its diffusion states. Artificial elevation of the ToxR level was found to promote transition of TcpP molecules away from the *toxT* promoter, reducing downstream virulence factor production. Our data describe the first biophysical model of promoter association between an MLTR and its target promoter.

Lastly, the unusual localization of MLTRs exposes them to unique forms of post-translational regulation compared to cytoplasmically-localized one-component regulators. TcpP and ToxR are both sensitive to Regulated Intramembrane Proteolysis (RIP), which is a form of post-translational regulation (56, 58, 59, 80, 440). Prior to this work, it was clear that RIP of TcpP is inhibited *in vivo*, but it was unknown what signals *in vivo* contributed to this. In Chapter 4, we present data demonstrating that α -linolenic acid, a dietary fatty acid, promotes inhibition of TcpP RIP via co-association of TcpP and TcpH within detergent-resistant membrane domains. These data are the first to identify an *in vivo* signal that stimulates inhibition of TcpP RIP, the first data indicating that detergent-resistant membranes influence signal transduction within *V. cholerae*, and the first direct evidence that TcpH inhibits RIP of TcpP via direct interaction.

5.2 – Future Directions

The work presented here demonstrates that there remain major gaps in our knowledge regarding MLTRs. Gaining deeper insight into MLTR function will increase our knowledge of bacterial signal transduction. To understand MLTRs at a deeper level we first need to understand what genes can be regulated by MLTRs. The bacterial chromosome is an ordered and dynamic structure that is not thought to be freely available to the cytoplasmic membrane (308–317). Furthermore, the evolution of two-component signal transduction regulators implies that there are genes unavailable to the cytoplasmic membrane. We hypothesize that genes directly regulated by MLTRs are encoded near genes for integral membrane proteins and that transertion of the neighboring membrane protein drives association of the target gene and its MLTR. To test this hypothesis bioinformatic analysis of the genetic neighborhood of MLTR genes across bacterial species would be critical. In addition, experimental evidence would also be required. Alteration of the genetic coordinates of the *toxT* promoter to different areas of the chromosome with distant (>10 Kbp) or close to integral membrane proteins within *V. cholerae* would also be required.

Currently, we have a working model for how TcpP, and possibly other single pass MLTRs, functions to find the *toxT* promoter from the work presented in Chapter 3. In the future we plan to investigate how host factors (such as bile salts, bicarbonate, temperature, pH, dietary fatty acids, and microbiota derived chemicals and proteins) influence TcpP single molecule dynamics. However, this requires that we have a deeper understanding of the biological role of the intermediate diffusion state.

One possibility is that TcpP molecules are non-specifically interacting with chromosomal DNA within the intermediate diffusion state. Given that there is no definitive evidence that TcpP directly regulates genes in addition to *toxT*, combined with the fact that deletion of the entire *toxT* promoter or mutation of the DNA binding domain of TcpP (i.e., TcpP[K94E]) has little effect on the intermediate diffusion state, we view this hypothesis as unlikely. However, this hypothesis could be tested by increasing the number of *toxT* promoter copies, either plasmid encoded or on the chromosome. If the intermediate diffusion state is occupied by TcpP molecules non-specifically interacting with DNA then the overall occupancy of this diffusion state would reduce by increasing the number of specific promoter targets (i.e., the *toxT* promoter). Secondly, if the intermediate diffusion state is occupied by TcpP molecules interacting with DNA then by restricting interaction between the cytoplasmic membrane and chromosomal DNA, via treatment of cells with chloramphenicol, this would also reduce the total percentage of TcpP molecules within the intermediate diffusion state.

However, it is also possible that TcpP molecules within the intermediate diffusion state do not interact with DNA at all. SMT studies have consistently shown that TcpP molecules must enter the intermediate diffusion state to interact with the *toxT* promoter. This suggests that the conformation of the cytoplasmic domain of TcpP molecules in the fast diffusion state is fundamentally different from TcpP molecules within the intermediate diffusion state. Considering this hypothesis, this raises two additional hypotheses regarding how the transmembrane domain may impact the cytoplasmic domain of TcpP molecules in the intermediate diffusion state: 1) TcpP molecules within the intermediate diffusion state are associated with detergent resistant membrane (DRM) domains (i.e.,

lipid rafts) and, due to reduced membrane fluidity and increased membrane thickness, this alters the conformation of the cytoplasmic DNA-binding domain thereby promoting interaction with the *toxT* promoter; and 2) TcpP molecules within the intermediate diffusion state associate with an unknown high molecular weight membrane localized protein complex, composed of one or more proteins, and this in turn influences the conformation of the cytoplasmic DNA-binding domain thereby promoting interaction with the *toxT* promoter.

Testing these hypotheses will require a range of different experiments. Regarding our primary hypothesis, defining the regions of the chromosome TcpP is capable of interacting with, likely via chromatin immunoprecipitation sequencing (ChiP), will be critical to determine if TcpP is capable of regulating additional genes.

To investigate the biological role of the intermediate diffusion state, defining the protein interaction network of TcpP molecules, using a combination of coimmunoprecipitation and proteomics, will be critical to decipher the biological function of the intermediate diffusion state. Interaction between TcpP and high molecular weight membrane localized protein(s) would indicate that these interactions occur within the intermediate diffusion state. To determine if this potential TcpP-protein interaction is relevant to biophysical dynamics of TcpP molecules, deletion of the gene encoding the high molecular weight protein(s) followed by investigation of TcpP single molecule dynamics will be required. If interaction between TcpP and an unknown high molecular weight protein is promoting transition of TcpP molecules from the intermediate diffusion state to the slow diffusion state, I would minimally expect the rate of transition between the intermediate and slow diffusion state to decrease upon deletion of the gene for the

high molecular weight protein. It is also likely that, if critical for TcpP molecules to efficiently interact with the *toxT* promoter, deletion of this unknown high molecular weight protein would result in the loss of the intermediate diffusion state altogether and thereby reduce virulence factor production.

Lastly, it is also possible that TcpP molecules within the intermediate diffusion state alter the conformation of their DNA binding domain due to local membrane properties. In Chapter 4, we demonstrate that TcpP molecules are capable of associating with DRM and detergent soluble membranes (DSM). DRM are also known as lipid ordered membrane domains (i.e., lipid rafts), and these membrane domains have been described as possessing a lower degree of membrane fluidity and an increase in thickness relative to detergent soluble membranes. To test this hypothesis, alteration of the TcpP transmembrane domain (i.e., decrease the total length and increase the overall surface area) will be required to reduce the affinity of TcpP molecules with DRM. If association of TcpP molecules within DRM is critical for transition of TcpP molecules from the intermediate diffusion state to the slow diffusion state then alteration of the TcpP transmembrane domain (i.e., decrease the total length and increase the overall surface area) will reduce the rate of transition between these biophysical states. Additionally, this would also reduce *toxT* transcription and production of downstream virulence factors.

From the work presented here we have uncovered substantial knowledge regarding how TcpP locates the *toxT* promoter. From work discussed in Chapter 4, we have also gained significant insights into the mechanism by which TcpH inhibits RIP of TcpP. Our data indicate that TcpH protects TcpP from RIP via direct interaction, interaction between TcpP and TcpH likely occurs in both DRM and DSM, and that TcpP-

TcpH interaction occurs via different mechanisms within DRM and DSM. More specifically, our data suggest that the C-terminus of TcpP must be available for TcpP-TcpH interaction to occur and for elevated *toxT* transcription in the presence of α -linolenic acid. Due to low specificity of our TcpP and TcpH anti-serum we are unable to perform coimmunoprecipitation experiments with native TcpP and TcpH. Thus, we require a different approach to determine if TcpP and TcpH molecules interact via different residues within DRM and DSM.

Future experiments to define the precise mechanism of interaction between TcpP and TcpH within DRM and DSM will require purification of TcpP-His-Hsv, TcpH-His-Hsv, and Hsv-His-Tsp. Prior to cleavage of the His-Hsv tag, the TcpP-His-Hsv and TcpH-His-Hsv molecules will be reconstituted together into synthetic liposomes. Once TcpP and TcpH molecules are reconstituted into liposomes, confirmation of function and orientation of TcpP and TcpH molecules will be required. To confirm the orientation of TcpP and TcpH within liposomes, liposomes containing TcpP-His-Hsv or TcpH-His-Hsv will be purified using anti-Hsv antibodies conjugated to A-sepharose beads. This purification will yield only liposomes containing TcpP or TcpH molecules with their C-termini on the exterior of the liposome. Once purified, the His-Hsv tag will be cleaved from TcpP-His-Hsv and TcpH-His-Hsv. To confirm TcpH function, purified Tsp will be added to TcpP/TcpH containing liposomes buffered with low pH (pH 6.5) or alkaline pH (pH8.5). If reconstituted TcpP molecules are resistant to Tsp proteolysis at low pH (in the presence of TcpH) and sensitive to Tsp proteolysis at alkaline pH it would indicate that purified TcpH remains functional. We will also test if purified TcpP molecules are able to interact with the *toxT* promoter using electromobility shift assays. If we are able to confirm that

TcpP and TcpH remain functional when purified and reconstituted into a liposome, this would allow us to manipulate the liposome environment to further test our hypothesis that association of TcpP and TcpH within DRMs enhances TcpH-dependent inhibition of RIP, and allow us to determine if TcpP and TcpH interact via different residues, by mutating specific residues, within DRM and DSM.

APPENDICES

APPENDIX A:
Supplemental Material for Chapter 2

A.1 – Supplemental Tables and Figures

Table A.1. **Characterized MLTRs and their known cellular response and associated proteins.** `: indicates this MLTR is not discussed at length in the main text. *: indicates that 01/0139 classical and El Tor biotypes encode *tcpPH* within their genomes. #: indicates that there are possible TcpH/ToxS-like gene that is uncharacterized immediately upstream or downstream of the indicated MLTR.

MLTR	Organisms	Cellular Response	Associated Protein	References
<i>ToxR</i>	<i>Vibrio spp.</i> <i>Photobacterium spp.</i>	Bile salt resistance, cationic antimicrobial peptides, pressure response, biofilm formation, and virulence factor transcription	ToxS	(39–41, 53, 55, 71, 72, 104, 120, 124–127, 207, 441–443)
<i>TcpP</i>	<i>Vibrio cholerae</i> * and <i>Vibrio fischeri</i>	Virulence factor (<i>toxT</i> transcription), motility, chemotaxis, and reduction of extracellular polysaccharides	TcpH	(52, 96, 143, 351, 352)
<i>CadC</i>	<i>Vibrio spp.</i> <i>Escherichia spp.</i> <i>Salmonella spp.</i> <i>Yersinia spp.</i>	Acid resistance	LysP	(107, 156–160, 163, 164, 166, 444, 445)
<i>TfoS</i>	<i>Vibrio spp.</i>	Natural Competence	Na	(110, 167)
<i>VtrA/VttrA</i>	<i>Vibrio spp.</i>	Type-3 secretion systems	VtrC	(101, 102, 148, 154, 155)
<i>VtrB/VttrB</i>	<i>Vibrio spp.</i> <i>Salmonella spp.</i>	Type-3 secretion systems	Na	(101, 102, 149)
<i>MarT</i>	<i>Salmonella spp.</i> <i>Yersinia ruckeri</i>	Fibronectin binding	#	(181, 190, 234, 235)
<i>GvrA</i>	<i>Escherichia coli</i>	Promotes transcription of LEE in response to bicarbonate	Na	(184, 203)
<i>YqeI</i>	<i>Escherichia coli</i>	Serum resistance, flagella synthesis, and host cell adhesion	YqeJ	(186)

Table A.1 (cont'd)

<i>PsaE</i>	<i>Yersinia pestis</i>	Fimbriae transcription	PsaF	(221, 224, 230)
<i>MyfE</i>	<i>Yersinia enterocolitica</i>	Fimbriae transcription	MyfF	(231–233)
<i>PypB</i>	<i>Yersinia enterocolitica</i> and <i>Yersinia ruckeri</i>	Flp type IVb pillin transcription	#	(239)
<i>BcrR</i>	<i>Enterococcus</i> spp. <i>Lactobacillus</i> spp.	Bacitracin resistance	Na	(106, 246–248)
<i>BreG</i>	<i>Lactobacillus</i> spp. <i>Enterococcus</i> spp.	Bacteriocin synthesis	Na	(242, 253)
<i>AguR</i>	<i>Enterococcus</i> spp.	Acid tolerance	Na	(243, 257–259)
<i>LP_2991</i>	<i>Enterococcus</i> spp. <i>Lactobacillus</i> spp.	Immune modulation	Na	(114, 267)
<i>HcrR</i>	<i>Lactobacillus planatarium</i>	Hydroxycinnamic acid metabolism	Na	(103, 279)
<i>MmsR</i>	<i>Lactobacillus bif fermentans</i>	Isobutyryl-CoA metabolism	Na	(112)
<i>MtbS</i>	<i>Staphylococcus</i> spp. <i>Enterococcus</i> spp. <i>Lactobacillus</i> spp.	Virulence factors, phosphate transport, tRNAs, etc.	Na	(285)
<i>NanR</i>	<i>Staphylococcus</i> spp.	Sialic acid metabolism	Na	(112, 113)
<i>WmpR</i>	<i>Pseudomonas tunicate</i>	Type IV pilin, pigmentation, iron uptake, amino acid metabolism, biofilm formation, and anti-fouling	Na	(446, 447)

Table A.2: **Membrane localized transcription regulators (MLTRs) within the *Vibrio* genus.** Underlined MLTRs had a minimum percent identity of 25% or greater to their respective MLTR. MLTRs with “” were previously characterized. *: indicates that the MLTR has a TcPH/ToxS like gene immediately upstream or downstream of its coding sequence. &: indicates that the MLTR has an unknown multi-transmembrane (YitT-like) gene immediately upstream or downstream of its coding sequence. #: indicates that the MLTR has a similar primary sequence structure to TcpP, ToxR, and CadC but lacks sequence homology.

<i>Organism</i>	# of	<i>TcpP</i>	<i>ToxR</i>	<i>CadC</i>	<i>TfoS</i>	<i>VtrA</i>	<i>VtrB</i>	<i>MT-MLTR</i>	<i>Uncharacterized</i>
	ML TR								
<i>Vibrio cholerae</i> 01 El Tor	5	<u>VC0826</u> *	<u>VC0984</u> *	<u>VC0278</u>	<u>VC2080</u>			<u>VCA0926</u>	
<i>Vibrio cholerae</i> 0395 Classical	5	<u>RS0710</u> 5*	<u>AVK7916</u> 0.1*	<u>RS1857</u> 5	<u>RS1370</u> 0			<u>RS01510</u>	
<i>Vibrio cholerae</i> AM-19226 (non-01/0139)	5			<u>RS1576</u> 5	<u>RS0224</u> 5	<u>RS03</u> 865*	<u>RS03</u> 800	<u>RS085</u> 60	
<i>Vibrio cholerae</i> RC385 (non-01/0139)	1				<u>RS1305</u> 0				
<i>Vibrio parahaemolyticus</i>	5		<u>VP0820</u>	<u>RS0097</u> 0	<u>RS0610</u> 0	<u>RS23</u> 940	<u>RS24</u> 000		
<i>Vibrio alginolyticus</i>	4		SQA465 27.1	RS1021 0	<u>RS1528</u> 5				RS20210 RS14510#

Table A.2 (cont'd)

<i>Vibrio campbellii</i>	6	<u>RS07705</u> <u>RS06270</u> *	<u>RS0099</u> <u>0</u>	<u>RS0645</u> <u>0</u>	<u>RS11</u> <u>600*</u>	RS25150
<i>Vibrio diazotrophicus</i>	3			<u>RS1725</u> <u>5</u>		<u>RS129</u> <u>20</u> RS02285
<i>Vibrio fischeri</i>	9	<u>VF_A04</u> <u>73*</u> <u>VF_A08</u> <u>60*</u>	<u>VF_0791</u> * <u>VF_A02</u> <u>59\$</u> <u>VF_A03</u> <u>04</u>	<u>VF_206</u> <u>0</u> <u>VF_111</u> <u>6</u> <u>VF_083</u> <u>2</u>		VF_1086*
<i>Vibrio fluvialis</i>	6	<u>RS26105</u> <u>RS39125</u> *		<u>RS3285</u> <u>5</u>	<u>RS27</u> <u>425</u>	<u>RS233</u> <u>40</u> RS33410*
<i>Vibrio gazogenes</i>	2	<u>RS13720</u> *		<u>RS0204</u> <u>0</u>		
<i>Vibrio mediterranei</i>	11		<u>RS1879</u> <u>0</u> <u>RS1884</u> <u>0</u> <u>RS1826</u> <u>0</u> <u>RS0537</u> <u>0&</u>	<u>RS2290</u> <u>5</u>		RS13975 RS12645# RS12640# RS06645*# RS25540*# RS19560*#
<i>Vibrio proteolyticus</i>	5	<u>RS15940</u> * <u>RS02825</u> *		<u>RS0325</u> <u>5</u>		<u>RS148</u> <u>70</u> RS18455
<i>Vibrio vulnificus</i>	3	<u>RS12130</u> *		<u>RS1193</u> <u>0</u>		RS12725&#

Table A.3: **Membrane localized transcription regulators (MLTRs) within the *Escherichia* and *Salmonella* genera.** Underlined MLTRs had a minimum percent identity of 25% or greater to their respective MLTR. MLTRs with “” were previously characterized. *: indicates that the MLTR has a TcPH/ToxS like gene immediately upstream or downstream of its coding sequence. !: Fimbriae genes encoded immediately upstream or downstream of its coding sequence. #: indicates that the MLTR has a similar primary sequence structure to TcpP, ToxR, and CadC but lacks sequence homology. %: possible motility gene regulator (211). ^: Probable Type-3 secretion system regulator (214). STM1575 does contain a C-terminal transmembrane domain, but is predicted to encode a null protein within the MIST database and as such was not included in our analysis.

Organism	Number of MLTFs	VtrB-like	CadC-like	MarT-Like	Uncharacterized
<i>Escherichia coli</i> O157:H7	4		<u>“ECs5115”</u>	<u>ECs1274*</u> <u>ECs3704*</u>	ECs0796
<i>Salmonella enterica</i> subsp. <i>enterica</i> serovar <i>Enteritidis</i>	6	<u>RS00150!</u>	<u>RS13195</u>	<u>RS18610*</u>	RS07670 RS00085 RS00160^ RS07670%
<i>Salmonella enterica</i> subsp. <i>enterica</i> serovar <i>Typhimurium</i>	4	<u>STM0029</u>		<u>“STM3759*”</u>	STM0017 STM0031^
<i>Salmonella enterica</i> subsp. <i>enterica</i> serovar <i>Typhi</i>	3	<u>STY0035!</u>	<u>STY2804</u>		STY0017
<i>Salmonella enterica</i> subsp. <i>enterica</i> serovar <i>Paratyphi</i>	1			<u>RS18300*</u>	
<i>Salmonella enterica</i> subsp. <i>enterica</i> serovar <i>Newport</i>	5	<u>RS01170!</u>	<u>RS14145</u>	<u>RS20100*</u>	RS01180^ RS01105

Table A.4: **Membrane localized transcription regulators (MLTRs) within the *Yersinia* genus.** Underlined MLTRs had a minimum percent identity of 25% or greater to their respective MLTR. MLTRs with "" were previously characterized. *: indicates that the MLTR has a TcpH/ToxS like gene immediately upstream or downstream of its coding sequence.

Organism	Number of MLTR	PsaE	MyfE	MarT	CadC	PypB	MT-MLTR	Uncharacterized
<i>Yersinia pestis</i>	3	<u>YPO_130</u> <u>1*</u>			YPO0804			YPO0736*
<i>Yersinia enterocolitica</i> subsp. <i>enterocolitica</i>	5		<u>YE145</u> <u>0*</u>		<u>YE3340</u> *	<u>YE3632</u> "	YE0935	YE1942
<i>Yersinia ruckeri</i>	6			RS16705*	<u>RS0349</u> <u>5</u> RS06955	<u>RS0749</u> <u>0*</u> <u>RS1367</u> <u>0*</u>		RS16645*

Table A.5: **Membrane localized transcription regulators (MLTRs) within the *Enterococcus* genus.** Underlined MLTRs had a minimum percent identity of 25% or greater to their respective MLTR. MLTRs that are bolded maintained high sequence identity to indicated MLTR, but lacked homology to their predicted extracellular domain. MLTRs with “” were previously characterized. *: indicates that the MLTR has a TcpH/ToxS like gene immediately upstream or downstream of its coding sequence. ~: indicates that there is a multi-transmembrane domain protein of unknown function directly upstream or downstream of the indicated MLTR. BcrR was not found within the *E. faecalis* genome within the MIST database. As such the BcrR sequence was obtained from NCBI and included in our analysis here.

Organism	Number of MLTFs	BcrR	BreG	MbtS	AguR	Lp_2991	Uncharacterized
<i>Enterococcus asini</i>	1						RS00345
<i>Enterococcus aquimarinus</i>	3						RS00615 RS02785 RS07540
<i>Enterococcus columbae</i>	4						RS08195 RS03755 RS08590 RS02640
<i>Enterococcus cecorum</i>	2	<u>RS0110</u> <u>0</u>					RS01715
<i>Enterococcus casseliflavus</i>	8		RS05 555	<u>RS134</u> <u>05</u>			RS12830/RS1051 0/RS15855*/RS15 110/RS07240/RS 15005
<i>Enterococcus canis</i>	2						RS00645 RS09835
<i>Enterococcus dispar</i>	1						RS07360
<i>Enterococcus devriesei</i>	1						RS07030
<i>Enterococcus faecium</i>	2						HMPREF0351_10 607 HMPREF0351_12 753

Table A.5 (cont'd)

<i>Enterococcus faecalis</i>	3			<u>EF073</u> <u>1</u>		EF1531 EF0600
<i>Enterococcus gilvus</i>	8			<u>RS143</u> <u>65</u>	<u>RS162</u> <u>65</u>	<u>RS02100</u> RS00880 RS06585 RS18200 RS10460 RS14805
<i>Enterococcus hirae</i>	2	<u>RS1305</u> <u>5</u>		<u>RS025</u> <u>70*</u>		
<i>Enterococcus hermanniensis</i>	1					RS11415
<i>Enterococcus haemoperoxidus</i>	5			<u>RS076</u> <u>75</u>	<u>RS043</u> 35	RS14655 RS07770 RS10820
<i>Enterococcus italicus</i>	4	RS11 425	<u>RS043</u> <u>85</u>			RS00315 RS04425
<i>Enterococcus mundtii</i>	1					RS04320
<i>Enterococcus massiliensis</i>	4	RS03 730~				RS05900 RS09315 RS12565*
<i>Enterococcus malodoratus</i>	11	<u>RS0629</u> <u>0~</u>	RS21 210	<u>RS118</u> <u>50~</u>	<u>RS104</u> <u>25</u>	RS07765 RS20630 RS05940 RS22780 RS15880 RS05495 RS12085~
<i>Enterococcus thailandicus</i>	6					RS09800 RS00180 RS09185

Table A.5 (cont'd)

<i>Enterococcus sulfureus</i>	4		<u>RS112</u> <u>25</u>	RS04980 RS04765 RS11240
<i>Enterococcus saccharolyticus</i>	2	RS0681 0		RS02430
<i>Enterococcus rivorum</i>	4			RS05980 RS05970 RS00735 RS01425
<i>Enterococcus pseudoavium</i>	6		<u>RS095</u> <u>RS049</u> <u>05</u> <u>30</u>	RS02475 RS09190 RS06660~ RS13025
<i>Enterococcus phoeniculicola</i>	12	RS17 900 RS05 905	<u>RS05900</u> <u>RS00705</u>	RS17765 RS13510 RS03560 RS17715 RS08900 RS02805
<i>Enterococcus pallens</i>	8		<u>RS116</u> <u>RS016</u> <u>55</u> <u>10</u>	RS26705 RS12270 RS03020 RS02430 RS09675 RS11665

Table A.6: **Membrane localized transcription regulators (MLTRs) within the *Lactobacillus* genus.** Underlined MLTRs had a minimum percent identity of 25% or greater to their respective MLTR. MLTRs that are bolded maintained high sequence identity to indicated MLTR, but lacked homology to their predicted extracellular domain. MLTRs with “” were previously characterized. *: indicates that the MLTR has a TcPH/ToxS like gene immediately upstream or downstream of its coding sequence. ~: indicates that there is a multi-transmembrane domain protein of unknown function directly upstream or downstream of the indicated MLTR.

Organism	Number of MLTR	BcrR	BreG	MbtS	HcrR	MmsR	Lp_2991	Uncharacterized
<i>Lactobacillus animalis</i>	1							RS00095
<i>Lactobacillus amylovorus</i>	2							RS01185~ RS10235
<i>Lactobacillus amylophilus</i>	2							RS04890 RS05100
<i>Lactobacillus agilis</i>	1	<u>RS0955</u>						<u>5</u>
<i>Lactobacillus acidophilus</i>	3							LBA0244~ LBA1955 LBA1936
<i>Lactobacillus acetotolerans</i>	1							RS06700
<i>Lactobacillus buchneri</i>	3			<u>RS0829</u>				<u>0</u> RS00895 RS11590
<i>Lactobacillus brevis</i>	5		<u>RS22905</u>	<u>RS2290</u>			<u>RS11990</u>	<u>0</u> RS21830 RS21965
<i>Lactobacillus bifementans</i>	7		RS05860			RS0953	0	RS14570 RS05925 RS15695 RS01745~

Table A.6 (cont'd)

<i>Lactobacillus coryniformis</i>	5	RS1196 5	<u>RS001</u> <u>60</u>	RS11875 RS00280 RS00240
<i>Lactobacillus farciminis</i>	10	<u>RS087</u> <u>20</u>	<u>RS0025</u> <u>0</u>	<u>RS064</u> <u>35</u> RS06350 RS01610 RS06300 RS03750 RS12580
<i>Lactobacillus fermentum</i>	1			RS08365
<i>Lactobacillus gasseri</i>	3			RS01145 RS09185 RS04740
<i>Lactobacillus hilgardii</i>	1			RS01600
<i>Lactobacillus reuteri</i>	3	<u>RS0934</u> <u>5</u>	<u>RS0934</u> <u>5</u>	RS08535
<i>Lactobacillus ruminis</i>	4	RS0523 5		RS09095 RS10010 RS02285
<i>Lactobacillus sakei</i>	2			RS01090 RS09720
<i>Lactobacillus sharpeae</i>	3	<u>RS0895</u> <u>0</u>		RS02445 RS03380
<i>Lactobacillus plantarum</i>	6	<u>RS1205</u> <u>0</u> <u>RS1327</u> <u>0~</u>	<u>RS060</u> <u>15</u>	<u>RS1327</u> <u>0</u> "RS1205" <u>0"</u> RS03925
<i>Lactobacillus paracasei</i>	3			LSEI_1084 LSEI_2759 LSEI_0132

Table A.7: **Membrane localized transcription regulators (MLTRs) within the *Staphylococcus* genus.** 66 total MLTRs were identified in our search. Underlined MLTRs had a minimum percent identity of 25% or greater to their respective MLTR. MLTRs that are bolded maintained high sequence identity to indicated MLTR, but lacked homology to their predicted extracellular domain. MLTRs with "" were previously characterized. *: indicates that the MLTR has a Tcph/ToxS like gene immediately upstream or downstream of its coding sequence. ~: indicates that there is a multi-transmembrane domain protein of unknown function directly upstream or downstream of the indicated MLTR. #: indicates that a CPBP family metalloprotease is encoded immediately upstream or downstream of the indicated MLTR.

Organism	Number of MLTFs	MtbS	NanR	Uncharacterized
<i>Staphylococcus arlettae</i>	2			RS09735
				RS10965
<i>Staphylococcus aureus</i> <i>str. Newman</i>	3	<u>"RS14925"</u>		RS06710
				RS13825
<i>Staphylococcus auricularis</i>	2			RS09160
				RS00495
<i>Staphylococcus cohnii</i>	5	<u>RS04280</u>	<u>RS06235</u>	RS03660
				RS11745
				RS06375
<i>Staphylococcus condimenti</i>	2			RS02300
				RS00310
<i>Staphylococcus epidermidis</i>	4	<u>SE2409</u>		SE_p609
				SE0959
				SE2048
<i>Staphylococcus equorum</i>	3	<u>RS00040</u>		RS00830
				RS00605
<i>Staphylococcus gallinarum</i>	2	<u>RS12330</u>		RS09010
<i>Staphylococcus haemolyticus</i>	3	<u>RS12905</u>		RS02640
				RS01135#
<i>Staphylococcus hominis</i>	4	<u>RS00360</u>		RS10595
				RS02415
				RS10980

Table A.7 (cont'd)

<i>Staphylococcus hyicus</i>	1	<u>RS00530</u>	RS10980
			RS0101280
<i>Staphylococcus lentus</i>	4		RS0114085
			RS0109075
<i>Staphylococcus lugdunensis</i>	4	<u>RS12095</u>	RS07885
			RS02430
			RS03175#
<i>Staphylococcus lutrae</i>	1		RS06365
<i>Staphylococcus massiliensis</i>	2		RS0110280
			RS0103355
			RS07660
<i>Staphylococcus microti</i>	3		RS00195
			RS10565
<i>Staphylococcus pettenkoferi</i>	2		RS06300
			RS07860#
<i>Staphylococcus pseudintermedius</i>	1	<u>RS12210</u>	
<i>Staphylococcus saprophyticus</i>	3	<u>RS02440</u>	<u>RS04325</u> RS01945
<i>Staphylococcus sciuri</i>	3	<u>RS26220~</u>	RS14815
			RS14640
<i>Staphylococcus simiae</i>	1		RS05740
<i>Staphylococcus simiae2</i>	1		RS23340
<i>Staphylococcus succinus</i>	1		RS09190*
<i>Staphylococcus vitulinus</i>	3	<u>RS0105830</u>	RS0100350
			RS0106810
<i>Staphylococcus warneri</i>	2	<u>RS24325</u>	RS19740
<i>Staphylococcus xylosus</i>	4	<u>RS12090</u>	<u>RS08695</u> RS03545
			RS09645

APPENDIX B:

Distribution of Membrane-Localized Transcription Regulators within the Prokaryotic Domain

B.1 – Introduction

To gain a deeper understanding of membrane localized transcription regulators (MLTRs) we collaborated with Vadim Gumervo and Igor Jouline to mine the genomes within the Microbial Signal Transduction Database (MIST) database to gain a better understanding of the distribution and prevalence of MLTRs within the Prokaryotic domain. In Chapter 2 we focus on specific Prokaryotic genera that have been described to encode MLTRs in the literature. Here we expanded our analysis to all Prokaryotic genomes within the MIST database. Overall, we found that MLTRs are far more common and diverse within the Prokaryotic domain, similar as in Chapter 2. We also found that specific Prokaryotic genera are enriched with MLTRs. Below we summarize our findings.

B.2 – Materials and Methods

B.2.1 – Identification and Transmembrane Domain analysis of MLTRs within the MIST database

MLTRs for a representative set of genomes were collected from MiST database by running a custom python script on the local computational cluster (449). For each genome all DNA-binding signal transduction proteins that contain transmembrane regions were retrieved. Transmembrane regions of the protein sequences were identified by running TMHMM, domains were verified using TREND and Pfam profile Hidden Markov Models (116, 450, 451). The average length, number of amino acids, and surface area for each MLTR transmembrane domain was calculated using a custom script. Of note,

the MIST database did not define ToxR, a known MLTR, as having a transmembrane domain. As such, this indicates that MLTRs presented here are a conservative estimate at the true prevalence of MLTRs within the bacterial domain. Sequences corresponding to transmembrane regions were extracted using a custom python script. Taxonomy information for the genomes was retrieved from GTDB and NCBI databases.

B.3 – Results

B.3.1 – Distribution of Membrane Localized Transcription Regulators in the Prokaryotic Domain

To gain a deeper understanding of the prevalence and distribution of membrane localized transcription factors (MLTRs) within the Prokaryotic domain we mined the genomes of 10,933 bacterial species for genes that encoded a DNA binding domain and at least one transmembrane domain. We found that of the 9,306 out of 10,933 bacterial species screened (~85%) encoded at least one MLTR (Supplemental File B.1). Within these MLTR positive genomes we identified a total of 48,918 MLTRs (Supplemental File B.2). On average bacterial genomes contain ~5 MLTRs (Supplemental File B.1). However, the number of MLTRs per genome varies dramatically with the range of MLTRs per genome is also quite broad with some bacterial species encoding only 1 MLTR and others encoding up to 158 MLTRs (*Raoultibacter timonensis*) (Supplemental File B.1). At the phylum level, the *Bacteroides*, *Firmicutes*, *Proteobacteria*, and *Spirochaetes* contained the most bacterial species that were enriched with MLTRs (Table B.1 and Supplemental Table B.1). Only a small fraction of bacterial genera (180 out of 2,342) are

enriched with MLTRs containing an average of 12 or more MLTRs per genome (Supplemental Table B.1).

B.3.2 –Input and Output Domains within MLTRs

Among the MLTRs identified ~96% of MLTRs were found to encode a Helix turn Helix DNA binding domains (Supplemental Table B.2 and Supplemental File B.2). The most common non-DNA/RNA binding domain within MLTRs is the response regulator domain commonly found within two component signal transduction systems (Supplemental Table B.3 and Supplemental File B.2) (452). Response regulators catalyze the transfer of a phosphate from a histidine kinase donor and also have intrinsic dephosphorylation activity (453). Response regulators are commonly multi-domain proteins typically containing a C-terminal effector domain that is commonly a DNA binding domain (453). Phosphorylation of the response regulator domain stabilizes a conformation that allows for activity of the effector domain (453). Additionally, among the top five most common non-DNA binding domains in MLTRs are the HATPase_c (an ATP cleavage domain), HisKA (a histidine kinase domain), and the Y_Y_Y domains (an extracellular domain found in two-component systems) (Supplemental Table B.3). These domains are all commonly found within two component signal transduction pathways (452, 454–456). In fact, ~9.5% of all MLTRs identified by our analysis contain domains commonly associated with two component regulatory systems, which we refer to as hybrid MLTRs (Supplemental File B.1 and B.2). Prior studies revealed that *Bacteroides thetaiotaomicron* contains 32 hybrid histidine kinases with DNA-binding domains (i.e., hybrid MLTRs) (457). Our data indicate that not only is the *Bacteroides* genus enriched with MLTRs but that a majority of the MLTRs within the *Bacteroides* genus are hybrid

MLTRs (~72%) (Supplemental File B.1 and B.2). It remains unclear if these hybrid MLTRs evolved from canonical two component regulatory systems. However, Prior studies indicate that hybrid two component regulatory systems, which do not encode DNA binding domains, were the result of recent evolutionary events and that canonical two component regulatory systems were adapted to generate these hybrid two component regulatory systems (458). Our data suggest that hybrid MLTRs are the product of recent evolutionary events as they are not conserved at the genus level and maintain domains only found within two component regulatory systems that would have no obvious role for a MLTR.

B.3.3 – TM Domain Properties of MLTRs

There is evidence that these hybrid MLTRs function to sense and respond to disaccharides (459). However, it is not obvious how a hybrid MLTR, or MLTRs in general, have a functional advantage over canonical two component regulatory systems, which are not restricted to the cytoplasmic membrane. Given that a majority of MLTRs within *Bacteroides* species are hybrid MLTRs, this implies that two component regulatory systems had already evolved to achieve this task. So why bring the response regulator and DNA-binding domain to the membrane? Currently the exact evolutionary pressure that selects for hybrid MLTRs, specifically within the *Bacteroides* genus, is not known. One possibility is that the cytoplasmic membrane itself serves as a signal to further fine tune these signal transduction pathways. It is generally recognized that the membrane environment in both bacterial and eukaryotic cells is not a homogenous environment. Direct evidence within *Bacillus subtilis* demonstrates that a vast majority of integral

membrane proteins are heterogeneously distributed within *B. subtilis* cells indicating that their diffusion within the cytoplasmic membrane is restricted (328, 329).

Bacteria and Eukaryotes are both known to support lipid ordered and lipid disordered membrane domains within their membrane(s) (367, 368, 372). Generally speaking, liquid-ordered and liquid-disordered membrane domains differ by their overall fluidity and thickness, with liquid-ordered membrane domains having a lower fluidity and increased thickness, as a consequence of the phospholipid species that occupy these membrane environments (372, 373, 375, 377, 460, 461). These membrane domains have been shown to influence many signaling pathways in Eukaryotic cells, in particular T-cells (462). Association with liquid-ordered and liquid-disordered membrane domains is determined by the properties of the transmembrane domain with length and overall surface area of the transmembrane domain being the most critical factors (435). There is also evidence that dietary polyunsaturated fatty acids can influence formation and stability of lipid ordered membrane domains thereby influencing signal transduction (430, 463). Given that there is a clear evolutionary pressure to evolve MLTRs, we hypothesized that MLTRs may respond to their local membrane environment (i.e., liquid-ordered or liquid-disordered membrane domains) which can be influenced by extracellular conditions. As the overall length and surface area of transmembrane domains controls the association of membrane proteins within lipid ordered and lipid disordered membrane domains, we calculated the overall surface area for all transmembrane domains for MLTRs analyzed here (Supplemental File B.3). We found that a majority (~68%) of MLTR transmembrane domains have a surface area equal to or below 172 Å² per amino acid (Supplemental File B.3). In Chapter 4 we demonstrate that TcpP, an MLTR that positively modulates

virulence in *Vibrio cholerae*, increases its association with detergent resistant membranes (i.e., liquid-ordered membrane domain) in the presence of α -linolenic acid, a dietary fatty acid. The surface area of the TcpP transmembrane domain is 172 Å per amino acid. This indicates that a majority of MLTRs have the capacity to associate with liquid-ordered membrane domains. However, it does not rule out the possibility that MLTRs with transmembrane domain surface area above 172 Å per amino acid cannot associate with liquid-ordered membrane domains or are not influenced by liquid-ordered membrane domains. Due to a lack of information on liquid-ordered and liquid-disordered membrane domains in bacteria, particularly Gram-negative bacteria, and a lack of studies to understand transmembrane domain properties that influence protein association in bacterial membranes our analysis remains limited.

B.4 – Discussion

Our analysis has revealed that the abundance of MLTRs is far greater within the Prokaryotic domain than previously understood and suggests that they play a significant regulatory role in some bacterial genera. Among the top 10 genera most enriched for MLTRs (totaling to 1,272 MLTRs across the 15 species) there was little homology to characterized MLTRs (Supplemental Figure B.1). The majority of the genera most highly enriched with MLTRs belong to the *Eggerthellaceae* family which are members of mammalian gastrointestinal tracts (464–468). This family is composed of Gram-positive rods or cocci, anaerobic, nonmotile, non-spore forming, and are generally unable to utilize carbohydrates as an energy source (469). The majority of MLTRs within these species is a multi-transmembrane domain MLTR with a C-terminal LuxR-type DNA-binding HTH domain (Supplemental Figure B.1). The function of these MLTRs remains unknown but

given the abundance of these multi-transmembrane domain MLTRs within the genomes of these bacteria it is likely that they play an important regulatory role.

Furthermore, a large number of MLTRs identified in our screen (~9.5%) contain domains commonly found in two-component regulatory systems suggesting that these hybrid MLTRs were originally two-component regulatory systems (Supplemental File B.1 and B.2). Taken together, our data suggest that there is an evolutionary pressure to evolve MLTRs in specific bacterial species, most of which are associated with mammalian gastrointestinal tracts. However, it remains unclear what these evolutionary pressure(s) are. Compared to the number of MLTRs identified by our analysis the number of experimentally validated MLTRs is extremely low indicating that a large fraction of MLTRs function remains to be understood (Table A.1). In support of this, the majority of MLTRs identified here (~56%) encode only a DNA binding domain and no additional domains of known function (Supplemental File B.4). Our data show that MLTRs are enriched within genera that are commonly associated with mammalian gastrointestinal tracts thus gaining deeper insights into the regulatory roles of these MLTRs will likely contribute to developing a more complete understanding of the gastrointestinal microbiome.

B.5 – Supplemental Figures and Tables

Due to the size of Supplemental Figure B.1, Supplemental File B.1, Supplemental File B.2, Supplemental File B.3, Supplemental File B.4, Supplemental Table B.1, Supplemental Table B.2, and Supplemental Table B.3 these data are included as attachments and are not within this document.

Table B.1: Distribution of MLTRs within Bacterial Phyla.

GTDB Taxonomy	# of phylum members enriched with MLTRs	# of phylum members with at least 1 MLTR	Percentage of phylum members enriched with MLTRs
<i>p__Acidobacteria</i>	3	27	11.11111111
<i>p__Actinobacteria</i>	30	1625	1.846153846
<i>p__Aquificae</i>	0	8	0
<i>p__Armatimonadetes</i>	0	2	0
<i>p__Bacteroidetes</i>	555	1220	45.49180328

Table B.1 (cont'd)

<i>p__Balneolaeota</i>	0	11	0
<i>p__Caldiserica</i>	0	1	0
<i>p__Calditrichaeota</i>	0	1	0
<i>p__Chlamydiae</i>	0	17	0
<i>p__Chlorobi</i>	0	13	0
<i>p__Chloroflexi</i>	0	28	0
<i>p__Chrysiogenetes</i>	0	2	0
<i>p__Cyanobacteria</i>	0	103	0
<i>p__Deferribacteres</i>	0	5	0
<i>p__Deinococcus-Thermus</i>	0	62	0

Table B.1 (cont'd)

<i>p__Dictyoglomi</i>	0	2	0
<i>p__Elusimicrobia</i>	0	1	0
<i>p__Firmicutes</i>	191	1932	9.886128364
<i>p__Fusobacteria</i>	0	19	0
<i>p__Ignavibacteriae</i>	0	2	0
<i>p__Kiritimatiellaeota</i>	0	1	0
<i>p__Lentisphaerae</i>	0	2	0
<i>p__Nitrospinae</i>	0	1	0
<i>p__Nitrospirae</i>	0	9	0
<i>p__Planctomycetes</i>	0	29	0

Table B.1 (cont'd)

<i>p__Proteobacteria</i>	81	3961	2.044938147
<i>p__Rhodothermaeota</i>	0	3	0
<i>p__Spirochaetes</i>	67	129	51.9379845
<i>p__Synergistetes</i>	0	9	0
<i>p__Tenericutes</i>	0	26	0
<i>p__Thermodesulfobacteria</i>	0	6	0
<i>p__Thermotogae</i>	0	23	0
<i>p__Verrucomicrobia</i>	0	25	0

APPENDIX C:

Supplemental Material for Chapter 3

C.1 – Supplemental Tables and Figures

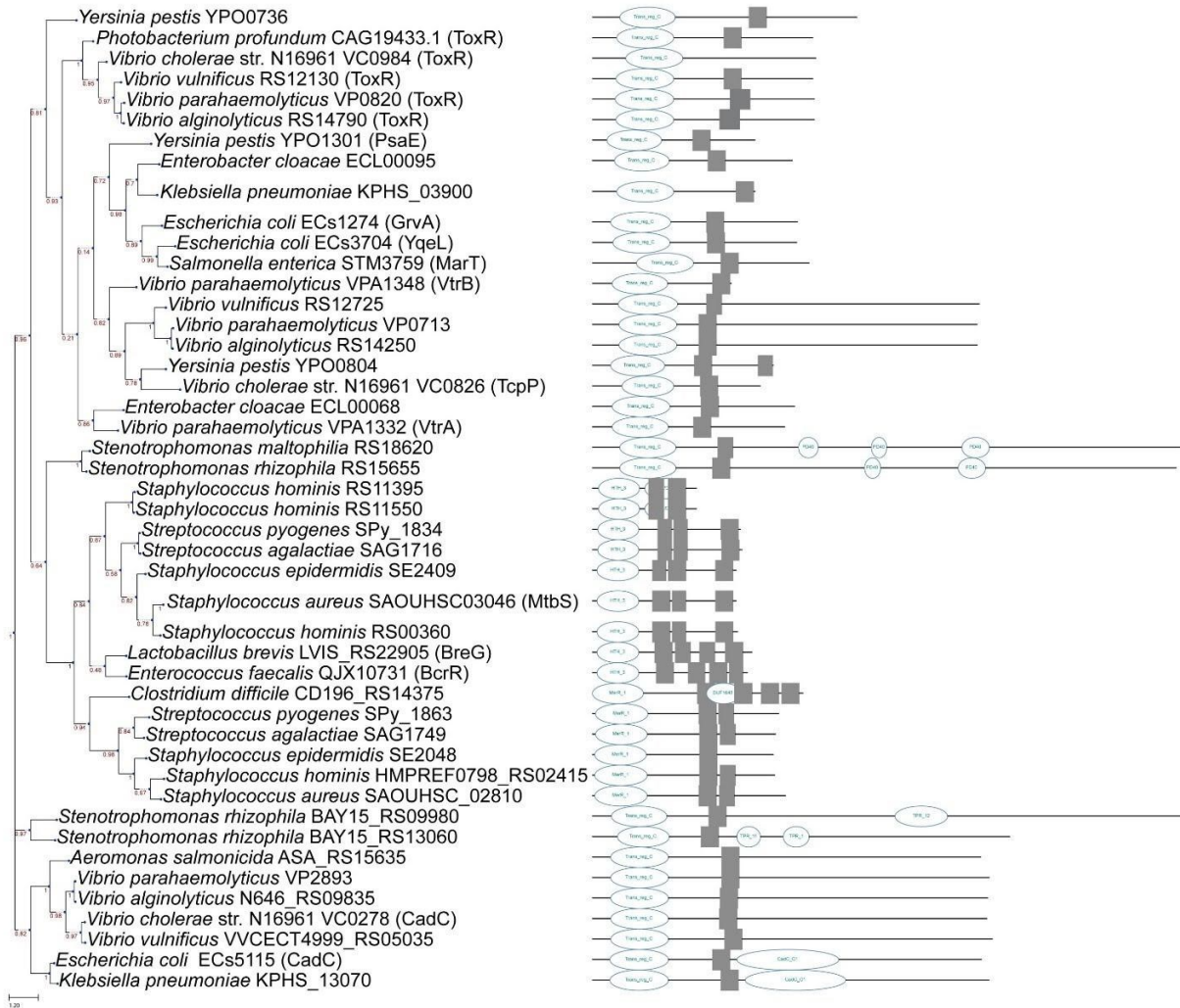


Figure C.1: Possible membrane localized transcription regulators (MLTRs) within Gram-negative and Gram-positive bacteria. Maximum likelihood phylogenetic tree of MLTRs collected from the MiST database, phylogenetic tree generated using the TREND server (449, 450). MLTRs displayed here represent a portion of the total MLTRs identified in our small survey. Genus and species information displayed on each branch followed by locus tag and gene designation, where applicable. Numbers next to branch points indicate the bootstrap value. Bootstrap values were generated from 100 replicates. The corresponding MLTRs genes are displayed on the right with their predicted domain(s) (in blue) and transmembrane domain(s) in gray.

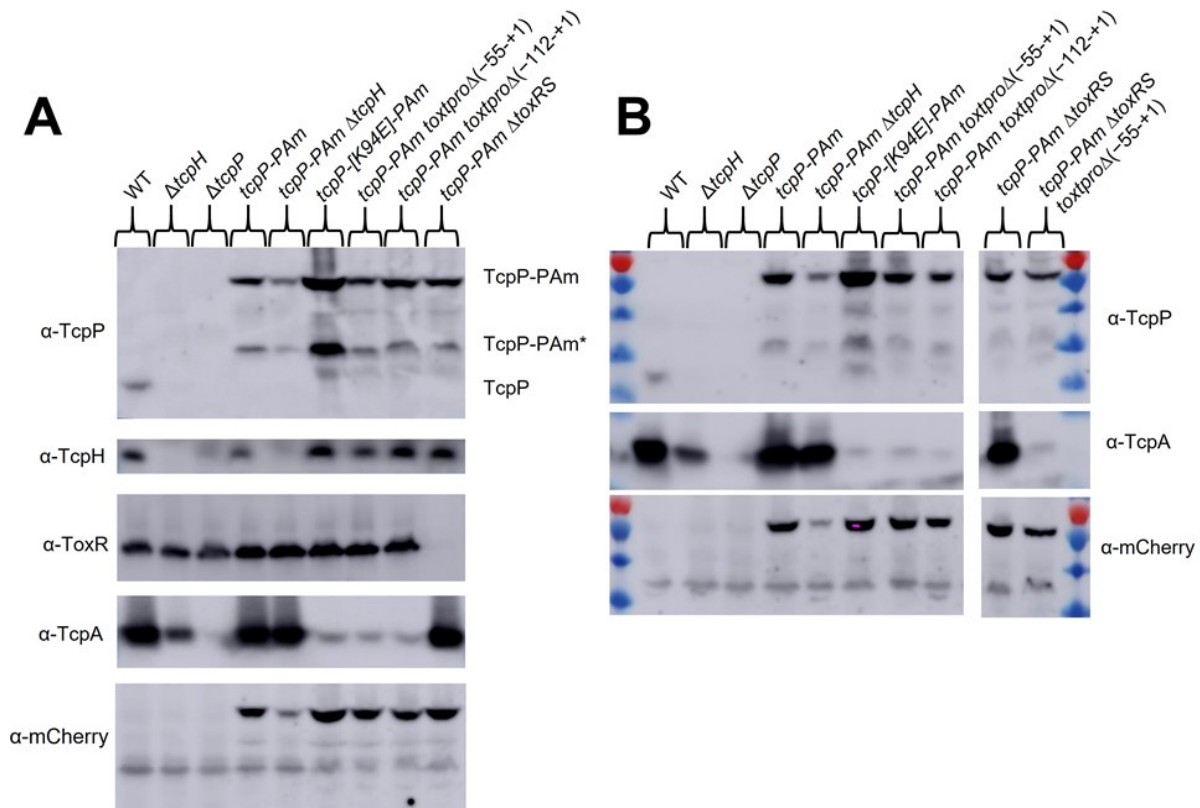


Figure C.2: **Biochemical characterization of *tcpP-PAm* strains.** A and B) Western blots of cultures grown under virulence-inducing conditions for 6 hrs, see methods for primary antibody dilution. Photoactivatable mCherry (PAmCherry) is fused to the C-terminus of TcpP and is under the control of its endogenous promoter on the chromosome. Addition of PAmCherry to TcpP results in two species: TcpP-PAmCherry (~70KDa) and TcpP-PAmCherry* (~36KDa). Deletion of *tcpH* yields lower levels of TcpP-PAmCherry and TcpP-PAmCherry*, likely due to an increase in regulated intramembrane proteolysis (RIP).

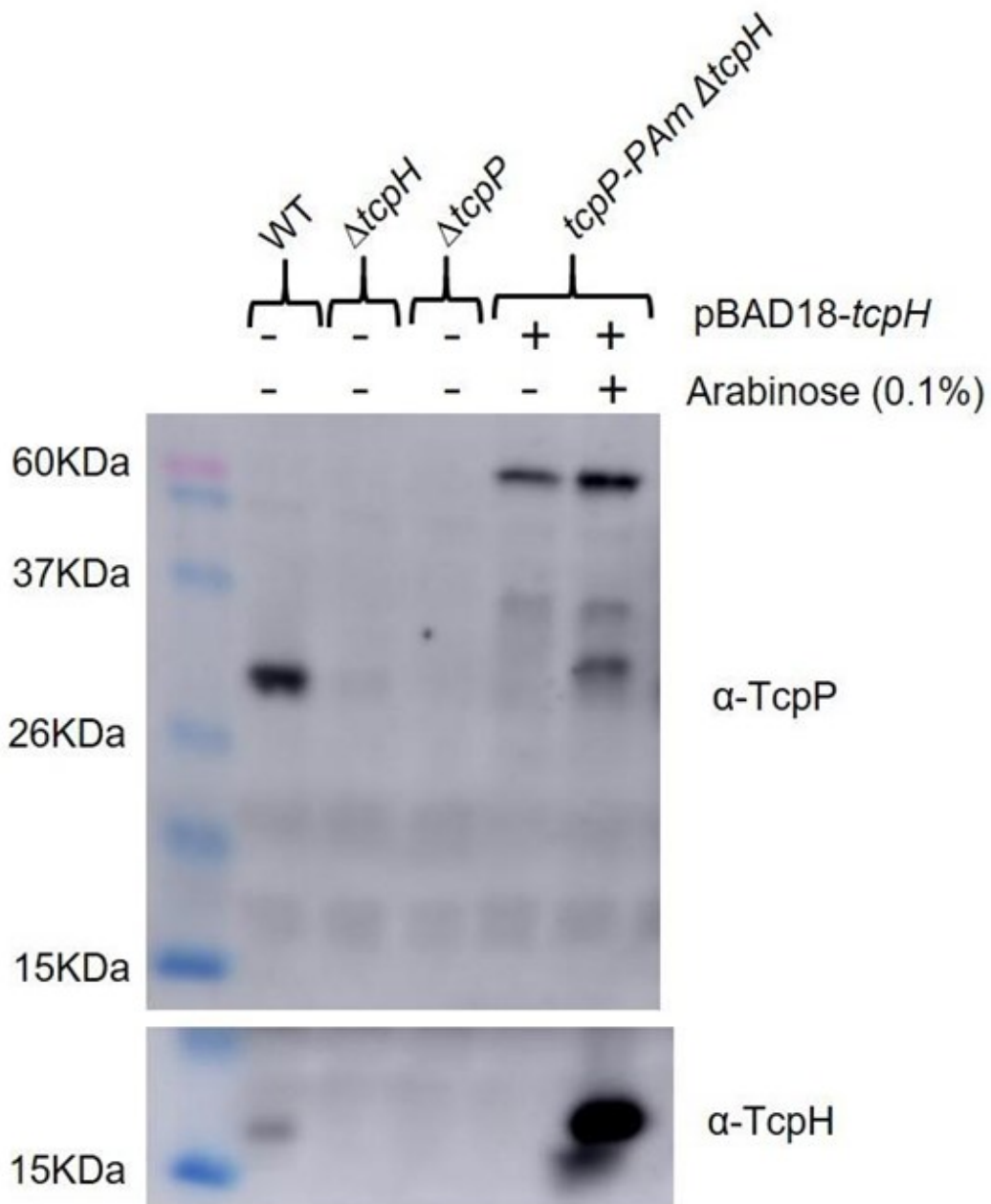


Figure C.3: **TcpH protects TcpP-PAM from proteolysis.** Western blots of cultures grown under virulence-inducing conditions for 6 hrs with or without arabinose, see methods for primary antibody dilution. *tcpP-PAMCherry* Δ *tcpH* cells harbor an arabinose-inducible vector (pBAD18) encoding *tcpH*. Ectopic transcription of *tcpH* complemented deletion of *tcpH*. Complementation of *tcpH* also resulted in an additional TcpP band, ~29KDa, that corresponds to native TcpP.

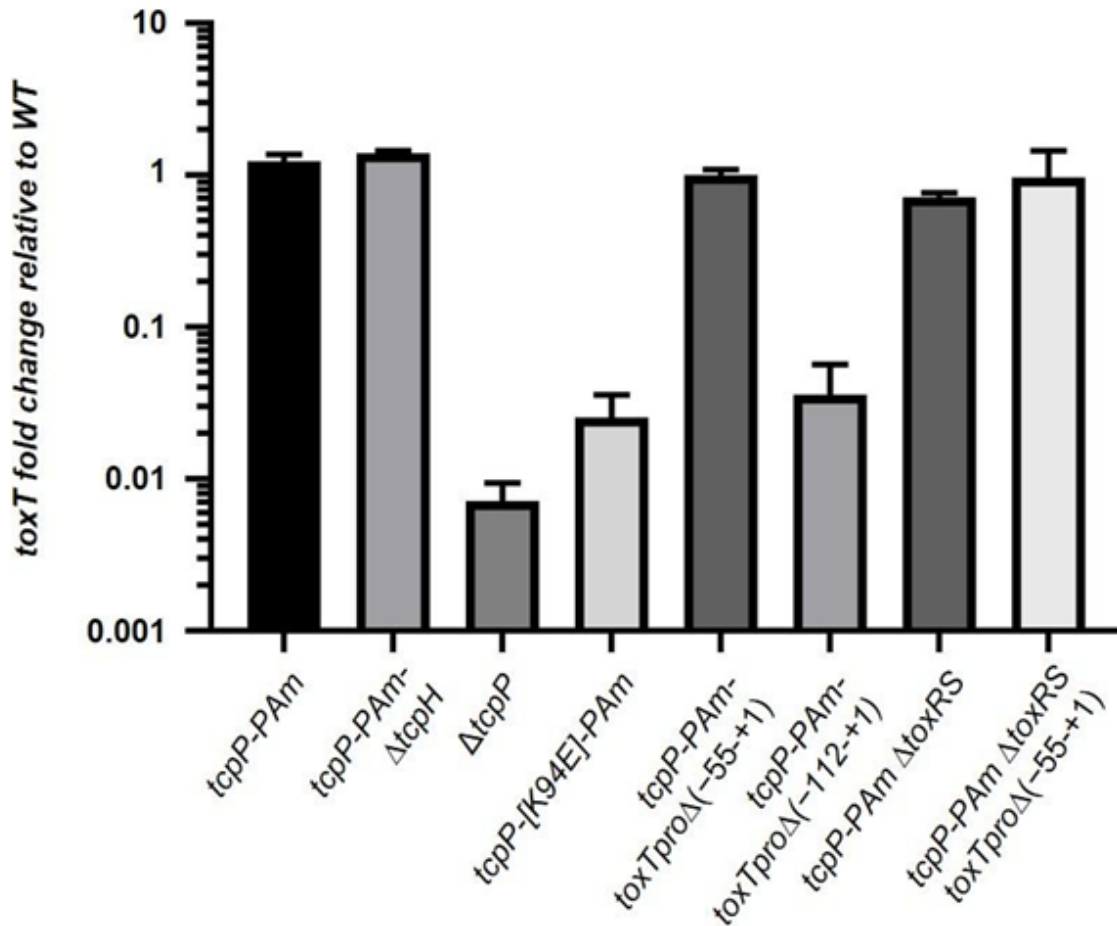


Figure C.4: ***toxT* transcription profile in *tcpP-PAm* strains.** Average *toxT* fold change, relative to WT, across three biological replicates (determined via the $\Delta\Delta C_T$ method) (322). mRNA was collected from cells after 2 hrs in virulence-inducing conditions, and error bars represent standard error of the mean.

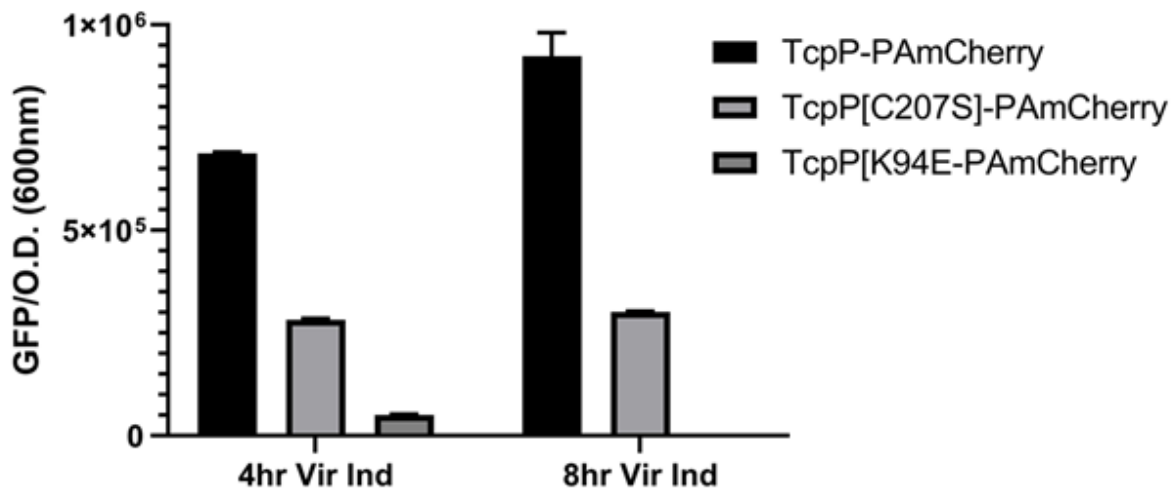


Figure C.5: **PAmCherry does not promote dimerization of TcpP.** *toxT* transcription in *V. cholerae* cells determined using a plasmid based *toxT::GFP* transcriptional reporter. At each time point, *toxT* transcription was determined by measuring GFP fluorescence (excitation 488nm and emission 515nm) and optical density (600nm). The data here are an average of three biological replicates. Error bars represent the standard error of the mean.

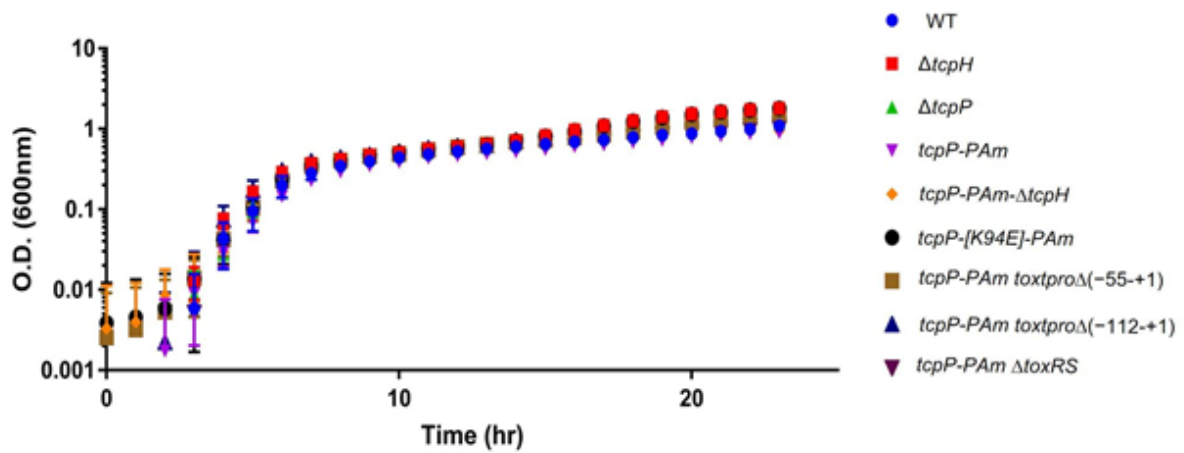


Figure C.6: ***tcpP-PAm* strains have growth dynamics similar to WT.** *in vitro* growth curve under virulence-inducing conditions. Optical density (O.D.) values are the average of three biological replicates and error bars represent standard error of the mean.

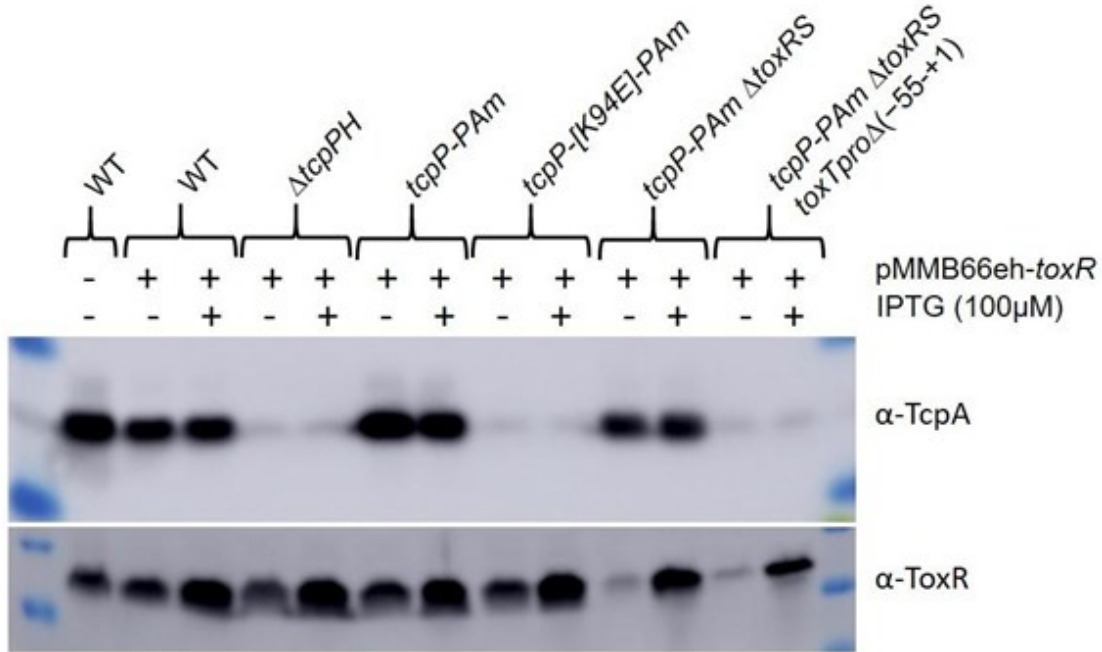


Figure C.7: Complementation and overexpression of ToxR in *tcpP-PAm* strains. Western blots of cellular lysates collected after growth under virulence-inducing conditions for 6 hrs with or without IPTG, see methods for primary antibody dilution. ToxR does not stimulate TcpA production without TcpPH, and ToxR cannot complement TcpPK94E-PAmCherry or *toxTpro*Δ(-55-+1). Low levels of ToxR were detected in *tcpP-PAmCherry* Δ*toxRS* and *tcpP-PAmCherry* Δ*toxRS* *toxTpro*Δ(-55-+1) without IPTG, likely due to leaky transcription of *toxRS* at the IPTG promoter. Multiple copies of the lac promoter are known to result in leaky transcription due to insufficient levels of LacI (470, 471).

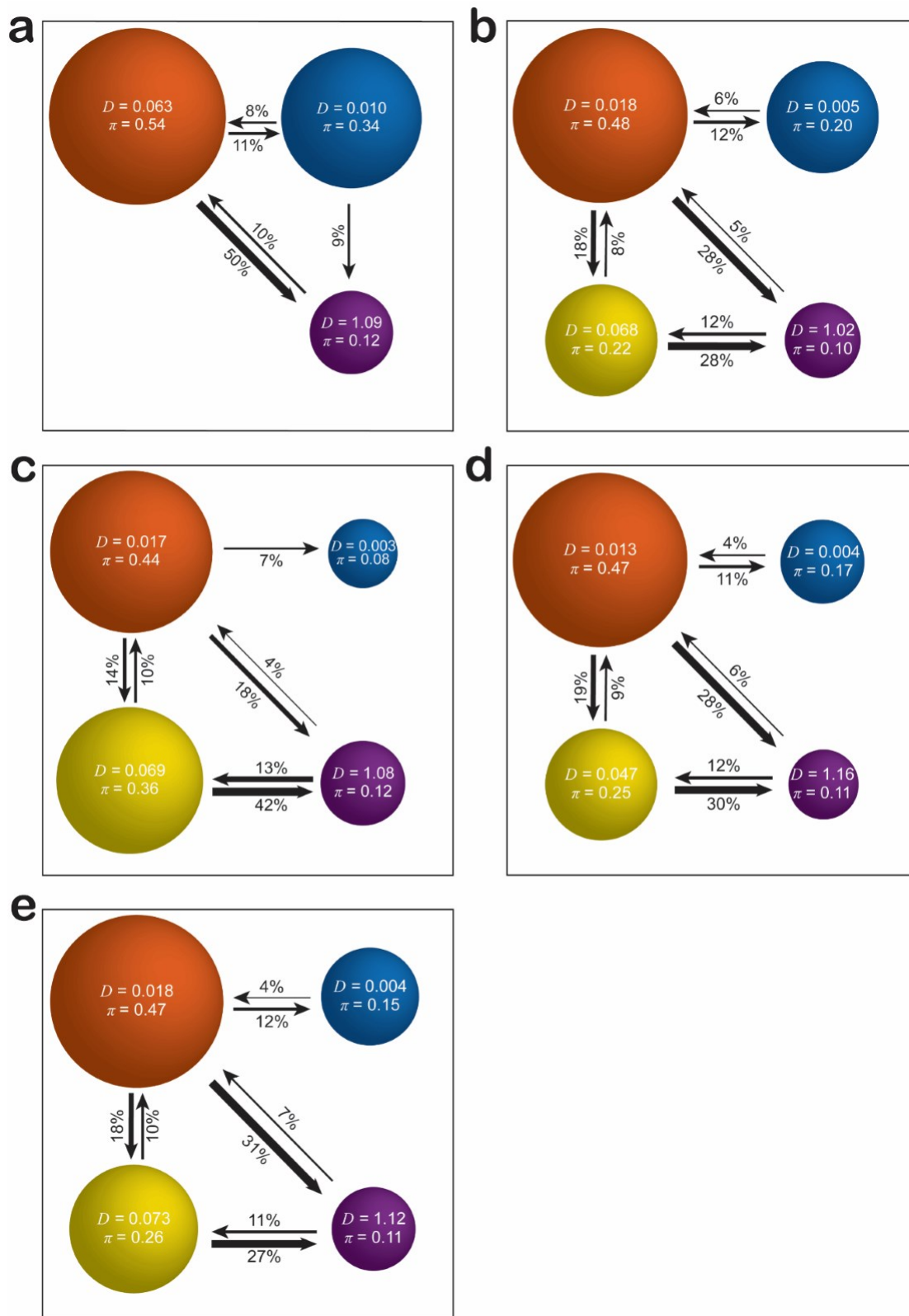


Figure C.8: **TcP-PAMCherry transition plots**. Based on the identification of distinct diffusion states for TcP-PAMCherry (circles with colors as in Figure 3.1C and with

Figure C.8 (cont'd)

average single-molecule diffusion coefficient, D , indicated in $\mu\text{m}^2/\text{s}$), the average probabilities of transitioning between mobility states at each step are indicated as arrows between those two circles, and the circle areas are proportional to the weight fractions. Low significance transition probabilities less than 4% are not displayed. Numbers above the arrows indicate the probability of transition. a) *V. cholerae tcpP-PAmCherry toxTpro* $\Delta(-55-+1)$, corresponding to main text Figure 3.2D. b) *V. cholerae tcpP-PAmCherry Δ toxRS*, corresponding to main text Figure 3.3B. c) *V. cholerae tcpP-PAmCherry Δ toxRS toxTpro* $\Delta(-55-+1)$, corresponding to main text Figure 3.3D. d) *V. cholerae tcpP-PAmCherry pMMB66eh-toxR*, corresponding to main text Figure 3.3F e) *V. cholerae tcpP-K94E-PAmCherry*, corresponding to main text Figure 3.4B.

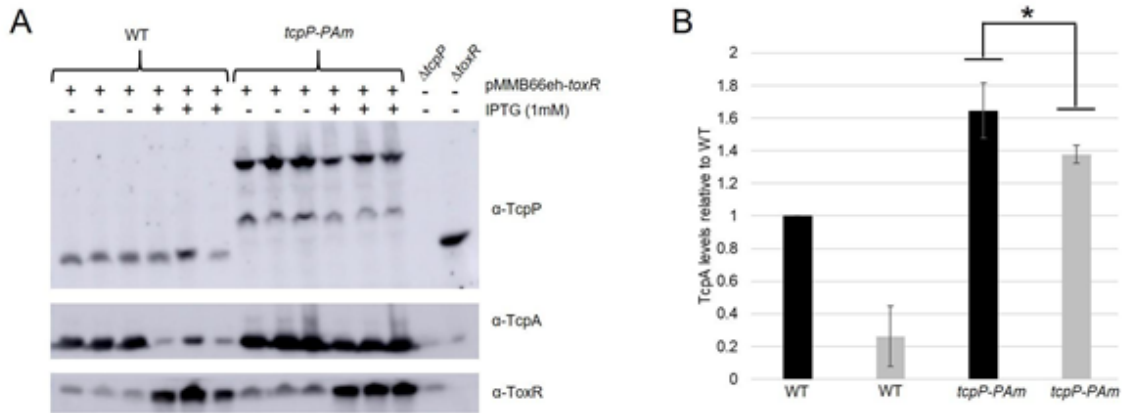


Figure C.9: **ToxR overexpression reduces virulence factor production.** A) Western blots of cell lysates, three biological replicates, collected after 6 hrs of virulence-inducing conditions with or without IPTG. B) Densitometry analysis of the TcpA western blot in panel A. ImageJ was used to perform the densitometry analysis. Black bars: -IPTG; gray bars: +IPTG. Error bars represent standard deviation. One-tailed Student's *t*-test was used to determine statistical significance. *indicates a P-value of 0.029.

Table C.1: **Chapter 3 strain list.**

Strain	Description	Reference
<i>V. cholerae</i> 0395 classical biotype	Wild type	DiRita lab collection
<i>V. cholerae</i> $\Delta tcpH$	Isogenic deletion	Beck, N.A., et. al. 2004. <i>Journal of bacteriology</i> , 186(24), p.8309.
<i>V. cholerae</i> $\Delta tcpP$	Isogenic deletion	Häse, C.C. and Mekalanos, J.J., 1998. <i>Proceedings of the National Academy of Sciences</i> , 95(2), pp.730-734.
<i>V. cholerae</i> $\Delta toxRS$	Isogenic deletion	DiRita lab collection

Table C.1 (cont'd)

<i>V. cholerae tcpP-PAmCherry</i>	Isogenic construct; TcpP-PAmCherry (C-terminal fusion), native <i>tcpH</i> start codon and 3rd amino acid mutated (ATG to GTG and AAA to TAA respectively), and both ribosomal binding site and coding sequence of <i>tcpH</i> cloned downstream of PAmCherry.	
<i>V. cholerae tcpP-PAmCherry ΔtcpH</i>	Isogenic construct	This study
<i>V. cholerae tcpP-PAmCherry ΔtoxRS</i>	Isogenic construct	This study
<i>V. cholerae tcpP-PAmCherry ΔtoxRS toxTproΔ(-55-+1)</i>	Isogenic construct	This study
<i>V. cholerae tcpPK94E-PAmCherry</i>	Isogenic construct	This study

Table C.1 (cont'd)

<i>V. cholerae tcpP-PAmCherry</i> toxTproΔ(-55-+1)	Isogenic construct	This study
<i>V. cholerae tcpP-PAmCherry</i> toxTproΔ(-112-+1)	Isogenic construct	This study
<i>V. cholerae tcpP-PAmCherry</i> pMMB66eh-toxR	Isogenic construct	This Study
<i>E. coli</i> ET12567 Δ <i>dapA</i>	Cloning vector recipient	Allard, N., et. al. 2015. Canadian journal of microbiology, 61(8), pp.565-574.
<i>E. coli</i> ET12567 Δ <i>dapA</i> pKAS32- (empty vector)	Plasmid vector strain	Skorupski, K. and Taylor, R.K., 1996. <i>Gene</i> , 169(1), pp.47-52.

Table C.2: **Chapter 3 primer list.** Kpn1-HiFi restriction sites were included in forward primers and Xba1 restriction sites were included in all reverse primers to provide homology between insert and vector sequences.

Description	Sequence
pKAS-TcpP promoter FW	ctaacgtaacaaccggtacTTTCGAGTGATAGAAAAAG G
pKAS-TcpP FW	ctaacgtaacaaccggtacATGGGGTATGTCCGCGTG
TcpP-PAmCherry FW	atgactaaaaatATGGTGAGCAAGGGCGAGGA
TcpP-PAmCherry RV	ccttgctcaccatATTTTTAGTGCATTCTAATGTCTTCT GTTC
TcpH-PAmCherry FW	ctaagtcttCTTGACAGCTCGTCCATGC
TcpH-PAmCherry RV	gctgtacaagAAGACATTAGAATGCACAAAAATTAA AAG
Downstream TcpH-PAmCherry RV	tcatgataagaccCTTGACAGCTCGTCCATGCC
Downstream TcpH-PAmCherry FW	cgagctgtacaagGGTCTTATCATGAGCCGCCTAG
pKAS-downstream TcpH RV	aaattgcatgctagctatagttCTTGGTCTTTTTTAGATA ACGTAAGC
TcpPK94E RV	GATCAACGTCTCATGTTTCATC
TcpPK94E FW	GATGAACATGAGACGTTGATC
<i>toxTpro</i> Δ(-55-+1) RV	tccaatcatATCTTAAAATCGAAGTTAATATAAAACT AC

Table C.2 (cont'd)

<i>toxTpro</i> Δ(-55-+1) FW	gattttaagatATGATTGGGAAAAAATCTTTTC
pKAS- <i>toxTpro</i> Δ(-112-+1) FW	ctaacgtaacaaccggtacGTTGGTGGTGTTCAGATA ATAC
<i>toxTpro</i> Δ(-112-+1) RV	ttcccaatcaGTATTACATAAGAAAAACATAAAGTAA CTCATG
<i>toxTpro</i> Δ(-112-+1) FW	tatgtaatacTGATTGGGAAAAAATCTTTTC
pKAS- <i>toxTpro</i> Δ(-112-+1) RV	tgcgcatgctagctatagttATCATCAGTAATAAATATAGA GTTATATTTTTTTTC
<i>recA</i> FW	ATTGAAGGCGAAATGGGCGATAG
<i>recA</i> RV	TACACATACAGTTGGATTGCTTG AGG
<i>toxT</i> FW	ACTGATGATCTTGATGCTATGGAG
<i>toxT</i> RV	CATCCGATTCGTTCTTAATTCACC

APPENDIX D:
Supplemental Material for Chapter 4

D.1 – Supplemental Methods

D.1.1 – Mass-spectroscopy methods

Samples analyzed via Mass-spectroscopy were run on an SDS page gel (12.5% acrylamide) for 20 minutes at 100 volts. The mobilized protein was then excised from SDS page gel (using a methanol washed razor) and suspended in 5% methanol. Samples were then analyzed by the Michigan State University Proteomics core to identify all peptides within the samples. Below is a brief description of their methods.

Gel bands were digested in-gel according to Shevchenko, et. al. with modifications (472). Briefly, gel bands were washed with 100mM ammonium bicarbonate and dehydrated using 100% acetonitrile. Sequencing grade modified trypsin was prepared to 0.01 $\mu\text{g}/\mu\text{L}$ in 50mM ammonium bicarbonate and $\sim 100 \mu\text{L}$ of this was added to each gel band so that the gel was completely submerged. Bands were then incubated at 37°C overnight. Peptides were extracted from the gel by water bath sonication in a solution of 60% acetonitrile and 1% TFA and vacuum dried to $\sim 2 \mu\text{L}$. Peptides were then re-suspended in 2% acetonitrile and 0.1% TFA to 20 μL . From this, 5 μL were automatically injected by a Thermo EASYnLC 1200 onto a Thermo Acclaim PepMap RSLC C18 peptide trap (5 μm , 0.1mm x 20mm) and washed with buffer A for ~ 5 min. Bound peptides were then eluted onto a Thermo Acclaim PepMap RSLC 0.075mm x 250mm C18 resolving column and eluted over 35min with a gradient of 8% B to 40% B in 24min, ramping to 90% B at 25 min and held at 90% B for the duration of the run (Buffer A = 99.9% Water, 0.1% Formic Acid, Buffer B = 80% Acetonitrile, 0.1% Formic Acid, 19.9%

Water) at a constant flow rate of 300 nL/min. Column temperature was maintained at 50°C using an integrated column heater (PRSO-V2).

Eluted peptides were sprayed into a ThermoFisher Q-Exactive HF-X mass spectrometer using a FlexSpray spray ion source. Survey scans were taken in the Orbitrap (60000 resolution, determined at m/z 200) and the top 15 ions in each survey scan were then subjected to automatic higher energy collision induced dissociation (HCD) with fragment spectra acquired at 15,000 resolution. The resulting MS/MS spectra are converted to peak lists using Mascot Distiller, v2.7 (www.matrixscience.com) and searched against a database containing all *V. cholerae* strain ATCC39541/Classical Ogawa 395/0395 protein entries available from UniProt (downloaded from www.uniprot.org) appended with customer provided sequences and common laboratory contaminants (www.thegpm.org). Searches were performed using the Mascot searching algorithm, v 2.7, on an in-house server. The Mascot output was then analyzed using Scaffold, v4.11.0 (www.proteomesoftware.com) to probabilistically validate protein identifications. Assignments validated using the Scaffold 1% FDR confidence filter are considered true.

D.1.2 – Fatty acid analysis

Analysis of fatty acids from whole *V. cholerae* cells was done as previously described (473). Briefly, *V. cholerae* cells were grown with and without α -linolenic acid (500 μ M) as described in section D.1.3 – Supplemental virulence inducing culture conditions. Cells were collected by centrifugation (2450 X g 15 minutes) and then washed with PBS. Cells were then lysed via addition of 300 μ l of extraction solvent (composed of

methanol, chloroform and formic acid [20:10:1, v/v/v]). After lipids were extracted the Fatty Acyl Methylene Ester (FAME) reactions were carried out as described (473). After the FAME reactions, fatty acid content was measured via Gas-Liquid Chromatography using a DB-23 column (Agilent, part number: 122-2332). Molar values of each peak was then normalized to an internal standard (15:0) to calculate the total molar percentage of each fatty acid detected.

D.1.3 – Supplemental virulence inducing culture conditions

To test if crude bile (Ox gal, Sigma Aldrich), as well as components of crude bile, we opted to pretreat all *V. cholerae* strains under Vir Ind conditions before exposing cells to these additional factors. *V. cholerae* cells were subcultured from overnight cultures to an optical density (600 nm) of 0.01 in 100 ml of LB pH 6.5 in a 250 ml Erlenmeyer flask. *V. cholerae* strains were grown for 4 hours under Vir Ind conditions, centrifuged (2450 X g 15 minutes), resuspended in 0.8 ml LB. 200 µl of resuspended cells were transferred to 50 ml of fresh Vir Ind media in 125 ml Erlenmeyer flasks. The remaining 200 µl of cells were lysed and analyzed via western blot. A maximum of 4 different conditions were tested per strain per biological replicate due to limited incubator space. The following were supplemented to Vir Ind media: crude bile (CB; final concentration), α -linolenic acid (LA; final concentration 500µM), palmitic acid (PA; final concentration 500µM), purified bile salts cholate and deoxycholate (PB; final concentration 100µM). All compounds were purchased from Sigma Aldrich. CB and PB were solubilized in Vir Ind media and filter sterilized (0.22 µM) before addition to Vir Ind. LA and PA were dissolved in 1 ml of

Dimethyl sulfoxide (DMSO) and then added to Vir Ind media. LA and PA sterility were confirmed by spreading 100µl of DMSO solubilized LA and PA on LB agar plates (data not shown).

D.2 – Supplemental Tables and Figures

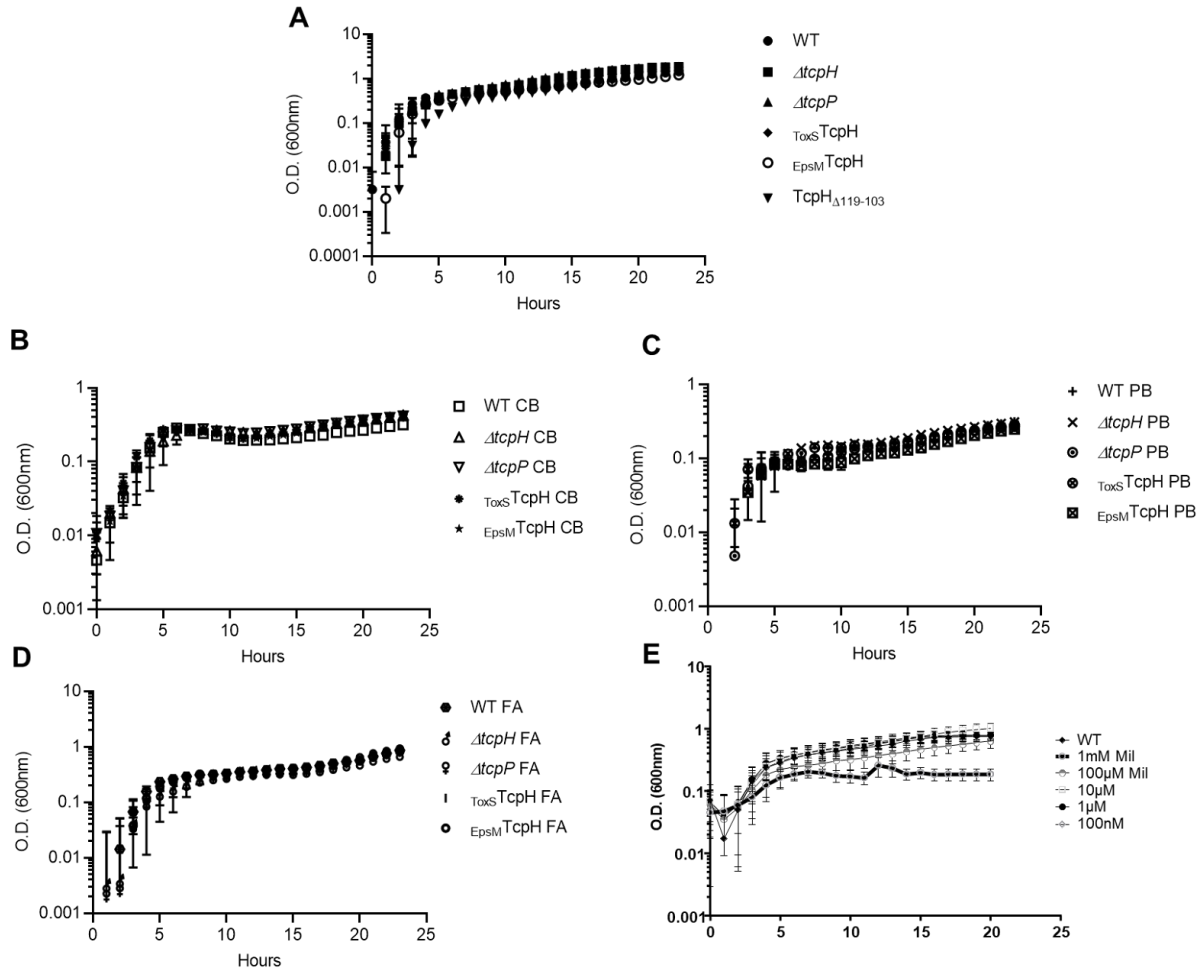


Figure D.1: TcpH transmembrane and periplasmic constructs growth dynamics are similar to WT. A) Virulence inducing conditions growth curve of TcpH TM and Peri constructs respectively. B) Virulence inducing condition growth curve supplemented with crude bile (0.4%). C) Virulence inducing condition growth curve supplemented with purified bile salts (cholate/deoxycholate 100 μ M). D) Virulence inducing condition growth curve supplemented with α -linolenic acid (500 μ M). E) LB, 37°C, growth curve with 1mM to 100nM Miltefosine.

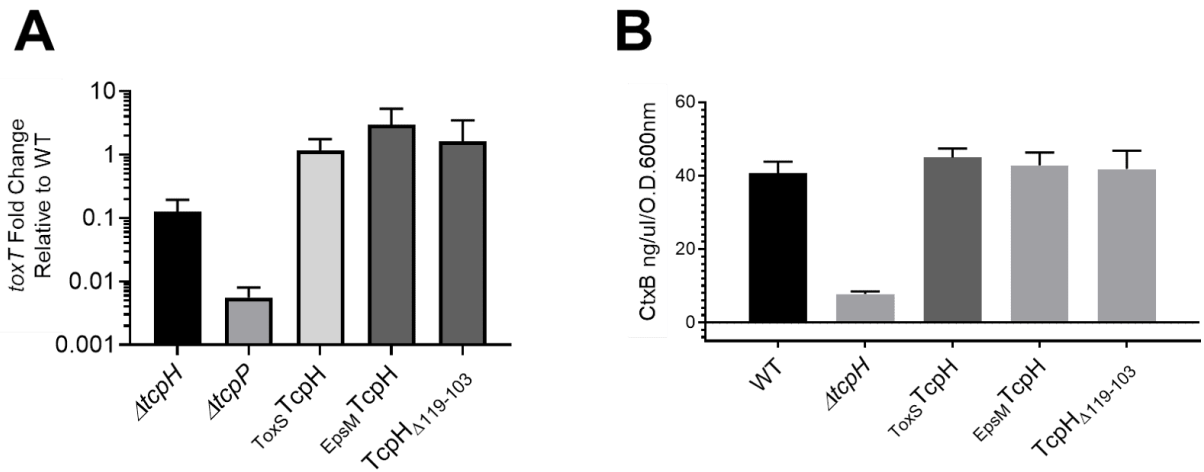


Figure D.2: **TcpH transmembrane and periplasmic constructs support *toxT* transcription and CtxB production.** A) Average *toxT* transcription of three biological replicates, determined via $\Delta\Delta C_T$ method. *toxT* fold change is relative to WT *V. cholerae* (i.e., *toxT* transcription=1). B) CtxB levels, measured via ELISA, in culture supernatants collected from cultures incubated with *V. cholerae* cells cultured in virulence inducing conditions for 24hrs. Error bars represent standard error of the mean.

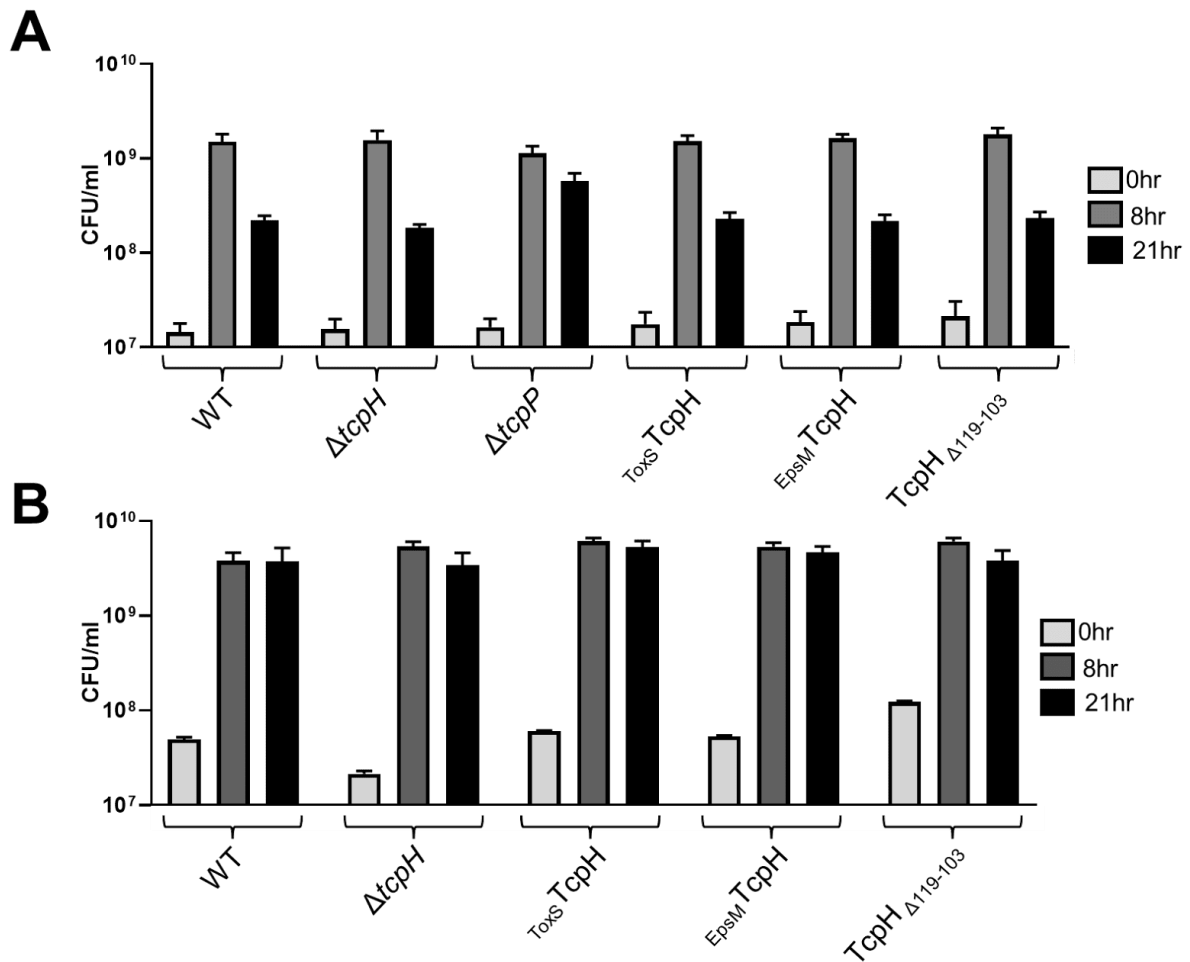


Figure D.3: **TcpH transmembrane and periplasmic constructs display WT growth in adult mice feces.** A) Filter sterilized mice fecal growth curve. B) Non-filtered (i.e., non-sterile) mice fecal growth curve. *ΔtcpP* was excluded from non-sterile mice fecal growth experiment due to limited supply of non-sterile mice fecal media. For all data presented here, averages represent three biological replicates. Error bars represent standard error of the mean.

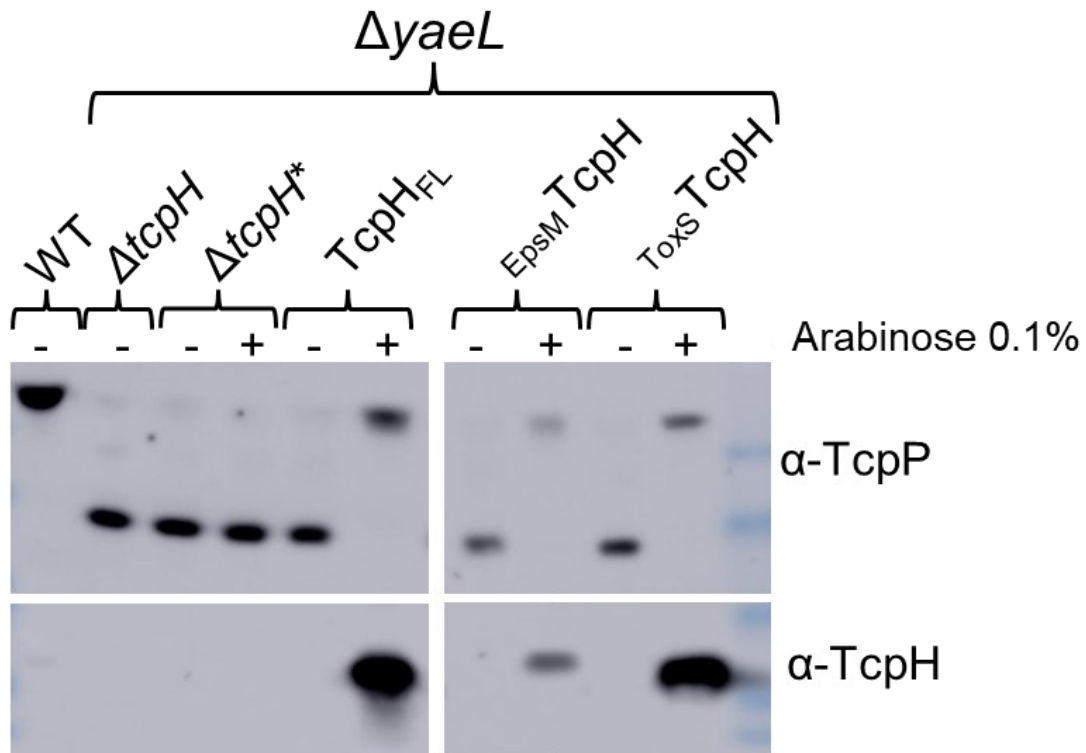


Figure D.4: **TcpH transmembrane constructs inhibit RIP of TcpP**. Western blots of spheroplast fractions (cytoplasm and cytoplasmic membrane fractions). TcpH transmembrane constructs ($ToxS$ TcpH and Eps^M TcpH) and native TcpH were expressed from pBAD18 in $\Delta tcpH \Delta yaeL$ background under virulence inducing conditions for 6hrs. All strains, excluding WT, are $\Delta tcpH \Delta yaeL$. $\Delta tcpH^*$ harbors pBAD18 (empty vector). See Figure E.5 for full view of these western blots.

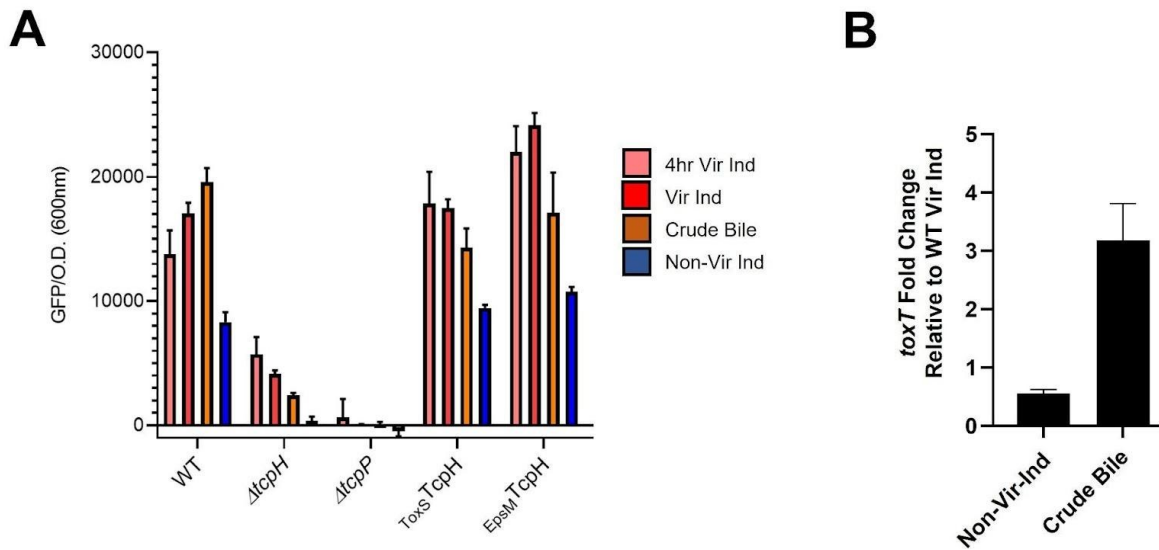


Figure D.5: Crude bile stimulates *toxT* transcription in a Tcph dependent manner. A) *toxT* transcription in Tcph transmembrane constructs in *V. cholerae* cells. *toxT* transcription was measured using a plasmid based *toxT::GFP* transcriptional reporter. The data here are an average of three or more biological replicates and error bars represent the standard error of the mean. Data for these strains for 4hr Vir Ind, Vir Ind, crude bile, and Non-Vir Ind can also be found in Figure D.6. B) *toxT* transcription in WT *V. cholerae* cells using RT-qPCR, determined via $\Delta\Delta$ CT method. Cells were incubated in Vir Ind for 4hrs and then transferred to indicated conditions for an additional 4hrs. RNA was collected at the 8hr time point. *toxT* transcription is relative to WT Vir Ind. Averages represent three biological replicates and error bars represent standard error of the mean. The data presented in panel B can also be found in Figure D.8A.

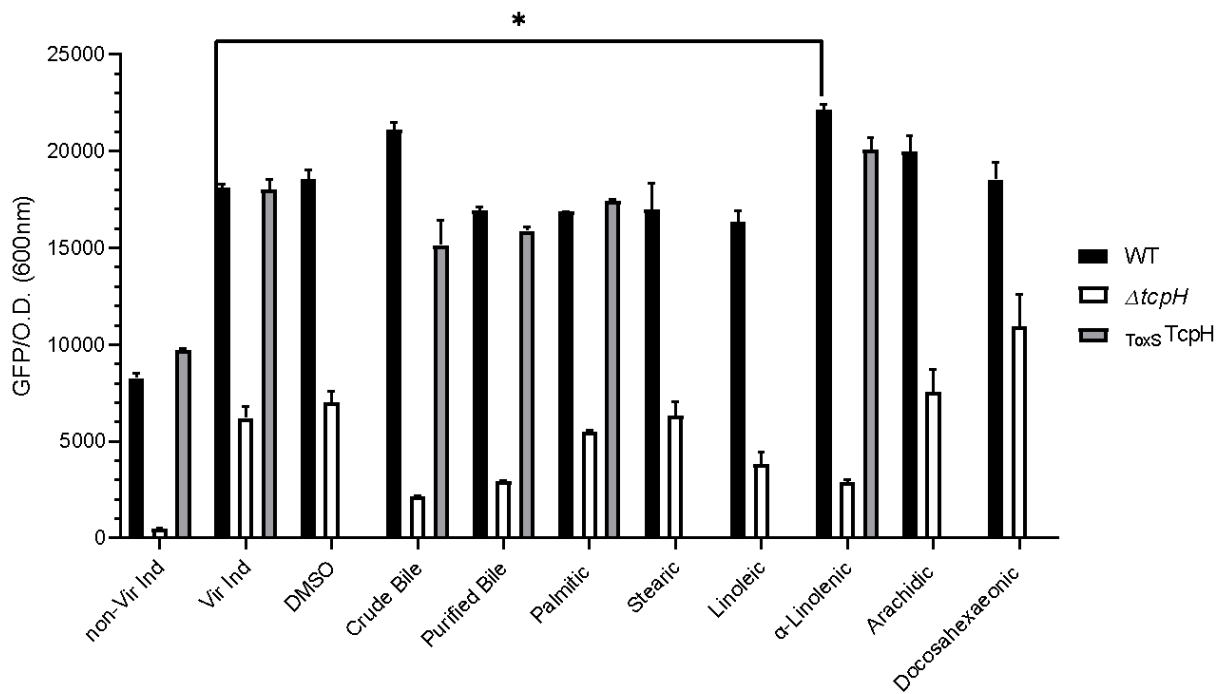


Figure D.6: **α -Linolenic acid stimulates *toxT* transcription in a *TcpH* dependent manner.** A) *toxT* transcription in WT (black bars), $\Delta tcpH$ (white bars), and $ToxS TcpH$ (dark gray bars) was determined using a plasmid based *toxT::GFP* transcriptional reporter. The data here are an average of three or more biological replicates and error bars represent the standard error of the mean. Two-tailed Student's t-test was used to determine statistical significance. *indicates a P-value of < 0.05 .

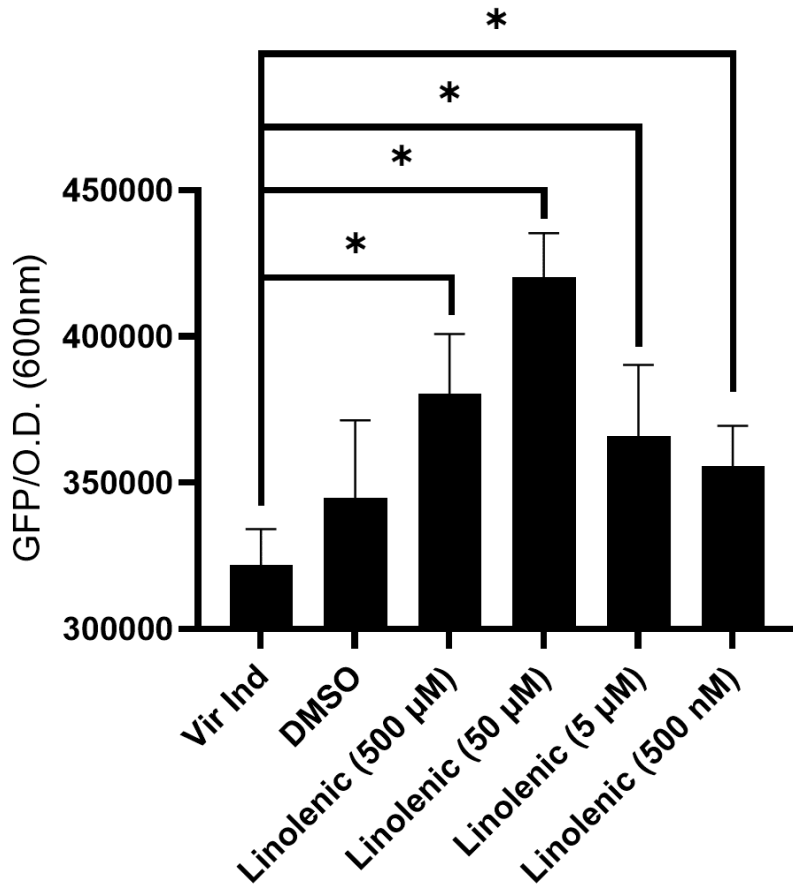


Figure D.7: **α -Linolenic acid stimulates *toxT* transcription in a dose dependent manner.** *toxT* transcription in WT (black bars), $\Delta tcpH$ (white bars), and $E_{psM}TcpH$ (grey bars) was determined using a plasmid based *toxT::GFP* transcription reporter. Concentrations of α -linolenic acid (LA) used are displayed below each bar. Lower concentrations of LA (50 μ M) were tested with control groups ($\Delta tcpH$ and $E_{psM}TcpH$) and were found to have similar levels of *toxT* transcription as virulence inducing conditions (Vir Ind), data not shown. Error bars represent standard deviation. A two-tailed Student's t-test was used to determine statistical significance. *indicates a P-value of < 0.05.

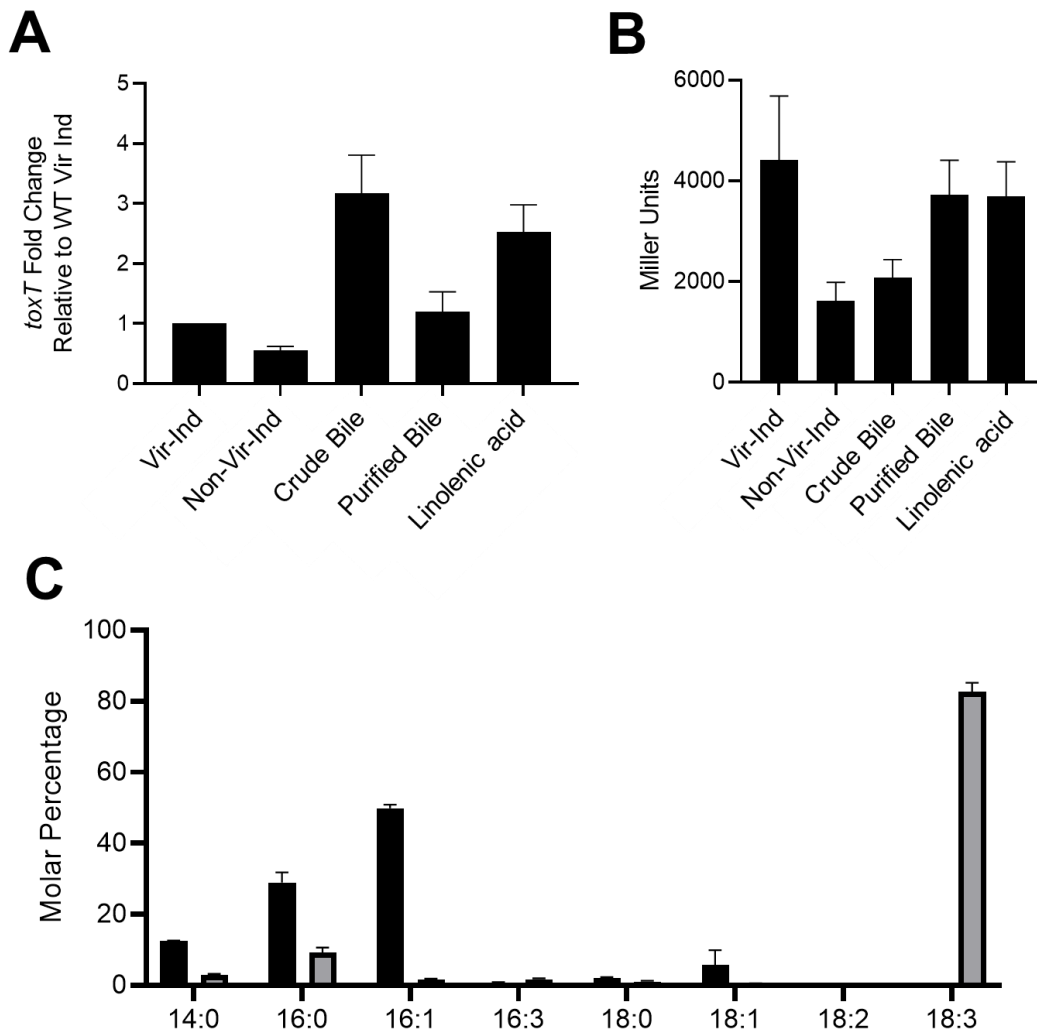


Figure D.8: ***toxT* transcription is stimulated by crude bile and α -linolenic acid, but *tcpP* transcription does not change.** A) *toxT* transcription in WT *V. cholerae* cells using RT-qPCR, determined via $\Delta\Delta$ CT method. Cells were incubated in Vir Ind for 4hrs and then transferred to indicated conditions for an additional 4hrs. RNA was collected at the 8hr time point. *toxT* transcription is relative to WT Vir Ind. Averages represent three biological replicates and error bars represent standard error of the mean. B) *tcpP* transcription in WT *V. cholerae* cells determined using *tcpP::lacZ* transcription. *tcpP* transcription was determined by quantifying LacZ activity (i.e., calculating Miller Units). *V. cholerae* cells were grown as in panel A. Averages represent five biological replicates for panel B. Error bars represent the standard error of the mean. D) Percentage of fatty acids present in whole *V. cholerae* cells cultured with α -linolenic acid (gray bars) and without (black bars). Error bars represent the standard deviation, and the average values here represent two biological replicates.

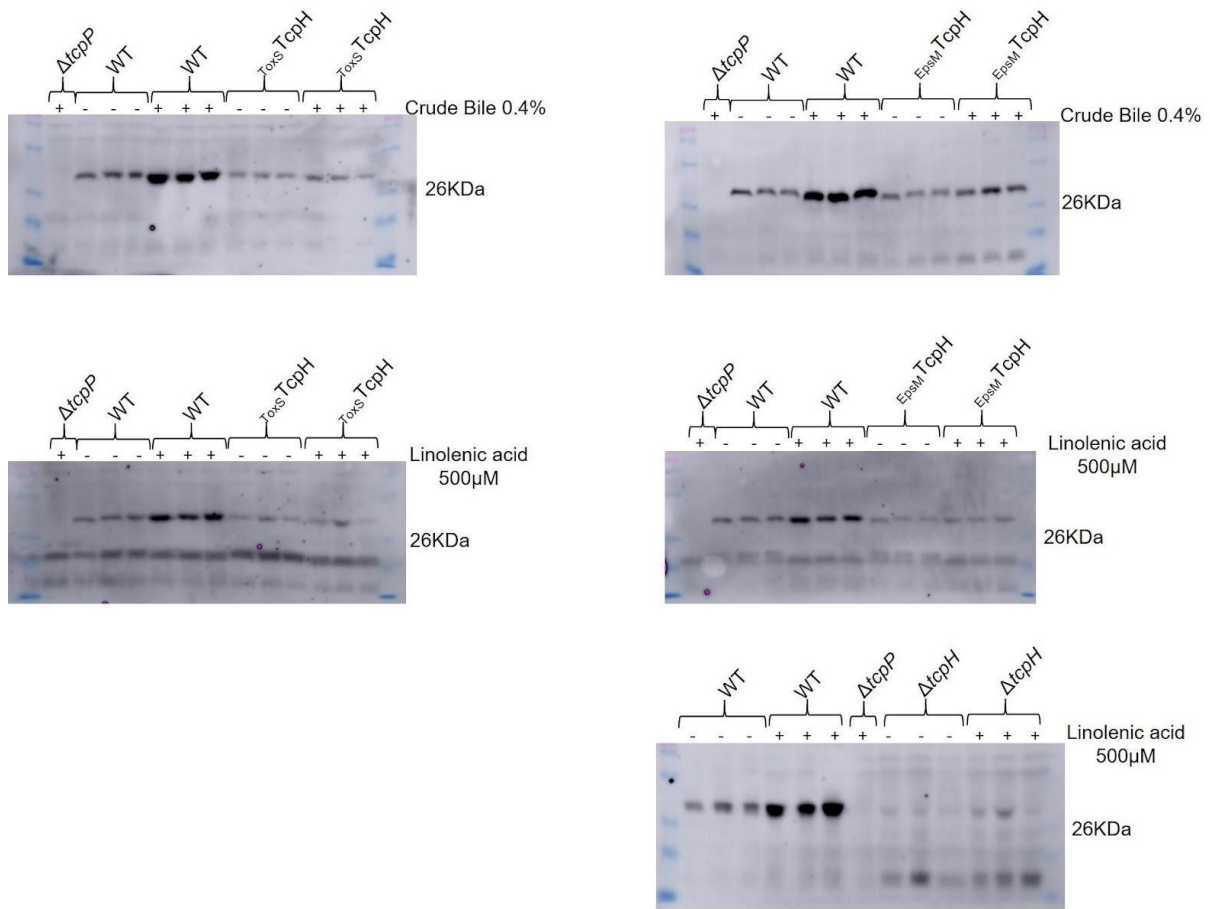


Figure D.9: **TcpP levels are elevated in the presence of crude bile and α -linolenic acid.** Western blots used to quantify TcpP levels in Figure 4.3C. TcpP is approximately 29KDa. Bands above and below 29KDa are non-specific bands.

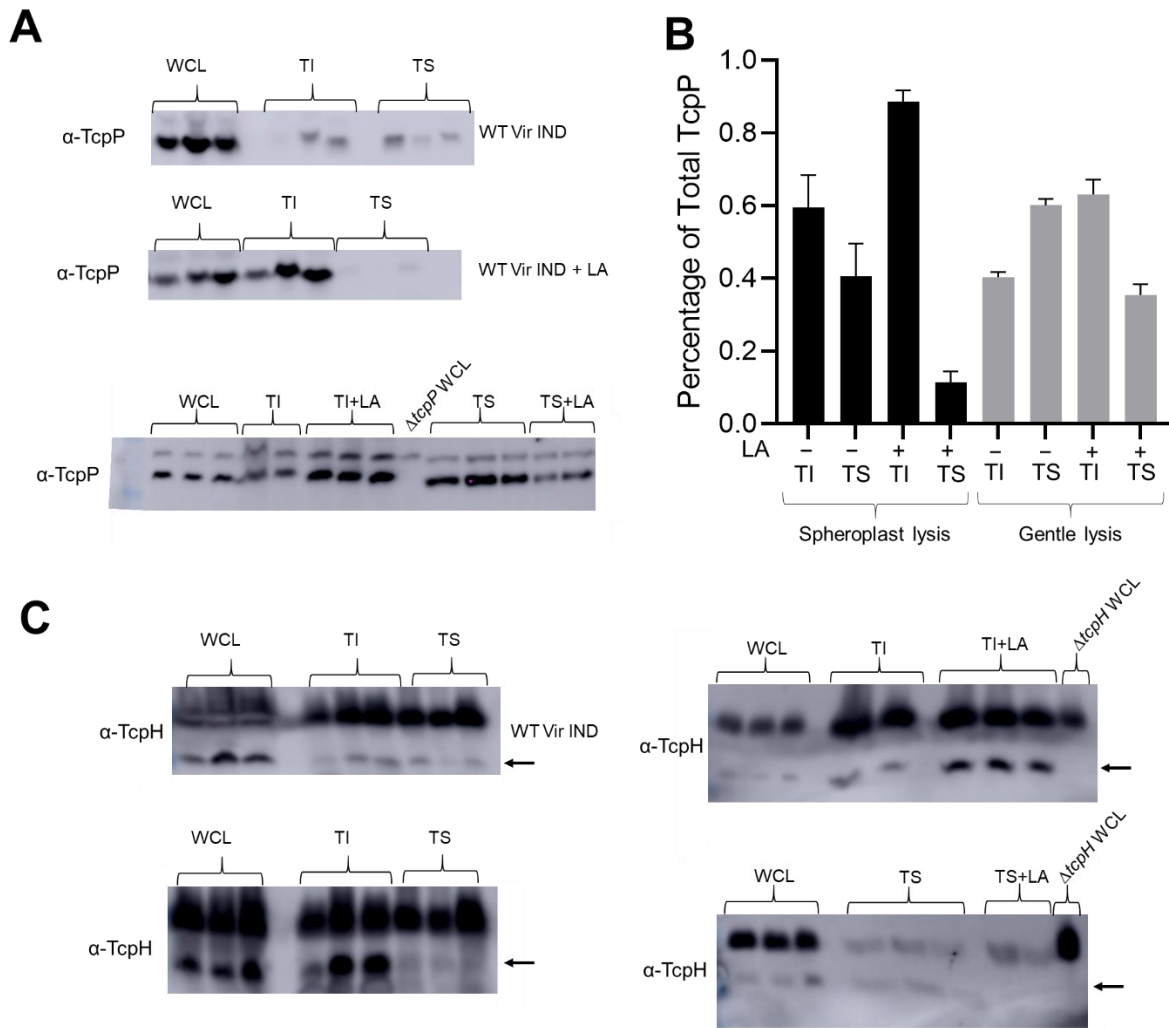


Figure D.10: **α -Linolenic acid promotes association of TcpP and TcpH with detergent resistant membranes (DRM).** Western blots of Triton X-100 soluble (lipid disordered) and Triton X-100 insoluble (lipid ordered) membrane fractions with and without α -linolenic acid supplementation (LA). A) Three Western blots probed with α -TcpP from WT *V. cholerae* cells. Samples in the top two western blots were collected using the spheroplast method of cell lysis, and samples in the bottom western blot were collected using the gentle cell lysis method. Samples were collected from three biological replicates. For gentle cell lysis samples, only two biological replicates were analyzed for the TI and TS+LA samples due to sample mishandling. B) Densitometry analysis of western blots in panel A. ImageJ was used to perform the densitometry analysis. Error bars represent the standard error. C) Four Western blots probed with α -TcpH from WT *V. cholerae* cells. Samples in the left two western blots were collected using the spheroplast method of cell lysis, and samples in the right two western blots were collected using the gentle cell lysis method. Samples were collected from three biological replicates. Arrows indicate TcpH specific bands.

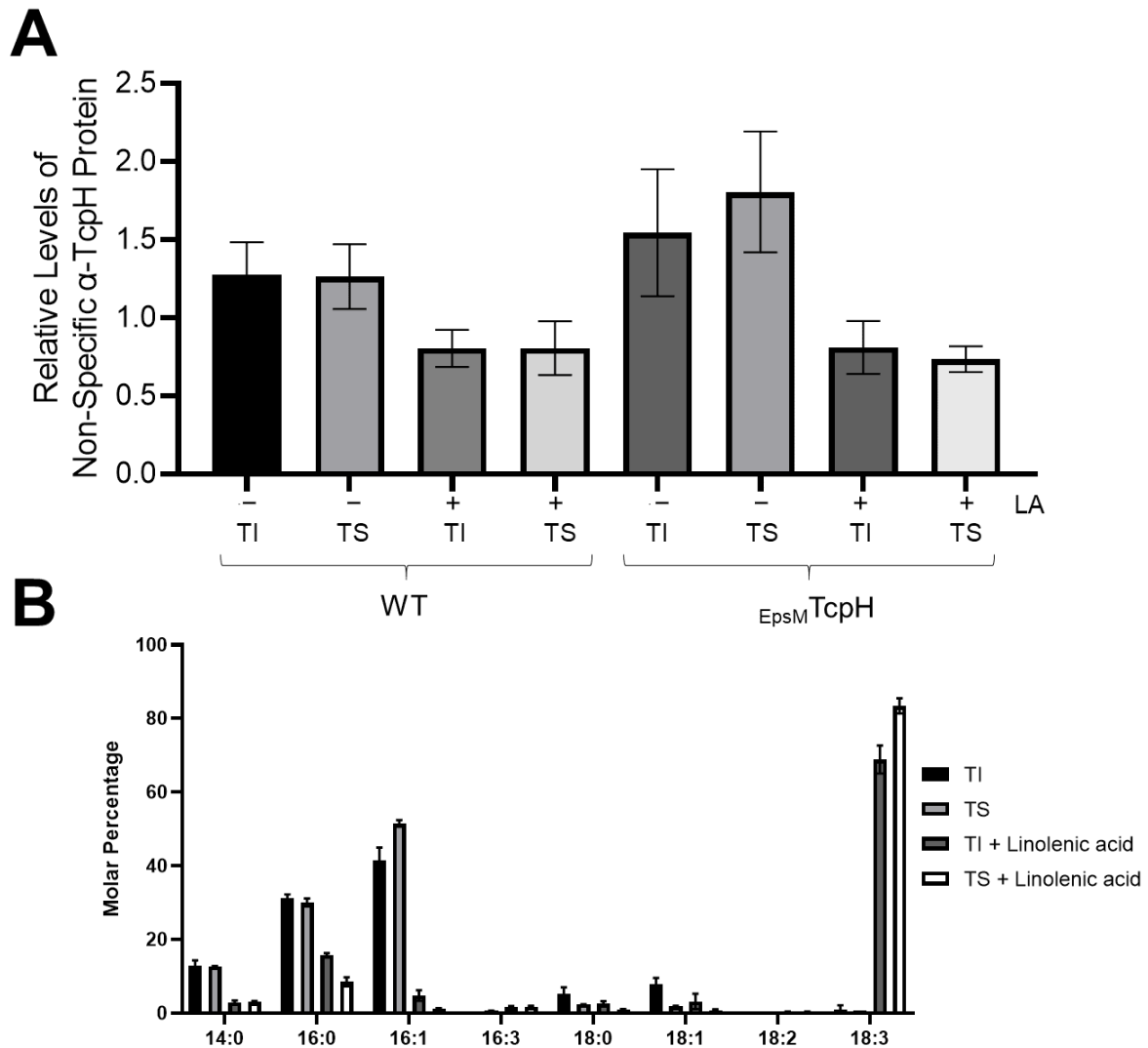


Figure D.11: α -Linolenic acid does not promote non-specific protein association with detergent resistant membranes. A) Relative levels of the non-specific loading control in α -TcpH westerns is equally distributed among Triton soluble (i.e., TS; lipid disordered) and Triton insoluble (i.e., TI; lipid ordered) fractions. Addition of α -linolenic acid (LA, 500 μ M), indicated by +/-, does not change this distribution. Relative levels of the non-specific loading control were determined via densitometry analysis. Densitometry analysis was conducted using ImageJ. Error bars represent the standard error. B) Fatty acid analysis of Triton soluble (i.e., TS; lipid disordered) and Triton insoluble (i.e., TI; lipid ordered) fractions. Error bars represent the standard deviation, and the average values here represent two biological replicates.

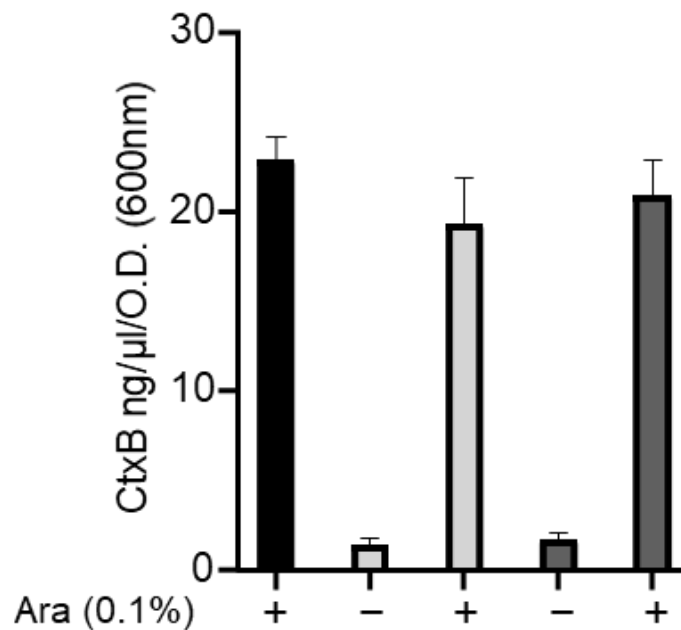


Figure D.12: **Hsv-His(6x) tagged TcpP constructs remain functional.** CtxB levels, measured via ELISA, in culture supernatants collected from cultures incubated with *V. cholerae* cells cultured in virulence inducing conditions for 24hrs. Black bars represent WT cells. Light gray bars represent $\Delta tcpP$ complemented with pBAD18-Hsv-His(6x)-tcpP, and dark gray bars represent $\Delta tcpP$ complemented with pBAD18-tcpP-His(6x)-Hsv. tcpP constructs were ectopically expressed from pBAD18 using arabinose (Ara 0.1% w/v). + indicates arabinose was added to the culture.

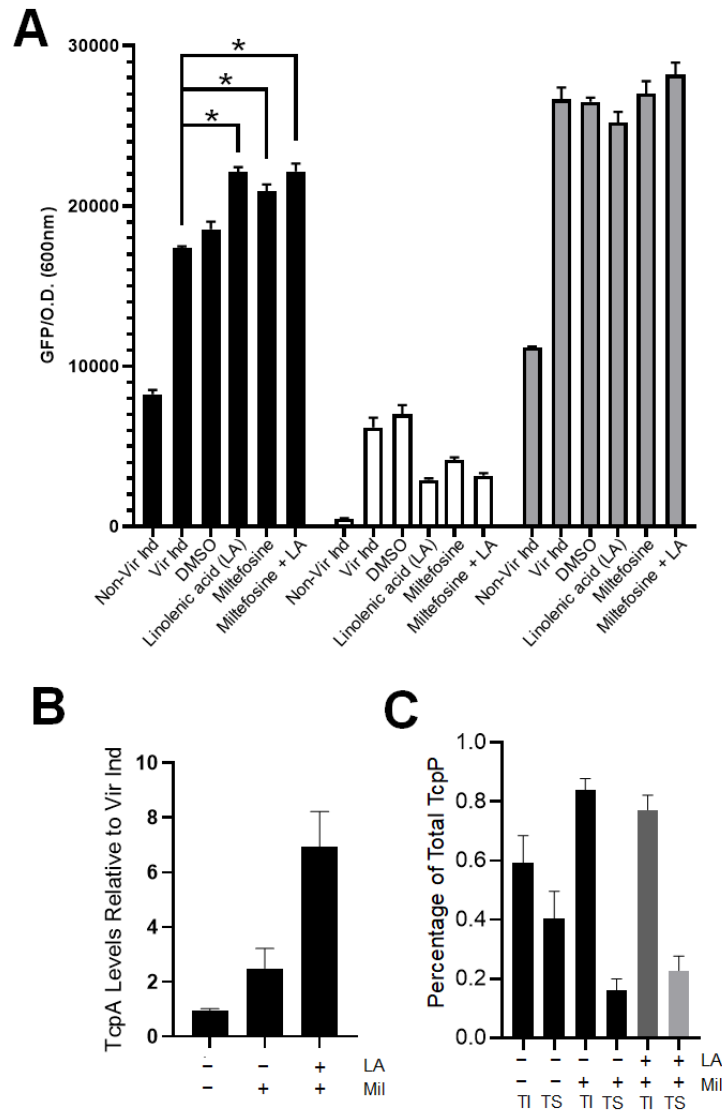


Figure D.13: **Miltefosine and α -linolenic acid function synergistically to stimulate *toxT* transcription.** A) *toxT* transcription in WT (black bars), $\Delta tcpH$ (white bars), and $EpsM$ TcpH (gray bars) was determined using a plasmid based *toxT::GFP* transcriptional reporter. Values displayed here are an average of three or more biological replicates. Error bars represent the standard error of the mean. A two-tailed Student's t-test was used to determine statistical significance. *Indicates a P-value of < 0.05. Data from Non-Vir Ind, Vir Ind, DMSO, and α -linolenic acid (LA) conditions can be found in Figure 4.4A and Figure D.6. B) TcpP levels relative to WT *V. cholerae* cells grown in Vir Ind conditions for 8 hours. C) Percentage of TcpP molecules present in the TI (Triton insoluble; lipid ordered membrane domain) and TS (Triton soluble; lipid disordered membrane domain) membrane fractions within WT *V. cholerae* cells. B and C) Densitometry analysis was done using ImageJ to quantify TcpP levels. Averages represent three biological replicates, and error bars represent standard error of the mean. LA: α -linolenic acid (500 μ M) Mil: miltefosine (10 μ M).

Table D.1: Chapter 4 strain list.

Strain	Description	Reference
<i>V. cholerae</i> 0395 classical biotype	Wild type	DiRita lab collection
<i>V. cholerae</i> $\Delta tcpH$	Isogenic deletion	DiRita lab collection
<i>V. cholerae</i> $\Delta tcpP$	Isogenic deletion	DiRita lab collection
<i>V. cholerae</i> $\Delta tcpH$ pBAD18-empty vector	Overexpression plasmid vector	DiRita lab collection
<i>V. cholerae</i> $\Delta tcpH$ pBAD18 TcpH	$\Delta tcpH$ complementation with ectopic <i>tcpH</i>	This study
<i>V. cholerae</i> $\Delta tcpPH$ pBAD18 _{CtxB} TcpH	$\Delta tcpH$ complementation with ectopic <i>tcpH</i> TM construct	This study
<i>V. cholerae</i> $\Delta tcpH$; $\Delta yaeL$ pBAD18-empty vector	Overexpression plasmid	This study
<i>V. cholerae</i> $\Delta tcpH$; $\Delta yaeL$ pBAD18 _{CtxB} TcpH	$\Delta tcpH$ complementation with ectopic <i>tcpH</i> TM construct	This study
<i>V. cholerae</i> $\Delta tcpH$; $\Delta yaeL$ pBAD18 _{ToxS} TcpH	$\Delta tcpH$ complementation with ectopic <i>tcpH</i> TM construct	This study

Table D.1 (cont'd)

<i>V. cholerae</i> $\Delta tcpH$; $\Delta yaeL$ pBAD18 _{EpsM} TcpH	$\Delta tcpH$ complementation with ectopic <i>tcpH</i> TM construct	This study	
<i>V. cholerae</i> $\Delta tcpH$; $\Delta yaeL$ pBAD18 TcpH Δ_{136-} 119	$\Delta tcpH$ complementation with ectopic <i>tcpH</i> Peri construct	This study	
<i>V. cholerae</i> $\Delta tcpH$; $\Delta yaeL$ pBAD18 TcpH Δ_{136-} 103	$\Delta tcpH$ complementation with ectopic <i>tcpH</i> Peri construct	This study	
<i>V. cholerae</i> $\Delta tcpP$ pBAD18 <i>Hsv-</i> <i>His(6x)-tcpP</i>	N-terminal immuno construct	<i>tcpP</i> co- precipitation	This study
<i>V. cholerae</i> $\Delta tcpP$ pBAD18 <i>tcpP-His(6x)-Hsv</i>	C-terminal immuno construct	<i>tcpP</i> co- precipitation	This study
<i>V. cholerae</i> $\Delta tcpH$ pBAD18 <i>Hsv-His(6x)-tcpH</i>	N-terminal immuno construct	<i>tcpH</i> co- precipitation	This study
<i>V. cholerae</i> $\Delta tcpH$ pBAD18 <i>tcpH-His(6x)-Hsv</i>	C-terminal immuno construct	<i>tcpH</i> co- precipitation	This study

Table D.1 (cont'd)

<i>V. cholerae</i> $\Delta yaeL$ pBAD18 <i>Hsv-</i> <i>His(6x)-tcpP</i>	N-terminal immuno construct	<i>tcpP</i> co- precipitation	This study
<i>V. cholerae</i> $\Delta yaeL$ pBAD18 <i>tcpP-His(6x)-Hsv</i>	C-terminal immuno construct	<i>tcpP</i> co- precipitation	This study
<i>V. cholerae</i> CtxB TcpH	chromosomal construct		This study
<i>V. cholerae</i> ToxS TcpH	chromosomal construct		This study
<i>V. cholerae</i> EpsM TcpH	chromosomal construct		This study
<i>V. cholerae</i> TcpH $\Delta_{136-119}$	chromosomal construct		This study
<i>V. cholerae</i> TcpH $\Delta_{136-103}$	chromosomal construct		This study
<i>V. cholerae</i> TcpH $\Delta_{119-103}$	chromosomal construct		This study
<i>V. cholerae</i> TcpH Δ_{103-79}	chromosomal construct		This study
<i>V. cholerae</i> TcpH Δ_{79-55}	chromosomal construct		This study
<i>V. cholerae</i> TcpHC114S	isogenic mutant		This study
<i>V. cholerae</i> TcpHC114S/C132S	isogenic mutant		This study

Table D.1 (cont'd)

<i>V. cholerae</i> pBH6119- <i>toxT::GFP</i>	<i>toxT</i> transcription reporter	Anthouard R, and DiRita VJ. mBio. 2013.
<i>V. cholerae</i> Δ <i>tcpH</i> pBH6119- <i>toxT::GFP</i>	<i>toxT</i> transcription reporter	This study
<i>V. cholerae</i> Δ <i>tcpP</i> pBH6119- <i>toxT::GFP</i>	<i>toxT</i> transcription reporter	This study
<i>V. cholerae</i> _{CtxB} TcpH pBH6119- <i>toxT::GFP</i>	<i>toxT</i> transcription reporter	This study
<i>V. cholerae</i> _{ToxS} TcpH pBH6119- <i>toxT::GFP</i>	<i>toxT</i> transcription reporter	This study
<i>V. cholerae</i> _{EpsM} TcpH pBH6119- <i>toxT::GFP</i>	<i>toxT</i> transcription reporter	This study
<i>V. cholerae</i> TcpH Δ ₁₃₆₋₁₁₉ pBH6119- <i>toxT::GFP</i>	<i>toxT</i> transcription reporter	This study
<i>V. cholerae</i> TcpH Δ ₁₃₆₋₁₀₃ pBH6119- <i>toxT::GFP</i>	<i>toxT</i> transcription reporter	This study
<i>V. cholerae</i> TcpH Δ ₁₁₉₋₁₀₃ pBH6119- <i>toxT::GFP</i>	<i>toxT</i> transcription reporter	This study

Table D.1 (cont'd)

<i>V. cholerae</i> TcpH Δ 103-79 pBH6119- <i>toxT</i> :: <i>GFP</i>	<i>toxT</i> transcription reporter	This study
<i>V. cholerae</i> TcpH Δ 79-55 pBH6119- <i>toxT</i> :: <i>GFP</i>	<i>toxT</i> transcription reporter	This study
<i>V. cholerae</i> TcpHC114S pBH6119- <i>toxT</i> :: <i>GFP</i>	<i>toxT</i> transcription reporter	This study
<i>V. cholerae</i> TcpHC114S/C132S pBH6119- <i>toxT</i> :: <i>GFP</i>	<i>toxT</i> transcription reporter	This study
<i>E. coli</i> ET12567 Δ <i>dapA</i>	Cloning vector recipient	Allard, N., et. al. 2015. Canadian Journal of Microbiology, 61(8), pp.565- 574.
<i>E. coli</i> ET12567 Δ <i>dapA</i> pKAS32-empty vector	Plasmid vector strain	DiRita lab collection
<i>E. coli</i> ET12567 Δ <i>dapA</i> pBAD18-empty vector	Plasmid vector strain	DiRita lab collection

Table D.2: **Chapter 4 primer list.** Each primer contains Kpn1-HiFi (forward primers) and Xba1 (reverse primers) restriction sites.

Description	Sequence
pKAS FW	gcctctaaggttttaagt
pKAS RV	ctttcaaggtagcggttacc
pBAD18 FW	ctgtttctccatacccgtt
pBAD18 RV	ggctgaaaatcttctct
pKAS-TcpP promoter FW	ctaacgttaacaaccggtactttcgagtgatagaaaaagg
pKAS-TcpP FW	ctaacgttaacaaccggtacatggggtatgtccgctg
pKAS-downstream TcpH RV	aaatttgcgcatgctagctatagtcttggctcttttagataacgtaagc
TcpP-CtxBss FW	atgcactaaaaattaaagacattagaatgattaaattaaatttg
TcpP-CtxBss RV	aatttaacattctaattgtcttttaatttttagtgattctaattgtcttc
CtxBss-TcpHperi FW	tcttcagcatatgcacatggaccgatgacgacaaaaaac
CtxBss-TcpHperi RV	gtcgcacatcggtccatgtgcatatgctgaaga

Table D.2 (cont'd)

TcpP-EpsMss RV	tctaagtcttttaatttttagtgcattctaattgtcttc
EpsMss-TcpHperi FW	gggaatatggccgatgacgacaaaaaac
EpsMss-TcpHperi RV	gtcgcacggccatattccccaataagc
TcpP-ToxSss FW	atgcactaaaaattaagacattagaatgcaaaatagacacatcg
TcpP-ToxSss RV	cgatgtgtctatttgacattctaattgtcttttaatttttagtgcattctaattgtcttc
ToxSss-TcpHperi FW	ttgggggagtcggatgacgacaaaaaac
ToxSss-TcpHperi RV	tgatgcctgcaggctgactctaaaaatcgctttgacag
TcpH _{Δ136-119} FW	cgcctcccttagggcttatcatgagccgc
TcpH _{Δ136-119} RV	tgataagaccctaaggggaaggcgagaaaaacaac
TcpH _{Δ136-103} FW	tgattacaattagggcttatcatgagccgc
TcpH _{Δ136-103} RV	tgataagaccctaattgtaatcacggctcacattactttc
TcpH _{Δ119-103} FW	tgattacaattacaagcagcttacggctg
TcpH _{Δ119-103} RV	taagctgcttgtaattgtaatcacggctcac

Table D.2 (cont'd)

TcpH _{Δ103-79} FW	tcaaacattggtgttgagtattatcaactc
TcpH _{Δ103-79} RV	tactcaacaccaatgtttgataacgtgtag
TcpH _{Δ79-55} FW	taatctatcccagatcctagctctcag
TcpH _{Δ79-55} RV	taggatctggggatagattaccttgataagtag
TcpHC114S FW	tcaactcggcaaaggtagttttctcgcttccc
TcpHC114S RV	gggaaggcgagaaaactaccttggccgagttga
TcpHC132S FW	ggtttccagtcaaagcgatttttag
TcpHC132S RV	ctaaaaatcgctttgactggaaaacc
pBAD18-CtxBss FW	agcgaattcgagctcggtaccaaagggagcattataagacattagaatgattaaattaa aatttg
pBAD18-ToxSss RV	agcgaattcgagctcggtaccaaagggagcattatatgcaaaatagacacatcg
pBAD18-EpsMss FW	agcgaattcgagctcggtaccaaagggagcattatatgatgaaagaattattggctc
pBAD18-TcpH FW	agcgaattcgagctcggtaccaaagggagcattatatgcacaaaaaattaaagcttg
pBAD18-TcpH RV	tgcatgcctgcaggtcgactctaaaaatcgctttgacag

Table D.2 (cont'd)

pBAD18-TcpH Δ 136- 119 RV	tgcatgcctgcaggctgactctaaggggaaggcgagaaaacaac
pBAD18-TcpH Δ 136- 103 RV	tgcatgcctgcaggctgactctaattgtaatcacggctcacattacttc
pBAD18 Hsv- His(6x) FW	ttcgagctcggtaccaaagggagcattatatgcagccggaactggcgccggaagatcc g
Hsv-His(6x)-TcpP FW	ccggaagatccggaagattgccatcatcatcatcatatggggatgtccgctg
Hsv-His(6x)-TcpP RV	cagtccggctgatgatgatgatgatgatgatttttgtgcattctaattgtcttc
pBAD18-TcpP RV	tgcatgcctgcaggctgactttaatttttgtgcattctaattgtcttctgttc
pKT25-TcpP FW	ggctgcagggtcgactatggggatgtccgc
pKT25-TcpP RV	attcttactacttaggtacttaatttttgtgcattctaattgtcttctgttc
pUT18C-TcpH FW	aacgccactgcaggctgactcagcgggtggagggttcgaaatgcacaaaaaattaa ag
pUT18C-TcpH RV	gatgaattcgagctcggtacctaaaaatcgcttgacaggaaaacc
<i>recA</i> FW RT-qPCR	attgaaggcgaaatgggcatag

Table D.2 (cont'd)

recA RV RT-qPCR tacacatacagttggattgcttg agg

toxT FW RT-qPCR actgatgatcttgatgctatggag

toxT RV RT-qPCR catccgattcgttctaattcacc

tcpP FW RT-qPCR tgagtgggggaagataaacg

tcpP RV RT-qPCR ttggattgtatccccggta

APPENDIX E:

Identifying Regions within TcpH Critical for its Function

E.1 – Introduction

TcpP is essential for *toxT* transcription, presumably as TcpP facilitates transcription through direct interaction with RNA polymerase due to its binding sequence being near the -35 site (340, 347). Furthermore, TcpP is post-translationally regulated by two proteases, Tail-specific protease (Tsp) and YaeL, and this process is also known as Regulated Intramembrane Proteolysis (RIP) (96, 351, 352). The literature suggests that TcpP is constitutively sensitive to RIP, by Tsp and YaeL, and requires TcpH to inhibit RIP under specific conditions (96, 351, 352). However, the mechanism by which TcpH inhibits RIP of TcpP remains unclear. TcpP and TcpH both lack significant sequence similarity to other proteins with similar function. Thus, we aimed to understand how TcpH protects TcpP from RIP by identifying regions within that are critical for its function. To do this we generated chimeric transmembrane (TM) domain fusions and periplasmic (Peri) TcpH deletion constructs to identify regions within TcpH that are critical for its protective function. We generated a total of 10 chromosomal TcpH constructs, 3 TM and 7 Peri, that do not disrupt the coding sequence of TcpP and are subject to WT transcriptional control (Figure E.1A). Below we discuss our findings and outline future experiments to eventually identify specific residues within TcpH that are critical for its function. Some of the data presented in this section can also be found in Chapter 4 (specifically data with T_{oxS} TcpH, E_{psM} TcpH, and $TcpH_{\Delta 119-103}$). This data has also been included in this section for direct comparison with TcpH constructs not discussed in Chapter 4 due to stability issues.

E.2 – Results

E.2.1 – TcpH Maintains Remains Functional Upon Alteration of its Transmembrane and its Periplasmic Domains.

TcpH has a single transmembrane domain (also a Sec signal sequence), at its N-terminus, and two periplasmic cysteine residues (C114 and C132), represented by “s”. TcpH sequence is highly conserved among *V. cholerae* strains. Thus, it was unclear what region of TcpH was critical to inhibit RIP. To that end, we took a broad approach and made modifications to the transmembrane and periplasmic domain of TcpH. To determine if the transmembrane domain of TcpH has a direct role in protecting TcpP the transmembrane domain of TcpH was replaced with the transmembrane domain of ToxS (ToxSTcpH) and EpsM (EpsMTcpH) as both ToxS and EpsM are known to be localized to the cytoplasmic membrane (207, 389). Additionally, we hypothesized that membrane localization of TcpH may not be essential for its function. To test this we replaced the native TcpH Sec signal sequence (which is not cleaved) with the Sec signal sequence from the B subunit of cholera toxin (*ctxB*), termed *ctxB*TcpH, that is cleaved and has also been utilized to localized proteins to the periplasmic space (474). A majority of TcpH coding sequence reside in the periplasmic space (residues 26-136). Thus, in-frame deletions of periplasmic regions were made based on TcpH secondary structure, resulting in TcpH Δ 136-119, TcpH Δ 136-103, TcpH Δ 119-103, TcpH Δ 103-79, and TcpH Δ 79-55 (Figure E.1A). In addition, prior studies have shown that C114 within the periplasmic domain of TcpH may have a role in inhibiting RIP of TcpP (475). To determine if C114 and C132 play a role in TcpH function we made point mutations to both C114 and C132 resulting in TcpHC114S and TcpHC114S/C132S (Figure E.1A).

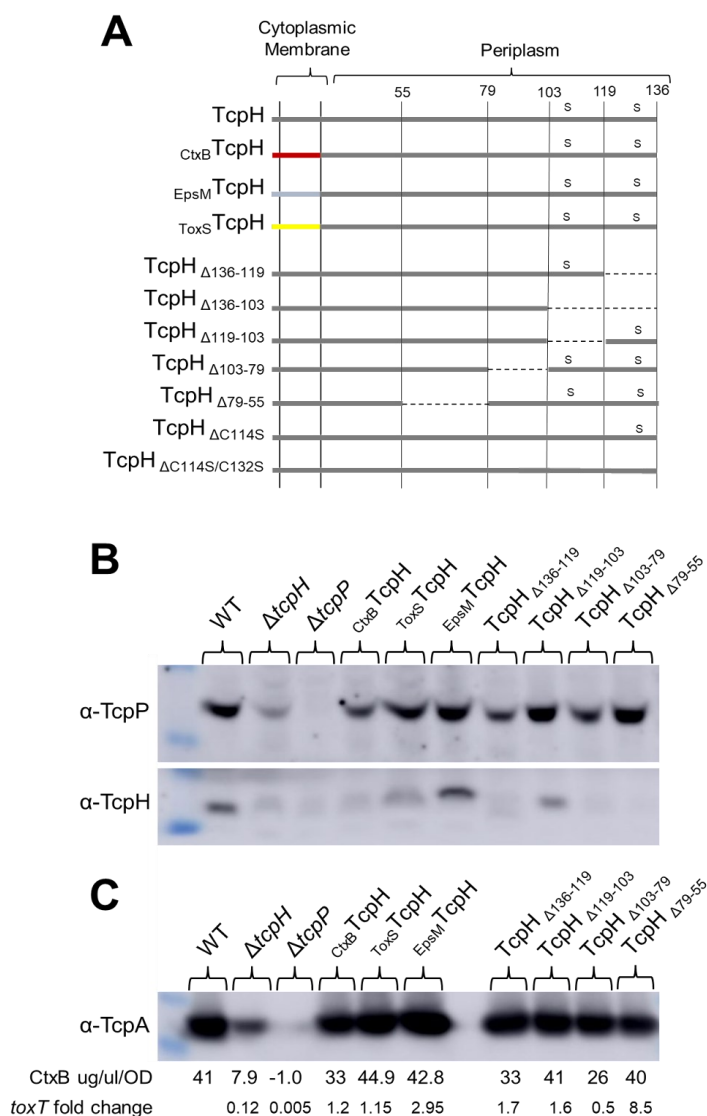


Figure E.1: **TcpH transmembrane and periplasmic constructs remain functional *in vitro***. A) Diagram of TcpH transmembrane constructs (CtxB-TcpH, EpsM-TcpH, and ToxS-TcpH) and periplasmic constructs (TcpH $_{\Delta 136-119}$, TcpH $_{\Delta 119-103}$, TcpH $_{\Delta 103-79}$, and TcpH $_{\Delta 79-55}$). B and C) *in vitro* characterization of TcpH transmembrane and periplasmic chromosomal constructs grown under virulence inducing conditions. B) Western blots of whole-cell lysates probed with α -TcpP (top), α -TcpH (middle). C) Western blot of whole-cell lysates probed with α -TcpA. In addition, CtxB levels and *toxT* transcription were also determined for the TcpH transmembrane and periplasmic constructs. Average CtxB levels and *toxT* fold change (relative to WT) for each strain are indicated below the western blot. See Figure E.2 for full view of the data.

We evaluated the function of TcpH TM and specific Peri constructs by first measuring levels of TcpP, *toxT* transcription, and virulence factor (TcpA and CtxB) production *in vitro* (Figure E.1B). All of the TcpH constructs tested prevented complete degradation of TcpP, similar to WT TcpH (Figure E.1B). This suggests that the TcpH constructs are capable of inhibiting RIP of TcpP and thereby the TcpH TM and Peri constructs support TcpP function to stimulate *toxT* transcription. We also assessed the ability of TcpH TM and Peri constructs to support WT *toxT* transcription in the presence of crude bile (0.4%) (Figure E.2D). We found that TcpH Peri constructs were unable to support WT *toxT* transcription in the presence of crude bile, similar to ToxS TcpH and EpsM TcpH in Chapter 4.

We found that *toxT* transcription was not significantly different for TcpH TM or Peri constructs compared to WT (Figure E.1C and Figure E.2A). Similar to *toxT* transcription, we found that all the TcpH constructs tested were able to support production of CtxB and TcpA, which are positively regulated by *toxT*, production better than $\Delta tcpH$ (Figure E.1C and Figure E.2B). However, CtxB levels did not reach that of WT for all of the TcpH Peri constructs tested (Figure E.1C and Figure E.2B). In addition, despite *toxT* transcription and TcpA production, TcpH Peri constructs $\text{TcpH}_{\Delta 136-103}$ and $\text{TcpH}_{\Delta 103-79}$, did not support WT production of CtxB (Figure E.1C and Figure E.2B). Currently, it is unclear as to why $\text{TcpH}_{\Delta 136-103}$ and $\text{TcpH}_{\Delta 103-79}$ do not support WT CtxB production *in vitro*. However, these data indicate that residues 136-103 and 103-79 are important, but not essential, for TcpH to inhibit RIP.

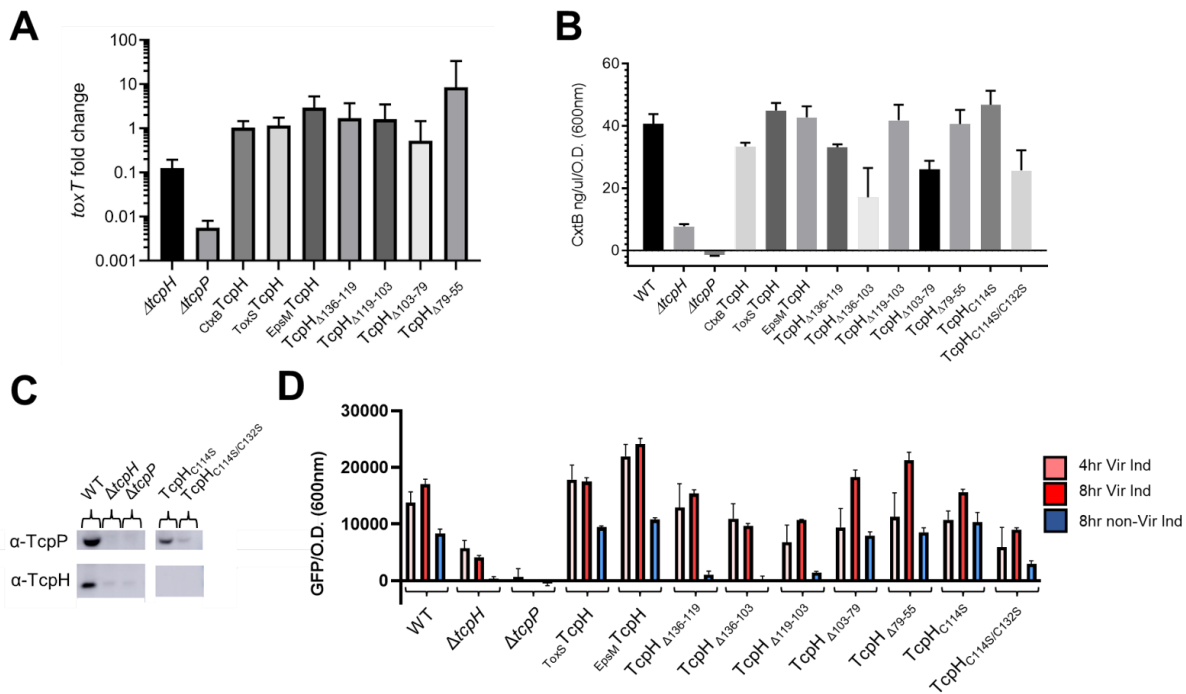


Figure E.2: Residues within region 136-103 in the periplasmic domain of TcpH are critical for protecting TcpP under non-virulence inducing conditions. A) Average *toxT* transcription of three biological replicates, determined via $\Delta\Delta C_T$ method. *toxT* fold change is relative to WT *V. cholerae* (i.e., *toxT* transcription=1). B) CtxB levels, measured via ELISA, in culture supernatants collected from cultures incubated with *V. cholerae* cells cultured in virulence inducing conditions for 24hrs. C) Western blots of WCL collected after 6hrs of growth under virulence inducing conditions. D) *toxT* transcription in TcpH transmembrane and periplasmic constructs in *V. cholerae* cells. *toxT* transcription was measured using a plasmid based *toxT::GFP* transcriptional reporter. The data here are an average of three or more biological replicates and error bars represent the standard error of the mean.

Furthermore, some of the TcpH constructs are not detectable via western blot (CtxB TcpH, ToxS TcpH, TcpH_{Δ136-119}, TcpH_{Δ103-79}, and TcpH_{Δ79-55}) (Figure E.1B). This was expected for TcpH₁₀₃₋₇₉ and 79-55, as they lack the epitope for our TcpH antibody. However, since the remaining TcpH constructs still support WT TcpP levels and virulence factor production (Figure E.1), it is likely that these TcpH constructs are not detectable via western blot due to reduced stability compared to WT. To confirm that these TcpH

constructs are indeed translated, we overexpressed each construct from an arabinose inducible vector (pBAD18). Overexpression of these remaining TcpH constructs supported CtxB production and allowed for visualization of CtxB-TcpH, ToxS-TcpH, and TcpH Δ 136-119 via western blot (Figure E.3) suggesting that a lack of detection of the chromosomal TcpH constructs by western blot is due to decreased stability of the modified protein rather than a lack of translation.

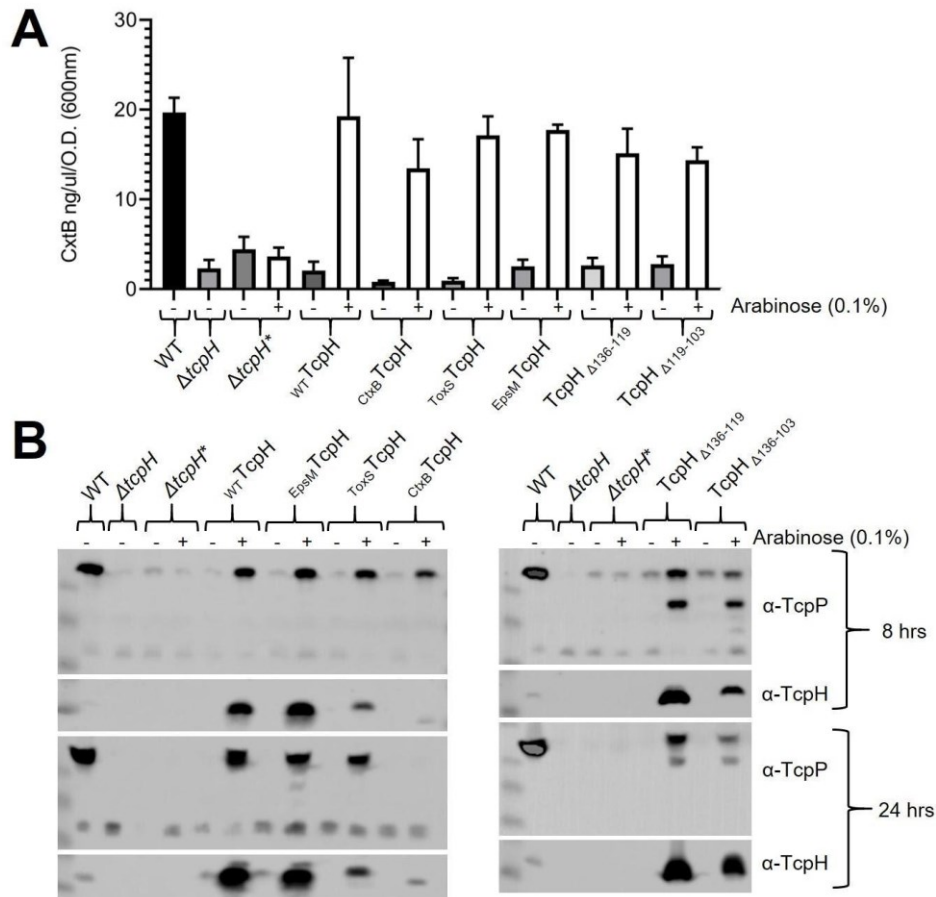


Figure E.3: Overexpression of TcpH transmembrane and periplasmic constructs allows for visualization via western blot. A) CtxB levels in culture supernatants after 24 hrs of incubation in virulence inducing conditions, measured by ELISA. White bars indicate samples that were induced with 0.1% arabinose (w/v) and black/gray bars indicate that no arabinose was added. B) Western blot of whole cell lysates collected

Figure E.3 (cont'd)

after 8hrs and 24 hrs. Western blots probed with α -TcpP (Top) and α -TcpH (bottom) for both 8hr and 24hr time points. Samples with a black asterisk (*) indicate that strain carries an empty overexpression vector (pBAD18).

These data show that, *in vitro*, the sequence of the TcpH TM domain sequence can be modified and without inhibiting its ability to inhibit RIP of TcpP. However, loss of some C-terminal regions of TcpH results in minor defects in CtxB production despite being able to protect TcpP. These data indicate that the Peri domain (particularly regions 136-119 and 103-79) of TcpH is important for inhibition of RIP of TcpP *in vitro*. In addition to the TcpH TM and Peri chromosomal constructs discussed above, we also characterized the function and the ability to support *toxT* transcription in TcpH_{C114S} and TcpH_{C114S/C132S} (Figure E.3CD). These data indicate that the periplasmic cysteine residues (C114 and C132) are not entirely essential for TcpH function *in vitro*. Taken together, this indicates that other non-cysteine residues within regions 136-119 are important for TcpH function *in vitro*.

E.2.2 – TcpH Peri Constructs Display WT Colonization of Infant Mice

In vitro experiments indicate that the TM and Peri domain of TcpH can withstand considerable modifications and still maintain function. However, *in vitro* virulence inducing conditions do not represent the conditions found in the gastrointestinal tract. Thus, we tested the fitness of the TcpH TM and Peri constructs *in vivo*. To accomplish this, we infected infant mice with the TcpH TM and Peri constructs (Figure E.4A). Overall, we found that the TcpH TM constructs were unable to colonize mice as well as WT, and we found that the Peri TcpH constructs colonized mice to WT levels. A detailed discussion

and additional data regarding the TM TcpH constructs can be found in Chapter 4. It remained possible that the TM TcpH constructs were sensitive to the gastrointestinal microbiota. To test this, we cultured WT and the TcpH constructs (TM and Peri) aerobically in both sterile and non-sterile mice fecal media (9% w/vol in M9 minimal media) for 21hrs at 37°C (Figure E.4BC). We found that WT and the TcpH TM and Peri constructs had similar growth rates and final cell densities in both sterile and non-sterile mice fecal media (Figure E.5BC). In addition, we also quantified TcpA levels in cell lysates after 21 hours of growth in sterile mice fecal media. While the growth rates were very similar between WT and the TcpH constructs, the TM TcpH constructs did not support WT levels of TcpA while the Peri TcpH constructs did (Figure E.4A). These data indicate that the TM domain of TcpH is critical for TcpH to respond to cues present in the gastrointestinal tract to protect TcpP from RIP and support downstream virulence factor production.

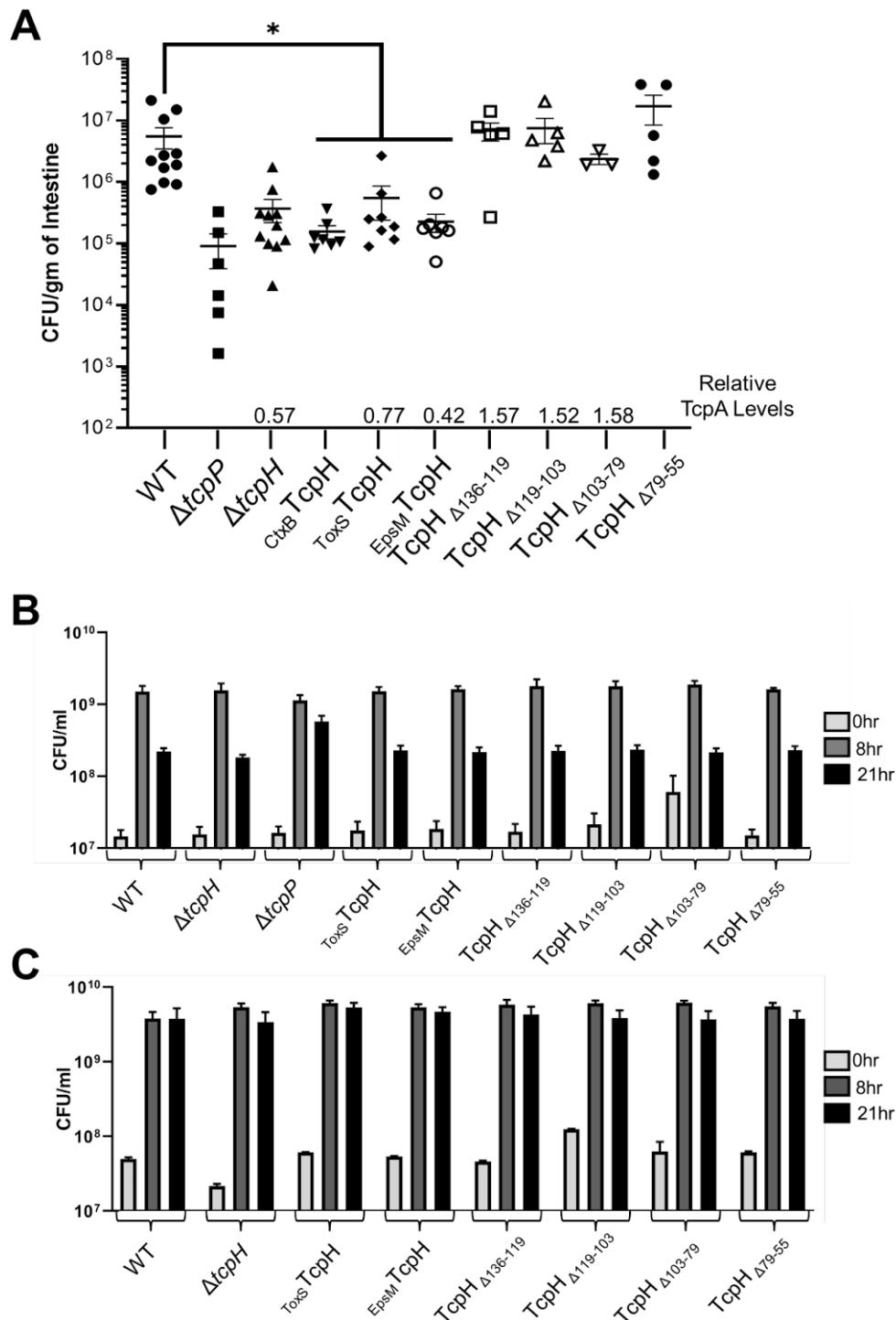


Figure E.4: **TcpH transmembrane and periplasmic constructs Infant mouse colonization and growth in adult mice feces.** A) Colony forming units per gram of 3-6 day old infant mouse intestine infected with TM and Peri TcpH constructs following the same protocol in Figure 4.2A. Due to inclement weather during the pandemic we

Figure E.4 (cont'd)

were unable to acquire a sufficient number of infant mice for the TcpH peri constructs. Asterisk indicates a p-value of less than 0.05. A mann-whitney U test was used to determine statistical significance between WT and each TcpH transmembrane construct. The horizontal line indicates the average CFU/gm of the intestine and is an average of 3-11 biological replicates. Error bars indicate the standard error of the mean. B) Filter sterilized mice fecal growth curve. D) Non-filtered (i.e., non-sterile) mice fecal growth curve. For all data presented here, averages represent three biological replicates. Error bars represent standard error of the mean. Two-tailed Student's t-test was used to determine.

E.2.3 – TcpH TM Constructs Specifically Inhibit RIP of TcpP

In Chapter 4 we demonstrate that the T_{OxS} TcpH and E_{psM} TcpH specifically inhibit RIP of TcpP (Figure D.4). Here we C_{txB} TcpH is also able to inhibit RIP of TcpP due to lack of accumulation of TcpP* (Figure E.5A). These data show that RIP of TcpP is inhibited by all TM constructs. Construction of C_{txB} TcpH was intended to localize the periplasmic domain of TcpH to the periplasm. To accomplish this, we replaced the predicted N-terminal transmembrane domain (residues 1-25) of TcpH with the Sec signal sequence from *ctxB* as it has been used to localize other proteins to the periplasmic space (476). However, we observed that TcpH, C_{txB} TcpH and $\Delta tcpP$ C_{txB} TcpH all associated within the membrane fraction (Figure E.5B). TcpH does not have any predicted “lipidation” motifs (palmitoylation, etc) indicating that C_{txB} TcpH may associate with an integral membrane protein (possibly via its cysteine residues), or that TcpH has a non-canonical transmembrane domain that was not predicted by sequence alone. Due to its unexpected sub-cellular localization we opted to exclude C_{txB} TcpH from additional experiments.

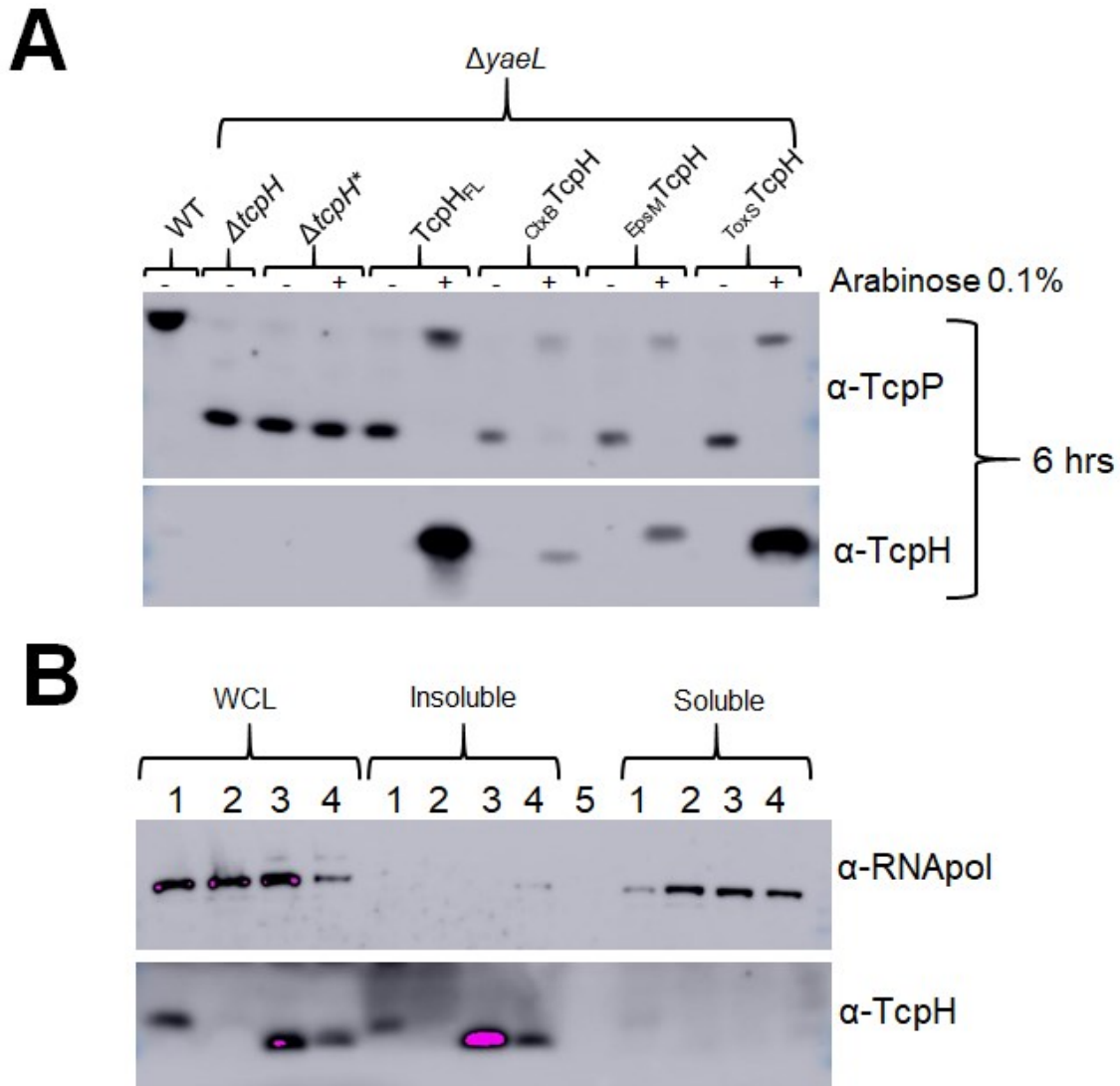


Figure E.5: **TcpH transmembrane constructs inhibit RIP of TcpP and $CtxB$ TcpH remains localized to the cytoplasmic membrane.** A) Western blots of spheroplast fractions (cytoplasm and cytoplasmic membrane fractions). TcpH transmembrane constructs ($ToxS$ TcpH and $EpsM$ TcpH) and native TcpH were expressed from pBAD18 in $\Delta tcpH \Delta yaeL$ background under virulence inducing conditions for 6hrs. All strains, excluding WT, are $\Delta tcpH \Delta yaeL$. $\Delta tcpH^*$ harbors pBAD18 (empty vector). B) Cellular fractionation of *V. cholerae* cells (i.e., insoluble=membrane fraction) collected after 6hrs of growth under virulence inducing conditions, and cells were fractionated using a French Press (10,000 psi). Numbers above the western blot correspond to the following: 1=WT, 2= $\Delta tcpH$, 3= $CtxB$ TcpH, 4= $\Delta tcpP$, $CtxB$ TcpH, 5= empty lane. RNA polymerase was used as a control to determine if the cellular fraction contained soluble proteins. TcpH remains in the insoluble fraction (i.e., membrane fraction) in the absence of TcpP and upon modification of its transmembrane domain. Bands that are pink were overexposed.

E.3 – Future Directions

Taken together these data indicate that, similar as in Chapter 4, that the transmembrane domain of TcpH is critical for its function *in vivo* and the periplasmic domain of TcpH is not critical for colonization of infant mice. This is somewhat surprising given that the majority of TcpH coding sequence is present in the periplasmic domain. From our studies in Chapter 4 we believe that the periplasmic domain is critical for TcpP-TcpH interaction. These data indicate that large portions of the periplasmic domain of TcpH can be lost without affecting colonization of the infant mouse. It is possible that these regions of the TcpH periplasmic domain are relevant in other animal models with mature immune systems and with an established diverse microbiota. Secondly, it is also possible that multiple regions within TcpH contribute to its ability to protect TcpP and larger deletions are required to affect function (e.g., TcpH Δ 136-103). Lastly, it is also possible that periplasmic deletions we generated, while decreasing stability of TcpH, also functioned to promote its ability to protect TcpP. If true, it would imply that there are regions within TcpH that actively inhibit its ability to protect TcpP from RIP. Future experiments will be required to test these hypotheses. Data presented in Chapter 4 indicate that TcpP-TcpH interaction is critical for inhibition of RIP. Thus, future experiments might include identifying peptides purified TcpH and TcpP recognize using a peptide array (477). These experiments would identify peptides that both TcpP and TcpH recognize thereby informing about what regions within TcpP and TcpH interact. This would allow for targeted point mutations within TcpP and TcpH that will likely yield variants that are more stable than the TcpH Peri constructs discussed above.

APPENDIX F:

Defining the Mechanism of Action of Toxtazin A and Toxtazin B

F.1 – Introduction

Vibrio cholerae is a Gram-negative gastrointestinal pathogen that causes the diarrheal disease cholera. Its two major virulence determinants are cholera toxin (*ctxAB*) and the toxin co-regulated pilus (*tcpA-F*), and they are regulated by ToxT, an AraC-like activator, and indirectly by ToxR and TcpP (23, 31, 39–42)(39–41, 52–55). Despite our extensive knowledge of *V. cholerae* pathogenicity mechanisms, cholera continues to persist and afflicts millions every year. Conventional methods to combat *V. cholerae* have been developed, including vaccines, oral-rehydration therapy, and antibiotic therapy (7–10)(4–6). However, they have been ineffective at reducing the incidence of *V. cholerae* infections globally. Thus, new strategies are needed and targeting the *toxT* regulatory pathway is one such strategy as loss of ToxT, ToxR or TcpP severely attenuates *V. cholerae in vivo*. We identified two small molecules, toxtazin A and toxtazin B, that inhibit *toxT* transcription and significantly reduce toxin and pilus production (383). The Toxtazins do not inhibit growth of *V. cholerae* (383). Oral administration of toxtazin B was effective *in vivo*, decreasing colonization of *V. cholerae* strain O395 by approximately 1000-fold (383). The precise mechanism of action for both toxtazin A and B have yet to be determined. Currently, the data show that toxtazin A does not alter localization or DNA binding of both TcpP and ToxR, and yet still reduces *toxT* transcription considerably (383). Proteomics analysis showed that toxtazin A stimulates many proteins, including several involved in oxidative stress responses, and suggests that toxtazin A inhibits *toxT* via a novel regulatory mechanism (Anthouard R. and DiRita V. unpublished). Secondly, toxtazin B, on the other hand, inhibits *toxT* transcription by reducing levels of *tcpP* transcription (Anthouard R. and DiRita V. unpublished). The mechanism by which toxtazin

B affects *tcpP* transcription is not currently known and elucidating this mechanism will add new knowledge to our understanding of *tcpP* transcription regulatory mechanisms (Anthouard R. and DiRita V. unpublished). As toxtazin A had no effect on localization or DNA binding of ToxR and TcpP, we focused on identifying the mechanism of action of toxtazin A.

F.2 – Results

Prior experiments have revealed that Toxtazin A treated *V. cholerae* cells have an increase (~4 fold) in the abundance of proteins involved in cell redox homeostasis (35% of upregulated proteins), amino acid biosynthesis and transport (15% of upregulated proteins), and metabolic enzymes (20% of upregulated proteins) (unpublished work Anthouard et. al.). A protein that was of particular interest was malate synthase, which was not detected in DMSO treated cells (unpublished work Anthouard et. al.). Malate synthase produces malate and CoA from acetyl-CoA and glyoxylate. Previous work has established that central metabolism is critical for *toxT* transcription (478). Specifically, acetyl-CoA levels are hypothesized to directly correlate with *toxT* transcription (i.e., high levels of acetyl-CoA leads to elevated *toxT* transcription) (478). We hypothesized that elevated levels of malate synthase in toxtazin A treated cells inhibited *toxT* transcription by depleting the cell of acetyl-CoA levels. The mechanism by which acetyl-CoA stimulates *toxT* transcription is not known. Acetyl-CoA is essential for de novo fatty acid synthesis. Thus, it is possible that acetyl-CoA influences *toxT* transcription via de novo phospholipid synthesis. In Chapter 4 we present data that demonstrates that RIP of TcpP is influenced

by the cytoplasmic membrane. As toxtazin A has been shown to not reduce levels of TcpP, we hypothesized that toxtazin A would inhibit *toxT* transcription independent of RIP of TcpP. To test this, we measured *toxT* transcription in WT and in *tcpP-PAmCherry* cells. In Chapter 3 we demonstrate that TcpP-PAmCherry is resistant to RIP (Figure C.1A). We found that *tcpP-PAmCherry* cells were sensitive to toxtazin A (Figure F.1A). These data indicated that toxtazin A inhibits *toxT* transcription independent of RIP of TcpP. These data also showed that our toxtazin B stock was no longer effective at inhibiting virulence factor production in WT cells (Figure F.1A). Follow up studies with working with a malate synthase revealed that WT cells were also insensitive to toxtazin A. Taken together, these data indicated that our toxtazin A and B compounds had degraded while in cold storage. Unfortunately acquisition of fresh toxtazin A compound was not possible. An analog of toxtazin A (toxtazin A') was available as a fresh powder, but was not effective at inhibiting *toxT* transcription, data not shown.

Prior to our toxtazin A and B stocks becoming ineffective, we screened for spontaneous *V. cholerae* mutants that were insensitive to toxtazin A or toxtazin B. Synthesis of toxin co-regulated pilus (Tcp) is known to promote autoagglutination of *V. cholerae* cells (32). Thus, we selected for cells that stimulated synthesis of the Tcp in the presence of toxtazin A or B. To do this WT cells were inoculated in virulence inducing media and cultured for 8hrs with or without the toxtazin's. Cultures were then incubated at room temperature under static conditions for an additional 16hrs. Cells that aggregated at the bottom of the flask were collected and inoculated into fresh virulence inducing media with toxtazin A or B. The cells were passaged for 5 days to in the presence of toxtazin A or B. After day 5 400 colonies were selected at random (200 toxtazin A and

200 toxtazin B passaged cells). The colonies were then cultured in virulence inducing conditions for 24hrs with and without toxtazin A or B and CtxB levels were quantified from culture supernatants. Out of 120 possible mutants we identified 6 toxtazin B and 1 toxtazin A insensitive mutants (Figure F.1B). Follow up validation of these possible mutants revealed that they remained sensitive to toxtazin A or toxtazin B (Figure F.1C). These data indicate that our screen was not sufficient to identify tolerant toxtazin A and B mutants.

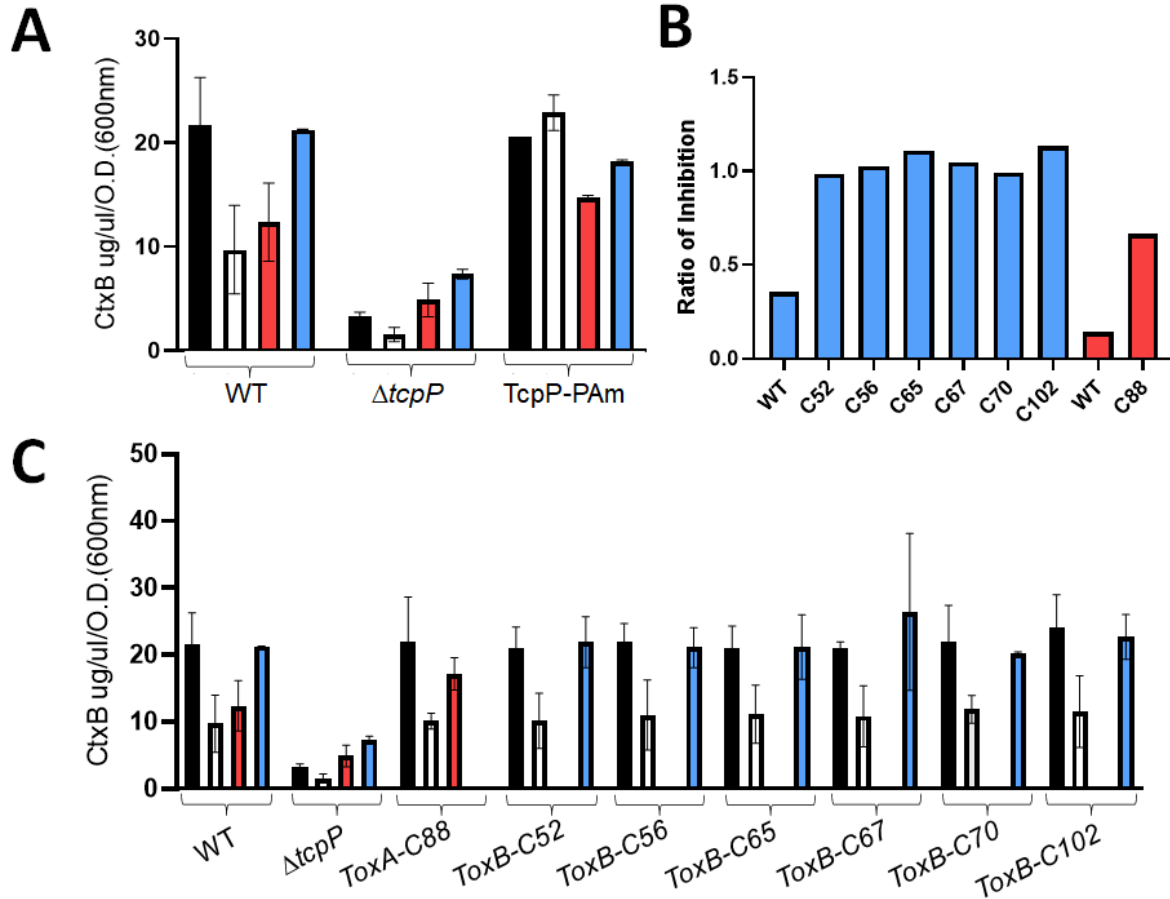


Figure F.1: **Characterization of toxtazin A and B mechanism of action.** A-C) CtxB levels collected after 24hrs from culture supernatants. Black bars represent virulence inducing conditions. White bars represent non-virulence inducing conditions. Red bars indicate virulence inducing conditions supplemented with 10 μ M toxtazin A. Blue bars

Figure F.1 (cont'd)

virulence inducing conditions supplemented with 10 μ M toxtazin B. B) WT and possible toxtazin A and B tolerant cells were grown in LB with and without toxtazin A or B for 24hrs. After 24hrs CtxB levels were quantified for both conditions. Levels of CtxB produced by the indicated strain in the presence and absence of toxtazin A or B was used to calculate the ratio of inhibition (i.e., CtxB ug/ul/O.D.600nm produced in the presence of toxtazin A or B divided by CtxB ug/ul/O.D.600nm produced without toxtazin A or B). A ratio of inhibition below 1 indicates less CtxB was produced in the presence of toxtazin A or B.

F.3 – Future Directions

As we were unable to acquire active toxtazin A or active toxtazin A analogs, acquiring fresh toxtazin A is essential for defining the mechanism of action of toxtazin A. Future experiments will entail testing malate synthase mutants tolerance to toxtazin A. We hypothesize that a malate synthase mutant will be resistant to toxtazin A, and thereby synthesize WT levels of *toxT* transcripts. Secondly, we hypothesize that upregulation of malate synthase will inhibit *toxT* transcription independent of toxtazin A treatment. Acetyl-CoA is essential for de novo fatty acid synthesis in bacteria (479). As TcpP and ToxR are localized in the cytoplasmic membrane, it stands to reason that increased malate synthase activity influences the composition of phospholipids that compose the cytoplasmic membrane due to depletion of acetyl-CoA levels. Our data show that toxtazin A inhibits *toxT* transcription independent of RIP of TcpP. Thus, it remains possible that phospholipid composition can impede TcpP activity. Future experiments are aimed at testing this hypothesis.

APPENDIX G:

Heterogeneous Single-Cell *toxT* Transcription

G.1 – Introduction

It was previously demonstrated that TcpA transcription is highly heterogeneous among individual *V. cholerae* cells *in vitro* and *in vivo*, and it is driven by the *toxT* autoregulatory loop (337). The remaining question is why do these sub-population of *V. cholerae* cells continue to stimulate *toxT* transcription? We hypothesized that a sub-population of *V. cholerae* cells stimulates elevated *toxT* transcription, increasing the overall pool of ToxT within the cell, and this thereby drives heterogeneous single-cell transcription of TcpA.

G.2 – Results and Discussion

In line with these data, we also see that *toxT* transcription is highly heterogeneous among single *V. cholerae* cells (Figure G.1). Furthermore, cells stimulate high *toxT* transcription independent of cell density, temperature, pH, RIP, direct cell contact, culture age, and the *toxT* autoregulatory loop (Figure G.1). However, TcpP and ToxR are required for heterogeneous *toxT* transcription (data not shown). Furthermore, addition of PAmCherry to the C-terminus of TcpP does not result in constitutive *toxT* transcription in all cells (Figure G.1). These data suggest that elevated *toxT* transcription within a sub-population of *V. cholerae* cells is due to TcpP and ToxR. At any time, a high percentage of the TcpP-PAmCherry molecules in the *V. cholerae* cells are in intermediate diffusion states and therefore are not actively associated with DNA/*toxT**pro*, it remains possible that diffusion states of TcpP molecules differ between individual cells and promote high transition rates of TcpP molecules from the fast and intermediate diffusion states to the slow diffusion state via an unknown mechanism.

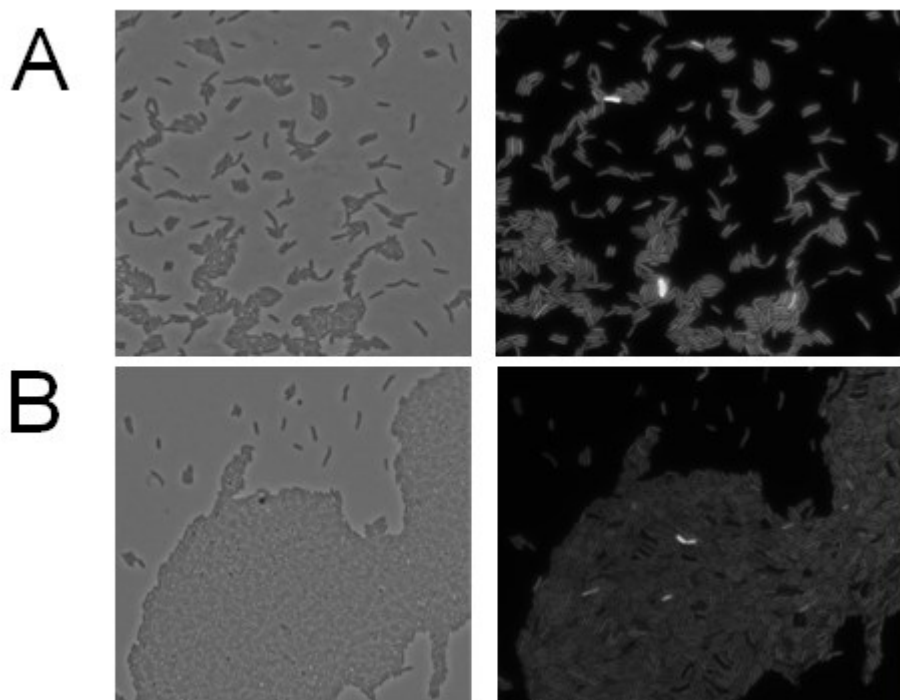


Figure G.1: **Single-cell *toxT* transcription is heterogeneous in *V. cholerae*.** Cultures were grown under virulence inducing conditions (VIC) for 6hrs unless otherwise stated. A) TcpP-PAm. B) WT. Images on the left are phase contrast images of *V. cholerae* cells harboring pBH6119 (*toxT*::GFP) and images on the right are fluorescent images of the same cells. Heterogeneous *toxT* transcription as seen in WT cells was also observed in $\Delta tcpH$, Δtsp , $\Delta yaeL$, $\Delta tsp \Delta yaeL$, 4- 24hrs VIC, and 4-24hrs under non-virulence inducing conditions, data not shown. $\Delta tcpP$ and $\Delta toxR$ cells displayed no fluorescence whatsoever, data not shown.

Regardless of the specific mechanism, we reasoned that heterogeneous diffusion dynamics of TcpP are important for heterogeneous *toxT* transcription among *V. cholerae* cells. Using an ectopic *toxT*::GFP transcriptional reporter, we observed that only a small percentage of WT *V. cholerae* cells have high *toxT* transcription. Furthermore, we found that heterogeneous *toxT* transcription is independent of cell density, temperature, pH, direct cell contact, culture age, and the *toxT* autoregulatory loop (Figure G.1). TcpP and ToxR are required to support heterogeneous *toxT* transcription in *V. cholerae* cells, data not shown. Taken together, these results suggest heterogeneous transcription of *toxT* in

V. cholerae cells is due to TcpP and ToxR, not transcription or RIP of TcpP and ToxR. Currently, RIP of TcpP is only known to be mediated by Tsp and YaeL. Deletion of both *tsp* and *yaeL* results in a reduction in TcpA and TcpP levels under virulence inducing and non-virulence inducing conditions (Figure G.2). Secondly, an additional non-TcpP* band can be observed in overnight cultures of $\Delta t s p \Delta y a e L$ cells (Figure G.2A). This indicates that TcpP is undergoing proteolysis via an unknown protease and is only capable of degrading TcpP in the absence of both *tsp* and *yaeL*.

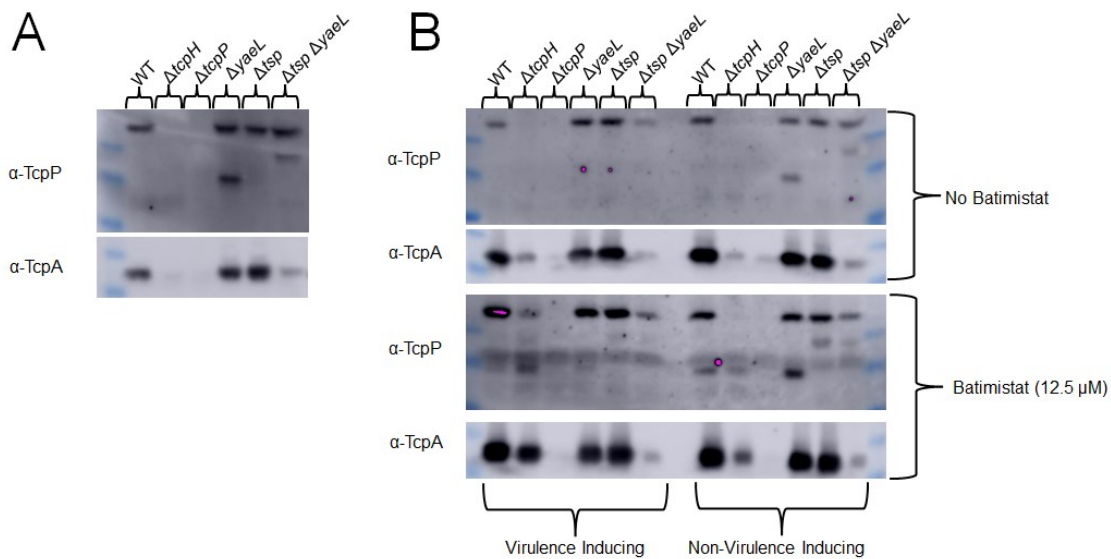


Figure G.2: **TcpP is sensitive to an unknown protease upon mutation of *tsp* and *yaeL*.** A) overnight cultures of *V. cholerae*. B) 8hrs of growth under virulence inducing conditions or non-virulence inducing conditions (indicated at the bottom of the gel) supplemented with or without 12.5 μ M batimastat. Levels of TcpP and TcpA were probed for each samples. Batimastat is a metalloprotease inhibitor that has been shown to inhibit RseP (a homolog of YaeL) within *Escherichia coli* (480).

G.3 – Future Directions

Currently, the data indicate that *toxT* transcription is highly heterogeneous within *V. cholerae* cells. Our data show that heterogeneous *toxT* transcription is dependent on TcpP and ToxR, but it is independent of cell density, culture age, TcpH, RIP via Tsp and YaeL, pH, temperature, and direct cell contact. As discussed in Chapter 3, the intermediate and fast diffusion states of TcpP-PAmCherry are critical for this sub-population of *V. cholerae* cells to *toxT* transcription. As TcpP and ToxR are localized to the cytoplasmic membrane, we hypothesize that phospholipid composition within the sub-population of constitutive *toxT* expressing cells to differs and promotes the transition probability of TcpP molecules from the intermediate diffusion state to the slow diffusion state. Alternatively, heterogeneous single-cell *toxT* transcription could be mediated by downregulation of the unidentified protease within the sub-population of constitutive *toxT* expressing cells. Testing these hypotheses will be the subject of future research.

REFERENCES

REFERENCES

1. Centers for Disease Control and Prevention (CDC). 1993. Imported cholera associated with a newly described toxigenic *Vibrio cholerae* O139 strain--California, 1993. *MMWR Morb Mortal Wkly Rep* 42:501–503.
2. Ali M, Nelson AR, Lopez AL, Sack DA. 2015. Updated global burden of cholera in endemic countries. *PLoS Negl Trop Dis* 9:e0003832.
3. Gil AI, Louis VR, Rivera ING, Lipp E, Huq A, Lanata CF, Taylor DN, Russek-Cohen E, Choopun N, Bradley Sack R, Colwell RR. 2004. Occurrence and distribution of *Vibrio cholerae* in the coastal environment of Peru. *Environmental Microbiology* <https://doi.org/10.1111/j.1462-2920.2004.00601.x>.
4. Pierce NF, Banwell JG, Mitra RC, Caranasos GJ, Keimowitz RI, Mondal A, Manji PM. 1968. Effect of Intragastric Glucose-Electrolyte Infusion Upon Water and Electrolyte Balance in Asiatic Cholera. *Gastroenterology* [https://doi.org/10.1016/s0016-5085\(19\)34043-0](https://doi.org/10.1016/s0016-5085(19)34043-0).
5. Hirschhorn N, Kinzie JL, Sachar DB, Northrup RS, Taylor JO, Ahmad SZ, Phillips RA. 1968. Decrease in net stool output in cholera during intestinal perfusion with glucose-containing solutions. *N Engl J Med* 279:176–181.
6. Wallace CK, Anderson PN, Brown TC, Khanra SR, Lewis GW, Pierce NF, Sanyal SN, Segre GV, Waldman RH. 1968. Optimal antibiotic therapy in cholera. *Bull World Health Organ* 39:239–245.
7. Jelinek T, Kollaritsch H. 2008. Vaccination with Dukoral® against travelers' diarrhea (ETEC) and cholera. *Expert Review of Vaccines*.
8. Saha A, Chowdhury MI, Khanam F, Bhuiyan MS, Chowdhury F, Khan AI, Khan IA, Clemens J, Ali M, Cravioto A, Qadri F. 2011. Safety and immunogenicity study of a killed bivalent (O1 and O139) whole-cell oral cholera vaccine Shanchol, in Bangladeshi adults and children as young as 1 year of age. *Vaccine* 29:8285–8292.
9. Cabrera A, Lepage JE, Sullivan KM, Seed SM. 2017. Vaxchora: A Single-Dose Oral Cholera Vaccine. *Ann Pharmacother* 51:584–589.
10. Sinha R, Koley H, Nag D, Mitra S, Mukhopadhyay AK, Chattopadhyay B. 2015. Pentavalent outer membrane vesicles of *Vibrio cholerae* induce adaptive immune response and protective efficacy in both adult and passive suckling mice models. *Microbes Infect* 17:215–227.
11. Hoge CW, Bodhidatta L, Echeverria P, Deesuan M, Kitporaka P. 1996. Epidemiologic Study of *Vibrio cholerae* O1 and O139 in Thailand: At the Advancing Edge of the Eighth Pandemic. *American Journal of Epidemiology* <https://doi.org/10.1093/oxfordjournals.aje.a008737>.
12. Swerdlow DL, Ries AA. 1993. *Vibrio cholerae* non-O1--the eighth pandemic? *Lancet*.

13. Nair GB, Faruque SM, Bhuiyan NA, Kamruzzaman M, Siddique AK, Sack DA. 2002. New variants of *Vibrio cholerae* O1 biotype El Tor with attributes of the classical biotype from hospitalized patients with acute diarrhea in Bangladesh. *J Clin Microbiol* 40:3296–3299.
14. Chunara R, Andrews JR, Brownstein JS. 2012. Social and news media enable estimation of epidemiological patterns early in the 2010 Haitian cholera outbreak. *Am J Trop Med Hyg* 86:39–45.
15. Chowdhury FR, Nur Z, Hassan N, von Seidlein L, Dunachie S. 2017. Pandemics, pathogenicity and changing molecular epidemiology of cholera in the era of global warming. *Ann Clin Microbiol Antimicrob* 16:10.
16. Mooi FR, Bik EM. 1997. The evolution of epidemic *Vibrio cholerae* strains. *Trends Microbiol* 5:161–165.
17. Faruque SM, Albert MJ, Mekalanos JJ. 1998. Epidemiology, genetics, and ecology of toxigenic *Vibrio cholerae*. *Microbiol Mol Biol Rev* 62:1301–1314.
18. Keasler SP, Hall RH. 1993. Detecting and biotyping *Vibrio cholerae* O1 with multiplex polymerase chain reaction. *Lancet* 341:1661.
19. Dziejman M, Balon E, Boyd D, Fraser CM, Heidelberg JF, Mekalanos JJ. 2002. Comparative genomic analysis of *Vibrio cholerae*: Genes that correlate with cholera endemic and pandemic disease. *Proceedings of the National Academy of Sciences* <https://doi.org/10.1073/pnas.042667999>.
20. Thomas S, Williams SG, Manning PA. 1995. Regulation of tcp genes in classical and E1 Tor strains of *Vibrio cholerae* O1. *Gene* [https://doi.org/10.1016/0378-1119\(95\)00610-x](https://doi.org/10.1016/0378-1119(95)00610-x).
21. Phillips RA. 1964. WATER AND ELECTROLYTE LOSSES IN CHOLERA. *Fed Proc* 23:705–712.
22. Nelson EJ, Harris JB, Morris JG Jr, Calderwood SB, Camilli A. 2009. Cholera transmission: the host, pathogen and bacteriophage dynamic. *Nat Rev Microbiol* 7:693–702.
23. Angelichio MJ, Spector J, Waldor MK, Camilli A. 1999. *Vibrio cholerae* intestinal population dynamics in the suckling mouse model of infection. *Infect Immun* 67:3733–3739.
24. Millet YA, Alvarez D, Ringgaard S, von Andrian UH, Davis BM, Waldor MK. 2014. Insights into *Vibrio cholerae* intestinal colonization from monitoring fluorescently labeled bacteria. *PLoS Pathog* 10:e1004405.
25. Camilli A, Beattie DT, Mekalanos JJ. 1994. Use of genetic recombination as a reporter of gene expression. *Proceedings of the National Academy of Sciences*.
26. Ho BT, Dong TG, Mekalanos JJ. 2014. A view to a kill: the bacterial type VI secretion system. *Cell Host Microbe* 15:9–21.
27. Wu Z, Nybom P, Magnusson KE. 2000. Distinct effects of *Vibrio cholerae* haemagglutinin/protease on the structure and localization of the tight junction-associated proteins occludin and ZO-1. *Cell Microbiol* 2:11–17.
28. Uzzau S, Lu R, Wang W, Fiore C, Fasano A. 2001. Purification and preliminary

- characterization of the zonula occludens toxin receptor from human (CaCo2) and murine (IEC6) intestinal cell lines. *FEMS Microbiol Lett* 194:1–5.
29. Goldblum SE, Rai U, Tripathi A, Thakar M, De Leo L, Di Toro N, Not T, Ramachandran R, Puche AC, Hollenberg MD, Fasano A. 2011. The active Zot domain (aa 288–293) increases ZO-1 and myosin 1C serine/threonine phosphorylation, alters interaction between ZO-1 and its binding partners, and induces tight junction disassembly through proteinase activated receptor 2 activation. *The FASEB Journal* <https://doi.org/10.1096/fj.10-158972>.
 30. Herrington DA, Hall RH, Losonsky G, Mekalanos JJ, Taylor RK, Levine MM. 1988. Toxin, toxin-coregulated pili, and the *toxR* regulon are essential for *Vibrio cholerae* pathogenesis in humans. *J Exp Med* 168:1487–1492.
 31. Taylor RK, Miller VL, Furlong DB, Mekalanos JJ. 1987. Use of *phoA* gene fusions to identify a pilus colonization factor coordinately regulated with cholera toxin. *Proc Natl Acad Sci U S A* 84:2833–2837.
 32. Chiang SL, Taylor RK, Koomey M, Mekalanos JJ. 1995. Single amino acid substitutions in the N-terminus of *Vibrio cholerae* TcpA affect colonization, autoagglutination, and serum resistance. *Mol Microbiol* 17:1133–1142.
 33. Stern AM, Hay AJ, Liu Z, Desland FA, Zhang J, Zhong Z, Zhu J. 2012. The NorR regulon is critical for *Vibrio cholerae* resistance to nitric oxide and sustained colonization of the intestines. *MBio* 3:e00013–12.
 34. Bitar A, Aung KM, Wai SN, Hammarström M-L. 2019. *Vibrio cholerae* derived outer membrane vesicles modulate the inflammatory response of human intestinal epithelial cells by inducing microRNA-146a. *Sci Rep* 9:7212.
 35. Woida PJ, Satchell KJF. 2020. The MARTX toxin silences the inflammatory response to cytoskeletal damage before inducing actin cytoskeleton collapse. *Sci Signal* 13.
 36. Bharati K, Ganguly NK. 2011. Cholera toxin: a paradigm of a multifunctional protein. *Indian J Med Res* 133:179–187.
 37. Somarny WMZ, Mariana NS, Neela V, Rozita R, Raha AR. 2002. Optimization of Parameters for Accessory Cholera Enterotoxin (Ace) Protein Expression. *Journal of Medical Sciences* <https://doi.org/10.3923/jms.2002.74.76>.
 38. Trucksis M, Conn TL, Wasserman SS, Sears CL. 2000. *Vibrio cholerae* ACE stimulates Ca(2+)-dependent Cl(-)/HCO(3)(-) secretion in T84 cells *in vitro*. *Am J Physiol Cell Physiol* 279:C567–77.
 39. Krukonis ES, Yu RR, Dirita VJ. 2000. The *Vibrio cholerae* ToxR/TcpP/ToxT virulence cascade: distinct roles for two membrane-localized transcriptional activators on a single promoter. *Mol Microbiol* 38:67–84.
 40. DiRita VJ, Parsot C, Jander G, Mekalanos JJ. 1991. Regulatory cascade controls virulence in *Vibrio cholerae*. *Proc Natl Acad Sci U S A* 88:5403–5407.
 41. Higgins DE, DiRita VJ. 1994. Transcriptional control of *toxT*, a regulatory gene in the ToxR regulon of *Vibrio cholerae*. *Mol Microbiol* 14:17–29.

42. Higgins DE, Nazareno E, DiRita VJ. 1992. The virulence gene activator ToxT from *Vibrio cholerae* is a member of the AraC family of transcriptional activators. *J Bacteriol* 174:6974–6980.
43. Plecha SC, Withey JH. 2015. Mechanism for inhibition of *Vibrio cholerae* ToxT activity by the unsaturated fatty acid components of bile. *J Bacteriol* 197:1716–1725.
44. Cruite JT, Kovacicova G, Clark KA, Woodbrey AK, Skorupski K, Jon Kull F. 2019. Structural basis for virulence regulation in *Vibrio cholerae* by unsaturated fatty acid components of bile. *Communications Biology* <https://doi.org/10.1038/s42003-019-0686-x>.
45. Childers BM, Cao X, Weber GG, Demeler B, Hart PJ, Klose KE. 2011. N-terminal residues of the *Vibrio cholerae* virulence regulatory protein ToxT involved in dimerization and modulation by fatty acids. *J Biol Chem* 286:28644–28655.
46. Withey JH, Nag D, Plecha SC, Sinha R, Koley H. 2015. Conjugated Linoleic Acid Reduces Cholera Toxin Production *In vitro* and *In vivo* by Inhibiting *Vibrio cholerae* ToxT Activity. *Antimicrob Agents Chemother* 59:7471–7476.
47. Abuaita BH, Withey JH. 2011. Termination of *Vibrio cholerae* virulence gene expression is mediated by proteolysis of the major virulence activator, ToxT. *Mol Microbiol* 81:1640–1653.
48. Thomson JJ, Plecha SC, Withey JH. 2015. A small unstructured region in *Vibrio cholerae* ToxT mediates the response to positive and negative effectors and ToxT proteolysis. *J Bacteriol* 197:654–668.
49. Hogan DL, Ainsworth MA, Isenberg JI. 1994. Review article: gastroduodenal bicarbonate secretion. *Aliment Pharmacol Ther* 8:475–488.
50. Thomson JJ, Withey JH. 2014. Bicarbonate increases binding affinity of *Vibrio cholerae* ToxT to virulence gene promoters. *J Bacteriol* 196:3872–3880.
51. Shakhnovich EA, Hung DT, Pierson E, Lee K, Mekalanos JJ. 2007. Virstatin inhibits dimerization of the transcriptional activator ToxT. *Proc Natl Acad Sci U S A* 104:2372–2377.
52. Häse CC, Mekalanos JJ. 1998. TcpP protein is a positive regulator of virulence gene expression in *Vibrio cholerae*. *Proc Natl Acad Sci U S A* 95:730–734.
53. Miller VL, Taylor RK, Mekalanos JJ. 1987. Cholera toxin transcriptional activator ToxR is a transmembrane DNA binding protein. *Cell*.
54. Crawford JA, Krukoni ES, DiRita VJ. 2003. Membrane localization of the ToxR winged-helix domain is required for TcpP-mediated virulence gene activation in *Vibrio cholerae*. *Mol Microbiol* 47:1459–1473.
55. Krukoni ES, DiRita VJ. 2003. DNA binding and ToxR responsiveness by the wing domain of TcpP, an activator of virulence gene expression in *Vibrio cholerae*. *Mol Cell* 12:157–165.
56. Beck NA, Krukoni ES, DiRita VJ. 2004. TcpH Influences Virulence Gene Expression in *Vibrio cholerae* by Inhibiting Degradation of the Transcription Activator TcpP. *Journal of Bacteriology*.

57. Almagro-Moreno S, Root MZ, Taylor RK. 2015. Role of ToxS in the proteolytic cascade of virulence regulator ToxR in *Vibrio cholerae*. *Mol Microbiol* 98:963–976.
58. Teoh WP, Matson JS, DiRita VJ. 2015. Regulated intramembrane proteolysis of the virulence activator TcpP in *Vibrio cholerae* is initiated by the tail-specific protease (Tsp). *Mol Microbiol* 97:822–831.
59. Matson JS, DiRita VJ. 2005. Degradation of the membrane-localized virulence activator TcpP by the YaeL protease in *Vibrio cholerae*. *Proc Natl Acad Sci U S A* 102:16403–16408.
60. Skorupski K, Taylor RK. 1997. Cyclic AMP and its receptor protein negatively regulate the coordinate expression of cholera toxin and toxin-coregulated pilus in *Vibrio cholerae*. *Proc Natl Acad Sci U S A* 94:265–270.
61. Kovacikova G, Skorupski K. 2001. Overlapping binding sites for the virulence gene regulators AphA, AphB and cAMP-CRP at the *Vibrio cholerae* tcpPH promoter. *Molecular Microbiology* <https://doi.org/10.1046/j.1365-2958.2001.02518.x>.
62. Behari J, Stagon L, Calderwood SB. 2001. pepA , a Gene Mediating pH Regulation of Virulence Genes in *Vibrio cholerae*. *Journal of Bacteriology* <https://doi.org/10.1128/jb.183.1.178-188.2001>.
63. Kovacikova G, Lin W, Skorupski K. 2010. The LysR-Type Virulence Activator AphB Regulates the Expression of Genes in *Vibrio cholerae* in Response to Low pH and Anaerobiosis. *Journal of Bacteriology* <https://doi.org/10.1128/jb.00193-10>.
64. Taylor JL, De Silva RS, Kovacikova G, Lin W, Taylor RK, Skorupski K, Jon Kull F. 2012. The crystal structure of AphB, a virulence gene activator from *Vibrio cholerae*, reveals residues that influence its response to oxygen and pH. *Molecular Microbiology* <https://doi.org/10.1111/j.1365-2958.2011.07919.x>.
65. Liu Z, Wang H, Zhou Z, Naseer N, Xiang F, Kan B, Goulian M, Zhu J. 2016. Differential Thiol-Based Switches Jump-Start *Vibrio cholerae* Pathogenesis. *Cell Rep* 14:347–354.
66. Kovacikova G, Skorupski K. 2002. Regulation of virulence gene expression in *Vibrio cholerae* by quorum sensing: HapR functions at the aphA promoter. *Molecular Microbiology* <https://doi.org/10.1046/j.1365-2958.2002.03229.x>.
67. Zhu J, Miller MB, Vance RE, Dziejman M, Bassler BL, Mekalanos JJ. 2002. Quorum-sensing regulators control virulence gene expression in *Vibrio cholerae*. *Proc Natl Acad Sci U S A* 99:3129–3134.
68. Ball AS, Chaparian RR, van Kessel JC. 2017. Quorum Sensing Gene Regulation by LuxR/HapR Master Regulators in *Vibrios*. *J Bacteriol* 199.
69. Martínez-Hackert E, Stock AM. 1997. Structural relationships in the OmpR family of winged-helix transcription factors. *J Mol Biol* 269:301–312.
70. Goss TJ, Seaborn CP, Gray MD, Krukoni ES. 2010. Identification of the TcpP-binding site in the toxT promoter of *Vibrio cholerae* and the role of ToxR in TcpP-mediated activation. *Infect Immun* 78:4122–4133.
71. Goss TJ, Morgan SJ, French EL, Krukoni ES. 2013. ToxR recognizes a direct repeat

- element in the *toxT*, *ompU*, *ompT*, and *ctxA* promoters of *Vibrio cholerae* to regulate transcription. *Infect Immun* 81:884–895.
72. Kazi MI, Conrado AR, Mey AR, Payne SM, Davies BW. 2016. ToxR Antagonizes H-NS Regulation of Horizontally Acquired Genes to Drive Host Colonization. *PLoS Pathog* 12:e1005570.
 73. Higgins DE, DiRita VJ. 1996. Genetic analysis of the interaction between *Vibrio cholerae* transcription activator ToxR and *toxT* promoter DNA. *J Bacteriol* 178:1080–1087.
 74. Fan F, Liu Z, Jabeen N, Birdwell LD, Zhu J, Kan B. 2014. Enhanced interaction of *Vibrio cholerae* virulence regulators TcpP and ToxR under oxygen-limiting conditions. *Infect Immun* 82:1676–1682.
 75. Bina TF, Kunkle DE, Bina XR, Mullet SJ, Wendell SG, Bina JE. 2021. Bile salts promote ToxR regulon activation during growth under virulence inducing conditions. *Infect Immun* IAI0044121.
 76. Shi M, Li N, Xue Y, Zhong Z, Yang M. 2020. The 58th Cysteine of TcpP Is Essential for *Vibrio cholerae* Virulence Factor Production and Pathogenesis. *Frontiers in Microbiology* <https://doi.org/10.3389/fmicb.2020.00118>.
 77. Hay AJ, Yang M, Xia X, Liu Z, Hammons J, Fenical W, Zhu J. 2017. Calcium Enhances Bile Salt-Dependent Virulence Activation in *Vibrio cholerae*. *Infect Immun* 85.
 78. Yang M, Liu Z, Hughes C, Stern AM, Wang H, Zhong Z, Kan B, Fenical W, Zhu J. 2013. Bile salt-induced intermolecular disulfide bond formation activates *Vibrio cholerae* virulence. *Proc Natl Acad Sci U S A* 110:2348–2353.
 79. Lembke M, Pennetzdorfer N, Tutz S, Koller M, Vorkapic D, Zhu J, Schild S, Reidl J. 2018. Proteolysis of ToxR is controlled by cysteine-thiol redox state and bile salts in *Vibrio cholerae*. *Molecular Microbiology* <https://doi.org/10.1111/mmi.14125>.
 80. Almagro-Moreno S, Kim TK, Skorupski K, Taylor RK. 2015. Proteolysis of virulence regulator ToxR is associated with entry of *Vibrio cholerae* into a dormant state. *PLoS Genet* 11:e1005145.
 81. Gubensäk N, Wagner GE, Schrank E, Falsone FS, Berger TMI, Pavkov-Keller T, Reidl J, Zangger K. 2021. The periplasmic domains of *Vibrio cholerae* ToxR and ToxS are forming a strong heterodimeric complex independent on the redox state of ToxR cysteines. *Molecular Microbiology* <https://doi.org/10.1111/mmi.14673>.
 82. Carroll PA, Tashima KT, Rogers MB, DiRita VJ, Calderwood SB. 1997. Phase variation in *tcpH* modulates expression of the ToxR regulon in *Vibrio cholerae*. *Molecular Microbiology*.
 83. Midgett CR, Almagro-Moreno S, Pellegrini M, Taylor RK, Skorupski K, Kull FJ. 2017. Bile salts and alkaline pH reciprocally modulate the interaction between the periplasmic domains of *Vibrio cholerae* ToxR and ToxS. *Mol Microbiol* 105:258–272.
 84. Midgett CR, Swindell RA, Pellegrini M, Kull FJ. 2020. Publisher Correction: A disulfide constrains the ToxR periplasmic domain structure, altering its interactions with ToxS and bile-salts. *Sci Rep* 10:12085.

85. Lembke M, Höfler T, Walter A-N, Tutz S, Fengler V, Schild S, Reidl J. 2020. Host stimuli and operator binding sites controlling protein interactions between virulence master regulator ToxR and ToxS in *Vibrio cholerae*. *Mol Microbiol* 114:262–278.
86. Sirisaengtaksin N, Odem MA, Bosserman RE, Flores EM, Krachler AM. 2020. The *E. coli* transcription factor GrlA is regulated by subcellular compartmentalization and activated in response to mechanical stimuli. *Proceedings of the National Academy of Sciences* <https://doi.org/10.1073/pnas.1917500117>.
87. Muro-Pastor AM, Ostrovsky P, Maloy S. 1997. Regulation of gene expression by repressor localization: biochemical evidence that membrane and DNA binding by the PutA protein are mutually exclusive. *J Bacteriol* 179:2788–2791.
88. Parkinson JS, Kofoid EC. 1992. Communication modules in bacterial signaling proteins. *Annu Rev Genet* 26:71–112.
89. Ulrich LE, Koonin EV, Zhulin IB. 2005. One-component systems dominate signal transduction in prokaryotes. *Trends Microbiol* 13:52–56.
90. Paget MS. 2015. Bacterial Sigma Factors and Anti-Sigma Factors: Structure, Function and Distribution. *Biomolecules* 5:1245–1265.
91. Staroń A, Sofia HJ, Dietrich S, Ulrich LE, Liesegang H, Mascher T. 2009. The third pillar of bacterial signal transduction: classification of the extracytoplasmic function (ECF) sigma factor protein family. *Mol Microbiol* 74:557–581.
92. 2011. *Two-Component Signaling Systems*. Elsevier.
93. Zarrella TM, Bai G. 2020. The Many Roles of the Bacterial Second Messenger Cyclic di-AMP in Adapting to Stress Cues. *J Bacteriol* 203.
94. Römling U, Galperin MY, Gomelsky M. 2013. Cyclic di-GMP: the first 25 years of a universal bacterial second messenger. *Microbiol Mol Biol Rev* 77:1–52.
95. Hengge R, Gründling A, Jenal U, Ryan R, Yildiz F. 2016. Bacterial Signal Transduction by Cyclic Di-GMP and Other Nucleotide Second Messengers. *Journal of Bacteriology* <https://doi.org/10.1128/jb.00331-15>.
96. Beck NA, Krukonis ES, DiRita VJ. 2004. TcpH influences virulence gene expression in *Vibrio cholerae* by inhibiting degradation of the transcription activator TcpP. *J Bacteriol* 186:8309–8316.
97. Hobbs M, Collie ES, Free PD, Livingston SP, Mattick JS. 1993. PilS and PilR, a two-component transcriptional regulatory system controlling expression of type 4 fimbriae in *Pseudomonas aeruginosa*. *Mol Microbiol* 7:669–682.
98. Carrick CS, Fyfe JA, Davies JK. 2000. The genome of *Neisseria gonorrhoeae* retains the remnants of a two-component regulatory system that once controlled piliation. *FEMS Microbiol Lett* 186:197–201.
99. Bischof LF, Haurat MF, Albers S-V. 2019. Two membrane-bound transcription factors regulate expression of various type-IV-pili surface structures in *Sulfolobus acidocaldarius*. *PeerJ* <https://doi.org/10.7717/peerj.6459>.

100. Lassak K, Peeters E, Wróbel S, Albers S-V. 2013. The one-component system ArnR: a membrane-bound activator of the crenarchaeal archaellum. *Mol Microbiol* 88:125–139.
101. Kodama T, Gotoh K, Hiyoshi H, Morita M, Izutsu K, Akeda Y, Park K-S, Cantarelli VV, Dryselius R, Iida T, Honda T. 2010. Two regulators of *Vibrio parahaemolyticus* play important roles in enterotoxicity by controlling the expression of genes in the Vp-PAI region. *PLoS One* 5:e8678.
102. Alam A, Tam V, Hamilton E, Dziejman M. 2010. *vttRA* and *vttRB* Encode ToxR family proteins that mediate bile-induced expression of type three secretion system genes in a non-O1/non-O139 *Vibrio cholerae* strain. *Infect Immun* 78:2554–2570.
103. Miller KA, Hamilton E, Dziejman M. 2012. The *Vibrio cholerae* *trh* Gene Is Coordinately Regulated *In vitro* with Type III Secretion System Genes by *VttRA/VttRB* but Does Not Contribute to Caco2-BBE Cell Cytotoxicity. *Infection and Immunity* <https://doi.org/10.1128/iai.00832-12>.
104. Ante VM, Bina XR, Howard MF, Sayeed S, Taylor DL, Bina JE. 2015. *Vibrio cholerae* *leuO* Transcription Is Positively Regulated by ToxR and Contributes to Bile Resistance. *J Bacteriol* 197:3499–3510.
105. Provenzano D, Schuhmacher DA, Barker JL, Klose KE. 2000. The Virulence Regulatory Protein ToxR Mediates Enhanced Bile Resistance in *Vibrio cholerae* and Other Pathogenic *Vibrio* Species. *Infection and Immunity* <https://doi.org/10.1128/iai.68.3.1491-1497.2000>.
106. Manson JM, Keis S, Smith JMB, Cook GM. 2004. Acquired Bacitracin Resistance in *Enterococcus faecalis* Is Mediated by an ABC Transporter and a Novel Regulatory Protein, *BcrR*. *Antimicrobial Agents and Chemotherapy*.
107. Kuper C, Jung K. 2005. CadC-mediated activation of the *cadBA* promoter in *Escherichia coli*. *J Mol Microbiol Biotechnol* 10:26–39.
108. Gu D, Wang K, Lu T, Li L, Jiao X. 2021. *Vibrio parahaemolyticus* CadC regulates acid tolerance response to enhance bacterial motility and cytotoxicity. *J Fish Dis* 44:1155–1168.
109. Choi SH. 2008. Activation of the *Vibrio vulnificus* *cadBA* Operon by Leucine-Responsive Regulatory Protein is Mediated by CadC. *Journal of Microbiology and Biotechnology* <https://doi.org/10.4014/jmb.0800.121>.
110. Dalia AB, Lazinski DW, Camilli A. 2014. Identification of a membrane-bound transcriptional regulator that links chitin and natural competence in *Vibrio cholerae*. *MBio* 5:e01028–13.
111. Santamaría L, Reverón I, López de Felipe F, de Las Rivas B, Muñoz R. 2018. Unravelling the Reduction Pathway as an Alternative Metabolic Route to Hydroxycinnamate Decarboxylation in *Lactobacillus plantarum*. *Appl Environ Microbiol* 84.
112. Steele MI, Lorenz D, Hatter K, Park A, Sokatch JR. 1992. Characterization of the *mmsAB* operon of *Pseudomonas aeruginosa* PAO encoding methylmalonate-semialdehyde dehydrogenase and 3-hydroxyisobutyrate dehydrogenase. *J Biol Chem* 267:13585–13592.
113. Olson ME, King JM, Yahr TL, Horwill AR. 2013. Sialic acid catabolism in *Staphylococcus aureus*. *J Bacteriol* 195:1779–1788.

114. Meijerink M, van Hemert S, Taverne N, Wels M, de Vos P, Bron PA, Savelkoul HF, van Bilsen J, Kleerebezem M, Wells JM. 2010. Identification of genetic loci in *Lactobacillus plantarum* that modulate the immune response of dendritic cells using comparative genome hybridization. *PLoS One* 5:e10632.
115. Gumerov VM, Ortega DR, Adebali O, Ulrich LE, Zhulin IB. 2020. MiST 3.0: an updated microbial signal transduction database with an emphasis on chemosensory systems. *Nucleic Acids Research* <https://doi.org/10.1093/nar/gkz988>.
116. Krogh A, Larsson B, von Heijne G, Sonnhammer ELL. 2001. Predicting transmembrane protein topology with a hidden markov model: application to complete genomes. Edited by F. Cohen. *Journal of Molecular Biology* <https://doi.org/10.1006/jmbi.2000.4315>.
117. Gumerov VM, Zhulin IB. 2020. TREND: a platform for exploring protein function in prokaryotes based on phylogenetic, domain architecture and gene neighborhood analyses. *Nucleic Acids Research* <https://doi.org/10.1093/nar/gkaa243>.
118. Johnson M, Zaretskaya I, Raytselis Y, Merezhuk Y, McGinnis S, Madden TL. 2008. NCBI BLAST: a better web interface. *Nucleic Acids Research* <https://doi.org/10.1093/nar/gkn201>.
119. Korf I, Yandell M, Bedell J. 2003. BLAST. "O'Reilly Media, Inc."
120. Welch TJ, Bartlett DH. 1998. Identification of a regulatory protein required for pressure-responsive gene expression in the deep-sea bacterium *Photobacterium* species strain SS9. *Mol Microbiol* 27:977–985.
121. Osorio CR, Klose KE. 2000. A region of the transmembrane regulatory protein ToxR that tethers the transcriptional activation domain to the cytoplasmic membrane displays wide divergence among *Vibrio* species. *J Bacteriol* 182:526–528.
122. Colwell RR, Huq A. 1994. Environmental reservoir of *Vibrio cholerae*. The causative agent of cholera. *Ann N Y Acad Sci* 740:44–54.
123. Baker-Austin C, Trinanès J, Gonzalez-Escalona N, Martínez-Urtaza J. 2017. Non-Cholera Vibrios: The Microbial Barometer of Climate Change. *Trends Microbiol* 25:76–84.
124. Bina XR, Howard MF, Ante VM, Bina JE. 2016. *Vibrio cholerae* LeuO Links the ToxR Regulon to Expression of Lipid A Remodeling Genes. *Infect Immun* 84:3161–3171.
125. Mey AR, Craig SA, Payne SM. 2012. Effects of amino acid supplementation on porin expression and ToxR levels in *Vibrio cholerae*. *Infect Immun* 80:518–528.
126. Hung DT, Mekalanos JJ. 2005. Bile acids induce cholera toxin expression in *Vibrio cholerae* in a ToxT-independent manner. *Proc Natl Acad Sci U S A* 102:3028–3033.
127. Provenzano D, Lauriano CM, Klose KE. 2001. Characterization of the role of the ToxR-modulated outer membrane porins OmpU and OmpT in *Vibrio cholerae* virulence. *J Bacteriol* 183:3652–3662.
128. Provenzano D, Klose KE. 2000. Altered expression of the ToxR-regulated porins OmpU and OmpT diminishes *Vibrio cholerae* bile resistance, virulence factor expression, and intestinal colonization. *Proc Natl Acad Sci U S A* 97:10220–10224.

129. Mathur J, Waldor MK. 2004. The *Vibrio cholerae* ToxR-Regulated Porin OmpU Confers Resistance to Antimicrobial Peptides. *Infection and Immunity* <https://doi.org/10.1128/iai.72.6.3577-3583.2004>.
130. Lin Z, Kumagai K, Baba K, Mekalanos JJ, Nishibuchi M. 1993. *Vibrio parahaemolyticus* has a homolog of the *Vibrio cholerae* toxRS operon that mediates environmentally induced regulation of the thermostable direct hemolysin gene. *Journal of Bacteriology* <https://doi.org/10.1128/jb.175.12.3844-3855.1993>.
131. Lee SE, Shin SH, Kim SY, Kim YR, Shin DH, Chung SS, Lee ZH, Lee JY, Jeong KC, Choi SH, Rhee JH. 2000. *Vibrio vulnificus* Has the Transmembrane Transcription Activator ToxRS Stimulating the Expression of the Hemolysin Gene vvhA. *Journal of Bacteriology* <https://doi.org/10.1128/jb.182.12.3405-3415.2000>.
132. Fan F, Liu Z, Jabeen N, Birdwell LD, Zhu J, Kan B. 2014. Enhanced interaction of *Vibrio cholerae* virulence regulators TcpP and ToxR under oxygen-limiting conditions. *Infect Immun* 82:1676–1682.
133. Zheng B, Jiang X, Cheng H, Guo L, Zhang J, Xu H, Yu X, Huang C, Ji J, Ying C, Feng Y, Xiao Y, Li L. 2017. Genome characterization of two bile-isolated *Vibrio fluvialis* strains: an insight into pathogenicity and bile salt adaption. *Sci Rep* 7:11827.
134. Bennett BD, Essock-Burns T, Ruby EG. 2020. HbtR, a Heterofunctional Homolog of the Virulence Regulator TcpP, Facilitates the Transition between Symbiotic and Planktonic Lifestyles in *Vibrio fischeri*. *MBio* 11.
135. Koch EJ, Miyashiro T, McFall-Ngai MJ, Ruby EG. 2014. Features governing symbiont persistence in the squid-vibrio association. *Mol Ecol* 23:1624–1634.
136. Visick KL, Foster J, Doino J, McFall-Ngai M, Ruby EG. 2000. *Vibrio fischeri* lux genes play an important role in colonization and development of the host light organ. *J Bacteriol* 182:4578–4586.
137. Moriano-Gutierrez S, Koch EJ, Bussan H, Romano K, Belcaid M, Rey FE, Ruby EG, McFall-Ngai MJ. 2019. Critical symbiont signals drive both local and systemic changes in diel and developmental host gene expression. *Proc Natl Acad Sci U S A* 116:7990–7999.
138. Mandel MJ, Schaefer AL, Brennan CA, Heath-Heckman EAC, DeLoney-Marino CR, McFall-Ngai MJ, Ruby EG. 2012. Squid-Derived Chitin Oligosaccharides Are a Chemotactic Signal during Colonization by *Vibrio fischeri*. *Applied and Environmental Microbiology* <https://doi.org/10.1128/aem.00377-12>.
139. Ruby EG, Asato LM. 1993. Growth and flagellation of *Vibrio fischeri* during initiation of the sepiolid squid light organ symbiosis. *Arch Microbiol* 159:160–167.
140. Graf J, Ruby EG. 1998. Host-derived amino acids support the proliferation of symbiotic bacteria. *Proc Natl Acad Sci U S A* 95:1818–1822.
141. Jones BW, Nishiguchi MK. 2004. Counterillumination in the Hawaiian bobtail squid, *Euprymna scolopes* Berry (Mollusca: Cephalopoda). *Marine Biology* <https://doi.org/10.1007/s00227-003-1285-3>.

142. Lee KH, Ruby EG. 1994. Effect of the Squid Host on the Abundance and Distribution of Symbiotic *Vibrio fischeri* in Nature. *Appl Environ Microbiol* 60:1565–1571.
143. Thompson LR, Nikolakakis K, Pan S, Reed J, Knight R, Ruby EG. 2017. Transcriptional characterization of *Vibrio fischeri* during colonization of juvenile *Euprymna scolopes*. *Environ Microbiol* 19:1845–1856.
144. Kovach ME, Shaffer MD, Peterson KM. 1996. A putative integrase gene defines the distal end of a large cluster of ToxR-regulated colonization genes in *Vibrio cholerae*. *Microbiology* 142 (Pt 8):2165–2174.
145. Karaolis DK, Johnson JA, Bailey CC, Boedeker EC, Kaper JB, Reeves PR. 1998. A *Vibrio cholerae* pathogenicity island associated with epidemic and pandemic strains. *Proc Natl Acad Sci U S A* 95:3134–3139.
146. Ruby EG, Urbanowski M, Campbell J, Dunn A, Faini M, Gunsalus R, Lostroh P, Lupp C, McCann J, Millikan D, Schaefer A, Stabb E, Stevens A, Visick K, Whistler C, Greenberg EP. 2005. Complete genome sequence of *Vibrio fischeri*: a symbiotic bacterium with pathogenic congeners. *Proc Natl Acad Sci U S A* 102:3004–3009.
147. Visick KL, Quirke KP, McEwen SM. 2013. Arabinose induces pellicle formation by *Vibrio fischeri*. *Appl Environ Microbiol* 79:2069–2080.
148. Okada R, Matsuda S, Iida T. 2017. *Vibrio parahaemolyticus* VtrA is a membrane-bound regulator and is activated via oligomerization. *PLoS One* 12:e0187846.
149. Miller KA, Sofia MK, Weaver JWA, Seward CH, Dziejman M. 2016. Regulation by ToxR-Like Proteins Converges on vttRB Expression To Control Type 3 Secretion System-Dependent Caco2-BBE Cytotoxicity in *Vibrio cholerae*. *J Bacteriol* 198:1675–1682.
150. Dziejman M, Serruto D, Tam VC, Sturtevant D, Diraphat P, Faruque SM, Rahman MH, Heidelberg JF, Decker J, Li L, Montgomery KT, Grills G, Kucherlapati R, Mekalanos JJ. 2005. Genomic characterization of non-O1, non-O139 *Vibrio cholerae* reveals genes for a type III secretion system. *Proc Natl Acad Sci U S A* 102:3465–3470.
151. Chaand M, Miller KA, Sofia MK, Schlesener C, Weaver JWA, Sood V, Dziejman M. 2015. Type 3 Secretion System Island Encoded Proteins Required for Colonization by Non-O1/non-O139 Serogroup. *Infect Immun* 83:2862–2869.
152. Makino K, Oshima K, Kurokawa K, Yokoyama K, Uda T, Tagomori K, Iijima Y, Najima M, Nakano M, Yamashita A, Kubota Y, Kimura S, Yasunaga T, Honda T, Shinagawa H, Hattori M, Iida T. 2003. Genome sequence of *Vibrio parahaemolyticus*: a pathogenic mechanism distinct from that of *V. cholerae*. *Lancet* 361:743–749.
153. Izutsu K, Kurokawa K, Tashiro K, Kuhara S, Hayashi T, Honda T, Iida T. 2008. Comparative Genomic Analysis Using Microarray Demonstrates a Strong Correlation between the Presence of the 80-Kilobase Pathogenicity Island and Pathogenicity in Kanagawa Phenomenon-Positive *Vibrio parahaemolyticus* Strains. *Infection and Immunity* <https://doi.org/10.1128/iai.01535-07>.
154. Li P, Rivera-Cancel G, Kinch LN, Salomon D, Tomchick DR, Grishin NV, Orth K. 2016. Bile salt receptor complex activates a pathogenic type III secretion system. *Elife* 5.

155. Rivera-Cancel G, Orth K. 2017. Biochemical basis for activation of virulence genes by bile salts in *Vibrio parahaemolyticus*. *Gut Microbes* 8:366–373.
156. Ante VM, Bina XR, Bina JE. 2015. The LysR-type regulator LeuO regulates the acid tolerance response in *Vibrio cholerae*. *Microbiology* 161:2434–2443.
157. Rhee JE, Jeong HG, Lee JH, Choi SH. 2006. AphB influences acid tolerance of *Vibrio vulnificus* by activating expression of the positive regulator CadC. *J Bacteriol* 188:6490–6497.
158. Merrell DS, Scott Merrell D, Camilli A. 2000. Regulation of *Vibrio cholerae* Genes Required for Acid Tolerance by a Member of the “ToxR-Like” Family of Transcriptional Regulators. *Journal of Bacteriology* <https://doi.org/10.1128/jb.182.19.5342-5350.2000>.
159. Neely MN, Dell CL, Olson ER. 1994. Roles of LysP and CadC in mediating the lysine requirement for acid induction of the *Escherichia coli* cad operon. *J Bacteriol* 176:3278–3285.
160. Casalino M, Prosseda G, Barbagallo M, Iacobino A, Ceccarini P, Latella MC, Nicoletti M, Colonna B. 2010. Interference of the CadC regulator in the arginine-dependent acid resistance system of *Shigella* and enteroinvasive *E. coli*. *Int J Med Microbiol* 300:289–295.
161. Lee YH, Kim BH, Kim JH, Yoon WS, Bang SH, Park YK. 2007. CadC Has a Global Translational Effect during Acid Adaptation in *Salmonella enterica* Serovar Typhimurium. *Journal of Bacteriology* <https://doi.org/10.1128/jb.01277-06>.
162. Lee YH, Kim JH. 2017. Direct interaction between the transcription factors CadC and OmpR involved in the acid stress response of *Salmonella enterica*. *Journal of Microbiology* <https://doi.org/10.1007/s12275-017-7410-7>.
163. Hsieh P-F, Lin H-H, Lin T-L, Wang J-T. 2010. CadC regulates cad and tdc operons in response to gastrointestinal stresses and enhances intestinal colonization of *Klebsiella pneumoniae*. *J Infect Dis* 202:52–64.
164. Tetsch L, Koller C, Haneburger I, Jung K. 2008. The membrane-integrated transcriptional activator CadC of *Escherichia coli* senses lysine indirectly via the interaction with the lysine permease LysP. *Mol Microbiol* 67:570–583.
165. Lee YH, Kim JH, Bang IS, Park YK. 2008. The membrane-bound transcriptional regulator CadC is activated by proteolytic cleavage in response to acid stress. *J Bacteriol* 190:5120–5126.
166. Dell CL, Neely MN, Olson ER. 1994. Altered pH lysine signalling mutants of cadC, a gene encoding a membrane-bound transcriptional activator of the *Escherichia coli* cadBA operon. *Molecular Microbiology* <https://doi.org/10.1111/j.1365-2958.1994.tb01262.x>.
167. Debnath A, Mizuno T, Miyoshi S-I. 2020. Regulation of Chitin-Dependent Growth and Natural Competence in. *Microorganisms* 8.
168. Antonova ES, Hammer BK. 2015. Genetics of Natural Competence in *Vibrio cholerae* and other *Vibrios*. *Microbiol Spectr* 3.
169. Pollack-Berti A, Wollenberg MS, Ruby EG. 2010. Natural transformation of *Vibrio fischeri*

- requires *tfoX* and *tfoY*. *Environ Microbiol* 12:2302–2311.
170. Gulig PA, Tucker MS, Thiaville PC, Joseph JL, Brown RN. 2009. USER friendly cloning coupled with chitin-based natural transformation enables rapid mutagenesis of *Vibrio vulnificus*. *Appl Environ Microbiol* 75:4936–4949.
 171. Souza CP, Almeida BC, Colwell RR, Rivera ING. 2011. The importance of chitin in the marine environment. *Mar Biotechnol* 13:823–830.
 172. Huq A, Small EB, West PA, Huq MI, Rahman R, Colwell RR. 1983. Ecological relationships between *Vibrio cholerae* and planktonic crustacean copepods. *Appl Environ Microbiol* 45:275–283.
 173. Dumontet S, Krovacek K, Baloda SB, Grottoli R, Pasquale V, Vanucci S. 1996. Ecological relationship between *Aeromonas* and *Vibrio* spp. and planktonic copepods in the coastal marine environment in Southern Italy. *Comparative Immunology, Microbiology and Infectious Diseases* [https://doi.org/10.1016/0147-9571\(96\)00012-4](https://doi.org/10.1016/0147-9571(96)00012-4).
 174. Herzig A. 1983. The ecological significance of the relationship between temperature and duration of embryonic development in planktonic freshwater copepods. *Hydrobiologia* <https://doi.org/10.1007/bf00027423>.
 175. Kasuga T. 1986. An ecological study of *Vibrio cholerae* O-1 and *Vibrio cholerae* non O-1, with special regard to behavior in foodstuffs and living shellfish. *Journal of Nippon Medical School* <https://doi.org/10.1272/jnms1923.53.388>.
 176. Martin RG, Rosner JL. 2001. The AraC transcriptional activators. *Curr Opin Microbiol* 4:132–137.
 177. Popoff MY, Le Minor LE. 2015. *Salmonella*. *Bergey's Manual of Systematics of Archaea and Bacteria* <https://doi.org/10.1002/9781118960608.gbm01166>.
 178. Gut AM, Vasiljevic T, Yeager T, Donkor ON. 2018. *Salmonella* infection - prevention and treatment by antibiotics and probiotic yeasts: a review. *Microbiology* 164:1327–1344.
 179. Bula-Rudas FJ, Rathore MH, Maraqa NF. 2015. *Salmonella* Infections in Childhood. *Advances in Pediatrics* <https://doi.org/10.1016/j.yapd.2015.04.005>.
 180. Gomes TAT, Elias WP, Scaletsky ICA, Guth BEC, Rodrigues JF, Piazza RMF, Ferreira LCS, Martinez MB. 2016. Diarrheagenic *Escherichia coli*. *Braz J Microbiol* 47 Suppl 1:3–30.
 181. Tükel C, Akçelik M, de Jong MF, Simsek O, Tsolis RM, Bäumler AJ. 2007. MarT activates expression of the MisL autotransporter protein of *Salmonella enterica* serotype Typhimurium. *J Bacteriol* 189:3922–3926.
 182. Dorsey CW, Laarakker MC, Humphries AD, Weening EH, Bäumler AJ. 2005. *Salmonella enterica* serotype Typhimurium MisL is an intestinal colonization factor that binds fibronectin. *Mol Microbiol* 57:196–211.
 183. Eran Z, Akçelik M, Yazıcı BC, Özcengiz G, Akçelik N. 2020. Regulation of biofilm formation by marT in *Salmonella* Typhimurium. *Molecular Biology Reports* <https://doi.org/10.1007/s11033-020-05573-6>.

184. Morgan JK, Carroll RK, Harro CM, Vendura KW, Shaw LN, Riordan JT. 2016. Global Regulator of Virulence A (GrvA) Coordinates Expression of Discrete Pathogenic Mechanisms in Enterohemorrhagic *Escherichia coli* through Interactions with GadW-GadE. *J Bacteriol* 198:394–409.
185. Aquino P, Honda B, Jaini S, Lyubetskaya A, Hosur K, Chiu JG, Ekladius I, Hu D, Jin L, Sayeg MK, Stettner AI, Wang J, Wong BG, Wong WS, Alexander SL, Ba C, Bensussen SI, Bernstein DB, Braff D, Cha S, Cheng DI, Cho JH, Chou K, Chuang J, Gastler DE, Grasso DJ, Greifenberger JS, Guo C, Hawes AK, Israni DV, Jain SR, Kim J, Lei J, Li H, Li D, Li Q, Mancuso CP, Mao N, Masud SF, Meisel CL, Mi J, Nykyforchyn CS, Park M, Peterson HM, Ramirez AK, Reynolds DS, Rim NG, Saffie JC, Su H, Su WR, Su Y, Sun M, Thommes MM, Tu T, Varongchayakul N, Wagner TE, Weinberg BH, Yang R, Yaroslavsky A, Yoon C, Zhao Y, Zollinger AJ, Stringer AM, Foster JW, Wade J, Raman S, Broude N, Wong WW, Galagan JE. 2017. Coordinated regulation of acid resistance in *Escherichia coli*. *BMC Syst Biol* 11:1.
186. Xue M, Xiao Y, Fu D, Raheem MA, Shao Y, Song X, Tu J, Xue T, Qi K. 2020. Transcriptional Regulator Yqel, Locating at ETT2 Locus, Affects the Pathogenicity of Avian Pathogenic. *Animals (Basel)* 10.
187. Hansen-Wester I, Hensel M. 2001. *Salmonella* pathogenicity islands encoding type III secretion systems. *Microbes Infect* 3:549–559.
188. Hensel M, Shea JE, Bäumlér AJ, Gleeson C, Blattner F, Holden DW. 1997. Analysis of the boundaries of *Salmonella* pathogenicity island 2 and the corresponding chromosomal region of *Escherichia coli* K-12. *J Bacteriol* 179:1105–1111.
189. Shea JE, Hensel M, Gleeson C, Holden DW. 1996. Identification of a virulence locus encoding a second type III secretion system in *Salmonella typhimurium*. *Proc Natl Acad Sci U S A* 93:2593–2597.
190. Blanc-Potard AB, Solomon F, Kayser J, Groisman EA. 1999. The SPI-3 pathogenicity island of *Salmonella enterica*. *J Bacteriol* 181:998–1004.
191. Kyrova K, Stepanova H, Rychlik I, Faldyna M, Volf J. 2012. SPI-1 encoded genes of *Salmonella Typhimurium* influence differential polarization of porcine alveolar macrophages *in vitro*. *BMC Vet Res* 8:115.
192. Raffatellu M, Wilson RP, Chessa D, Andrews-Polymenis H, Tran QT, Lawhon S, Khare S, Adams LG, Bäumlér AJ. 2005. SipA, SopA, SopB, SopD, and SopE2 contribute to *Salmonella enterica* serotype typhimurium invasion of epithelial cells. *Infect Immun* 73:146–154.
193. Ochman H, Soncini FC, Solomon F, Groisman EA. 1996. Identification of a pathogenicity island required for *Salmonella* survival in host cells. *Proc Natl Acad Sci U S A* 93:7800–7804.
194. Walia B, Castaneda FE, Wang L, Kolachala VL, Bajaj R, Roman J, Merlin D, Gewirtz AT, Sitaraman SV. 2004. Polarized fibronectin secretion induced by adenosine regulates bacterial-epithelial interaction in human intestinal epithelial cells. *Biochem J* 382:589–596.
195. Makino S-I, Tobe T, Asakura H, Watarai M, Ikeda T, Takeshi K, Sasakawa C. 2003.

- Distribution of the secondary type III secretion system locus found in enterohemorrhagic *Escherichia coli* O157:H7 isolates among Shiga toxin-producing *E. coli* strains. *J Clin Microbiol* 41:2341–2347.
196. Ren C-P, Chaudhuri RR, Fivian A, Bailey CM, Antonio M, Barnes WM, Pallen MJ. 2004. The ETT2 gene cluster, encoding a second type III secretion system from *Escherichia coli*, is present in the majority of strains but has undergone widespread mutational attrition. *J Bacteriol* 186:3547–3560.
 197. Wang S, Liu X, Xu X, Zhao Y, Yang D, Han X, Tian M, Ding C, Peng D, Yu S. 2016. *Escherichia coli* type III secretion system 2 (ETT2) is widely distributed in avian pathogenic *Escherichia coli* isolates from Eastern China. *Epidemiol Infect* 144:2824–2830.
 198. Hartleib S, Prager R, Hedenström I, Löfdahl S, Tschäpe H. 2003. Prevalence of the new, SPI1-like, pathogenicity island ETT2 among *Escherichia coli*. *International Journal of Medical Microbiology* <https://doi.org/10.1078/1438-4221-00224>.
 199. Ideses D, Gophna U, Paitan Y, Chaudhuri RR, Pallen MJ, Ron EZ. 2005. A degenerate type III secretion system from septicemic *Escherichia coli* contributes to pathogenesis. *J Bacteriol* 187:8164–8171.
 200. McDaniel TK, Jarvis KG, Donnenberg MS, Kaper JB. 1995. A genetic locus of enterocyte effacement conserved among diverse enterobacterial pathogens. *Proc Natl Acad Sci U S A* 92:1664–1668.
 201. Yao Y, Xie Y, Perace D, Zhong Y, Lu J, Tao J, Guo X, Kim KS. 2009. The type III secretion system is involved in the invasion and intracellular survival of *Escherichia coli* K1 in human brain microvascular endothelial cells. *FEMS Microbiol Lett* 300:18–24.
 202. Shulman A, Yair Y, Biran D, Sura T, Otto A, Gophna U, Becher D, Hecker M, Ron EZ. 2018. The *Escherichia coli* Type III Secretion System 2 Has a Global Effect on Cell Surface. *mBio* <https://doi.org/10.1128/mbio.01070-18>.
 203. Morgan JK, Vendura KW, Stevens SM, Riordan JT. 2013. RcsB determines the locus of enterocyte effacement (LEE) expression and adherence phenotype of *Escherichia coli* O157 : H7 spinach outbreak strain TW14359 and coordinates bicarbonate-dependent LEE activation with repression of motility. *Microbiology* 159:2342–2353.
 204. Kailasan Vanaja S, Bergholz TM, Whittam TS. 2009. Characterization of the *Escherichia coli* O157:H7 Sakai GadE regulon. *J Bacteriol* 191:1868–1877.
 205. Tree JJ, Roe AJ, Flockhart A, McAteer SP, Xu X, Shaw D, Mahajan A, Beatson SA, Best A, Lotz S, Woodward MJ, La Ragione R, Murphy KC, Leong JM, Gally DL. 2011. Transcriptional regulators of the GAD acid stress island are carried by effector protein-encoding prophages and indirectly control type III secretion in enterohemorrhagic *Escherichia coli* O157:H7. *Mol Microbiol* 80:1349–1365.
 206. Elliott SJ, Sperandio V, Girón JA, Shin S, Mellies JL, Wainwright L, Hutcheson SW, McDaniel TK, Kaper JB. 2000. The Locus of Enterocyte Effacement (LEE)-Encoded Regulator Controls Expression of Both LEE- and Non-LEE-Encoded Virulence Factors in Enteropathogenic and Enterohemorrhagic *Escherichia coli*. *Infection and Immunity* <https://doi.org/10.1128/iai.68.11.6115-6126.2000>.

207. DiRita VJ, Mekalanos JJ. 1991. Periplasmic interaction between two membrane regulatory proteins, ToxR and ToxS, results in signal transduction and transcriptional activation. *Cell* [https://doi.org/10.1016/0092-8674\(91\)90206-e](https://doi.org/10.1016/0092-8674(91)90206-e).
208. Muse WB, Bender RA. 1998. The *nac* (nitrogen assimilation control) gene from *Escherichia coli*. *J Bacteriol* 180:1166–1173.
209. Wурpel DJ, Beatson SA, Totsika M, Petty NK, Schembri MA. 2013. Chaperone-Usher Fimbriae of *Escherichia coli*. *PLoS ONE* <https://doi.org/10.1371/journal.pone.0052835>.
210. Deditius JA, Felgner S, Spöring I, Kühne C, Frahm M, Rohde M, Weiß S, Erhardt M. 2015. Characterization of Novel Factors Involved in Swimming and Swarming Motility in *Salmonella enterica* Serovar Typhimurium. *PLoS One* 10:e0135351.
211. Bogomolnaya LM, Aldrich L, Ragoza Y, Talamantes M, Andrews KD, McClelland M, Andrews-Polymenis HL. 2014. Identification of novel factors involved in modulating motility of *Salmonella enterica* serotype typhimurium. *PLoS One* 9:e111513.
212. Cuthbertson L, Nodwell JR. 2013. The TetR Family of Regulators. *Microbiology and Molecular Biology Reviews* <https://doi.org/10.1128/mnbr.00018-13>.
213. Ramos JL, Martínez-Bueno M, Molina-Henares AJ, Terán W, Watanabe K, Zhang X, Gallegos MT, Brennan R, Tobes R. 2005. The TetR family of transcriptional repressors. *Microbiol Mol Biol Rev* 69:326–356.
214. Wang Y, Sun M'an, Bao H, White AP. 2013. T3_MM: a Markov model effectively classifies bacterial type III secretion signals. *PLoS One* 8:e58173.
215. Elfenbein JR, Endicott-Yazdani T, Porwollik S, Bogomolnaya LM, Cheng P, Guo J, Zheng Y, Yang H-J, Talamantes M, Shields C, Maple A, Ragoza Y, DeAtley K, Tatsch T, Cui P, Andrews KD, McClelland M, Lawhon SD, Andrews-Polymenis H. 2013. Novel determinants of intestinal colonization of *Salmonella enterica* serotype typhimurium identified in bovine enteric infection. *Infect Immun* 81:4311–4320.
216. Bennett JE, Dolin R, Blaser MJ. 2019. *Mandell, Douglas, and Bennett's Principles and Practice of Infectious Diseases: 2-Volume Set*. Elsevier.
217. Tobbäck E, Decostere A, Hermans K, Haesebrouck F, Chiers K. 2007. *Yersinia ruckeri* infections in salmonid fish. *J Fish Dis* 30:257–268.
218. Kumar G, Menanteau-Ledouble S, Saleh M, El-Matbouli M. 2015. *Yersinia ruckeri*, the causative agent of enteric redmouth disease in fish. *Vet Res* 46:103.
219. Furones MD, Rodgers CJ, Munn CB. 1993. *Yersinia ruckeri*, the causal agent of enteric redmouth disease (ERM) in fish. *Annual Review of Fish Diseases* [https://doi.org/10.1016/0959-8030\(93\)90031-6](https://doi.org/10.1016/0959-8030(93)90031-6).
220. Schilling J, Wagner K, Seekircher S, Greune L, Humberg V, Schmidt MA, Heusipp G. 2010. Transcriptional activation of the *tad* type IVb pilus operon by PypB in *Yersinia enterocolitica*. *J Bacteriol* 192:3809–3821.
221. Quinn JD, Weening EH, Miner TA, Miller VL. 2019. Temperature Control of Expression by *PsaE* and *PsaF* in *Yersinia pestis*. *J Bacteriol* 201.

222. Quinn JD, Weening EH, Miner TA, Miller VL. 2019. Temperature Control of *psaA* Expression by *PsaE* and *PsaF* in *Yersinia pestis*. *Journal of Bacteriology* <https://doi.org/10.1128/jb.00217-19>.
223. Li P, Wang X, Smith C, Shi Y, Wade JT, Sun W. 2021. Dissecting Locus Regulation in *Yersinia pestis*. *J Bacteriol* 203:e0023721.
224. Yang Y, Isberg RR. 1997. Transcriptional regulation of the *Yersinia pseudotuberculosis* pH6 antigen adhesin by two envelope-associated components. *Mol Microbiol* 24:499–510.
225. Price SB, Freeman MD, Yeh KS. 1995. Transcriptional analysis of the *Yersinia pestis* pH 6 antigen gene. *J Bacteriol* 177:5997–6000.
226. Lindler LE, Klempner MS, Straley SC. 1990. *Yersinia pestis* pH 6 antigen: genetic, biochemical, and virulence characterization of a protein involved in the pathogenesis of bubonic plague. *Infect Immun* 58:2569–2577.
227. Huang X-Z, Lindler LE. 2004. The pH 6 antigen is an antiphagocytic factor produced by *Yersinia pestis* independent of *Yersinia* outer proteins and capsule antigen. *Infect Immun* 72:7212–7219.
228. Zav'yalov VP, Abramov VM, Cherepanov PG, Spirina GV, Chernovskaya TV, Vasiliev AM, Zav'yalova GA. 1996. pH6 antigen (*PsaA* protein) of *Yersinia pestis*, a novel bacterial Fc-receptor. *FEMS Immunol Med Microbiol* 14:53–57.
229. Lindler LE, Tall BD. 1993. *Yersinia pestis* pH 6 antigen forms fimbriae and is induced by intracellular association with macrophages. *Molecular Microbiology* <https://doi.org/10.1111/j.1365-2958.1993.tb01575.x>.
230. Quinn JD, Weening EH, Miller VL. 2021. *PsaF* Is a Membrane-Localized pH Sensor That Regulates *psaA* Expression in *Yersinia pestis*. *Journal of Bacteriology* <https://doi.org/10.1128/jb.00165-21>.
231. Iriarte M, Vanooteghem JC, Delor I, Díaz R, Knutton S, Cornelis GR. 1993. The Myf fibrillae of *Yersinia enterocolitica*. *Mol Microbiol* 9:507–520.
232. Levine MM, Ristaino P, Marley G, Smyth C, Knutton S, Boedeker E, Black R, Young C, Clements ML, Cheney C. 1984. Coli surface antigens 1 and 3 of colonization factor antigen II-positive enterotoxigenic *Escherichia coli*: morphology, purification, and immune responses in humans. *Infect Immun* 44:409–420.
233. Iriarte M, Cornelis GR. 1995. MyfF, an element of the network regulating the synthesis of fibrillae in *Yersinia enterocolitica*. *Journal of Bacteriology* <https://doi.org/10.1128/jb.177.3.738-744.1995>.
234. Cascales D, Guijarro JA, García-Torrico AI, Méndez J. 2017. Comparative genome analysis reveals important genetic differences among serotype O1 and serotype O2 strains of *Y. ruckeri* and provides insights into host adaptation and virulence. *MicrobiologyOpen* <https://doi.org/10.1002/mbo3.460>.
235. Emmerth M, Goebel W, Miller SI, Hueck CJ. 1999. Genomic Subtraction Identifies *Salmonella typhimurium* Prophages, F-Related Plasmid Sequences, and a Novel Fimbrial

- Operon, *stf*, Which Are Absent in *Salmonella typhi*. *Journal of Bacteriology*
<https://doi.org/10.1128/jb.181.18.5652-5661.1999>.
236. Cornelis GR, Boland A, Boyd AP, Geuijen C, Iriarte M, Neyt C, Sory MP, Stainier I. 1998. The virulence plasmid of *Yersinia*, an antihost genome. *Microbiol Mol Biol Rev* 62:1315–1352.
237. Foultier B, Troisfontaines P, Müller S, Opperdoes FR, Cornelis GR. 2002. Characterization of the *ysa* pathogenicity locus in the chromosome of *Yersinia enterocolitica* and phylogeny analysis of type III secretion systems. *J Mol Evol* 55:37–51.
238. Haller JC, Carlson S, Pederson KJ, Pierson DE. 2000. A chromosomally encoded type III secretion pathway in *Yersinia enterocolitica* is important in virulence. *Mol Microbiol* 36:1436–1446.
239. Liu T, Wang K-Y, Wang J, Chen D-F, Huang X-L, Ouyang P, Geng Y, He Y, Zhou Y, Min J. 2016. Genome Sequence of the Fish Pathogen *Yersinia ruckeri* SC09 Provides Insights into Niche Adaptation and Pathogenic Mechanism. *Int J Mol Sci* 17:557.
240. Holzapfel WHN, Wood BJB. 2012. *The Genera of Lactic Acid Bacteria*. Springer.
241. 2017. *Biology of Microorganisms on Grapes, in Must and in Wine*
<https://doi.org/10.1007/978-3-319-60021-5>.
242. Noda M, Miyauchi R, Danshiitsoodol N, Matoba Y, Kumagai T, Sugiyama M. 2018. Expression of Genes Involved in Bacteriocin Production and Self-Resistance in *Lactobacillus brevis* 174A Is Mediated by Two Regulatory Proteins. *Appl Environ Microbiol* 84.
243. Suárez C, Espariz M, Blancato VS, Magni C. 2013. Expression of the Agmatine Deiminase Pathway in *Enterococcus faecalis* Is Activated by the *AguR* Regulator and Repressed by *CcpA* and *PTSMAN* Systems. *PLoS ONE* <https://doi.org/10.1371/journal.pone.0076170>.
244. Růžičková M, Vítězová M, Kushkevych I. 2020. The characterization of *Enterococcus* genus: resistance mechanisms and inflammatory bowel disease. *Open Medicine*
<https://doi.org/10.1515/med-2020-0032>.
245. O'Donovan CA, Fan-Havard P, Tecson-Tumang FT, Smith SM, Eng RH. 1994. Enteric eradication of vancomycin-resistant *Enterococcus faecium* with oral bacitracin. *Diagn Microbiol Infect Dis* 18:105–109.
246. Charlebois A, Jalbert L-A, Harel J, Masson L, Archambault M. 2012. Characterization of genes encoding for acquired bacitracin resistance in *Clostridium perfringens*. *PLoS One* 7:e44449.
247. Darnell RL, Nakatani Y, Knottenbelt MK, Gebhard S, Cook GM. 2019. Functional characterization of *BcrR*: a one-component transmembrane signal transduction system for bacitracin resistance. *Microbiology* 165:475–487.
248. Gauntlett JC, Gebhard S, Keis S, Manson JM, Pos KM, Cook GM. 2008. Molecular analysis of *BcrR*, a membrane-bound bacitracin sensor and DNA-binding protein from *Enterococcus faecalis*. *J Biol Chem* 283:8591–8600.

249. Matos R, Pinto VV, Ruivo M, de Fátima Silva Lopes M. 2009. Study on the dissemination of the bcrABDR cluster in *Enterococcus* spp. reveals that the BcrAB transporter is sufficient to confer high-level bacitracin resistance. *International Journal of Antimicrobial Agents* <https://doi.org/10.1016/j.ijantimicag.2009.02.008>.
250. Dufour M, Manson JM, Bremer PJ, Dufour J-P, Cook GM, Simmonds RS. 2007. Characterization of monolaurin resistance in *Enterococcus faecalis*. *Appl Environ Microbiol* 73:5507–5515.
251. Tremblay C-L, Archambault M. 2013. Interference in pheromone-responsive conjugation of a high-level bacitracin resistant *Enterococcus faecalis* plasmid of poultry origin. *Int J Environ Res Public Health* 10:4245–4260.
252. Shang Y, Li D, Shan X, Schwarz S, Zhang S-M, Chen Y-X, Ouyang W, Du X-D. 2019. Analysis of two pheromone-responsive conjugative multiresistance plasmids carrying the novel mobile *optrA* locus from *Enterococcus faecalis*. *Infection and Drug Resistance* <https://doi.org/10.2147/idr.s206295>.
253. Noda M, Miyauchi R, Danshiitsoodol N, Higashikawa F, Kumagai T, Matoba Y, Sugiyama M. 2015. Characterization and Mutational Analysis of a Two-Polypeptide Bacteriocin Produced by Citrus Iyo-Derived *Lactobacillus brevis* 174A. *Biological & Pharmaceutical Bulletin* <https://doi.org/10.1248/bpb.b15-00505>.
254. Jack RW, Tagg JR, Ray B. 1995. Bacteriocins of gram-positive bacteria. *Microbiological reviews* <https://doi.org/10.1128/mubr.59.2.171-200.1995>.
255. David FL-R, Tania EVC, De la Fuente-Salcido Norma M. 2016. Bacteriocins of Gram-positive bacteria: Features and biotherapeutic approach. *African Journal of Microbiology Research* <https://doi.org/10.5897/ajmr2016.8376>.
256. Griswold AR, Chen Y-YM, Burne RA. 2004. Analysis of an agmatine deiminase gene cluster in *Streptococcus mutans* UA159. *J Bacteriol* 186:1902–1904.
257. Liu Y, Zeng L, Burne RA. 2009. *AguR* Is Required for Induction of the *Streptococcus mutans* Agmatine Deiminase System by Low pH and Agmatine. *Applied and Environmental Microbiology* <https://doi.org/10.1128/aem.02145-08>.
258. Del Rio B, Linares D, Ladero V, Redruello B, Fernandez M, Martin MC, Alvarez MA. 2016. Putrescine biosynthesis in *Lactococcus lactis* is transcriptionally activated at acidic pH and counteracts acidification of the cytosol. *Int J Food Microbiol* 236:83–89.
259. Linares DM, del Rio B, Redruello B, Ladero V, Cruz Martin M, de Jong A, Kuipers OP, Fernandez M, Alvarez MA. 2015. *AguR*, a Transmembrane Transcription Activator of the Putrescine Biosynthesis Operon in *Lactococcus lactis*, Acts in Response to the Agmatine Concentration. *Applied and Environmental Microbiology* <https://doi.org/10.1128/aem.00959-15>.
260. Del Rio B, Linares DM, Redruello B, Martin MC, Fernandez M, de Jong A, Kuipers OP, Ladero V, Alvarez MA. 2015. Transcriptomic profile of *aguR* deletion mutant of *Lactococcus lactis* subsp. *cremoris* CECT 8666. *Genom Data* 6:228–230.
261. Fabia R, Ar'Rajab A, Johansson ML, Willén R, Andersson R, Molin G, Bengmark S. 1993.

- The effect of exogenous administration of *Lactobacillus reuteri* R2LC and oat fiber on acetic acid-induced colitis in the rat. *Scand J Gastroenterol* 28:155–162.
262. Madsen KL, Doyle JS, Jewell LD, Tavernini MM, Fedorak RN. 1999. *Lactobacillus* species prevents colitis in interleukin 10 gene-deficient mice. *Gastroenterology* 116:1107–1114.
263. Mimura T. 2004. Once daily high dose probiotic therapy (VSL#3) for maintaining remission in recurrent or refractory pouchitis. *Gut* <https://doi.org/10.1136/gut.53.1.108>.
264. Rembacken BJ, Snelling AM, Hawkey PM, Chalmers DM, Axon AT. 1999. Non-pathogenic *Escherichia coli* versus mesalazine for the treatment of ulcerative colitis: a randomised trial. *Lancet* 354:635–639.
265. Kalliomäki M, Antoine J-M, Herz U, Rijkers GT, Wells JM, Mercenier A. 2010. Guidance for substantiating the evidence for beneficial effects of probiotics: prevention and management of allergic diseases by probiotics. *J Nutr* 140:713S–21S.
266. Dong H, Rowland I, Yaqoob P. 2012. Comparative effects of six probiotic strains on immune function *in vitro*. *Br J Nutr* 108:459–470.
267. van Hemert S, Meijerink M, Molenaar D, Bron PA, de Vos P, Kleerebezem M, Wells JM, Marco ML. 2010. Identification of *Lactobacillus plantarum* genes modulating the cytokine response of human peripheral blood mononuclear cells. *BMC Microbiol* 10:293.
268. Larché M, Robinson DS, Barry Kay A. 2003. The role of T lymphocytes in the pathogenesis of asthma. *Journal of Allergy and Clinical Immunology* <https://doi.org/10.1067/mai.2003.169>.
269. Smelt MJ, de Haan BJ, Bron PA, van Swam I, Meijerink M, Wells JM, Faas MM, de Vos P. 2013. Probiotics can generate FoxP3 T-cell responses in the small intestine and simultaneously inducing CD4 and CD8 T cell activation in the large intestine. *PLoS One* 8:e68952.
270. Smelt MJ, de Haan BJ, Bron PA, van Swam I, Meijerink M, Wells JM, Kleerebezem M, Faas MM, de Vos P. 2013. The impact of *Lactobacillus plantarum* WCFS1 teichoic acid D-alanylation on the generation of effector and regulatory T-cells in healthy mice. *PLoS One* 8:e63099.
271. Grangette C, Nutten S, Palumbo E, Morath S, Hermann C, Dewulf J, Pot B, Hartung T, Hols P, Mercenier A. 2005. Enhanced antiinflammatory capacity of a *Lactobacillus plantarum* mutant synthesizing modified teichoic acids. *Proc Natl Acad Sci U S A* 102:10321–10326.
272. Yeo W-S, Anokwute C, Marcadis P, Levitan M, Ahmed M, Bae Y, Kim K, Kostrominova T, Liu Q, Bae T. 2020. A Membrane-Bound Transcription Factor is Proteolytically Regulated by the AAA Protease FtsH in *Staphylococcus aureus*. *Journal of Bacteriology* <https://doi.org/10.1128/jb.00019-20>.
273. Law-Brown J, Meyers PR. 2003. *Enterococcus phoeniculicola* sp. nov., a novel member of the enterococci isolated from the uropygial gland of the Red-billed Woodhoopoe, *Phoeniculus purpureus*. *International Journal of Systematic and Evolutionary Microbiology* <https://doi.org/10.1099/ijs.0.02334-0>.

274. Law-Brown J. 2001. Chemical Defence in the Red-billed Woodhoopoe: *Phoeniculus Purpureus*.
275. Asnani MV, Ramachandran AV. 1993. Roles of adrenal and gonadal steroids and season in uropygial gland function in male pigeons, *Columba livia*. *Gen Comp Endocrinol* 92:213–224.
276. Ligon JD, David Ligon J, Ligon SH. 1978. Communal breeding in green woodhoopoes as a case for reciprocity. *Nature* <https://doi.org/10.1038/276496a0>.
277. Jacob J, Ziswiler V. 1982. THE UROPYGIAL GLAND. *Avian Biology* <https://doi.org/10.1016/b978-0-12-249406-2.50013-7>.
278. Levy EM, Strain PM. 1982. The composition of the preen gland waxes of some marine birds: A word of caution for chemotaxonomists. *Comparative Biochemistry and Physiology Part B: Comparative Biochemistry* [https://doi.org/10.1016/0305-0491\(82\)90043-8](https://doi.org/10.1016/0305-0491(82)90043-8).
279. Shahidi F, Naczki M. 2003. Phenolics in Food and Nutraceuticals <https://doi.org/10.1201/9780203508732>.
280. Nowell VJ, Kropinski AM, Songer JG, MacInnes JI, Parreira VR, Prescott JF. 2012. Genome sequencing and analysis of a type A *Clostridium perfringens* isolate from a case of bovine clostridial abomasitis. *PLoS One* 7:e32271.
281. Bakker HC den, den Bakker HC, Bowen BM, Rodriguez-Rivera LD, Wiedmann M. 2012. FSL J1-208, a Virulent Uncommon Phylogenetic Lineage IV *Listeria monocytogenes* Strain with a Small Chromosome Size and a Putative Virulence Plasmid Carrying Internalin-Like Genes. *Applied and Environmental Microbiology* <https://doi.org/10.1128/aem.06969-11>.
282. Rychli K, Müller A, Zaiser A, Schoder D, Allerberger F, Wagner M, Schmitz-Esser S. 2014. Genome sequencing of *Listeria monocytogenes* “Quargel” listeriosis outbreak strains reveals two different strains with distinct *in vitro* virulence potential. *PLoS One* 9:e89964.
283. Götz F, Bannerman T, Schleifer K-H. 2006. The Genera *Staphylococcus* and *Micrococcus*. *The Prokaryotes* https://doi.org/10.1007/0-387-30744-3_1.
284. Jenul C, Horswill AR. 2019. Regulation of *Staphylococcus aureus* Virulence. *Gram-Positive Pathogens* <https://doi.org/10.1128/9781683670131.ch41>.
285. Yeo W-S, Anokwute C, Marcadis P, Levitan M, Ahmed M, Bae Y, Kim K, Kostrominova T, Liu Q, Bae T. 2020. A Membrane-Bound Transcription Factor is Proteolytically Regulated by the AAA+ Protease FtsH in *Staphylococcus aureus*. *J Bacteriol* 202.
286. Ito K, Akiyama Y. 2005. Cellular functions, mechanism of action, and regulation of FtsH protease. *Annu Rev Microbiol* 59:211–231.
287. Herman C, Prakash S, Lu CZ, Matouschek A, Gross CA. 2003. Lack of a robust unfoldase activity confers a unique level of substrate specificity to the universal AAA protease FtsH. *Mol Cell* 11:659–669.
288. Liu Q, Hu M, Yeo W-S, He L, Li T, Zhu Y, Meng H, Wang Y, Lee H, Liu X, Li M, Bae T. 2020. Author Correction: Rewiring of the FtsH regulatory network by a single nucleotide change in *saeS* of *Staphylococcus aureus*. *Sci Rep* 10:17555.

289. Pei J, Mitchell DA, Dixon JE, Grishin NV. 2011. Expansion of type II CAAX proteases reveals evolutionary origin of γ -secretase subunit APH-1. *J Mol Biol* 410:18–26.
290. Dolence JM, Steward LE, Dolence EK, Wong DH, Poulter CD. 2000. Studies with recombinant *Saccharomyces cerevisiae* CaaX prenyl protease Rce1p. *Biochemistry* 39:4096–4104.
291. Kjos M, Snipen L, Salehian Z, Nes IF, Diep DB. 2010. The abi proteins and their involvement in bacteriocin self-immunity. *J Bacteriol* 192:2068–2076.
292. Diep DB, Håvarstein LS, Nes IF. 1996. Characterization of the locus responsible for the bacteriocin production in *Lactobacillus plantarum* C11. *J Bacteriol* 178:4472–4483.
293. Rojo-Bezares B, Sáenz Y, Navarro L, Jiménez-Díaz R, Zarazaga M, Ruiz-Larrea F, Torres C. 2008. Characterization of a new organization of the plantaric locus in the inducible bacteriocin-producing *Lactobacillus plantarum* J23 of grape must origin. *Arch Microbiol* 189:491–499.
294. Zuckerman JN, Rombo L, Fisch A. 2007. The true burden and risk of cholera: implications for prevention and control. *The Lancet Infectious Diseases*.
295. Baker-Austin C, Oliver JD, Alam M, Ali A, Waldor MK, Qadri F, Martinez-Urtaza J. 2018. *Vibrio* spp. infections. *Nature Reviews Disease Primers*.
296. Kim HB, Wang M, Ahmed S, Park CH, LaRocque RC, Faruque ASG, Salam MA, Khan WA, Qadri F, Calderwood SB, Jacoby GA, Hooper DC. 2010. Transferable quinolone resistance in *Vibrio cholerae*. *Antimicrob Agents Chemother* 54:799–803.
297. Glass RI, Huq MI, Lee JV, Threlfall EJ, Khan MR, Alim AR, Rowe B, Gross RJ. 1983. Plasmid-borne multiple drug resistance in *Vibrio cholerae* serogroup O1, biotype El Tor: evidence for a point-source outbreak in Bangladesh. *J Infect Dis* 147:204–209.
298. Pang B, Du P, Zhou Z, Diao B, Cui Z, Zhou H, Kan B. 2016. The Transmission and Antibiotic Resistance Variation in a Multiple Drug Resistance Clade of *Vibrio cholerae* Circulating in Multiple Countries in Asia. *PLOS ONE*.
299. Ramakrishna BS, Venkataraman S, Srinivasan P, Dash P, Young GP, Binder HJ. 2000. Amylase-resistant starch plus oral rehydration solution for cholera. *N Engl J Med* 342:308–313.
300. Krishna BVS, Patil AB, Chandrasekhar MR. 2006. Fluoroquinolone-resistant *Vibrio cholerae* isolated during a cholera outbreak in India. *Transactions of the Royal Society of Tropical Medicine and Hygiene*.
301. Nielsen AT, Dolganov NA, Rasmussen T, Otto G, Miller MC, Felt SA, Torrelles S, Schoolnik GK. 2010. A bistable switch and anatomical site control *Vibrio cholerae* virulence gene expression in the intestine. *PLoS Pathog* 6:e1001102.
302. Haas BL, Matson JS, DiRita VJ, Biteen JS. 2015. Single-molecule tracking in live *Vibrio cholerae* reveals that ToxR recruits the membrane-bound virulence regulator TcpP to the *toxT* promoter. *Mol Microbiol* 96:4–13.
303. Haas BL, Matson JS, DiRita VJ, Biteen JS. 2014. Imaging live cells at the nanometer-scale

with single-molecule microscopy: obstacles and achievements in experiment optimization for microbiology. *Molecules* 19:12116–12149.

304. Hanson BR, Lowe BA, Neely MN. 2011. Membrane topology and DNA-binding ability of the Streptococcal CpsA protein. *J Bacteriol* 193:411–420.
305. Cieslewicz MJ, Kasper DL, Wang Y, Wessels MR. 2001. Functional analysis in type Ia group B Streptococcus of a cluster of genes involved in extracellular polysaccharide production by diverse species of streptococci. *J Biol Chem* 276:139–146.
306. Gebhard S, Gaballa A, Helmann JD, Cook GM. 2009. Direct stimulus perception and transcription activation by a membrane-bound DNA binding protein. *Mol Microbiol* 73:482–491.
307. Hubbard TP, Chao MC, Abel S, Blondel CJ, Abel Zur Wiesch P, Zhou X, Davis BM, Waldor MK. 2016. Genetic analysis of *Vibrio parahaemolyticus* intestinal colonization. *Proc Natl Acad Sci U S A* 113:6283–6288.
308. Sobetzko P, Travers A, Muskhelishvili G. 2012. Gene order and chromosome dynamics coordinate spatiotemporal gene expression during the bacterial growth cycle. *Proceedings of the National Academy of Sciences*.
309. Browning DF, Grainger DC, Busby SJ. 2010. Effects of nucleoid-associated proteins on bacterial chromosome structure and gene expression. *Curr Opin Microbiol* 13:773–780.
310. Liu LF, Wang JC. 1987. Supercoiling of the DNA template during transcription. *Proceedings of the National Academy of Sciences* <https://doi.org/10.1073/pnas.84.20.7024>.
311. Harrington EW, Trun NJ. 1997. Unfolding of the bacterial nucleoid both *in vivo* and *in vitro* as a result of exposure to camphor. *J Bacteriol* 179:2435–2439.
312. Dorman CJ. 1991. DNA supercoiling and environmental regulation of gene expression in pathogenic bacteria. *Infection and Immunity*.
313. Badrinarayanan A, Le TBK, Laub MT. 2015. Bacterial Chromosome Organization and Segregation. *Annual Review of Cell and Developmental Biology*.
314. Brameyer S, Rösch TC, El Andari J, Hoyer E, Schwarz J, Graumann PL, Jung K. 2019. DNA-binding directs the localization of a membrane-integrated receptor of the ToxR family. *Commun Biol* 2:4.
315. Valens M, Penaud S, Rossignol M, Cornet F, Boccard F. 2004. Macrod domain organization of the *Escherichia coli* chromosome. *The EMBO Journal*.
316. Cagliero C, Grand RS, Jones MB, Jin DJ, O'Sullivan JM. 2013. Genome conformation capture reveals that the *Escherichia coli* chromosome is organized by replication and transcription. *Nucleic Acids Res* 41:6058–6071.
317. Le TBK, Imakaev MV, Mirny LA, Laub MT. 2013. High-resolution mapping of the spatial organization of a bacterial chromosome. *Science* 342:731–734.
318. Karslake JD, Donarski ED, Shelby SA, Demey LM, DiRita VJ, Veatch SL, Biteen JS. 2020. SMAUG: Analyzing single-molecule tracks with nonparametric Bayesian statistics.

Methods.

319. 2016. LB Liquid Medium. Cold Spring Harbor Protocols
<https://doi.org/10.1101/pdb.rec090928>.
320. Skorupski K, Taylor RK. 1996. Positive selection vectors for allelic exchange. *Gene*
[https://doi.org/10.1016/0378-1119\(95\)00793-8](https://doi.org/10.1016/0378-1119(95)00793-8).
321. Amin Marashi SM, Rajabnia R, Imani Fooladi AA, Hojati Z, Moghim S, Nasr Esfahani B. 2013. Determination of *ctxAB* expression in *Vibrio cholerae* Classical and El Tor strains using Real-Time PCR. *Int J Mol Cell Med* 2:9–13.
322. Schmittgen TD, Livak KJ. 2008. Analyzing real-time PCR data by the comparative C(T) method. *Nat Protoc* 3:1101–1108.
323. Isaacoff BP, Li Y, Lee SA, Biteen JS. 2019. SMALL-LABS: Measuring Single-Molecule Intensity and Position in Obscuring Backgrounds. *Biophys J* 116:975–982.
324. Liao Y, Schroeder JW, Gao B, Simmons LA, Biteen JS. 2015. Single-molecule motions and interactions in live cells reveal target search dynamics in mismatch repair. *Proc Natl Acad Sci U S A* 112:E6898–906.
325. Munkres J. 1957. Algorithms for the Assignment and Transportation Problems. *Journal of the Society for Industrial and Applied Mathematics*.
326. Park N-Y, Kim IH, Wen Y, Lee K-W, Lee S, Kim J-A, Jung K-H, Lee K-H, Kim K-S. 2019. Multi-Factor Regulation of the Master Modulator LeuO for the Cyclic-(Phe-Pro) Signaling Pathway in *Vibrio vulnificus*. *Sci Rep* 9:20135.
327. Bina XR, Taylor DL, Vikram A, Ante VM, Bina JE. 2013. *Vibrio cholerae* ToxR downregulates virulence factor production in response to cyclo(Phe-Pro). *MBio* 4:e00366–13.
328. Ramadurai S, Holt A, Krasnikov V, van den Bogaart G, Killian JA, Poolman B. 2009. Lateral diffusion of membrane proteins. *J Am Chem Soc* 131:12650–12656.
329. Lucena D, Mauri M, Schmidt F, Eckhardt B, Graumann PL. 2018. Microdomain formation is a general property of bacterial membrane proteins and induces heterogeneity of diffusion patterns. *BMC Biol* 16:97.
330. Lorent JH, Diaz-Rohrer B, Lin X, Spring K, Gorfe AA, Levental KR, Levental I. 2018. Author Correction: Structural determinants and functional consequences of protein affinity for membrane rafts. *Nat Commun* 9:1805.
331. Bina J, Zhu J, Dziejman M, Faruque S, Calderwood S, Mekalanos J. 2003. ToxR regulon of *Vibrio cholerae* and its expression in vibrios shed by cholera patients. *Proceedings of the National Academy of Sciences*.
332. Angelichio MJ, Spector J, Waldor MK, Camilli A. 1999. *Vibrio cholerae* Intestinal Population Dynamics in the Suckling Mouse Model of Infection. *Infection and Immunity*
<https://doi.org/10.1128/iai.67.8.3733-3739.1999>.
333. Millet YA, Alvarez D, Ringgaard S, von Andrian UH, Davis BM, Waldor MK. 2014. Insights

into *Vibrio cholerae* intestinal colonization from monitoring fluorescently labeled bacteria. *PLoS Pathog* 10:e1004405.

334. Taylor RK, Miller VL, Furlong DB, Mekalanos JJ. 1987. Use of *phoA* gene fusions to identify a pilus colonization factor coordinately regulated with cholera toxin. *Proc Natl Acad Sci U S A* 84:2833–2837.
335. Nelson EJ, Harris JB, Glenn Morris J, Calderwood SB, Camilli A. 2009. Cholera transmission: the host, pathogen and bacteriophage dynamic. *Nature Reviews Microbiology* <https://doi.org/10.1038/nrmicro2204>.
336. Camilli A, Beattie DT, Mekalanos JJ. 1994. Use of genetic recombination as a reporter of gene expression. *Proc Natl Acad Sci U S A* 91:2634–2638.
337. Nielsen AT, Dolganov NA, Rasmussen T, Otto G, Miller MC, Felt SA, Torreilles S, Schoolnik GK. 2010. A bistable switch and anatomical site control *Vibrio cholerae* virulence gene expression in the intestine. *PLoS Pathog* 6:e1001102.
338. Higgins DE, Nazareno E, DiRita VJ. 1992. The virulence gene activator ToxT from *Vibrio cholerae* is a member of the AraC family of transcriptional activators. *Journal of Bacteriology* <https://doi.org/10.1128/jb.174.21.6974-6980.1992>.
339. Higgins DE, DiRita VJ. 1994. Transcriptional control of *toxT*, a regulatory gene in the ToxR regulon of *Vibrio cholerae*. *Mol Microbiol* 14:17–29.
340. Krukoni ES, Yu RR, Dirita VJ. 2000. The *Vibrio cholerae* ToxR/TcpP/ToxT virulence cascade: distinct roles for two membrane-localized transcriptional activators on a single promoter. *Mol Microbiol* 38:67–84.
341. DiRita VJ, Parsot C, Jander G, Mekalanos JJ. 1991. Regulatory cascade controls virulence in *Vibrio cholerae*. *Proc Natl Acad Sci U S A* 88:5403–5407.
342. Miller VL, Taylor RK, Mekalanos JJ. 1987. Cholera toxin transcriptional activator *toxR* is a transmembrane DNA binding protein. *Cell* 48:271–279.
343. Crawford JA, Krukoni ES, DiRita VJ. 2003. Membrane localization of the ToxR winged-helix domain is required for TcpP-mediated virulence gene activation in *Vibrio cholerae*. *Mol Microbiol* 47:1459–1473.
344. Hase CC, Mekalanos JJ. 1998. TcpP protein is a positive regulator of virulence gene expression in *Vibrio cholerae*. *Proceedings of the National Academy of Sciences* <https://doi.org/10.1073/pnas.95.2.730>.
345. Carroll PA, Tashima KT, Rogers MB, DiRita VJ, Calderwood SB. 1997. Phase variation in *tcpH* modulates expression of the ToxR regulon in *Vibrio cholerae*. *Mol Microbiol* 25:1099–1111.
346. Martínez-Hackert E, Stock AM. 1997. Structural relationships in the OmpR family of winged-helix transcription factors 1 Edited by M. Gottesman. *Journal of Molecular Biology* <https://doi.org/10.1006/jmbi.1997.1065>.
347. Krukoni ES, DiRita VJ. 2003. DNA binding and ToxR responsiveness by the wing domain of TcpP, an activator of virulence gene expression in *Vibrio cholerae*. *Mol Cell* 12:157–165.

348. Goss TJ, Seaborn CP, Gray MD, Krukoni ES. 2010. Identification of the TcpP-Binding Site in the *toxT* Promoter of *Vibrio cholerae* and the Role of ToxR in TcpP-Mediated Activation. *Infection and Immunity* <https://doi.org/10.1128/iai.00566-10>.
349. Kovacicova G, Skorupski K. 2002. Regulation of virulence gene expression in *Vibrio cholerae* by quorum sensing: HapR functions at the *aphA* promoter. *Mol Microbiol* 46:1135–1147.
350. Liu Z, Yang M, Peterfreund GL, Tsou AM, Selamoglu N, Daldal F, Zhong Z, Kan B, Zhu J. 2011. *Vibrio cholerae* anaerobic induction of virulence gene expression is controlled by thiol-based switches of virulence regulator AphB. *Proc Natl Acad Sci U S A* 108:810–815.
351. Teoh WP, Matson JS, DiRita VJ. 2015. Regulated intramembrane proteolysis of the virulence activator TcpP in *Vibrio cholerae* is initiated by the tail-specific protease (Tsp). *Mol Microbiol* 97:822–831.
352. Matson JS, DiRita VJ. 2005. Degradation of the membrane-localized virulence activator TcpP by the YaeL protease in *Vibrio cholerae*. *Proc Natl Acad Sci U S A* 102:16403–16408.
353. Brown MS, Ye J, Rawson RB, Goldstein JL. 2000. Regulated intramembrane proteolysis: a control mechanism conserved from bacteria to humans. *Cell* 100:391–398.
354. Peñas ADL, De Las Peñas A, Connolly L, Gross CA. 1997. The σE -mediated response to extracytoplasmic stress in *Escherichia coli* is transduced by RseA and RseB, two negative regulators of σE . *Molecular Microbiology* <https://doi.org/10.1046/j.1365-2958.1997.3611718.x>.
355. Alba BM. 2002. DegS and YaeL participate sequentially in the cleavage of RseA to activate the sigma E-dependent extracytoplasmic stress response. *Genes & Development* <https://doi.org/10.1101/gad.1008902>.
356. Dartigalongue C, Missiakas D, Raina S. 2001. Characterization of the *Escherichia coli* σE Regulon. *Journal of Biological Chemistry* <https://doi.org/10.1074/jbc.m100464200>.
357. Rhodius VA, Suh WC, Nonaka G, West J, Gross CA. 2005. Conserved and Variable Functions of the σE Stress Response in Related Genomes. *PLoS Biology* <https://doi.org/10.1371/journal.pbio.0040002>.
358. Zhou R, Kroos L. 2005. Serine proteases from two cell types target different components of a complex that governs regulated intramembrane proteolysis of pro- σK during *Bacillus subtilis* development. *Mol Microbiol* 58:835–846.
359. Wakeley PR, Dorazi R, Hoa NT, Bowyer JR, Cutting SM. 2002. Proteolysis of SpoIVB is a critical determinant in signalling of Pro- σK processing in *Bacillus subtilis*. *Molecular Microbiology* <https://doi.org/10.1046/j.1365-2958.2000.01946.x>.
360. Kroos L, Yu YT. 2000. Regulation of sigma factor activity during *Bacillus subtilis* development. *Curr Opin Microbiol* 3:553–560.
361. Cezairliyan BO, Sauer RT. 2007. Inhibition of regulated proteolysis by RseB. *Proc Natl Acad Sci U S A* 104:3771–3776.
362. Wollmann P, Zeth K. 2007. The structure of RseB: a sensor in periplasmic stress response

- of *E. coli*. *J Mol Biol* 372:927–941.
363. Wilken C, Kitzing K, Kurzbauer R, Ehrmann M, Clausen T. 2004. Crystal structure of the DegS stress sensor: How a PDZ domain recognizes misfolded protein and activates a protease. *Cell* 117:483–494.
364. Zhou R, Kroos L. 2004. BofA protein inhibits intramembrane proteolysis of pro-sigmaK in an intercompartmental signaling pathway during *Bacillus subtilis* sporulation. *Proc Natl Acad Sci U S A* 101:6385–6390.
365. Resnekov O. 1999. Role of the sporulation protein BofA in regulating activation of the *Bacillus subtilis* developmental transcription factor sigmaK. *J Bacteriol* 181:5384–5388.
366. Ricca E, Cutting S, Losick R. 1992. Characterization of bofA, a gene involved in intercompartmental regulation of pro-sigma K processing during sporulation in *Bacillus subtilis*. *Journal of Bacteriology* <https://doi.org/10.1128/jb.174.10.3177-3184.1992>.
367. Bramkamp M, Lopez D. 2015. Exploring the existence of lipid rafts in bacteria. *Microbiol Mol Biol Rev* 79:81–100.
368. Toledo A, Huang Z, Coleman JL, London E, Benach JL. 2018. Lipid rafts can form in the inner and outer membranes of *Borrelia burgdorferi* and have different properties and associated proteins. *Mol Microbiol* 108:63–76.
369. Huang Z, Zhang X-S, Blaser MJ, London E. 2019. *Helicobacter pylori* lipids can form ordered membrane domains (rafts). *Biochim Biophys Acta Biomembr* 1861:183050.
370. Koch G, Wermser C, Acosta IC, Kricks L, Stengel ST, Yepes A, Lopez D. 2017. Attenuating *Staphylococcus aureus* Virulence by Targeting Flotillin Protein Scaffold Activity. *Cell Chem Biol* 24:845–857.e6.
371. Lopez D, Kolter R. 2010. Functional microdomains in bacterial membranes. *Genes & Development* <https://doi.org/10.1101/gad.1945010>.
372. Sezgin E, Levental I, Mayor S, Eggeling C. 2017. The mystery of membrane organization: composition, regulation and roles of lipid rafts. *Nat Rev Mol Cell Biol* 18:361–374.
373. Pike LJ. 2006. Rafts defined: a report on the Keystone Symposium on Lipid Rafts and Cell Function. *J Lipid Res* 47:1597–1598.
374. Nicolau DV, Burrage K, Parton RG, Hancock JF. 2006. Identifying Optimal Lipid Raft Characteristics Required To Promote Nanoscale Protein-Protein Interactions on the Plasma Membrane. *Molecular and Cellular Biology* <https://doi.org/10.1128/mcb.26.1.313-323.2006>.
375. Simons K, Vaz WLC. 2004. Model systems, lipid rafts, and cell membranes. *Annu Rev Biophys Biomol Struct* 33:269–295.
376. Yu J, Fischman DA, Steck TL. 1973. Selective solubilization of proteins and phospholipids from red blood cell membranes by nonionic detergents. *Journal of Supramolecular Structure* <https://doi.org/10.1002/jss.400010308>.
377. Simons K, Ikonen E. 1997. Functional rafts in cell membranes. *Nature* 387:569–572.

378. Ourisson G, Rohmer M. 1992. Hopanoids. 2. Biohopanoids: a novel class of bacterial lipids. *Accounts of Chemical Research* <https://doi.org/10.1021/ar00021a004>.
379. Sáenz JP, Grosser D, Bradley AS, Lagny TJ, Lavrynenko O, Broda M, Simons K. 2015. Hopanoids as functional analogues of cholesterol in bacterial membranes. *Proc Natl Acad Sci U S A* 112:11971–11976.
380. Nickels JD, Chatterjee S, Stanley CB, Qian S, Cheng X, Myles DAA, Standaert RF, Elkins JG, Katsaras J. 2017. The *in vivo* structure of biological membranes and evidence for lipid domains. *PLoS Biol* 15:e2002214.
381. 2016. LB Liquid Medium. *Cold Spring Harbor Protocols* <https://doi.org/10.1101/pdb.rec090928>.
382. Lycke N, Tsuji T, Holmgren J. 1992. The adjuvant effect of *Vibrio cholerae* and *Escherichia coli* heat-labile enterotoxins is linked to their ADP-ribosyltransferase activity. *European Journal of Immunology* <https://doi.org/10.1002/eji.1830220915>.
383. Anthouard R, DiRita VJ. 2013. Small-molecule inhibitors of toxT expression in *Vibrio cholerae*. *MBio* 4.
384. Schmittgen TD, Livak KJ. 2008. Analyzing real-time PCR data by the comparative CT method. *Nature Protocols* <https://doi.org/10.1038/nprot.2008.73>.
385. Amin Marashi SM, Rajabnia R, Imani Fooladi AA, Hojati Z, Moghim S, Nasr Esfahani B. 2013. Determination of *ctxAB* expression in *Vibrio cholerae* Classical and El Tor strains using Real-Time PCR. *Int J Mol Cell Med* 2:9–13.
386. Miller JH, Cold Spring Harbor Laboratory. 1974. *Experiments in Molecular Genetics*.
387. Quan S, Hiniker A, Collet J-F, Bardwell JCA. 2013. Isolation of Bacteria Envelope Proteins. *Methods in Molecular Biology* https://doi.org/10.1007/978-1-62703-245-2_22.
388. Jiang L, He L, Fountoulakis M. 2004. Comparison of protein precipitation methods for sample preparation prior to proteomic analysis. *Journal of Chromatography A* <https://doi.org/10.1016/j.chroma.2003.10.029>.
389. Sandkvist M, Hough LP, Bagdasarian MM, Bagdasarian M. 1999. Direct Interaction of the EpsL and EpsM Proteins of the General Secretion Apparatus in *Vibrio cholerae*. *Journal of Bacteriology* <https://doi.org/10.1128/jb.181.10.3129-3135.1999>.
390. Kameda K, Nunn WD. 1981. Purification and characterization of acyl coenzyme A synthetase from *Escherichia coli*. *J Biol Chem* 256:5702–5707.
391. Klein K, Steinberg R, Fiethen B, Overath P. 1971. Fatty acid degradation in *Escherichia coli*. An inducible system for the uptake of fatty acids and further characterization of old mutants. *Eur J Biochem* 19:442–450.
392. Nunn WD, Simons RW. 1978. Transport of long-chain fatty acids by *Escherichia coli*: mapping and characterization of mutants in the *fadL* gene. *Proc Natl Acad Sci U S A* 75:3377–3381.
393. Nunn WD, Colburn RW, Black PN. 1986. Transport of long-chain fatty acids in *Escherichia*

- coli. Evidence for role of fadL gene product as long-chain fatty acid receptor. *J Biol Chem* 261:167–171.
394. Giles DK, Hankins JV, Guan Z, Trent MS. 2011. Remodelling of the *Vibrio cholerae* membrane by incorporation of exogenous fatty acids from host and aquatic environments. *Mol Microbiol* 79:716–728.
395. Moravec AR, Siv AW, Hobby CR, Lindsay EN, Norbash LV, Shults DJ, Symes SJK, Giles DK. 2017. Exogenous Polyunsaturated Fatty Acids Impact Membrane Remodeling and Affect Virulence Phenotypes among Pathogenic *Vibrio* Species. *Appl Environ Microbiol* 83.
396. Plecha SC, Withey JH. 2015. Mechanism for Inhibition of *Vibrio cholerae* ToxT Activity by the Unsaturated Fatty Acid Components of Bile. *Journal of Bacteriology* <https://doi.org/10.1128/jb.02409-14>.
397. Jiang Y, Morgan-Kiss RM, Campbell JW, Chan CH, Cronan JE. 2010. Expression of *Vibrio harveyi* acyl-ACP synthetase allows efficient entry of exogenous fatty acids into the *Escherichia coli* fatty acid and lipid A synthetic pathways. *Biochemistry* 49:718–726.
398. Yao J, Rock CO. 2017. Exogenous fatty acid metabolism in bacteria. *Biochimie* <https://doi.org/10.1016/j.biochi.2017.06.015>.
399. Kim W, Fan Y-Y, Barhoumi R, Smith R, McMurray DN, Chapkin RS. 2008. n-3 Polyunsaturated Fatty Acids Suppress the Localization and Activation of Signaling Proteins at the Immunological Synapse in Murine CD4 T Cells by Affecting Lipid Raft Formation. *The Journal of Immunology* <https://doi.org/10.4049/jimmunol.181.9.6236>.
400. Chapkin RS, Wang N, Fan Y-Y, Lupton JR, Prior IA. 2008. Docosahexaenoic acid alters the size and distribution of cell surface microdomains. *Biochimica et Biophysica Acta (BBA) - Biomembranes* <https://doi.org/10.1016/j.bbamem.2007.11.003>.
401. Lorent JH, Diaz-Rohrer B, Lin X, Spring K, Gorfe AA, Levental KR, Levental I. 2017. Structural determinants and functional consequences of protein affinity for membrane rafts. *Nature Communications* <https://doi.org/10.1038/s41467-017-01328-3>.
402. Schuck S, Honsho M, Ekroos K, Shevchenko A, Simons K. 2003. Resistance of cell membranes to different detergents. *Proceedings of the National Academy of Sciences* <https://doi.org/10.1073/pnas.0631579100>.
403. Lichtenberg D, Goñi FM, Heerklotz H. 2005. Detergent-resistant membranes should not be identified with membrane rafts. *Trends in Biochemical Sciences* <https://doi.org/10.1016/j.tibs.2005.06.004>.
404. Miller VL, DiRita VJ, Mekalanos JJ. 1989. Identification of toxS, a regulatory gene whose product enhances toxR-mediated activation of the cholera toxin promoter. *Journal of Bacteriology* <https://doi.org/10.1128/jb.171.3.1288-1293.1989>.
405. Midgett CR, Swindell RA, Pellegrini M, Jon Kull F. 2020. A disulfide constrains the ToxR periplasmic domain structure, altering its interactions with ToxS and bile-salts. *Scientific Reports* <https://doi.org/10.1038/s41598-020-66050-5>.
406. Burdge GC. 2006. Metabolism of α -linolenic acid in humans. *Prostaglandins, Leukotrienes*

- and Essential Fatty Acids <https://doi.org/10.1016/j.plefa.2006.05.013>.
407. Aluko RE. 2012. *Functional Foods and Nutraceuticals*. Springer Science & Business Media.
408. Destailats F, Trottier JP, Galvez JMG, Angers P. 2005. Analysis of α -Linolenic Acid Biohydrogenation Intermediates in Milk Fat with Emphasis on Conjugated Linolenic Acids. *Journal of Dairy Science* [https://doi.org/10.3168/jds.s0022-0302\(05\)73006-x](https://doi.org/10.3168/jds.s0022-0302(05)73006-x).
409. Plourde M, Destailats F, Chouinard PY, Angers P. 2007. Conjugated α -Linolenic Acid Isomers in Bovine Milk and Muscle. *Journal of Dairy Science* <https://doi.org/10.3168/jds.2007-0157>.
410. Bu DP, Wang JQ, Dhiman TR, Liu SJ. 2007. Effectiveness of Oils Rich in Linoleic and Linolenic Acids to Enhance Conjugated Linoleic Acid in Milk from Dairy Cows. *Journal of Dairy Science* [https://doi.org/10.3168/jds.s0022-0302\(07\)71585-0](https://doi.org/10.3168/jds.s0022-0302(07)71585-0).
411. Burdge GC, Calder PC. 2005. Conversion of α -linolenic acid to longer-chain polyunsaturated fatty acids in human adults. *Reproduction Nutrition Development* <https://doi.org/10.1051/rnd:2005047>.
412. Yang B, Chen H, Stanton C, Chen YQ, Zhang H, Chen W. 2017. Mining bifidobacteria from the neonatal gastrointestinal tract for conjugated linolenic acid production. *Bioengineered* 8:232–238.
413. Valenzuela R, Bascuñán K, Chamorro R, Barrera C, Sandoval J, Puigredon C, Parraguez G, Orellana P, Gonzalez V, Valenzuela A. 2015. Modification of Docosahexaenoic Acid Composition of Milk from Nursing Women Who Received Alpha Linolenic Acid from Chia Oil during Gestation and Nursing. *Nutrients* 7:6405–6424.
414. Oosting A, Verkade HJ, Kegler D, van de Heijning BJM, van der Beek EM. 2015. Rapid and selective manipulation of milk fatty acid composition in mice through the maternal diet during lactation. *J Nutr Sci* 4:e19.
415. Dupertuis YM, Meguid MM, Pichard C. 2007. Colon cancer therapy: new perspectives of nutritional manipulations using polyunsaturated fatty acids. *Current Opinion in Clinical Nutrition and Metabolic Care* <https://doi.org/10.1097/mco.0b013e3281e2c9d4>.
416. Larsson SC, Kumlin M, Ingelman-Sundberg M, Wolk A. 2004. Dietary long-chain n-3 fatty acids for the prevention of cancer: a review of potential mechanisms. *The American Journal of Clinical Nutrition* <https://doi.org/10.1093/ajcn/79.6.935>.
417. Coakley M, Banni S, Johnson MC, Mills S, Devery R, Fitzgerald G, Paul Ross R, Stanton C. 2009. Inhibitory Effect of Conjugated α -Linolenic Acid from Bifidobacteria of Intestinal Origin on SW480 Cancer Cells. *Lipids* <https://doi.org/10.1007/s11745-008-3269-z>.
418. Suzuki R, Noguchi R, Ota T, Abe M, Miyashita K, Kawada T. 2001. Cytotoxic effect of conjugated trienoic fatty acids on mouse tumor and human monocytic leukemia cells. *Lipids* <https://doi.org/10.1007/s11745-001-0746-0>.
419. Wahle KWJ, Heys SD, Rotondo D. 2004. Conjugated linoleic acids: are they beneficial or detrimental to health? *Progress in Lipid Research*

<https://doi.org/10.1016/j.plipres.2004.08.002>.

420. Tricon S, Burdge GC, Williams CM, Calder PC, Yaqoob P. 2005. The effects of conjugated linoleic acid on human health-related outcomes. *Proceedings of the Nutrition Society* <https://doi.org/10.1079/pns2005418>.
421. Bhattacharya A, Banu J, Rahman M, Causey J, Fernandes G. 2006. Biological effects of conjugated linoleic acids in health and disease. *The Journal of Nutritional Biochemistry* <https://doi.org/10.1016/j.jnutbio.2006.02.009>.
422. Leikin-Frenkel A, Liraz-Zaltsman S, Hollander KS, Atrakchi D, Ravid O, Rand D, Kandel-Kfir M, Israelov H, Cohen H, Kamari Y, Shaish A, Harats D, Schnaider-Beeri M, Cooper I. 2021. Dietary alpha linolenic acid in pregnant mice and during weaning increases brain docosahexaenoic acid and improves recognition memory in the offspring. *J Nutr Biochem* 91:108597.
423. Zhuang P, Shou Q, Wang W, He L, Wang J, Chen J, Zhang Y, Jiao J. 2018. Essential Fatty Acids Linoleic Acid and α -Linolenic Acid Sex-Dependently Regulate Glucose Homeostasis in Obesity. *Mol Nutr Food Res* 62:e1800448.
424. Kovacikova G, Lin W, Taylor RK, Skorupski K. 2017. The Fatty Acid Regulator FadR Influences the Expression of the Virulence Cascade in the El Tor Biotype of *Vibrio cholerae* by Modulating the Levels of ToxT via Two Different Mechanisms. *J Bacteriol* 199.
425. Shi W, Kovacikova G, Lin W, Taylor RK, Skorupski K, Kull FJ. 2015. The 40-residue insertion in *Vibrio cholerae* FadR facilitates binding of an additional fatty acyl-CoA ligand. *Nat Commun* 6:6032.
426. Feng Y, Cronan JE. 2011. The *Vibrio cholerae* fatty acid regulatory protein, FadR, represses transcription of *plsB*, the gene encoding the first enzyme of membrane phospholipid biosynthesis. *Mol Microbiol* 81:1020–1033.
427. Yang S, Xi D, Wang X, Li Y, Li Y, Yan J, Cao B. 2020. *Vibrio cholerae* VC1741 (PsrA) enhances the colonization of the pathogen in infant mice intestines in the presence of the long-chain fatty acid, oleic acid. *Microb Pathog* 147:104443.
428. Giles DK, Hankins JV, Guan Z, Trent MS. 2011. Remodelling of the *Vibrio cholerae* membrane by incorporation of exogenous fatty acids from host and aquatic environments. *Mol Microbiol* 79:716–728.
429. Nunn WD, Colburn RW, Black PN. 1986. Transport of long-chain fatty acids in *Escherichia coli*. Evidence for role of *fadL* gene product as long-chain fatty acid receptor. *J Biol Chem* 261:167–171.
430. Kim W, Fan Y-Y, Barhoumi R, Smith R, McMurray DN, Chapkin RS. 2008. n-3 Polyunsaturated Fatty Acids Suppress the Localization and Activation of Signaling Proteins at the Immunological Synapse in Murine CD4 T Cells by Affecting Lipid Raft Formation. *The Journal of Immunology* <https://doi.org/10.4049/jimmunol.181.9.6236>.
431. Chapkin RS, Wang N, Fan Y-Y, Lupton JR, Prior IA. 2008. Docosahexaenoic acid alters the size and distribution of cell surface microdomains. *Biochimica et Biophysica Acta (BBA) - Biomembranes* <https://doi.org/10.1016/j.bbamem.2007.11.003>.

432. Chatterjee E, Chowdhury R. 2013. Reduced virulence of the *Vibrio cholerae* fadD mutant is due to induction of the extracytoplasmic stress response. *Infect Immun* 81:3935–3941.
433. Ray S, Chatterjee E, Chatterjee A, Paul K, Chowdhury R. 2011. A fadD mutant of *Vibrio cholerae* is impaired in the production of virulence factors and membrane localization of the virulence regulatory protein TcpP. *Infect Immun* 79:258–266.
434. Komura N, Suzuki KGN, Ando H, Konishi M, Koikeda M, Imamura A, Chadda R, Fujiwara TK, Tsuboi H, Sheng R, Cho W, Furukawa K, Furukawa K, Yamauchi Y, Ishida H, Kusumi A, Kiso M. 2016. Raft-based interactions of gangliosides with a GPI-anchored receptor. *Nat Chem Biol* 12:402–410.
435. Lorent J, Diaz-Rohrer BB, Lin X, Gorfe A, Levental KR, Levental I. 2018. Structural Determinants and Functional Consequences of Protein Association with Membrane Domains. *Biophysical Journal* <https://doi.org/10.1016/j.bpj.2017.11.2103>.
436. Yuan Z, Zhang F, Davis MJ, Bodén M, Teasdale RD. 2006. Predicting the solvent accessibility of transmembrane residues from protein sequence. *J Proteome Res* 5:1063–1070.
437. Li N, Zheng Y, Shi M, Xue Y, Zhang T, Ji S, Yang M. 2019. TcpP L152A Constitutively Activating Virulence Gene Expression in *Vibrio cholerae*. *Curr Microbiol* 76:583–589.
438. Lim MS, Ng D, Zong Z, Arvai AS, Taylor RK, Tainer JA, Craig L. 2010. *Vibrio cholerae* El Tor TcpA crystal structure and mechanism for pilus-mediated microcolony formation. *Mol Microbiol* 77:755–770.
439. Abuaita BH, Withey JH. 2009. Bicarbonate Induces *Vibrio cholerae* virulence gene expression by enhancing ToxT activity. *Infect Immun* 77:4111–4120.
440. Lembke M, Pennetzdorfer N, Tutz S, Koller M, Vorkapic D, Zhu J, Schild S, Reidl J. 2018. Proteolysis of ToxR is controlled by cysteine-thiol redox state and bile salts in *Vibrio cholerae*. *Mol Microbiol* 110:796–810.
441. Mathur J, Waldor MK. 2004. The *Vibrio cholerae* ToxR-regulated porin OmpU confers resistance to antimicrobial peptides. *Infect Immun* 72:3577–3583.
442. Chen L, Qiu Y, Tang H, Hu LF, Yang WH, Zhu XJ, Huang XX, Wang T, Zhang YQ. 2018. ToxR Is Required for Biofilm Formation and Motility of *Vibrio Parahaemolyticus*. *Biomed Environ Sci* 31:848–850.
443. Provenzano D, Schuhmacher DA, Barker JL, Klose KE. 2000. The virulence regulatory protein ToxR mediates enhanced bile resistance in *Vibrio cholerae* and other pathogenic *Vibrio* species. *Infect Immun* 68:1491–1497.
444. Lee YH, Kim BH, Kim JH, Yoon WS, Bang SH, Park YK. 2007. CadC has a global translational effect during acid adaptation in *Salmonella enterica* serovar Typhimurium. *J Bacteriol* 189:2417–2425.
445. Lee YH, Kim JH. 2017. Direct interaction between the transcription factors CadC and OmpR involved in the acid stress response of *Salmonella enterica*. *J Microbiol* 55:966–972.
446. Stelzer S, Egan S, Larsen MR, Bartlett DH, Kjelleberg S. 2006. Unravelling the role of the

- ToxR-like transcriptional regulator WmpR in the marine antifouling bacterium *Pseudoalteromonas tunicata*. *Microbiology* 152:1385–1394.
447. Egan S, James S, Kjelleberg S. 2002. Identification and characterization of a putative transcriptional regulator controlling the expression of fouling inhibitors in *Pseudoalteromonas tunicata*. *Appl Environ Microbiol* 68:372–378.
448. Bischof LF, Haurat MF, Albers S-V. 2019. Two membrane-bound transcription factors regulate expression of various type-IV-pili surface structures in. *PeerJ* 7:e6459.
449. Gumerov VM, Ortega DR, Adebali O, Ulrich LE, Zhulin IB. 2020. MiST 3.0: an updated microbial signal transduction database with an emphasis on chemosensory systems. *Nucleic Acids Res* 48:D459–D464.
450. Gumerov VM, Zhulin IB. 2020. TREND: a platform for exploring protein function in prokaryotes based on phylogenetic, domain architecture and gene neighborhood analyses. *Nucleic Acids Res* 48:W72–W76.
451. Mistry J, Chuguransky S, Williams L, Qureshi M, Salazar GA, Sonnhammer ELL, Tosatto SCE, Paladin L, Raj S, Richardson LJ, Finn RD, Bateman A. 2021. Pfam: The protein families database in 2021. *Nucleic Acids Res* 49:D412–D419.
452. Hoch JA. 2000. Two-component and phosphorelay signal transduction. *Current Opinion in Microbiology* [https://doi.org/10.1016/s1369-5274\(00\)00070-9](https://doi.org/10.1016/s1369-5274(00)00070-9).
453. Gao R, Mack TR, Stock AM. 2007. Bacterial response regulators: versatile regulatory strategies from common domains. *Trends in Biochemical Sciences* <https://doi.org/10.1016/j.tibs.2007.03.002>.
454. Lowe EC, Basle A, Czjzek M, Firbank SJ, Bolam DN. 2012. A scissor blade-like closing mechanism implicated in transmembrane signaling in a *Bacteroides* hybrid two-component system. *Proceedings of the National Academy of Sciences* <https://doi.org/10.1073/pnas.1200479109>.
455. Wolanin PM, Thomason PA, Stock JB. 2002. Histidine protein kinases: key signal transducers outside the animal kingdom. *Genome Biol* 3:REVIEWS3013.
456. Dutta R, Inouye M. 2000. GHKL, an emergent ATPase/kinase superfamily. *Trends Biochem Sci* 25:24–28.
457. Xu J, Chiang HC, Bjursell MK, Gordon JI. 2004. Message from a human gut symbiont: sensitivity is a prerequisite for sharing. *Trends Microbiol* 12:21–28.
458. Zhang W, Shi L. 2005. Distribution and evolution of multiple-step phosphorelay in prokaryotes: lateral domain recruitment involved in the formation of hybrid-type histidine kinases. *Microbiology* 151:2159–2173.
459. Sonnenburg ED, Sonnenburg JL, Manchester JK, Hansen EE, Chiang HC, Gordon JI. 2006. A hybrid two-component system protein of a prominent human gut symbiont couples glycan sensing *in vivo* to carbohydrate metabolism. *Proc Natl Acad Sci U S A* 103:8834–8839.
460. Nicolau DV Jr, Burrage K, Parton RG, Hancock JF. 2006. Identifying optimal lipid raft

- characteristics required to promote nanoscale protein-protein interactions on the plasma membrane. *Mol Cell Biol* 26:313–323.
461. Yu J, Fischman DA, Steck TL. 1973. Selective solubilization of proteins and phospholipids from red blood cell membranes by nonionic detergents. *J Supramol Struct* 1:233–248.
462. Simons K, Toomre D. 2000. Lipid rafts and signal transduction. *Nat Rev Mol Cell Biol* 1:31–39.
463. Chapkin RS, Wang N, Fan Y-Y, Lupton JR, Prior IA. 2008. Docosahexaenoic acid alters the size and distribution of cell surface microdomains. *Biochim Biophys Acta* 1778:466–471.
464. Danylec N, Göbl A, Stoll DA, Hetzer B, Kulling SE, Huch M. 2018. *Rubneribacter badeniensis* gen. nov., sp. nov. and *Enteroscipio rubneri* gen. nov., sp. nov., new members of the Eggerthellaceae isolated from human faeces. *Int J Syst Evol Microbiol* 68:1533–1540.
465. Beltrán D, Romo-Vaquero M, Espín JC, Tomás-Barberán FA, Selma MV. 2018. *Ellagibacter isourolithinifaciens* gen. nov., sp. nov., a new member of the family Eggerthellaceae, isolated from human gut. *International Journal of Systematic and Evolutionary Microbiology* <https://doi.org/10.1099/ijsem.0.002735>.
466. Clavel T, Charrier C, Braune A, Wenning M, Blaut M, Haller D. 2009. Isolation of bacteria from the ileal mucosa of TNF δ ARE mice and description of *Enterorhabdus mucosicola* gen. nov., sp. nov. *Int J Syst Evol Microbiol* 59:1805–1812.
467. Clavel T, Duck W, Charrier C, Wenning M, Elson C, Haller D. 2010. *Enterorhabdus caecimuris* sp. nov., a member of the family Coriobacteriaceae isolated from a mouse model of spontaneous colitis, and emended description of the genus *Enterorhabdus* Clavel et al. 2009. *International Journal of Systematic and Evolutionary Microbiology* <https://doi.org/10.1099/ijs.0.015016-0>.
468. Lagkouvardos I, Pukall R, Abt B, Foessel BU, Meier-Kolthoff JP, Kumar N, Bresciani A, Martínez I, Just S, Ziegler C, Brugiroux S, Garzetti D, Wenning M, Bui TPN, Wang J, Hugenholtz F, Plugge CM, Peterson DA, Hornef MW, Baines JF, Smidt H, Walter J, Kristiansen K, Nielsen HB, Haller D, Overmann J, Stecher B, Clavel T. 2016. The Mouse Intestinal Bacterial Collection (miBC) provides host-specific insight into cultured diversity and functional potential of the gut microbiota. *Nat Microbiol* 1:16131.
469. Gupta RS. 2021. Eggerthellaceae. *Bergey's Manual of Systematics of Archaea and Bacteria* <https://doi.org/10.1002/9781118960608.fbm00384>.
470. Dalia TN, Chlebek JL, Dalia AB. 2020. A modular chromosomally integrated toolkit for ectopic gene expression in *Vibrio cholerae*. *Sci Rep* 10:15398.
471. Muller-Hill B, Crapo L, Gilbert W. 1968. Mutants that make more lac repressor. *Proceedings of the National Academy of Sciences* <https://doi.org/10.1073/pnas.59.4.1259>.
472. Shevchenko A, Wilm M, Vorm O, Mann M. 1996. Mass Spectrometric Sequencing of Proteins from Silver-Stained Polyacrylamide Gels. *Analytical Chemistry* <https://doi.org/10.1021/ac950914h>.

473. Wang Z, Benning C. 2011. Arabidopsis thaliana polar glycerolipid profiling by thin layer chromatography (TLC) coupled with gas-liquid chromatography (GLC). *J Vis Exp* <https://doi.org/10.3791/2518>.
474. Jobling MG, Palmer LM, Erbe JL, Holmes RK. 1997. Construction and characterization of versatile cloning vectors for efficient delivery of native foreign proteins to the periplasm of *Escherichia coli*. *Plasmid* 38:158–173.
475. Morgan SJ, French EL, Thomson JJ, Seaborn CP, Shively CA, Krukonis ES. 2016. Formation of an Intramolecular Periplasmic Disulfide Bond in TcpP Protects TcpP and TcpH from Degradation in *Vibrio cholerae*. *J Bacteriol* 198:498–509.
476. Jobling MG, Palmer LM, Erbe JL, Holmes RK. 1997. Construction and characterization of versatile cloning vectors for efficient delivery of native foreign proteins to the periplasm of *Escherichia coli*. *Plasmid* 38:158–173.
477. Amartely H, Iosub-Amir A, Friedler A. 2014. Identifying protein-protein interaction sites using peptide arrays. *J Vis Exp* e52097.
478. Minato Y, Fassio SR, Wolfe AJ, Häse CC. 2013. Central metabolism controls transcription of a virulence gene regulator in *Vibrio cholerae*. *Microbiology* 159:792–802.
479. Hardie DG, Grahame Hardie D. 1989. Regulation of fatty acid synthesis via phosphorylation of acetyl-CoA carboxylase. *Progress in Lipid Research* [https://doi.org/10.1016/0163-7827\(89\)90010-6](https://doi.org/10.1016/0163-7827(89)90010-6).
480. Konovalova A, Grabowicz M, Balibar CJ, Malinverni JC, Painter RE, Riley D, Mann PA, Wang H, Garlisi CG, Sherborne B, Rigel NW, Ricci DP, Black TA, Roemer T, Silhavy TJ, Walker SS. 2018. Inhibitor of intramembrane protease RseP blocks the σ^E response causing lethal accumulation of unfolded outer membrane proteins. *Proceedings of the National Academy of Sciences* <https://doi.org/10.1073/pnas.1806107115>.